

**UNIVERSIDAD COMPLUTENSE DE MADRID**

**FACULTAD DE CIENCIAS QUÍMICAS**  
**Departamento de Bioquímica y Biología Molecular**



**SMART SYSTEMS FOR TISSUE ENGINEERING:  
COMBINING NATURAL AND SYNTHETIC ORIGIN  
POLYMERS**

**MEMORIA PARA OPTAR AL GRADO DE DOCTOR**  
**PRESENTADA POR**

**Joana Cristina Silva Magalhaes**

Bajo la dirección del doctor  
Julio San Román del Barrio

**Madrid, 2008**

- **ISBN: 978-84-692-2933-0**

**JOANA CRISTINA SILVA MAGALHÃES**

**TESIS DOCTORAL**

**SISTEMAS SENSIBLES A ESTÍMULOS PARA  
INGENIERIA TISULAR: COMBINACIÓN DE  
POLÍMEROS NATURALES Y SINTÉTICOS**

**SMART SYSTEMS FOR TISSUE  
ENGINEERING: COMBINING NATURAL  
AND SYNTHETIC ORIGIN POLYMERS**

**DIRECTOR:**

**Julio San Román del Barrio**



**CONSEJO SUPERIOR DE INVESTIGACIONES CIENTÍFICAS  
Instituto de Ciencia y Tecnología de Polímeros  
Departamento de Biomateriales**



**UNIVERSIDAD COMPLUTENSE DE MADRID  
Facultad de Ciencias Químicas  
Departamento de Bioquímica y Biología Molecular**

**Madrid, 2008**





## Acknowledgements

It has been now three years since I started a new chapter of my life. I was selected to the Marie Curie FP6 Actions- *Alea Jacta Est*.

Since the beginning I felt highly committed to enrol in this project not only due to its excellence, the potentiality of the field and its applications as a key point for the progression of regenerative medicine and the improvement in quality of life expectancy but also due to the multidisciplinary advanced training offered in the most recent developments in biomaterials and tissue engineering research.

The other aspect that attracted me was the possibility of participating in international programs of great economic and social importance for Europe as they contribute to the rise of Europe towards a leading position in the market of Tissue Engineering. Working in associated institutions for the EXPERTISSUES program I was able to participate in the formation the most important network created within this field. This network enabled a unification of facilities, mobility of researchers and bringing together knowledge and expertise between a variety of cultures.

During this period I was given the opportunity to experience multicultural environments and improving my knowledge and skills in conducting multidisciplinary research within different disciplines of the Tissue Engineering field.

Besides all the scientific and professional acquirements within the PhD, I fell truly honoured to have shared ideals, thoughts, laugh, tears, travels.. my life with everyone that has been part of it.

Without ever losing my Portuguese identity, that I am so very proud of, I have embraced Madrid as my capital, Sheffield for the sweetest memories, Braga as a rediscovery of my own country and Brazil as my passion.

I will always cherish the moments we've spent together and I will keep in memory all the professors, colleagues, friends, family, places, cultures.. that have all contributed to the person I am today. You have all made me feel home and so very special.

Far beyond of dedicating this thesis to all of you, I dedicate every single moment behind it.

Thank you!!

## **España**

A Julio por todo el ánimo y conocimiento científico que me ha aportado a lo largo de mi tesis, siempre endulzándome la vida, más de lo que lo podría hacer cualquier caramelo, con su “Se Feliz!”.

A todos los Biomat. En especial a Blanca por sus sabios consejos, a Carlos y Mar por su ayuda en mis primeros pasos en el mundo de los biomateriales, a Luís “Australiano”, por tú amistad, consejos, por el cielo compartido. Y como no a los compartieron mi día a día desde el inicio, Luis García, Marisa, Diego, Gemma, Alberto, Curra, Luis el Rojo, Palo, David por la ayuda preciosa en el SEM, Lucena, Luciano. A Eva y Cesare.

A Roberto por las “luces” que me ha dado y la forma tan sencilla de explicar las cosas que hace parecer todo tan fácil. A mi familia adoptiva de Caucho- Alberto, Irene, Javi y Juan. Justyna por su ayuda en TGA. Eva, Dulce, Rodrigo, Lorena. Jaime, Zuli. Olga, David y Marimar. María Jesús y Marisol que tantas horas compartieron conmigo en la administración de mi beca y a todos los amigos y colegas del ICTP por toda la ayuda y por siempre hacerme sentir en casa.

A mi tutor de la UCM, Javier Turnay Abad. Por toda tú contribución a lo largo de mi doctorado. Ha sido totalmente fundamental!

A Fabi que junto con su familia me dan momentos únicos de felicidad, a Dani y a Justo por todo el cariño y apoyo. A mi familia madrileña Ricky, Emilio, Consu y Jacques. A Ana, Inés y Marifer por que estuvisteis todos los momentos y sigues estando a mi lado.

## **Portugal**

Ao Prof. Rui Reis, pelo seu exemplo de determinação e profissionalismo, por todas as pequenas conversas em que partilhou a sua visão do mundo científico e pela sua disponibilidade sempre que precisei.

Á Ana Leite e Ricardo Silva, os “pais” dos Alea. Sem vocês nada teria acontecido!

Ao Rui Amandi, por me apoiar a 100% em tudo!

A todo o grupo dos 3B's, em especial ao Prof. João Mano, Patricia, João, Sofia, Helena, Sangwon and to my dear Vitor.

Obviamente à minha família que tem de sofrer cada ausência minha, mas apoia-me em cada decisão e mesmo longe, está presente em todos os momentos da minha vida. Á Tita e á Inês, porque tudo começou ao vosso lado. Como não ás “de toda la vida”, Tita, Vilma, Diana, Ana e Lu. E ao Tiago, por fazer-me acreditar.

## **UK**

I would like to thank Paul and Aileen for all the scientific support, the way they have welcomed me and how they were concerned all the time about my work and adaptation.

To Sheffield's biomaterial group, especially Richard, mum Jen, Marie, Becci, Kathryn and Victoria.

## ***Alea Jacta Est***

To all the ALEA students, Boris, Wojtek, Cassilda, Tommaso, Elizabeth, Aga, Paula and my dear Sweds, Linda and to Harald for always be the first one to stand up for me. Together we have shared the benefits and drawbacks of our program, interests, labs, houses, congresses, but the most valuable, friendship.

For the next step of our lives, it is starting how it all began, “*alea jacta est*”..

Wish you all the best!



## Index

<b>Resumen y objetivos generales</b> .....	3
<b>General Introduction</b> .....	9
1. Role of Scaffolds in Tissue Engineering .....	9
2. Characteristics and Properties	
2.1. Structural (like Molecular weight, physical properties, surface area, shape and morphology) .....	12
2.2. Physical Dimension .....	12
2.3. Pore Structure .....	12
2.4. Mechanical Properties .....	14
2.5. Hydrophilicity .....	14
2.6. Release of Active Agents .....	14
2.7. Biodegradability .....	15
2.8. Biocompatibility .....	16
2.9. Processability for Clinicians .....	16
3. Interactions cell-extracellular matrix and mimetic approaches for the application of polymeric supports .....	17
4. Composition and Structure of Polymeric Scaffolds- From Natural to Synthetic Biodegradable Formulations .....	21
4.1. PVP based polymer .....	24
4.2. Hyaluronic Acid .....	24
5. Bone and Cartilage Tissue Engineering .....	26
5.1. Bone.....	26
5.2. Cell Biology .....	26
5.3. Application of polymeric scaffolds in bone tissue regeneration .....	27
5.4. Cartilage .....	28
5.5. Cell Biology .....	29
5.6. Application of polymeric scaffolds in cartilaginous tissue regeneration	30
6. General Objectives .....	31
7. Bibliography .....	32

## Chapter I- Polymeric Smart Systems- synthesis and characterization

<b>1. Introduction</b>	37
1.1. Radical Polymerization Reactions	37
1.2. Preparation of Smart Polymeric Systems	38
1.3. Techniques for the characterization of the polymeric systems	40
1.3.1. Spectroscopic Techniques	40
1.3.2. Chromatographic Techniques	40
1.3.3. Thermal Analysis Techniques	41
1.3.4. Microscopic Techniques	42
1.3.5. Dynamic Mechanical Analysis	42
1.4. Objective	42
<b>2. Material and Methods</b>	43
2.1. Material Synthesis	43
2.1.1. Monomer Synthesis Process	43
2.1.2. Polymer Synthesis Process	44
2.1.2.1. Semi IPN systems preparation (Free Radical Polymerization)	44
2.2. Characterization of the materials:	45
2.2.1. Spectroscopic Techniques	45
2.2.2. Chromatographic Techniques	45
2.2.3. Thermal Analysis Techniques	46
2.2.4. Microscopic Techniques	46
2.2.5. Picnometric techniques	46
2.2.6. Dynamic Mechanical Analysis	46
<b>3. Results and Discussion</b>	47
3.1. Preparation of the semi-IPN	47
3.2. Spectroscopic Characterization	49
3.3. Chromatographic Characterization	53
3.4. Thermal Analysis Characterization	54
3.5. Macroscopic Characterization	55
3.6. Porosity determination by pycnometry	60
3.7. Determination of the mechanical properties of PEPMHA polymeric systems	61
<b>4. Bibliography</b>	65

## Chapter II- Semi-IPN behaviour in hydrated environment

<b>1. Introduction</b>	67
1.1. Equilibrium Swelling Theory	67
1.2. Rubber Elasticity Theory	68
1.3. Objective	69
<b>2. Material and Methods</b>	69
2.1. Water Uptake/Swelling Studies	69
2.2. LCST determination by water uptake	70
2.3. Determination of the average molecular weight between cross-links	70
<b>3. Results and Discussion</b>	71
3.1. Water Uptake	71
3.1.1. Effect of the composition of hydrogels	72
3.1.1.1. pH sensitivity of hydrogels	72
3.1.1.2. Temperature sensitivity of hydrogels	79
3.2. LCST determination by water uptake	82
3.3. Determination of the average molecular weight between cross-links	85
3.3.1. Volume fractions determination	86
3.3.2. Determination of the $M_c$	87
3.4. Relation between swelling and mechanical properties of the PEPMHA hydrogels	88
<b>4. Conclusions</b>	90
<b>5. Bibliography</b>	92



## Chapter III- Evaluation of the cellular behaviour in PEPMHA cell-constructs

<b>1. Introduction</b>	94
1.1. Objective	94
<b>2. Materials and Methods</b>	95
2.1. Scaffolds production	95
2.2. Sample sterilisation	95
2.3. Sample preparation	95
2.4. Controls preparation- agarose gels	96
2.5. Cell isolation and expansion	96
2.5.1. Bovine cartilage dissection	96
2.5.2. Bovine chondrocyte isolation	96
2.6. Cell expansion	97
2.6.1. Cell seeding and expansion	97
2.6.1.1. Seeding scaffolds for preliminary cell activity test	97
2.6.1.2. Cell Activity- Alamar Blue	98
2.6.2. Seeding scaffolds for TE	98
2.6.2.1. Seeding agarose gels for TE	99
2.6.2.2. Seeding efficiency	99
2.6.2.3. Expansion and adhesion (7d)	99
2.6.2.4. Cartilage constructs maturation (40d)	100
2.7. Characterization of the constructs	100
2.7.1. Scanning electron microscopy	100
2.7.1.1. Fixation and alcohol dehydration	100
2.7.1.2. Mounting samples	101
2.8. Sample Processing	101
2.8.1. Histology	101
2.8.1.1. Hematoxylin and eosin stain	102
2.8.1.2. Toluidine blue stain	102
2.9. Immunohistochemistry	102
2.9.1. Immunolocalization of type I and II collagen	102
2.9.2. Quantitative assessment of glycosaminoglycans- 1,9-dimethylmethyle	
blue (DMB) assay	103
2.9.3. Statistical analysis	105

<b>3. Results and discussion</b> .....	105
3.1. Cell activity- Alamar Blue.....	105
3.2. SEM.....	109
3.3. Seeding Efficiency.....	111
3.4. Scaffolds for Tissue Engineering.....	113
3.4.1. Histology of cartilage engineered on PEPMHA scaffolds.....	113
3.4.2. Hematoxylin- Eosin stain .....	114
3.4.3. Toluidine blue stain.....	117
3.4.4. Immunohistochemistry stain.....	119
3.4.5. Quantification of glycosaminoglycans.....	121
<b>4. Conclusions</b> .....	125
<b>5. Bibliography</b> .....	126

## **Chapter IV – Prediction of bone ingrowth in PEPMHA scaffolds**

<b>1. Introduction</b> .....	129
1.1. Objective.....	130
<b>2. Materials and methods</b> .....	130
<b>3. Results and discussion</b> .....	131
3.1. SEM.....	131
3.2. EDS.....	138
3.3. FTIR.....	139
<b>4. Conclusions</b> .....	141
<b>5. Bibliography</b> .....	142

## **Chapter V- Photopolymerization of PEPMHA systems**

<b>1. Introduction</b> .....	145
1.1. Photopolymerization Reactions.....	146
1.2. Cell Encapsulation.....	147
1.2.1. Cell Incorporation Routes.....	148
1.3. Objectives.....	150

<b>2. Material and methods</b> .....	150
2.1. Bulk Photopolymerization Process.....	151
2.2. Characterization of the materials.....	151
2.2.1. Spectrometric Techniques.....	151
2.2.2. Spectroscopic Techniques.....	151
2.2.3. Thermal Analysis Techniques.....	152
2.2.4. Microscopic Techniques.....	152
2.2.5. Dynamic Mechanical Analysis.....	152
2.2.6. Swelling properties.....	152
<b>3. Results and discussion</b> .....	152
3.1. Preparation of PEPMHA hydrogels through bulk photopolymerization	153
3.2. Characterization of the materials.....	156
3.2.1. Spectroscopic Techniques.....	156
3.2.2. Thermal Analysis Characterization.....	157
3.2.3. Macroscopic Characterization.....	158
3.2.4. Swelling behaviour of the photopolymerized PEPMHA hydrogels.....	159
3.2.5. Mechanical Performance of the photopolymerized PEPMHA hydrogels.....	162
<b>4. Conclusions</b> .....	164
<b>5. Bibliography</b> .....	165
 <b>General Summary and Conclusions</b> .....	169
<b>Conclusiones Generales</b> .....	171
<b>Appendix</b>	





## Resumen

La Ingeniería de Tejidos (IT) y la Reparación Direccional de Tejidos son áreas científicas en desarrollos avanzados, que pretenden ofrecer soluciones primordiales en la reparación y sustitución parcial ó total de tejidos y órganos seriamente dañados ó disfuncionales, así como para potenciar las funciones biológicas de elementos de estos mismos tejidos y órganos.

Los biomateriales basados en polímeros sintéticos en combinación con polímeros naturales están siendo utilizados como sistemas innovadores en la reparación de tejidos. Una combinación de materiales de diferentes orígenes permitirá la manipulación de diversas propiedades (polímeros de origen sintética) y por otro lado el mantenimiento de características que les aproximan del material biológico (polímeros de origen natural).

Dentro de estos sistemas se destacan los hidrogeles, siendo excelentes candidatos para la Ingeniería de Tejidos debido a sus elevados contenidos en agua, sus propiedades de transporte y su similitud en comportamiento químico y físico con los tejidos vivos.

Este trabajo de investigación se basa en la producción y caracterización de sistemas inteligentes implantables, utilizando la polimerización en solución acuosa del metacrilato de 2-etil (2-pirrolidona) (EPM), que presenta una solubilidad dependiente de la temperatura en agua, en combinación con el ácido hialurónico (AH), un polímero de origen natural con sensibilidad al pH, muy reconocido por su elevado carácter hidrofílico.

Sistemas basados en el monómero EPM tienen la propiedad de ser insolubles en agua, por encima de su temperatura crítica o LCST (“lower critical solution temperature”) ó bien precipitando debajo de la misma. Lo mismo sucede con algunos sistemas basados en el AH en relación al pH, causando particular interés para su aplicación como sistemas de liberación de fármacos, así como para la activación de procesos regenerativos en los tejidos.

Otra aplicación posible sería la combinación de la fotosensibilidad del grupo metacrilato del EPM y la biocompatibilidad del AH, para fotopolimerizar estos sistemas para conseguir el encapsulamiento celular. Esta estrategia permitiría la formación de hidrogeles in situ, reduciendo el coste de los implantes biomateriales, y la aplicación de técnicas quirúrgicas mínimamente invasivas.

Es de extrema importancia el estudio de estos materiales para que puedan funcionar debidamente en su aplicación. Desde un punto de vista estructural, el soporte polimérico ideal debería cumplir los siguientes requisitos: tener una estructura tridimensional, con una porosidad que permita la proliferación celular, ser biocompatible y poseer las propiedades mecánicas que le permitan asistir en la regeneración tisular, y debe ser biodegradable, es decir que sus productos puedan ser eliminados por el organismo una vez finalizada su función.

## **Capítulo I - Polimerización de los materiales en condiciones de temperatura moderada y su caracterización**

El 2- hydroxyethyl-pyrrolidone (EP) fue modificado a través de una reacción con el cloruro de metacrilato en presencia de trietilamina obteniendo el monómero EPM. Este método es utilizado con frecuencia para introducir metacrilatos en las cadenas poliméricas, aumentando su reactividad. El EPM fue polimerizado en presencia del AH, formando redes semi-interpenetradas y utilizando el dimetacrilato de trietilenglicol ó N,N'-metilen-bisacrilamida.

El ácido hialurónico fue utilizado en concentraciones hasta un 5% para conseguir sistemas biocompatibles, pero intentando no alterar sensiblemente las propiedades mecánicas de los sistemas.

Los sistemas entrecruzados se caracterizaron mediante técnicas de FTIR, RMN y SEM, así como se determinó su modulo de almacenamiento ( $G'$ ) y su estructura porosa.

Los sistemas desarrollados poseen una estructura porosa que puede ser relacionada con su carácter de retención de agua. Mientras la porosidad del material aumenta, y su módulo disminuye, mayor será el área superficial, y consecuentemente la capacidad de retención de agua.

## **Capítulo II- Propiedades de los materiales frente a cambios de temperatura y del pH**

Las diferentes condiciones de preparación de los hidrogeles, como la variación en la concentración inicial del monómero, concentración del ácido hialurónico, naturaleza del agente entrecruzante utilizado, son factores responsables de la formación de materiales con diferentes características estudiadas en el capítulo anterior.

A parte de estos parámetros, se estudiaron el grado de hinchamiento de los materiales en distintas condiciones de temperatura y pH y se verificó que a pesar de que ambos influyen en el carácter hidrofílico de los sistemas entrecruzados, no se ha observado una LCST como se esperaba inicialmente, aunque sí es posible detectar un perfil de sensibilidad a los diferentes estímulos inducidos, y se cree que la presencia del ácido hialurónico es la responsable principal por estos.

Debido al carácter aniónico del AH los hidrogeles sintetizados presentan una mayor solubilidad por debajo de su pKa y los mismos sistemas presentan un mayor grado de hinchamiento a una temperatura más baja.

El grado de hinchamiento pudo relacionarse fácilmente con las propiedades mecánicas de los materiales, esto es un mayor grado de hinchamiento corresponde a propiedades mecánicas más bajas, como así se ha comprobado experimentalmente.

### **Capítulo III- Estudio del comportamiento celular frente a los materiales (aplicaciones en Ingeniería del Tejido Cartilaginoso)**

La elección de los materiales que constituyen los soportes poliméricos es muy importante a la hora de implantación en los tejidos dañados de forma que el organismo no les detecte como agentes extraños e inicie una respuesta de rechazo.

Se sembraron diferentes tipos de células (condrocitos primarios, ROS, L929 y células mesenquimales) en los sistemas de PEPMAH preparados y se observó que todas mantuvieran su viabilidad.

En un estudio más detallado en su aplicación en la ingeniería de tejido cartilaginoso se verificó la influencia positiva del ácido hialurónico, es decir un incremento de la concentración de este polímero en los hidrogeles conlleva un aumento en la producción de glicosaminoglicanos (GAGs), uno de los componentes principales de la matriz extracelular.

A parte de la producción de GAGs, la producción de colágeno de tipo II influye en la formación de una matriz extracelular de características hialinas, aunque concentrada sobretudo en la superficie de los materiales y de limitada proliferación en su interior.

Se pudo constatar que los sistemas poliméricos basados en PEPMHA soportaron el crecimiento y proliferación de condrocitos primarios a pesar de la reducida penetración celular en el interior de los materiales.



## **Capítulo IV- Estudio del efecto de un fluido fisiológico simulado en los materiales sintetizados (aplicaciones en Ingeniería del Tejido Óseo)**

Se llevaron a cabo ensayos de bioactividad en los que los materiales se incubaron en un fluido fisiológico simulado (“simulated body fluid”, SBF). La bioactividad de un sistema se puede definir como la capacidad de un material para soportar el crecimiento de células de tejido óseo, manteniendo su estructura.

Se supone que cuando un material se encuentra en contacto con una disolución de SBF puede ocurrir la formación de fosfatos de calcio (Ca-P), como la hidroxiapatita, depositándose sobre el material. La hidroxiapatita es uno de los principales componentes del hueso, así que su formación en la superficie del material es una forma de predecir la bioactividad de un material *in vivo*, a partir de ensayos *in vitro*.

La formación de una capa de Ca-P depositada en la superficie de las distintas formulaciones de PEPMAH utilizadas (espectro de EDS), con la formación de los característicos cristales en forma de aguja, aglomerados a los que presentan la llamada “morfología tipo coliflor” (SEM) demostró el carácter bioactivo que presentan estos materiales y su posible aplicación en la ingeniería de tejidos óseos.

## **Capítulo V- Polimerización de los materiales activada fotoquímicamente**

Como bien indica la palabra fotopolimerización, en este proceso juega un papel fundamental la luz, que interviene en la primera parte de la reacción dando lugar a las especies que iniciaran la polimerización.

El monómero utilizado en nuestros estudios (EPM), posee un grupo metacrilato que puede ser fácilmente activado para polimerizar por vía radical a través de un fotoiniciador. Se utilizó este método para la preparación de nuevos sistemas basados en PEPMAH.

Estos hidrogeles fueron sintetizados obteniendo elevado rendimiento, y con una mejora sustancial de su capacidad de hinchamiento y en sus propiedades mecánicas en relación a los hidrogeles producidos por polimerización utilizando la temperatura.

Así que, tanto el control como la rapidez de este método en condiciones de temperatura ambiente ó fisiológica en combinación con las características de estos materiales demuestran su potencialidad para una futura aplicación en la encapsulación celular.

Aunque para tal deberían ser estudiadas sistemáticamente las condiciones de la reacción de fotopolimerización y las variables que influyen en la velocidad de esta reacción.

### **Objetivos Generales:**

Se pretende con este trabajo de investigación el desarrollo y caracterización de nuevos hidrogeles basados en la combinación de polímeros de origen natural y sintética. Como tal y para más fácil comprensión se presentó el trabajo por capítulos.

El primer objetivo es el de aumentar el carácter hidrofílico de los hidrogeles basados en PEPM. Así que, en una primera parte (capítulos I y II) se estudian y caracterizan los materiales polimerizados, seguido del estudio de cómo sus propiedades, en medios acuosos y en condiciones fisiológicas, influyen en la respuesta a diferentes estímulos (cambios en la temperatura y/o pH).

En una segunda parte de esta memoria (capítulo III y IV) se pretende ver la aplicabilidad de los hidrogeles en la ingeniería de los tejidos cartilaginoso y óseo. Como tal, se pretende estudiar la respuesta de diferentes tipos de células de forma a evaluar el carácter biocompatible de estos materiales, así como a través del estudio de la formación de fosfatos cálcicos en la superficie de los hidrogeles predecir una bioactividad de los mismos.

Por fin, en una tercera parte (capítulo V) revisar un proceso distinto de polimerización desencadenado por la luz, por su vez, más rápido y realizado a temperaturas fisiológicas. Este método debido a sus características supondría una proliferación celular más homogénea. Así que se pretende hacer un estudio preliminar de algunas de las propiedades de los materiales obtenidos por fotopolimerización y compararlas con las propiedades de los hidrogeles formados a través de la polimerización con activación térmica, descritos en la primera parte de esta memoria.

En el apéndice se representan gráficas de las propiedades mecánicas de los materiales, en escala logarítmica y una descripción más detallada de los métodos utilizados para los estudios del comportamiento celular.



## **General Introduction**

### **1. Role of Scaffolds in Tissue Engineering**

Tissue loss or end stage organ failure resulting from an injury or a disease is a major health care problem, as the transplantation of tissues or organs for these patients is limited by the availability of compatible donors. With life expectancy increase, the body is submitted to a bigger wear, so innovative alternatives are needed to fulfil the requirements of the body in order to provide a better health quality to a more elder world population.

Until approximately 2 decades ago, clinicians only disposed of mechanical devices or artificial prostheses that were designed to be implanted in the human body but that did not focus on the incorporation of the materials to the surrounding tissue to repair nor in the assessment of the diseased organ function [1]. One of the main problems of those materials considered for long-term implant applications is that of biocompatibility. There is a higher risk of inflammatory response in the host tissue as the body tends to reject foreign objects by encapsulating them through platelet deposition. Certain breast implants would be an example of this rejection. Therefore, it would be desirable if the material could be biodegradable and avoid long term biological reactions.

Concerning the limitations of the solutions for the replacement and repair of tissue and organs, a new field in regenerative medicine aroused, designated Tissue Engineering (TE).

As R. Langer defined, 'Tissue Engineering is an interdisciplinary field that incorporates principles of engineering with the life sciences for the development of tissue or organ replacements [2]. Design and synthesis of biomaterials, analysis of biocompatibility and biostability, as well as dissection of the normal physiological processes that result in tissue formation and homeostasis are all features of modern tissue engineering.

Cells are primordial to tissue regeneration and repair due to their proliferation and differentiation, cell-to-cell signalling, biomolecule production, and formation of extracellular matrix. The functionality of an engineered tissue may be structural (bone, cartilage) or metabolic (liver, pancreas) or both. Cells may be part of an engineered tissue or may be recruited in vivo with the help of biomaterials and/or biomolecules.

Three general strategies for tissue engineering have been adopted since the early definition of this field, and they focus on:

1. the use of isolated cells
2. tissue inducing substances
3. cells placed on or encapsulated within matrices

In the latter one, a new strategy that concerns the integration of cells and tissue inductive substances within a matrix is used. These matrices also defined as tissue engineering constructs possess characteristics that make them appropriate for their use as a support for the new tissue formation, as a scaffold.

There has been given special attention to the study of scaffolds with specific characteristics that provide temporary support for cell growth, promote cell adhesion, as well as the transport of nutrients and metabolites necessary for the formation of new tissue. At the same time, the scaffolds should also provide the appropriate mechanical strength required during surgical implantation in the human body and guide the tissue development and its organization into a mature and healthy state [3]. Finally, the scaffold components undergo simultaneous or delayed degradation or resorption via production of biocompatible, excretable, or metabolizable by-products [4].

In this vein, the role of biomaterials is governed by the interactions between the material and the body, specifically, the effect of the body environment on the material and the effect of the material on the body [5].

Scaffold properties depend primarily on the nature of the biomaterial and the fabrication process. The nature of the biomaterial has been extensively reviewed, as for metals, ceramics, chemically synthesized polymers, natural polymers and combinations of these materials to form composites [6].

Synthetic and natural polymers have been used as novel biomaterials in diverse medical applications. Among these, hydrogels are advantageous due to their chemical similarity to the extracellular matrix, their ability to form three-dimensional hydrophilic networks, retaining a high amount of water while maintaining a certain degree of structural integrity and flexibility [7, 8]. Also, their permeability for small molecules, soft consistency, low interfacial tension and facility of purification, makes their physical properties similar to those of living tissues. Focus on the different materials composition will be given later on.

The requisites for a biomaterial to be used in Tissue Engineering besides their specificity for each end should match the market profit concerns and product commercialization. The materials would need to be universal rather than patient specific and require long-term storage without loss of function; the materials should be modified in a fast and reproducible method that would decrease the high cost of bringing a new material up; the mechanical properties normally lost in short period of time shouldn't interfere with the tissue function in long-term period; the products of biodegradation should present any local or systemic toxicity; finally the polymeric materials used should be compatible with the controlled release of bioactive substances as drugs or growth factors.

## **2. Characteristics and Properties**

In terms of a structural point of view, the ideal polymeric scaffold would have to fulfil essential requirements: have a tri-dimensional structure, where structures with different porosity with defined pore size that enhance cellular proliferation can be obtained; be biocompatible, this is, not to induce any inflammatory or immunogenic response neither possess cytotoxic character; possess determined mechanical properties that supports the tissue regeneration whilst allowing some minimal level of function immediately post-implantation (patient's mobility); finally, the scaffold should be biodegradable in order to be eliminated by the organism once its function has support has been accomplished [9].

The function of a degradable scaffold is to act as a temporary support matrix for the transplanted or host cells so as to restore, maintain or improve tissue.

The design of a scaffold plays a key role in the development of a proper matrix. Therefore, the study of the properties of these materials is crucial for their manipulation and understanding the effect and interaction of cell-material.

This section surveys some of the characteristics and properties of the different materials that must be considered: structure, mechanical properties, properties facing the water, biodegradability and biological properties [5].

## **2.1. Structural (like Molecular weight, physical properties, surface area, shape and morphology)**

In general increasing the molecular weight of a polymer corresponds to increasing the physical properties of the scaffold.

Surface characteristics of polymers for biomedical applications are extremely important, as the surface of the material is normally the only part of the material in contact with the human body.

Surface roughness therefore enhances the attachment of cells and cells recognition can be increased when bioactive compounds are added to materials surface, also diminishing the risk of inflammation and rejection.

## **2.2. Physical Dimension**

The physical dimension defines the boundary of regeneration. Rapid prototyping techniques longer used in the plastic and metal industry are now being adapted to the regenerative medical field, where scaffolds can be specifically moulded to a determined shape of the tissue to replace [10].

## **2.3. Pore Structure**

Porosity can be defined as the percentage of void space and it is a morphological property independent of the material [11].

Material porosity and pore size distribution greatly influence the attachment of the different cell types and the interaction with the host's tissue.

The most common techniques used to form pores in a biomaterial are salt leaching, gas foaming, phase separation, freeze-drying and sintering [11, 12].

Considering the porous structure 2 types of organization can be defined: micro and macro-structure:

### **- Micro-structure**

The scaffold should possess an ideal porosity and pore size. Cells migration is highly influenced by these two characteristics. Cells will prefer to attach to highly porous

materials and migrate within the bulk when the size of the pores is considerable larger than the cell's own size. It has been suggested that the pore size in the range of 100-400  $\mu\text{m}$  is optimal for tissue regeneration [5]. This is also the maximum distance between any cell and the nearest blood capillary, beyond which there is inadequate supply of oxygen and nutrients. In a study for bone regeneration of Hulbert et al., where large pores with dimensions 100-150  $\mu\text{m}$  showed a substantial bone ingrowth that is also correlated with normal haversian systems that reach an approximate diameter of 100-200  $\mu\text{m}$  [11].

Another property related to the pore size is the permeability of ions and macromolecules, especially important in the case of cells in the center of a matrix that do cannot obtain nutrients or remove waste effectively.

Mass transport rates into cells can be optimized using bioreactors. The use of rotating bioreactors also provides tissue with hydrodynamic and/or mechanical stimulation [13]. It is also generally advantageous that scaffolds possess a large surface area to volume ratio. Logically the cell proliferation is favoured in a large surface with enough volume to develop new tissue.

Additionally, a scaffold efficacy is also dependent on its interaction with cells. Thus, the surface properties that can be enhanced with adjuvant proteins for cells recognition should facilitate this interaction.

#### - Macro-structure

A scaffold can be formed into a number of different macro-structures including, fibre meshes, hydrogels and foams.

Using a broad variety of processes these macro-structures can be organized in 3 dimensional scaffolds.

One modern technique associated to these structures is the use of rapid prototyping technology, where the design of the scaffold is controlled and allows the construction of scaffolds with well defined arrangements.

A major concern involving the porous structure of a material is the balance between providing a highly porous network for cells attachment, proliferation and differentiation and the maintenance of the integrity and stability of the scaffold's architecture that supports the cellular processes until the regenerated tissue can assume its structural role.



## **2.4. Mechanical Properties**

The tensile properties of biomaterials can be characterized by their deformation and flow behaviour under stress.

The ultimate mechanical properties of polymers at large deformations are important in selecting particular polymers for biomedical applications. This involves the observation of the material as one applies tension stress is applied for it to elongate (strain) to the point where it ruptures.

The mechanical strength of a scaffold material is intended to mimic the mechanical properties of the tissue to repair or replace. Therefore, in the case of degradable materials, not only the initial mechanical strength is crucial, but also the gradual strength reduction of the partially resorbed material has to be compensated by a strength increase from the regenerated tissue, in a way that the total mechanical forces are maintained.

## **2.5. Hydrophilicity**

Hydration of an implant facilitates nutrient diffusion. The extent of hydration would also provide information about the space available for tissue ingrowth.

## **2.6. Release of Active Agents**

Controlled release systems deliver a drug at a predetermined rate for a defined and limited period of time. In general, release systems rates are determined by the design of the system and environmental conditions, such as temperature and/or pH. Examples of these systems are the PEPm and PEPyM [14].

Drug delivery polymeric systems have been found to be a suitable substitution in the release of active agents and being more locally efficient rather than the administration of conventional drug therapies.

On the forefront of controlled drug delivery are intelligent, stimuli-responsive hydrogels that possess oscillatory swelling and, hence, modulate release in the response to changes in the pH, temperature, ionic charge, electric or magnetic fields, enzymes among others [15, 16].

A major concern in the conventional drug therapies is to find the suitable therapeutic range where the drug is effective, avoiding a burst of drug release above this range, being toxic to the organism or reaching levels below this range where the drug is ineffective.

A controllable and local release of the drug would not only help to maintain this optimal range as it would even lower the systemic drug level.

The degradation profile is especially important in drug delivery systems, as it is one of the factors that determine the rate of drug liberation.

## **2.7. Biodegradability**

3 main aspects should be considered concerning biodegradation:

- The degradation profile might need to be synchronized based on different strategies;
- Material degradation rate should match the regenerating rate of the tissue;
- Degradation products should be non- toxic.

Basically, the material may degrade through two different processes that are critical in cell attachment and proliferation, drug delivery profiles and late inflammatory responses: bulk and surface erosion [15].

In the first type of processes, the polymer matrix becomes highly porous with time and eventually breaks. In drug delivery systems, this phenomenon could lead to dumping of the drug, which could be fatal if high levels of the drug are toxic. The fact that the surface is maintained intact, it may facilitate cell adhesion to a greater extent than surface eroding scaffolds. Also it will create empty spaces that can be filled with cells producing matrix. Hence it is critical that the scaffold degradation rate follows the rate of tissue repair.

Surface erosion is achieved via enzymatic or hydrolytic degradation and is defined by a gradual decrease in the dimensions of the scaffold with no change in the mechanical properties. However, when reached a critical point, both size and mechanical stability may be comprised by surface erosion.

Enzyme levels vary between different individuals and may provoke different cellular responses, as for the water, present at high levels in every organism may determine a reproducible response thus is the preferred process.

In cases where mechanical forces are intended to maintain cell growth and phenotype expression, a scaffold that displays surface eroding properties may be elected.

Material's composition also determines the type of degradation process.

Synthetic degradable polymers mainly suffer bulk erosion although they can degrade by surface, bulk or both. In the other hand, natural polymers essentially undergo surface erosion due since enzymes are normally too large to penetrate into the scaffold [15-17].

## **2.8. Biocompatibility**

Polymeric materials origin selection is important in the sense of being recognized by the organism not to elicit a foreign body attack and rejection response. It is known that any injury will elicit some inflammatory response [17]. So far it has not been implanted any polymeric scaffold without inducing any inflammatory response although many materials have shown to be successfully implanted with minor inflammatory response. The fibrotic capsule formed around the tissue, formed in the implanted engineered construct due to inflammatory response may further inhibit the tissue remodelling and function forming a barrier to the nutrient transport and angiogenesis.

Polymer surfaces can be tailored with specific recognition properties when in contact with biological fluids, cells, or cellular components [16].

Incorporation of signal peptides such as RGD has been widely studied in order to effectively mimic the extracellular matrix and induce cell migration. RGD peptides do not only trigger cell adhesion effectively as they can also be used to address selectively certain cell lines and elicit specific cell responses [18].

## **2.9. Processability for Clinicians**

Designing materials that can be useful in present surgical procedures or even develop new surgical procedures represents an important opportunity for biomaterials scientists.

In order to diminish the invasiveness of the techniques and to facilitate the recuperation of the patient, minimal invasive surgery displays the ultimate goal for tissue engineering and regenerative medicine applications.

### **3. Interactions cell-extracellular matrix and mimetic approaches for the application of polymeric supports**

The main focus of the body's response to injury is the repair and homeostasis for the purpose of survival. The first response of the body after injury is to balance the damages through homeostatic mechanisms, such as vasoconstriction and blood clot formation. Then, there is a combat to stop the infection and eradicate damaged tissue and foreign bodies. Meanwhile, the body must replace damaged tissue, supply nutrients, remove wastes, and cover exposed surfaces to prevent desiccation and microbial invasion. Finally, the newly formed matrix has to be modified and remodelled to provide strength and durability.

Although cells are the key players in the newly formed tissue, they have to be backed up with a suitable extracellular matrix (ECM).

In most tissues of the human body, cells reside anchored in a network of complex glycoproteins referred to collectively as the extracellular matrix.

Basically, the ECM is composed by fibbers (collagen and elastin) and a largely amorphous interfibrillary matrix (mainly proteoglycans, noncollagenous cell-binding adhesive glycoproteins, salts and water) [19].

Collagens and elastin: Collagens are the most abundant proteins in the mammals. In 1991 they are defined as “structural macromolecules of the ECM composed one or more domains with a triple helix conformation”. Among this super- family, 3 groups were assigned [20, 21]:

- Interstitial or fibrillar collagens; Examples of this group are collagens type I, II and III, forming resistant fibbers, stabilized by covalent bonds. This constitutes the most abundant group;
- Collagens associated with fibbers; type IX, XII and XIV that are molecules where the domains in triple helix are alternated with non collagenous regions;
- Non fibrillar (or amorphous) collagens; group that include the collagens that form networks (type IV, VIII and X), or that present themselves in globular filaments (type VI) and the ones constituted by bonding fibres (type XVI and XIX). A sub family of this group is the one that the collagens (type XIII and XVII) are coupled to the membrane.

Elastic fibres are essential constituents of the heart valves on the aorta, where the tissue is exposed to a continuous pulsatile flow and repeated stress, and of intervertebral disks, where the repetitive forces along the spine are dissipated. Unlike collagen, elastin can be stretched, restoring the form of the tissues where it can be encountered, like the artery's form between heartbeats.

Proteoglycans: The proteoglycans are macromolecules composed by a proteic nucleus to which are covalently linked long chains of sulphated carbohydrate polymers, designated glycosaminoglycans (GAG). The glycosaminoglycans are polyanionic chains, generated by the repetition of a disaccharide, where one of the residues is always a hexosamine (D-glucosamine or D-galactosamine) and the other a hexuronic acid (D-glucuronic or L-iduronic). According to the nature of the present disaccharide, different glycosaminoglycans can be obtained: hyaluronic acid, the only non sulphated GAG; chondroitin sulphate and dermatan sulphate; heparin sulphate and heparin; and keratin sulphate.

The proteoglycans are responsible for the lubrication of the ECM, participating in the organization of the ECM as well as modulating cell adhesion, migration, proliferation, differentiation and morphogenesis processes, through the capability of the GAG chains to interact with different proteins.

Noncollagenous adhesive molecules: Compose the most heterogeneous group of macromolecules present in the ECM. Their basic functions are related to promote interactive centres between macromolecules and mediate interactions with cells. They are also characterized by being multifunctional proteins, presenting different binding sites allowing the recognition and adhesion of cells and other matrix components. A well known sequence for cell recognition present in the majority of these molecules is the RGD.

Two families' examples of this group are:

- Fibronectin; A multidomain glycoprotein with binding sites for collagen, heparins A and B, fibrin and chondroitin sulphate via surface integrins. It is synthesized by a great variety of cells and beside the mentioned functions it is also responsible for the promotion of wound healing and elimination of damaged tissue after an aggression, acting as a marker for phagocytic processes.

- Laminin; responsible for the binding of epithelial and endothelial cells to the basal lamina or basement membrane. As fibronectin, laminin has a domain that bind to type IV collagen, heparin sulphate, and cell surface integrins.

The interaction between the ECM components is responsible for the formation of the robust yet flexible, three-dimensional structure of the body [21].

The principal functions of the ECM are therefore:

- Mechanical support for cell anchorage
- Determination of cell orientation
- Control of cell growth
- Maintenance of cell differentiation
- Scaffolding for tissue renewal
- Sequestration, storage and presentation of soluble regulatory molecules.

Matrix components and the mechanical forces that cells experience determine the maintenance of cellular phenotypes and affect cell shape, polarity, and differentiated function through receptors for specific ECM molecules on cell surface.

Fibronectin and laminin are two aforementioned examples of matrix components that are responsible for mediating the adhesive interactions which support anchorage, migration, and tissue organization and are responsible for the activation of signalling pathways directing cell survival, proliferation and differentiation. ECM components also interact with growth and differentiation factors, chemotropic agents, and other soluble factors that regulate cell cycle progression and differentiation to control their availability and activity.

Like cell-cell interactions, cell-matrix interactions have a high degree of specificity, requiring initial recognition, physical adhesion, electrical and chemical communication, and/or cell migration.

It is the ability of cells to specifically recognize and attach to the individual components of the ECM through cell surface receptors that would lead us to understand the influence that the ECM has on processes of tissue regeneration.

The diversity of the characteristics possessed by the ECM has long been used as a model for tissue engineering constructs for the production of tissues such as cartilage, bone, nerve, and skin, but looking towards the production of more complex organs.

The materials used for tissue engineering were initially relied on the readily available polymeric materials, both naturally and chemically synthesized. The polymers would be chosen for specific applications according to the properties they exhibit. The potential of the materials would be the design of surfaces that stimulate highly precise reactions with proteins and cells at molecular level. The binding domains of the ECM can be mimicked by a multifunctional cell-adhesive surface created by specific proteins, peptides, and other biomolecules immobilized onto the biomaterial. Proteins can be introduced by simple coating of the polymeric scaffolds with solutions of ECM proteins based on the adsorption via non-covalent interactions. As for peptides, they can be modified and posteriorly immobilized. The following methods are some of the frequently used for the attachment and immobilization of peptides [17]:

- Reaction of thiol-terminated peptide surfaces and polymers that are functionalized with maleimide, thiol and vinyl sulfone groups;
- Reaction of amine and carboxylic side chains, as the carbodiimide-activated coupling of amines with carboxylic acids;
- Covalent coupling of the peptide into the matrix upon matrix formation;
- Enzymatic attachment;

Protein versus peptide use for medical applications is a question commonly addressed. Proteins have to be isolated from other organisms and purified. This may elicit undesirable immune responses. Thus proteins are object of proteolytic degradation. Apart of this features, only a part of the proteins offers the appropriate orientation for cell adhesion due to their stochastic orientation on the surface. In the other hand, peptides exhibit higher stability and because of their size can be packed with higher density on material surface. This would compensate for possible lower cell adhesion activity. Other advantage is that peptides are much more specific for determined binding sites, being one able to modulate the right motif for the requested application [18].

Among the most commonly used materials are natural ECM-based polymers such as collagen, fibrin glues, hyaluronic acid and alginate. Some reviews of polymeric materials for TE applications can be found in the literature [16, 22].

The use of patterned surfaces is also attractive when it comes to direct and control cell behaviour creating adhesive and non adhesive regions.

With recent engineering techniques such as photolithography, self assembly and other new technologies for micropatterning, one can create and engineer scaffolds by varying

the size and chemistry of the various regions, and therefore control in a certain range the type, architecture, directional migration and cell's function [23].

In this way, a door to design devices with surfaces that have selective cell adhesion and that can potentially orient cells to organize and form a specialized tissue is open.

#### **4. Composition and Structure of Polymeric Scaffolds- From Natural to Synthetic Biodegradable Formulations**

The incorporation of polymeric scaffolds in tissue regeneration occurred in the early 1980s, and it continues to play a crucial role in tissue engineering.

The idea of building a biodegradable scaffold is that to mimic the normal tissue either in structure and/or function.

Scaffolds may be created from different material with different origins. This section will be focused on natural and synthetic based polymers.

Natural polymers present an attractive solution for scaffold preparation as they are typically biocompatible and enzymatically biodegradable.

These polymers present bioactive molecules that play a key role in the recognition of determined sequences for cell recognition, attachment and proliferation. Also they might be helpful in the maintenance of the phenotypic profile of cells. Although they present a high degree of biocompatibility a major concern when using these types of materials arises from their enzymatic degradation. This process may not always be controlled and the material might degrade at a much faster rate than the one required for tissue regeneration leading to failure of the scaffold function.

To circumvent the limitations of materials derived from natural products, the use of synthetic materials confers several advantages when they permits the tailoring of chemical, physical and mechanical properties making them suitable specified functions. Although the degradable rate of these polymers can be controlled, often they degrade into undesirable toxic products that are harmful for the surrounding tissue, thus claiming to exhibit inferior biocompatibility [24]. Examples of both types of materials used within TE applications are summarized in the following chart;



Table 1: Common natural and synthetic based polymers used for different tissue engineering applications.

Polymeric origin	Natural based:	Synthetic based:
	Agarose	Poly(glycolic) Acid (PGA)
	Alginate	Poly(L-lactic) Acid (PLLA)
	Hyaluronic acid	Poly (D,L-lactic acid-co-glycolic acid)-copolymerized PGA and PLA
	Chitosan	Poly( $\epsilon$ -caprolactone) (PCL)
	Collagen	Polyanhydride
	Gelatin	Poly(ethylene glycol)/Poly(ethylene oxide) (PEG/PEO)
	Silk	Polyurethane
	Elastin	Polycarbonate

The conjugation of materials with synthetic and natural origin resulting in a hybrid material, would be extremely beneficial as it would combine the advantages of the nature of the different materials this is, the high level of biocompatibility with the manipulation of properties to fit a specific application.

These biodegradable polymers would resorb to accommodate cell multiplication, allowing cells to organize and differentiate in the scaffolds. Examples of these systems include poly(vinyl alcohol)/chitosan blends and chitosan/poly(acrylamide) interpenetrating networks [24]. Although cells' seeding has been shown successful, the seeding is not homogenous throughout the scaffold and it is often difficult to find a balance between the biocompatibility of the material and the mechanical properties required. Another problem is that most of the hybrid materials are hydrophobic, repelling water and diminishing the adhesiveness of cells.

A class of hybrid materials with increasing importance in the tissue engineering field is the thermo-responsive hydrogels [25].

Thermo- responsive hydrogels are materials with high affiliation to water molecules, so fully soluble in aqueous solutions, at temperatures below their lower critical solution temperature (LCST). When the temperature elevates above this value, the polymer solidifies and becomes a hydrated hydrogel.

When a polymer is dissolved in water there can be found three types of interactions: between polymer molecules, polymer-water and between water molecules. So, when the temperature is below the LCST the polymer dissolves due to the predominance of the

hydrogen bonds between the hydrophilic segments of the polymeric chains and the water molecules. As the temperature increases, the hydrophobic interactions between the hydrophilic segments became predominant and the hydrogen bonds deficient and the polymer precipitates when the temperature overcomes the critical temperature.

The LCST of a thermosensitive polymer depends directly on the balance between hydrophilic and hydrophobic components present in the macromolecules chains. Thus it can be controlled by the introduction with the adequate proportion of hydrophilic/hydrophobic components. So, in the case of a desired increase in the LCST, a copolymerization with a more hydrophilic component could be performed. This would be desirable for the controlled release of drugs within the body temperature which is one of its functional applications.

Other applications include tissue culture with human chondrocytes, three-dimensional scaffolds for neural and bone tissue engineering, cell delivery agents and cell carriers [26].

It is also very interesting to consider these materials for cell sheet engineering. In this case, the implant required is to be a thin sheet without a polymer scaffold, as in endothelium or retinal pigmented epithelium. Using materials that have their LCST around body temperature, the cells would adhere and proliferate in the material due to their hydrophobic character and could be recovered by simply lowering the temperature to below the LCST instead of using detachment methods involving enzymatic or mechanical methods that damage cells. At present, the prospective applications of this method include regeneration of periodontal, heart, corneal, liver tissues, and reconstruction of the bladder [27].

In an attempt to use the strategy of hybrid materials, the aim of this research was to enhance the properties of a derivative of a methacrylic polymer based in poly(vinyl pyrrolidone) (PVP), which properties were already studied [28], as the synthetic origin type and enhance in combination of a well know naturally occurring biopolymer, hyaluronic acid (HA).

#### 4.1. PVP based polymer

Polymers such as poly (vinyl pyrrolidone) (PVP) have been widely used in commercial applications. However, the monomer of this particular polymer presents poor reactivity in free radical polymerization reactions. Gonzalez N. *et al.*, [14, 29] described hydrophilic monomers with similar chemical structures and behaviour to those of PVP. To these monomers were added methacrylic groups that increase their reactivity, maintaining the biocompatible character and their solubility in water. The obtained products were: ethyl pyrrolidone [2-ethyl-(2-pyrrolidone)methacrylate (EPM)] and ethyl pyrrolidine [2-ethyl-(2-pyrrolidine)methacrylate (EPyM)]. Copolymerization with MMA and DMA lead to the formation of hydrogels presenting sensitivity to temperature and/or pH, both with reversible character. This feature allows characterizing them as intelligent hydrogels, presenting a critical temperature, the lower critical solution temperature (LCST), below which the polymer is soluble.

#### 4.2. Hyaluronic Acid

HA is an abundant non-sulfated glycosaminoglycan present as a major constituent of the extracellular matrix, skin and the vitreous body of the eyeball. Due to its unique viscoelastic properties it plays an important role in lubrication, as a component of the synovial fluid of joints. HA is also a regulator of cell adhesion and it directly affects tissue organization via interactions with cell-surface receptors such as CD44 [30]. Composed by repeating units of glucuronic-acid and N-acetyl-glucosamine, this macromolecule exhibits molecular weights of up to  $4 \times 10^6$  Da [31, 32].

In aqueous neutral solutions, hydrogen bonds form between water molecules and the adjacent carboxyl and N-acetyl groups of the HA responsible for a conformational stiffness to the polymer, limiting its flexibility. Due to its highly negative charge, HA attracts positive ions, leading to an osmotic imbalance in aqueous solutions. Because of the unique water-binding retention capacity of this biopolymer it has proven to be ideal for hydrogels and other ECM substitute's preparation [33].

HA presents an attractive building block for new biocompatible and biodegradable polymers that have applications in drug delivery, tissue engineering, and viscosupplementation. And although it has proven its ability to bear compressive forces in cartilaginous tissues, intervertebral disks and heart valve leaflets [34, 35], the

fabrication of new biomaterials is often precluded by the poor biomechanical properties of HA [20, 36]. The fact that HA is highly soluble at room temperature and exhibits high rates of turnover in vivo are other obstacles to structural integrity. These problems are diminished when HA polymers are modified through both the carboxyl and hydroxyl groups to resist degradation upon implantation. Methods involving crosslinking using the water soluble carbodiimide crosslinking or photocrosslinking hydrogels can be found in the literature [37, 38].

The incorporation of HA into crosslinked polymeric scaffolds increases chondrocytes attachment and the exogenous addition of HA to scaffolds impacts the material properties in a molecular weight dependent manner, although may be less stimulatory to cells growth because of limited contact with the cells and the lack of HA stabilization when compared to direct incorporation of HA into the biomaterial [35, 39].

HA chain length also plays an important role in the biological functions played by this biopolymer. Low and high molecular weight HA can induce different cellular responses. The difference of the variability between molecular weights is mainly due to the degradation of HA into smaller fragments. It was shown that HA degradation products may interact with various cells and initiate a program of gene expression leading to cell proliferation, migration, or activation. These products cause a different impact from those of the native HA. So, in a study of stimulation of vascular endothelial cells, HA degradation products have induced angiogenesis whilst native high molecular weight HA inhibited angiogenesis. It was also reported that HA fragments are similar in size to the HA molecules found in vivo in inflammatory sites [34]. Thus, the size and fragmentation of HA will compromise the integrity of tissues [40].

HA has been extensively used in the bone and cartilage tissue engineering field. It has become an important treatment in patients suffering from osteoarthritis as well as in articular cartilage lesions [41, 42].

So, it would be advantageous allying the HA properties as the high water retention character, biocompatibility and essential role in biological functions, and incorporate this natural biopolymer into sensitive polymeric systems, whose properties (swelling degree, porosity, degradation rate..) can be controlled. The developed systems have applications in both, cartilage and bone tissue engineering as well as drug delivery systems.

## 5. Bone and Cartilage Tissue Engineering

### 5.1. Bone

Bone is a dynamic, highly vascularised tissue with a unique capacity to heal and remodel without leaving a scar. These properties, together with its capacity to rapidly mobilize mineral stores on metabolic demand, make it the ultimate smart material.

Bone is composed of hydroxyapatite ( $(\text{Ca}_{10})(\text{PO}_4)_6(\text{OH})_2$ ) crystals deposited within an organic matrix (approximately 95% is type I collagen). Morphologically it is composed of trabecular or spongy bone which creates a porous environment with 50-90% porosity[43], with pore size of 1mm in diameter, surrounded by a solid structure (3-12% porosity)[11], designated cortical or compact bone. Cortical bone can be divided into different groups: long bones, short bones and flat bones.

Apart from the two architectural forms, trabecular and cortical bone, that the bone tissue can form, there are two types of bone that can be found in the adult skeleton: woven and lamellar bone. Woven bone can be characterized by a random orientation of collagen fibres, with incorporated blood vessels that will form the hematopoietic bone marrow, whilst in the lamellar bone collagen fibres have a preferred orientation alternating between layers or *lamellae*, deposited around a series of voids (Haversian canals) containing blood vessels and osteocytes [4].

The main role of bone is therefore to provide structural support for the body. Furthermore, the skeleton supports muscular contraction, protects the internal organs of the body and acts as a mineral reservoir.

### 5.2. Cell Biology

Four cell types can be found in the bone tissue: osteoblasts, osteoclasts, osteocytes and bone lining cells.

Osteoblasts are known to be involved in the synthesis and regulation of extracellular matrix elaboration. In the other hand, osteocytes derive from osteoblasts that became incorporated in the newly elaborated matrix. They interact with the different bone cell types through the establishment of gap junctions that allows them the access to oxygen and nutrients before and during matrix synthesis [44].

Bone is at a constant state of remodelling with osteoblasts producing and mineralizing new bone matrix, osteocytes maintaining the matrix and osteoclasts resorbing the matrix. As for the bone lining cells, are mainly inactive cells that are presumably the precursors for the osteoblasts [11].

### **5.3. Application of polymeric scaffolds in bone tissue regeneration**

Applications of polymers for bone tissue repair and reinforcement, for regeneration of cartilage associated with bones, for helping in partial replacement of bones by metallic parts, and as carriers of antibiotics to the infected bone tissues, have been extensively studied.

Bone implants are the most common implants in the human body. They are implanted in order to replace surgically removed parts or minimize even if possible eliminate damages or defects caused by diseases, accidents, birth defects or wars.

The natural repair of osteochondral defects can be enhanced by using biocompatible materials that can support repair process.

The class of materials based in calcium phosphate ceramics (CaP) is the most commonly used for bone applications. CaP ceramics possess a macroporous structure that facilitates cells' and growth factors penetration into an implant, making it possible for the osteogenic process to start and leading to a possible bone neoformation.

Ceramic materials have been lately combined with other biocompatible, water soluble polymers based on N-vinylpyrrolidone having promising results [45].

(HA-based biomaterials have also been extensively studied due to their biocompatibility and biodegradability profile. As stated by Jagur-Grodzinski, these materials seem to allow faster cell infiltration and thus faster bone tissue formation than synthetic polylactides and their copolymers [27].)

Combining hydrogels with CaP ceramics could lead to new scaffolds for bone TE with a synergetic combination between the properties of both materials.

## 5.4. Cartilage

Cartilage is a highly specialised, avascular and aneural connective tissue that may be found in several forms at different sites throughout the human body. These have been broadly classified as hyaline, elastic and fibro-cartilage. Each type has a distinct composition and organisation, related in turn to the specific properties that underpin the function of the tissue.

Auricular cartilage is non-load bearing and elastic tissue found primarily in the ear and epiglottis, whose primary role is to maintain shape and structure.

Articular cartilage is a supporting connective tissue that functions as a weight bearing, shock absorbance, and reduction of surface friction being for that the major responsible for the correct functioning of the articulating skeleton [46]. What allows this feature is its constitution of chondrocytes surrounded by an extracellular matrix (ECM), composed primarily of interstitial fluid, proteoglycans, namely glycosaminoglycans, several forms of collagens and noncollagenous proteins [47].

Interstitial fluid is an essential part of the hyaline cartilage, constituting around 80% of cartilage's wet weight. The remaining weight is mainly composed by collagen fibres of type II associated to highly hydrated proteoglycans and adhesive glycoproteins. By its structure, collagen type II has a higher interaction with water when compared to the other collagen types, present in the interstitial fluid. It is also the most abundant form and therefore a good indicative of cell's proliferation.

Proteoglycans form a special class of glycoproteins with attached long unbranched and highly charged glycosaminoglycans chains. Until 200 units of these proteoglycans can establish covalent bonds with a single molecule of hyaluronic acid, to form an aggrecan molecule. This molecule is extremely important in the maintenance of the rigidity of the extracellular matrix, interacting with the collagen fibres that are responsible for the tensile properties, gives compression resistance to the tissue.

As aforementioned, articular cartilage main functions are to transmit compressive and shear forces and facilitate joint mobility. Once damaged, cartilage has only a limited capacity of self repair. This poor spontaneous repair strongly depends on the depth of the articular lesion. If the lesion only affects the superficial cartilage, it will not heal spontaneously, as if besides the cartilage the lesion also affects the subchondral bone, then a fibrocartilage will be formed.

A major problem in the formation of this type of cartilage is that it doesn't present the same mechanical properties as in the native articular cartilage [48]. Therefore the use of a scaffold with cells that can maintain their phenotype and resemble the native articular cartilage is mandatory for approaches in cartilage tissue repair.

## **5.5. Cell Biology**

As important as knowing the characteristics of the tissues to be repaired, is the nature and provenience of the cells to be used.

Chondrocytes are the only cell type found in mature articular cartilage, and account for approximately 2% - 10% of the total cartilage volume [4]. They present a rounded morphology and have a defined pericellular matrix containing collagen II fibrils and abundant collagen type VI and proteoglycans [47]. Together, the cell and pericellular matrix form an anatomical structure known as a 'chondron'.

Chondrocytes are responsible for the maintenance (both synthesis and degradation) of ECM components, and although the constituent cells of cartilage are synthetically active, they are also relatively non-proliferative when in their final differentiated state. Due to the relatively low cell to matrix volume ratio, cartilage has a low metabolic activity. This factor may also contribute to the tissue's poor capacity for self-repair.

Chondrocytes can be isolated from a variety of sources, and it has been proven that chondrocytes behaviour in a determined engineered material is dependent on where they were isolated from [49]. Various authors have studied the effect on survival and proliferation of auricular and articular chondrocytes, showing differences in the construct size, gene expression, biochemical content and mechanical properties [50-52]. So, data on the source-dependent differential responses of chondrocytes is important at the time of election of isolating a specific cell source for a determined application. Apart from the cell source, one should not neglect how the variables in the scaffold design will dictate the cellular behaviour.



## 5.6. Application of polymeric scaffolds in cartilaginous tissue regeneration

A wide range of materials have been investigated for use in cartilage tissue engineering applications, and these have been comprehensively reviewed [53, 54].

The following table compiles some of the materials more commonly used and both their advantages and limitations.

Table 2: Commonly used scaffolds in cartilage tissue engineering.

Material origin	Benefits	Limitations
<b>Natural</b>		
Collagen	Can be processed in a wide variety of forms. Stimulates cell binding and deposition of ECM components	Derived from xenogeneic sources; variation from batch-to-batch
Fibrin	Currently in use in clinic as fibrin glue. Supports the formation of cartilage constructs.	Poor mechanical properties. Usually of bovine origin.
Alginate	Cross-link in the presence of $\text{Ca}^{2+}$ or divalent cations to form hydrogels. Used for encapsulation of chondrocytes and growth factors delivery.	Concerns over immunogenicity due to incomplete degradation. Batch-to batch variation.
Agarose	Injectable. Induction of chondrogenesis.	Limited <i>in vivo</i> due to foreign body giant cell reaction. Poor degradation rate.
Hyaluronic Acid	ECM component, encourages cell binding and stimulates ECM deposition	Usually obtained from animal sources. Batch-to-batch variation.
Chitosan	Analogue of cartilage specific GAGs. Antimicrobial properties.	Batch-to-batch variation.
<b>Synthetic</b>		
PGA	Degradable and processable into a number of forms. No batch-to-batch variation. FDA approved.	Uncontrolled degradation and acidic degradation products when total degradation doesn't occur.
PLA/PLLA	Degradable and processable. No batch-to-batch variation. FDA approved	Acidic degradation products. Poor mechanical stability. Some evidence of inflammatory reactions.
PLGA	Variable degradation rates, faster than PLA or PGA.	Acidic degradation products, poor mechanical stability.
PCL	Used as a biodegradable suture material in clinic. Can be co-polymerised with PLA to vary degradation times. Long term drug delivery	Acidic degradation products. Poor mechanical properties. Slow degradation (>24 months).
PEO	Injectable material into irregular shaped defect sites. Normally needs to be photopolymerized <i>in situ</i> . Good biocompatibility.	Depth of injection site that permits sufficient light for photopolymerization reactions. Inadequate cartilage formation
PVA	Easily sterilised and moulded into desired shapes. Good biocompatibility.	Non-degradable material, wear particles may cause inflammatory reaction. Inadequate mechanical stability.
PEG	Good biocompatibility. Non-immunogenic. Drug delivery devices.	Unmodified PEG is non biodegradable.

Since no material used to date for cartilage tissue engineering has proved to be ideal, there is scope for the investigation of new biomaterials for these applications. Polymeric gels forming semi-interpenetrated networks, providing porous structures, have proved to be successful scaffold forms, and natural materials have provided good environments for the *in vitro* culture of chondrocytes and development of a hyaline-like cartilage. In fact, hydrogels have proven to provide successful three-dimensional scaffold forms for culture of cells due to their biomimetic nature. In the same way natural materials have provided good environments for the *in vitro* culture of chondrocytes and development of a hyaline-like cartilage. So a natural based hydrogel, cartilage and bone tissues alike would contain high amount of physiological fluids hold by a macromolecular matrix.

In addition, scaffolds with good mechanical properties have been suggested, to provide support and stability to the developing cartilage. Thermo-responsive materials have also proven their importance for cell sheet engineering, establishing a new basis for regenerative medicine [55]. For these reasons, the combination of synthetic and natural origin polymers into a hybrid material has been proposed as a suitable scaffold material for tissue engineering applications.

## **6. General Objectives**

The main goal of this work is the development of new sensitive hydrogels, based in the combination of a synthetic origin polymer PEPM and a natural origin one, HA, the study of their properties and the development of biomedical applications.

For better comprehension, this memorandum has been divided in five chapters and an appendix.

The first chapters (I and II) concern the study and characterization of the hydrogels and their properties in aqueous environments, when submitted to different stimulus, namely variations in the temperature and/or pH.

Chapter III and IV are directed towards the study of biological activity within this materials and future application in cartilage and bone tissue engineering.

Chapter V is a revising chapter about photopolymerization and the preliminary study of this technique to produce PEPMHA hydrogels in a faster and controllable manner, focusing on future cell encapsulation.

The Appendix contains complementary information on the mechanical properties of the materials and methodology from Chapter V.

## 7. Bibliography

1. M.S. Chapekar, Tissue engineering: challenges and opportunities. *J Biomed Mater Res*, 2000. 53(6): p. 617-20.
2. V. Langer R., J.P., Tissue Engineering. *Science*, 1993. 260(5110): p. 920-926.
3. C.H. Quek, J. Li and T. Sun, Photo-crosslinkable microcapsules formed by polyelectrolyte copolymer and modified collagen for rat hepatocyte. *Biomaterials*, 2004. 25: p. 3531-3540.
4. S.R.J. Reis R.L., Biodegradable Systems in Tissue Engineering and Regenerative Medicine. 2004.
5. B.J.D. Park J.B., Biomaterials: principles and applications. 2003.
6. A.G. Mikos, Temenoff, J.S., Formation of highly porous biodegradable scaffolds for tissue engineering. *Journal of Biotechnology*, 2000. 3(2): p. 1-6.
7. R. Landers, U. Hubner, R. Schmelzeisen and R. Mulhaupt, Rapid prototyping of scaffolds derived from thermoreversible hydrogels and tailored for applications in tissue engineering. *Biomaterials*, 2002. 23(23): p. 4437-47.
8. Q. Li, J. Wang, S. Shahani, D.D. Sun, B. Sharma, J.H. Elisseeff and K.W. Leong, Biodegradable and photocrosslinkable polyphosphoester hydrogel. *Biomaterials*, 2006. 27(7): p. 1027-34.
9. C.W. Patrick Jr., Mikos, A.G., McIntire, L.V., *Frontiers in Tissue Engineering*. 1st ed. 1998: Elsevier Science Inc.
10. S.J. Bryant, J.L. Cuy, K.D. Hauch and B.D. Ratner, Photo-patterning of porous hydrogels for tissue engineering. *Biomaterials*, 2007. 28(19): p. 2978-86.
11. V. Karageorgiou and D. Kaplan, Porosity of 3D biomaterial scaffolds and osteogenesis. *Biomaterials*, 2005. 26(27): p. 5474-91.
12. R.P. Lanza, Vacanti, J.P., Langer R., *Principles of Tissue Engineering*. 2nd ed. 2000: Academic Press.
13. M. Pei, L.A. Solchaga, J. Seidel, L. Zeng, G. Vunjak-Novakovic, A.I. Caplan and L.E. Freed, Bioreactors mediate the effectiveness of tissue engineering scaffolds. *Faseb J*, 2002. 16(12): p. 1691-4.
14. N. González, C. Elvira and J. San Román, Hydrophilic and hydrophobic copolymer systems based on acrylic derivatives of pyrrolidone and pyrrolidine. *Journal of Polymer Science, Part A: Polymer Chemistry*, 2003. 41(3): p. 395-407.

15. L. R, Biomaterials and Biomedical Engineering. Chemical Engineering Science, 1995. 50(24): p. 4109-4121.
16. P.N.A. Langer R., Advances in Biomaterials, Drug Delivery, and Bionanotechnology. AIChE Journal, 2003. 49(12): p. 2990-3006.
17. M.A.G. Fisher J.P., Bronzino J.D., Tissue Engineering. 2007: CRC Press.
18. U. Hersel, C. Dahmen and H. Kessler, RGD modified polymers: biomaterials for stimulated cell adhesion and beyond. Biomaterials, 2003. 24(24): p. 4385-415.
19. M.D. Pierschbacher, J.W. Polarek, W.S. Craig, J.F. Tschopp, N.J. Sipes and J.R. Harper, Manipulation of cellular interactions with biomaterials toward a therapeutic outcome: a perspective. J Cell Biochem, 1994. 56(2): p. 150-4.
20. M.A. Lizarbe, La célula en su entorno: Organización estructural de la matriz extracelular e interacciones célula-matriz. Rev.R.Acad.Cienc.Exact.Fis.Nat., 1998. 92(2-3): p. 139-184.
21. H.A.S. Ratner B.D., Schoen F.J., Lemons J.E., Biomaterials Science: An Introduction to Materials in Medicine. 2nd ed. 2004: Elsevier Academic Press.
22. P. Malafaya, Silva, G.A., Reis, R.L., Natural-origin polymers as carriers and scaffolds for biomolecules and cell delivery in tissue engineering applications. Adv Drug Deliv Rev, 2007. 59(4-5): p. 207-33.
23. T. Boland, Tao, X., Damon, B.J., et al, Drop-on-demand printing of cells and materials for designer tissue constructs. Materials Science and Engineering: C, 2007. 27(3): p. 372-376.
24. A. Au, J. Ha, A. Polotsky, K. Krzyminski, A. Gutowska, D.S. Hungerford and C.G. Frondoza, Thermally reversible polymer gel for chondrocyte culture. J Biomed Mater Res A, 2003. 67(4): p. 1310-9.
25. E. Ruel-Gariépy and J.-C. Leroux, In situ-forming hydrogels-Review of temperature-sensitive systems. European Journal of Pharmaceutics and Biopharmaceutics, 2004. 58(2): p. 409.
26. L. Klouda and A.G. Mikos, Thermoresponsive hydrogels in biomedical applications. Eur J Pharm Biopharm, 2008. 68(1): p. 34-45.
27. J. Jagur-Grodzinski, Polymers for tissue engineering, medical devices, and regenerative medicine. Concise general review of recent studies. Polymers for Advanced Technologies, 2006. 17(6): p. 395-418.

28. G. N., Nuevos Sistemas Poliméricos Sensibles al pH y Temperatura. Aplicaciones Biomédicas, in Department of Macromolecular Chemistry. 2006, Universidad Complutense: Madrid, Spain.
29. L.A. Solchaga, J.E. Dennis, V.M. Goldberg and A.I. Caplan, Hyaluronic Acid-Based Polymers as Cell Carriers for Tissue-Engineering Repair of Bone and Cartilage. *Journal of Orthopaedic Research*, 1999. 17(2): p. 205-213.
30. R. Barbucci, P. Torricelli, M. Fini, D. Pasqui, P. Favia, E. Sardella, R. d'Agostino and R. Giardino, Proliferative and re-differentiative effects of photo-immobilized micro-patterned hyaluronan surfaces on chondrocyte cells. *Biomaterials*, 2005. 26(36): p. 7596-605.
31. H.M. Kim, F. Miyaji and T. Kokubo, Bioactivity of Na<sub>2</sub>O-CaO-SiO<sub>2</sub> glasses. *J Am Ceram Soc*, 1995. 78(9): p. 2405-2411.
32. G. Ladam, Micromechanics of Surface-Grafted Hyaluronic Acid Gels. *Journal of Physical Chemistry B*, 2003. 107(34): p. 8965-8971.
33. D.D. Allison and K.J. Grande-Allen, Review. Hyaluronan: a powerful tissue engineering tool. *Tissue Eng*, 2006. 12(8): p. 2131-40.
34. V.B. Lokeshwar and M.G. Selzer, Differences in hyaluronic acid-mediated functions and signaling in arterial, microvessel, and vein-derived human endothelial cells. *J Biol Chem*, 2000. 275(36): p. 27641-9.
35. D.D. Allison, N. Vasco, K.R. Braun, T.N. Wight and K.J. Grande-Allen, The effect of endogenous over-expression of hyaluronan synthases on material, morphological, and biochemical properties of uncrosslinked collagen biomaterials. *Biomaterials*, 2007. 28(36): p. 5509-17.
36. M.R. Kim and T.G. Park, Temperature-responsive and degradable hyaluronic acid/Pluronic composite hydrogels for controlled release of human growth hormone. *J Control Release*, 2002. 80(1-3): p. 69-77.
37. Y. Liu, Shu, X.Z., Prestwich, G.D., Biocompatibility and stability of disulfide-crosslinked hyaluronan films. *Biomaterials*, 2005. 26(23): p. 4737-4746.
38. C. Chung, J. Mesa, M.A. Randolph, M. Yaremchuk and J.A. Burdick, Influence of gel properties on neocartilage formation by auricular chondrocytes photoencapsulated in hyaluronic acid networks. *J Biomed Mater Res A*, 2006. 77(3): p. 518-25.
39. M. Abe, Takahashi, M., Nagano, A., The effect of hyaluronic acid with different molecular weights on collagen crosslink synthesis in cultured chondrocytes

- embedded in collagen gels. *Journal of Biomedical Materials Research- Part A*, 2005. 75(2): p. 494-499.
40. H. El Hajjaji, Cole, A.A., Manicourt, D.H., Chondrocytes, synoviocytes and dermal fibroblasts all express PH-20, a hyaluronidase active at neutral pH. *Arthritis research & therapy*, 2005. 7(4): p. R756-768.
  41. A.M. Patti, A. Gabriele, A. Vulcano, M.T. Ramieri and C. Della Rocca, Effect of hyaluronic acid on human chondrocyte cell lines from articular cartilage. *Tissue Cell*, 2001. 33(3): p. 294-300.
  42. M. Marcacci, Kon, E., Zaffagnini, S. et al, Autologous chondrocytes in a hyaluronic acid scaffold. *Operative Techniques in Orthopaedics*, 2006. 16(4): p. 266-270.
  43. F.S. Kaplan, Hayes W.C., Keaveny T.M., Boskey A., Einborn T.A., Iannotti J.P., Form and function of bone, in *Orthopaedic basic science*, S. S.R., Editor. 1994, American Academy of Orthopaedic Surgeons: Rosemont. p. 128-84.
  44. R.C.T. Sommerfeldt D.W., Biology of bone and how it orchestrates the form and function of the skeleton. *Eur Spine J*, 2001. 10 (S86).
  45. E.G. Vlach, E.F. Panarin, T.B. Tennikova, K. Suck and C. Kasper, Development of multifunctional polymer-mineral composite materials for bone tissue engineering. *J Biomed Mater Res A*, 2005. 75(2): p. 333-41.
  46. C.A. Oliveira J.T., et al., A cartilage tissue engineering approach combining starch-polycaprolactone fibre mesh scaffolds with bovine articular chondrocytes. *Journal of Materials Science: Materials in Medicine*, 2007. 18(2): p. 295-302(8).
  47. M. A.C., The Evaluation of Spider Silk as a Scaffold for Cartilage Tissue Engineering, in *School of Clinical Dentistry, Faculty of Medicine*. 2006, University of Sheffield: Sheffield.
  48. G.J. Vinatier C., Daculsi G., Layrolle P., Weiss P., Cartilage and bone tissue engineering using hydrogels. *Biomed Mater Eng*, 2006. 16(4 Suppl): p. S107-13.
  49. C. Chung, I.E. Erickson, R.L. Mauck and J.A. Burdick, Differential Behavior of Auricular and Articular Chondrocytes in Hyaluronic Acid Hydrogels. *Tissue Eng Part A*, 2008.
  50. A. Panossian, S. Ashiku, C.H. Kirchhoff, M.A. Randolph and M.J. Yaremchuk, Effects of cell concentration and growth period on articular and ear chondrocyte transplants for tissue engineering. *Plast Reconstr Surg*, 2001. 108(2): p. 392-402.

51. J.W. Xu, Zaporozhan, V., Yaremchuk, M.J., et al, Injectable tissue-engineered cartilage with different chondrocyte sources. *Plast Reconstr Surg*, 2004. 15(113(5)): p. 1361-71.
52. N. Isogai, Kusuhara, H., Landis, W.J., et al, Comparison of different chondrocytes for use in tissue engineering of cartilage model structures. *Tissue Eng*, 2006. 12(4): p. 691-703.
53. W.-J. Li, Tuan, R.S., *Polymeric Scaffolds for Cartilage Tissue Engineering. Macromolecular Symposia*, 2005: p. 65-75.
54. K.-U. Lewandrowski, Wise, D.L., Trantolo, D.J., et al, *Tissue Engineering and Biodegradable Equivalents- Scientific and Clinical Applications*. 2002: Marcel Dekker, Inc.
55. S. Masuda, Shimizu, T., Okano, T., Kurosawa, H., Cell sheet engineering for heart tissue repair. *Adv Drug Deliv Rev*, 2008. 60(2): p. 277-285.

## **Chapter I- Polymeric Smart Systems- synthesis and characterization**

### **1. Introduction**

#### **1.1. Radical Polymerization Reactions**

Radical polymerization is a chain reaction that involves reactive and unstable species that normally contain an unpaired electron, designated radicals. The most important representative family of this kind of reaction is the family of the alkenes ( $>C=C<$ ).

The polymerization process can be divided in three steps: initiation, propagation and chain termination, with the possibility of occurrence of side reactions named chain transfer reactions (figure 1).

Initially, an initiator molecule originates primary free radicals using thermal, photochemical or redox energy, then the radical starts to bond to monomer molecules, forming chains. If a chain transfer reaction doesn't occur, the propagation of the chains will happen until two radicals species react with each other and terminate the chain reaction, originating a polymer.

The chain transfer reactions are also responsible for the suspension of the chain reaction, originating inert polymer chains. In this case, the polymer suffers from a premature deactivation through a process of atomic transfer, normally from a molecule present in the reaction. This molecule is designated of chain transfer agent and can be the monomer itself, the initiator, the polymer or the dissolvent [1].



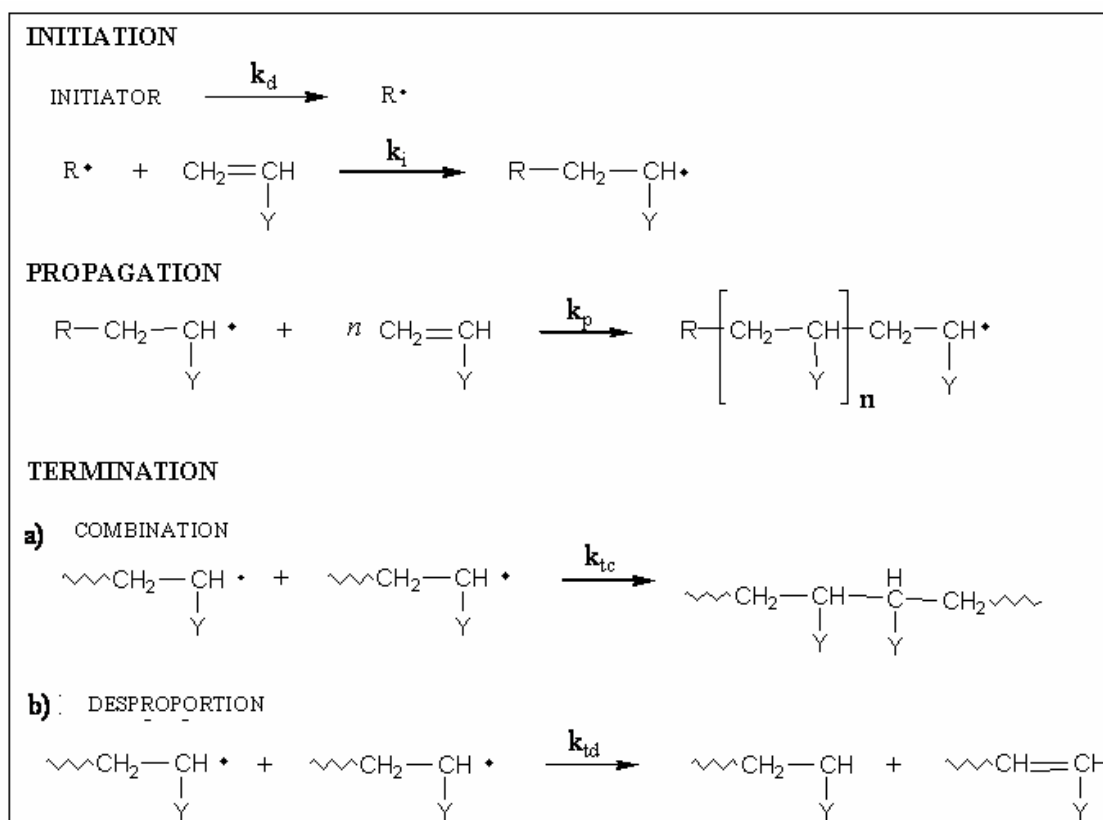


Figure 1. Schematic representation of the radical polymerization process: initiation, propagation and termination - a) combination or coupling and b) desproportion.

## 1.2. Preparation of Smart Polymeric Systems

Since the development of materials based on poly (2-hydroxyethyl methacrylate) in the 60s and due to their high content in water, soft consistency and low superficial tension that these systems have been considered in numerous biomedical applications [2].

As early mentioned, the reactivity of systems based on PVP can be enhanced by introducing a methacrylate group, leading to materials with similar properties to poly (2-hydroxyethyl methacrylate), thus maintaining their biocompatibility and solubility in water.

We aimed to use the methacrylic monomer derived from 2-Ethyl (2-pyrrolidone) methacrylate (EPM) (Figure 2) to form Semi-IPN with HA (Figure 3), in order to combine the temperature sensitivity (presents lower critical solution temperature-LCST) of the EPM with the high water retention character of the HA.

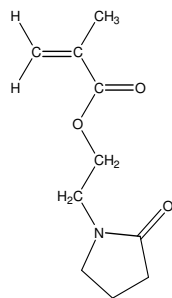


Figure 2. 2-Ethyl (2-pyrrolidone) methacrylate (EPM)

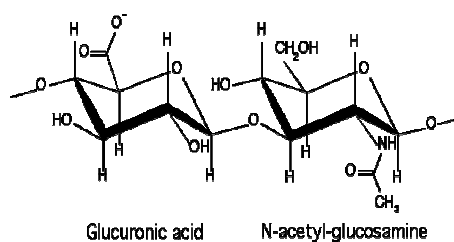


Figure 3. Hyaluronic Acid (HA).

Depending on their method of preparation, ionic charge, or physical structure features, hydrogels may be classified in several categories. Homopolymer hydrogels are crosslinked networks of one type of hydrophilic monomer unit, whereas copolymer hydrogels are produced by crosslinking of two comonomer units, at least one of which must be hydrophilic to render them swellable. Interpenetrating polymeric (IPN) hydrogels are produced by preparing a first network that is then swollen in a monomer. The latter reacts to form a second intermeshing network structure within the first [3].

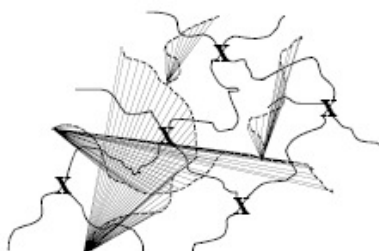


Figure 4. Semi-Interpenetrating Networks (semi-IPN), with PEPM crosslinked (X- crosslinker) in the presence of HA.

The concept of the IPN is the production of hydrogels with defined properties between two different materials, e.g., when a swelling polymer is mixed with a sensitive-responsive polymer, to obtain networks that have a defined profile of swelling, in response to environmental changes.

In the case of semi-IPN, the second component is entangled within the first network but not crosslinked. In the case of this study, EPM was crosslinked in the presence of the HA, resulting in porous structures (figure 4).

Porosity can occur only at the substrate surface or can completely penetrate throughout a bulk material. It consists of individual openings and spacings or interconnecting pores. Porosity can be created intentionally by a specific production process.

For many biomedical applications, there is a need for porous implant materials that have to fulfil determined requirements. These implants can be used for artificial skin, bone and cartilage reconstruction as well as tissue engineering [3].

### **1.3. Techniques for the characterization of the polymeric systems**

#### **1.3.1. Spectroscopic Techniques**

The materials were characterized using proton ( $^1\text{H}$ ) Nuclear Magnetic Resonance (NMR) and Fourier Transform Infra-Red (FTIR) techniques. These techniques allow both the identification of the synthesized monomers and polymers and to determine their purity.

NMR is one of the most effective analytical techniques that allow the detection of the chemical structure of molecules. It measures the absorption of radiofrequency radiation by a nucleus in a strong magnetic field. It considers how the system that has been oriented by the magnetic field responds to transitions of radiofrequency. Absorption of the radiation causes the nuclear spin to realign or switch to a higher energy direction. After absorbing energy, the nucleus will re-emit radiofrequency radiation and return to a lower energy state. The NMR spectrum allows the identification of atoms in a molecule and to study the interatomic distances and torsion angles between them.

FTIR spectroscopic technique is a very practical tool in a rapid qualitative analysis of the polymeric systems. It is used to measure the vibrational excitation of atoms around the bonds which connect them. The position of absorption signals depends of the type of functional groups present and the spectrum gives a unique identification of the molecule. The Infra-Red spectrum is interpreted by the use of known group frequencies, according to bibliography or theoretical assignation tables, being possible to characterize a substance as one containing a given type of group or groups.

### 1.3.2. Chromatographic Techniques

Many of the properties of the polymers are influenced by their molecular weight, constituting this, a fundamental parameter for its characterization.

Size Exclusion Chromatography (SEC) or Gel Permeation Chromatography (GPC) allows the determination of the distribution and the molecular weight of polymers. In this technique a diluted solution of the polymer is eluted into a chromatographic column composed of a porous gel. When the polymer solution flows, the bigger particles penetrate through the pores and the small particles are retained in the gel and for that take longer to go through the column. This way one can relate the elution time with the molecular weight. The resulting chromatogram in an SEC experiment thus represents a molecular size distribution. This technique doesn't allow the absolute determination of the molecular weight, for what is needed the comparison with commercial polymers with known molecular weight as the standard of calibration.

### 1.3.3. Thermal Analysis Techniques

Allowing the characterization of a material, this technique, through the weight variation of a sample whilst submitted to a temperature program, enables thermo-gravimetric curves for the analysis of the material's composition as it indicates the thermal stability of a polymer.

The sample can either be exposed to a linear increase of temperature or to an isothermal program where the weight variation is evaluated in function of time. An initial increase of temperature leads first to a loss of volatile products such as solvents with low boiling point, adsorbed water or gases within the sample. At higher temperatures, there is a weight loss of products like additives and/or plasticizers, water present in the interior of the polymer and products decomposed at lower temperatures; finally at even higher temperatures, normally above the 200°C, the thermal degradation of the polymer occurs. When the temperature is high enough the polymer is carbonized.

The process of thermal degradation can be characterized through the breakage of bonds in 2 processes: depolymerization and random decomposition. The first mechanism is typically observed in vinyl polymers due to a reversible mechanism of polymerization as for the second in condensation polymers [1].

#### 1.3.4. Microscopic Techniques

The scanning electron microscope (SEM) is a type of electron microscope capable of producing high-resolution images of a sample surface. The SEM images have a characteristic three-dimensional appearance and enable the study of the surface structure of a sample. Hereby we use this technique in order to speculate the porosity of the samples hence most constructs will require a high degree of porosity to enable mass transfer and tissue development, in conformance with the volume fraction of the scaffold that should be necessarily low [4].

#### 1.3.5. Dynamic Mechanical Analysis

Dynamic mechanical analysis (DMA) is a sensitive tool for characterizing polymers providing information about the small deformation behaviour of the materials. Materials are subjected to a cyclic deformation at a fixed frequency in the range of 1- 1000 Hz. The stress response is measured while the cyclic strain is applied and the temperature is slowly increased (typically at 2/3 degrees per min).

### 1.4. Objective

The goal of this first chapter is the development and characterization of the polymeric systems optimized through different combinations of the reaction components. All the mentioned techniques will be used.

## 2. Material and Methods

### 2.1. Material Synthesis

In the following table it is detailed the main materials used, commercial supplier and the purification process required before their use in chemical reactions (Table 3).

Table 3: Resumé of the main reagents and their process of purification.

<i>Reagent</i>	<i>Formula</i>	<i>Company</i>	<i>Purification</i>
EP, (N-2-hydroxyethyl) 2- pyrrolidone	$C_6H_{11}NO_2$	Fluka	
HA, Hyaluronic Acid	$[C_{14}H_20NNaO_{11}]_n$	Bioiberica	
Methacryloyl chloride	$C_4H_5ClO$	Fluka	Distillation
Et <sub>3</sub> N, triethylamine	$C_6H_{10}N$	Scharlau	Reflux with KOH, distillation
Chloroform	$CHCl_3$	SDS	
Potassium peroxodisulfate	$K_2S_2O_8$	Fluka	
BIS, N,N'-methylene- bisacrylamide	$(CH_2:CHCONH)_2CH_2$	Fluka AG	
TriEGDMA, Triethylene glycol dimethacrylate	$CH_2=C(CH_3)COC(CH_2CH_2O)_3COC(CH_3)=CH_2$		

#### 2.1.1. Monomer Synthesis Process

2-ethyl-2-pyrrolidone-methacrylate (EPM) was synthesized using the following procedure:

To a solution of 10g of 2-hydroxyethyl-pyrrolidone (0.087 mol) in chloroform (75 ml) with 12.1 ml (0.087 mol) of triethylamine, was added dropwise a solution of 8.3g (0.13 mol) of methacryloyl chloride (MeCl) in chloroform (25 ml), at 0°C under a N<sub>2</sub> atmosphere with magnetic stirring (Figure 5).

The solution was left overnight under magnetic stirring.

The obtained solution was washed several times with an aqueous solution of NaOH (5% wt) and dried over anhydrous Na<sub>2</sub>SO<sub>4</sub>. The solvent was removed at reduced pressure.

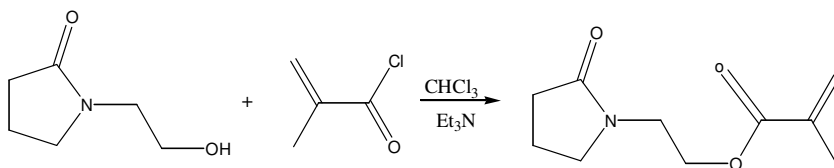


Figure 5. EPM Synthesis reaction.

### 2.1.2. Polymer Synthesis Process

PEPM was synthesized in a 2 step process:

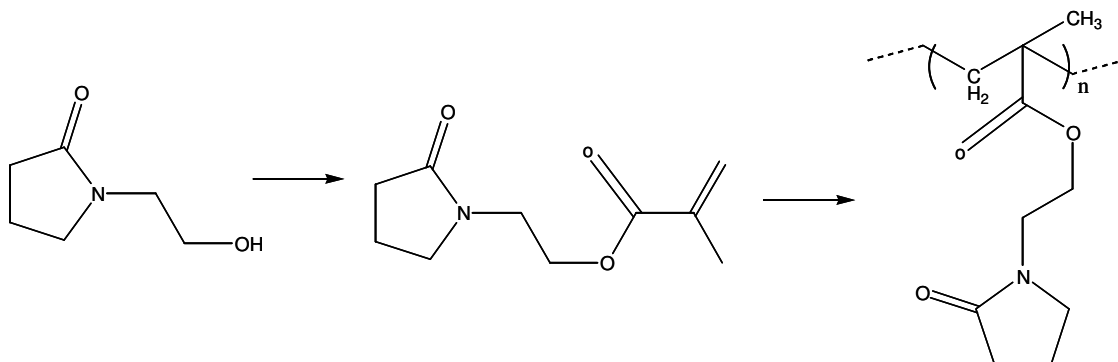


Figure 6. Schematic representation of PEPM synthesis.

Radical polymerization is the result of successive addition of monomer molecules with a double methacrylic bond to a growing polymeric chain with a radical active center.

#### 2.1.2.1. Semi IPN systems preparation (Free Radical Polymerization)

PEPM hydrogels crosslinked with *N,N'*-methylene-bisacrylamide or triethylene glycol dimethacrylate (2 and 1.7% molar fraction, Fluka) were prepared at 50°C by free radical polymerization in aqueous solutions with different concentrations of HA (1, 2.5 and 5%, Bioiberica) using  $2 \times 10^{-2}$  M  $K_2S_2O_8$  as radical initiator, forming Semi-IPN. After 4 hours of reaction the hydrogels were demoulded and consecutively washed against distilled water and finally freeze-dried (Figure 7).

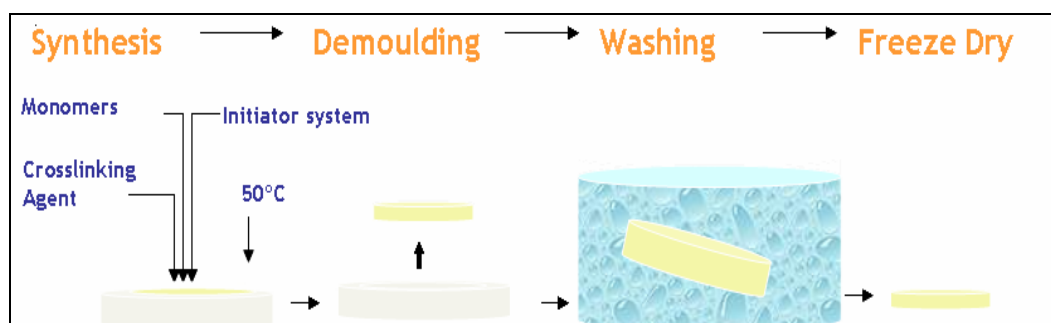


Figure 7. Synthesis of the polymeric systems using EPM as monomer,  $K_2S_2O_8$  as radical initiator, *N,N'*-methylene-bisacrylamide or triethylene glycol dimethacrylate as crosslinkers, in the presence of an aqueous solution of HA.

## 2.2. Characterization of the materials:

### 2.2.1. Spectroscopic Techniques

#### Nuclear Magnetic Resonance (NMR)

NMR spectra of EP, EPM and PEPM were obtained in deuterated chloroform ( $\text{CDCl}_3$ ).

NMR spectra of the samples containing HA were obtained in deuterated water ( $\text{D}_2\text{O}$ ).

The samples were characterized by the spectroscopic technique  $^1\text{H}$  NMR using a Bruker 500, operating at 500 MHz for proton, at room temperature.

#### Attenuated Total Reflectance Fourier Transform Infrared (ATR-FTIR)

FTIR spectra of the samples in dry form were recorded on a PerkinElmer Spectrum One (ATR- Diamond Se-Zn) spectrometer at room temperature. For ATR, the sample is placed in contact with a prism made of a material of high refractive index. As the IR beam passes through the prism, total internal reflection (TIR) occurs at each reflection from the sides. However, there is sufficient penetration into the sample, assuming good physical contact, at each reflection for structural information to be acquired.

### 2.2.2. Chromatographic Techniques

The chromatographs were registered by a GPC Waters 1515 Isocratic HPCL Pump, equipped with a pre-column, 2 columns connected in series (Waters Ultrahydrogel<sup>TM</sup> 500 y 250) thermostabilized at 30 °C, and a refractive index detector (Waters 2414).

For the calibration, monodisperse poly(ethylene-oxide) (POE) standards (Waters) were used, with a range of molecular weights of  $2.2 \times 10^4$  to  $8.4 \times 10^5$  g/mol. The eluent phase was acetonitrile/standard dissolution of  $\text{KNO}_3$  (0.1 M) (15:85 v/v), with a velocity of 0.5 mL/min.

The molecular weight distribution curves were obtained through polymer dissolutions previously microfiltered (filter Whatman, pore size 0.45  $\mu\text{m}$ ).

The analysis of the chromatographs was accessed by BREEZE software from Waters, without any excluded volume correction.



### 2.2.3. Thermal Analysis Techniques

The thermogravimetric analysis of the prepared polymers was obtained with a Perkin-Elmer TGA7 thermobalance. The experiments were performed under a helium flux of 90 mL/min, at a velocity of 10°C/min, from 0 to 500°C, using samples with approximately 10 mg (dry weight).

### 2.2.4. Microscopic Techniques

The pore size was estimated using Scanning Electron Microscopy images (Philips XL30-ESEM) at 15 kv.

Freeze-dried specimens of prepared PEPMHA hydrogels obtained by free radical polymerization were thinly metal-coated (Au:Pd/80:20) and observed with SEM.

The SEM photographs were taken at high (4.000x) and low magnifications (500x).

### 2.2.5. Picnometric techniques

Porosity was estimated by measuring the apparent density,  $\rho_{ap}$ , of the samples.

The apparent density of the porous structures was simply calculated by determining the ratio between the sample weight, when the material was immersed in ethanol, and its geometrical volume. As the real density,  $\rho_r$ , of the materials could be determined with a helium picnometer (AccuPyc 1330-gas picnometer). The porosity can be simply obtained, as an approximate estimation, from this expression:

$$\text{Porosity} = 1 - \rho_{ap} / \rho_r.$$

Experiments were made in triplicate.

### 2.2.6. Dynamic Mechanical Analysis

Tensile tests were performed using a TRITEC2000B DMA from Triton Technology (UK), equipped with a compression mode, with a displacement of 50 $\mu$ m, in a controlled environment at 37°C. PEPMHA hydrogels were previously immersed in distilled water, at 37°C, for 48h. The hydrogels were cut into a cylindrical shape (approx. 2mm) and

immersed in a liquid bath with distilled water, placed in a Teflon® reservoir. After equilibration at 37°C, the DMA spectra were obtained during a frequency scan between 0.1 and 10 Hz.

### 3. Results and Discussion

#### 3.1. Preparation of the semi-IPN

The methacrylic monomer EPM was synthesized with high yields (70-90%), by reaction of the hydroxyl group of the EP with the methacryloyl chloride, resulting in a methacrylic ester. This monomer was obtained as a viscous liquid of slight yellow color. For the radical polymerization of the EPM in the presence of HA, *N,N'*-methylene-bisacrylamide or triethylene glycol dimethacrylate were chosen as crosslinkers. *N,N'*-methylene-bisacrylamide (BIS) presents functional groups in common with the monomer and in that way it doesn't significantly alters the chemical structure of the ending hydrogels. Besides the similarity with the monomer, this free radical crosslinker is very hydrophilic and its flexibility provides highly water swellable hydrogels. It is non-biodegradable [5]. In the other hand, triethylene glycol dimethacrylate (TriEGDMA) is known to be a biodegradable and biocompatible difunctional crosslinker, non toxic but also known for its hydrophilic character, conferring flexibility around C–O–C bonds in the resultant polymers [6].

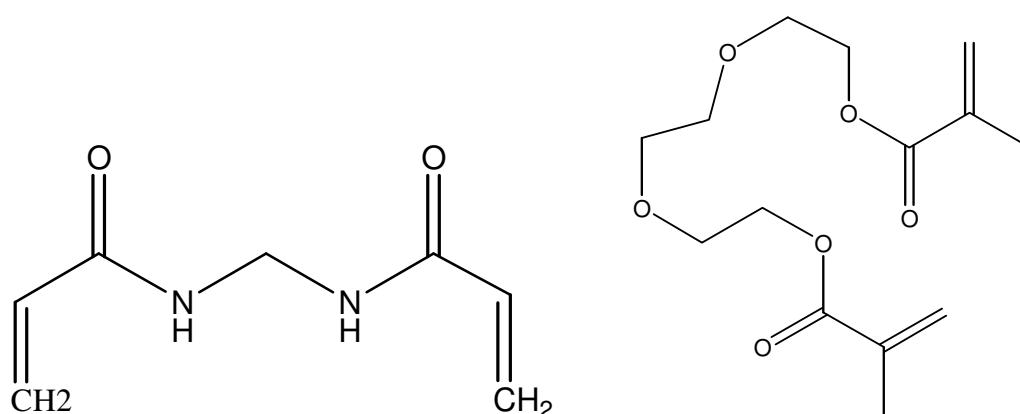


Figure 8. Chemical structure of *N,N'*-methylene-bisacrylamide (BIS) and triethylene glycol dimethacrylate (TriEGDMA).

The conditions for preparation of the hydrogels were optimized after careful investigation of the effects of the monomer concentration, crosslinker and initiator used, as well as their concentrations, concentration of hyaluronic acid and the temperature of the reaction.

The conditions that showed to be more efficient giving rise to more homogenous systems are summarized in table 4.

Table 4. Composition in weight (%) of the reactants for the preparation of the hydrogels.

Monomer	[ ]	Crosslinker	%	Initiator	[ ]	Polymer	%
EPM	0.725M 0.545M	BIS	2	$K_2S_2O_8$	$2 \times 10^{-2}$ M	HA	1
							2.5
							5
EPM	0.725M 0.545M	TriEGDMA	1.7	$K_2S_2O_8$	$2 \times 10^{-2}$ M	HA	1
							2.5
							5

The hydrogels produced had soft consistency appearance and had a white and opac color (figure 9).

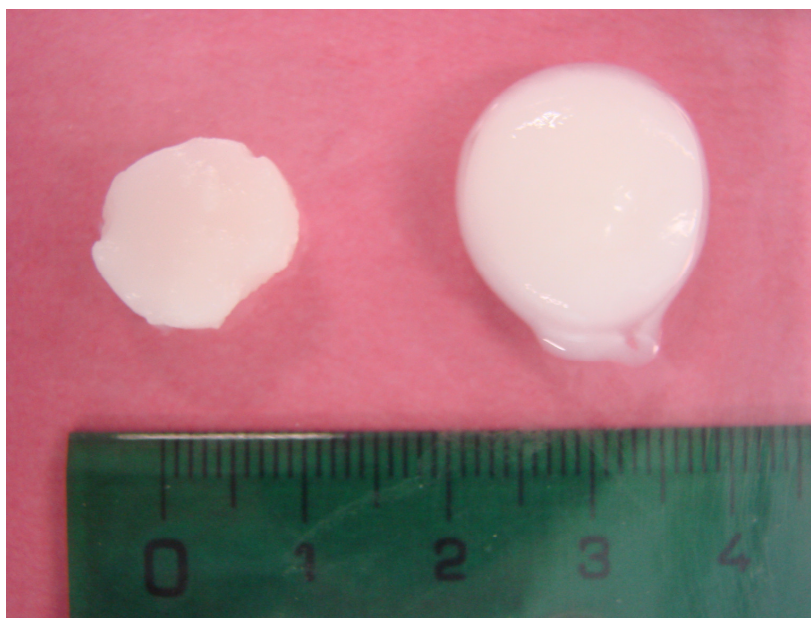


Figure 9. Photographs of PEPMHA hydrogels after free radical polymerization.

### 3.2. Spectroscopic Characterization

The products were characterized by NMR and FTIR spectra. Comparing the signals it is possible to detect the appearance of new groups formed during the synthesis reactions. In the following image (Figure 10) we show the NMR- $^1\text{H}$  spectra of the commercial product (EP), monomer (EPM) and homopolymer (PEPM) as also obtained in previous studies [7].

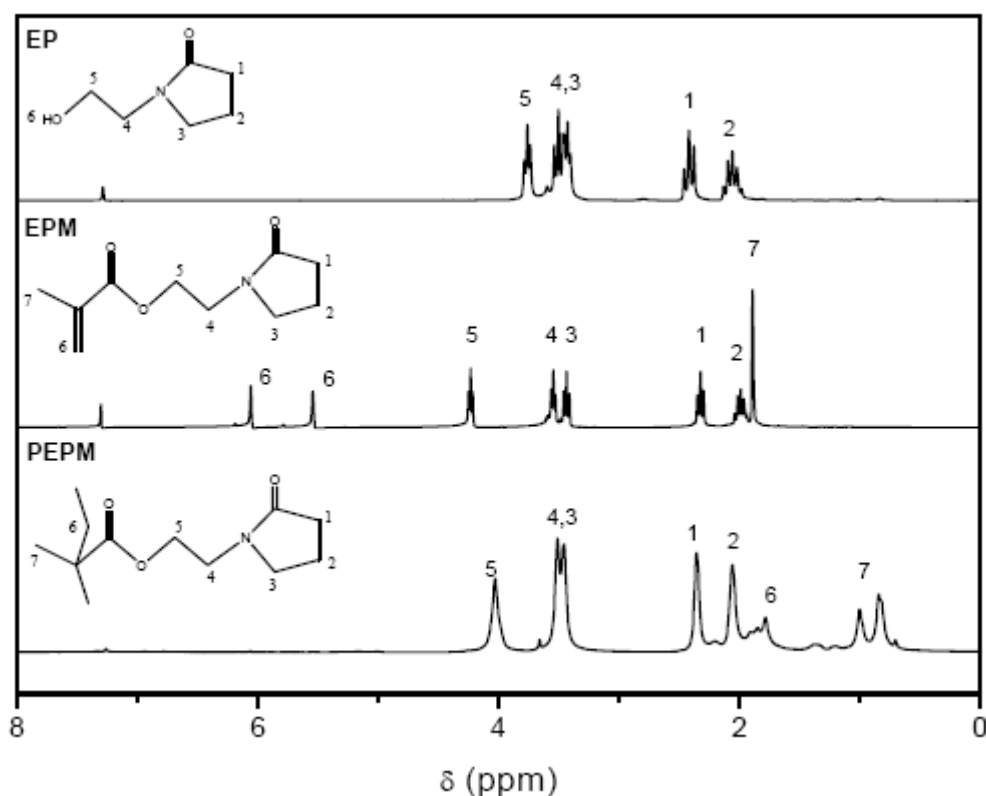


Figure 10. NMR- $^1\text{H}$  spectra of EP, EPM and PEPM [7].

The signal correspondent to the methacrylic group indicates the success of the reaction: double bond (6.05 ppm and 5.53 ppm) and methyl group (1.88 ppm). The polymer formation is provided by the disappearance of the signals correspondent to the double bond, confirming the progress of the reaction.

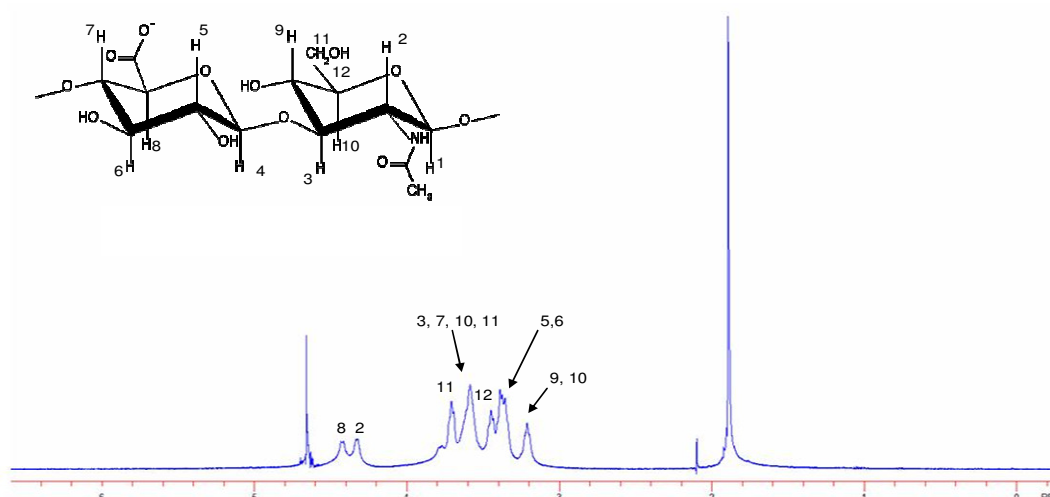


Figure 11. NMR- $^1\text{H}$  spectrum of HA.

In  $^1\text{H}$  NMR spectrum using  $\text{D}_2\text{O}$  as a solvent, all exchangeable protons from  $-\text{OH}$  and  $-\text{NH}$  groups were invisible, due to the group's dissociation [8]. The most important signals assigned in the hyaluronic acid  $^1\text{H}$  spectrum were: the protons  $-\text{CH}_2\text{OH}-$  (3.79 and 3.54 ppm),  $-\text{CH}-\text{NH}=\text{COOH}-$  (4.10 ppm) and  $\text{CH}-\text{C}=\text{OO}^-$  (4.55 ppm) (figure 11).

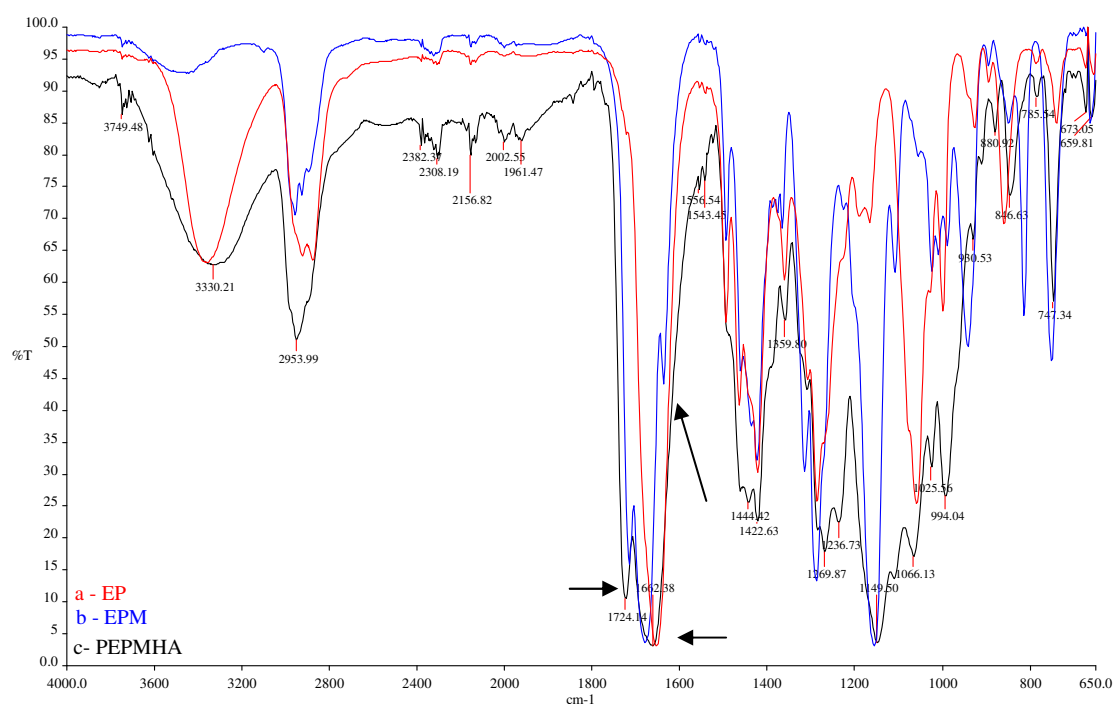


Figure 12. FTIR-ATR of EP, EPM and PEPM semi-interpenetrated with HA.

The FTIR-ATR results (Figure 12) confirm the evolution of the chemical reactions and the formation of a polymeric structure. We can assign the bands ( $\nu$ ,  $\text{cm}^{-1}$ ): from 1662 ( $\text{C}=\text{O}$ ), in the initial reagent EP; in the monomer EPM the assignment of 1600 ( $\text{CH}_2=\text{C}$ ) in result of the methacrylation; and finally the polymerized product, PEPM, with the characteristic ester bonds 1724 ( $\text{C}=\text{O}$ ) and 1650 ( $\text{C}=\text{O}$ ), and it is visible the disappearance of the double bond signal present in EPM, that gave rise to the polymeric chain.

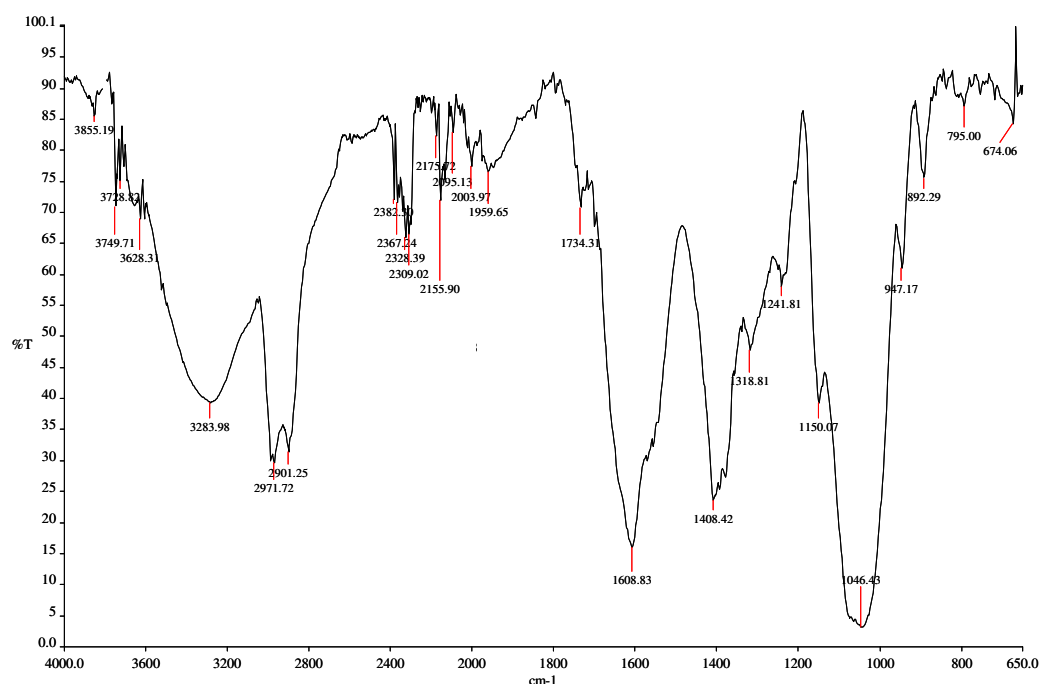


Figure 13. FTIR-ATR spectrum of HA.

Figure 13 shows the FT-IR spectrum of the hyaluronic acid. The absorption bands ( $\nu$ ,  $\text{cm}^{-1}$ ): located at 2971 and 2901 were assigned to the CH stretches. The absorption peak at 3283 to N-H in combination with  $\text{C}=\text{O}$ . The peak at 1608 assigned to amid II; 1408 to NH deformation; 1046 to C-O-C, C-O and C-O-H stretching.

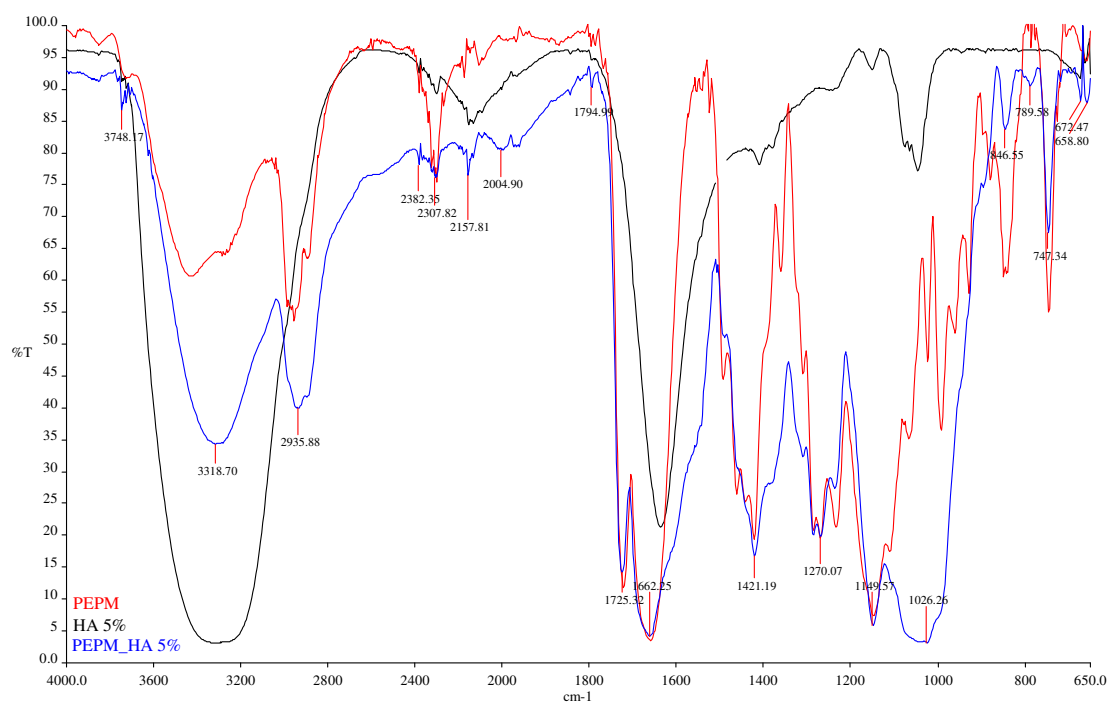


Figure 14. FTIR-ATR of PEPM, HA and PEPM interpenetrated with HA.

The FTIR-ATR for the prepared polymerized systems (PEPMHA) was as follows: ( $\nu$ ,  $\text{cm}^{-1}$ ), 3318 (N-H, O-H), 2935 (C-H), 1725 (C=O), 1662 (C=O cycle), 1421 ( $\text{CH}_2$ -N), 1270.07 (O- $\text{CH}_2$ ). Around 1550 we can assign a shift that can be attributed to possible HA and PEPM interactions (Figure 14).

### 3.3. Chromatographic Characterization

The molecular weight of a substance has great influence when in concern to the preparation of hydrogels. When preparing hydrogels in the presence of hyaluronic acid of different lots it was verified that the homogeneity of the materials prepared was different. For that, the molecular weight and  $M_w/M_n$  for the different lots was determined and the values of the lot finally used are represented in the following image (figure 15).

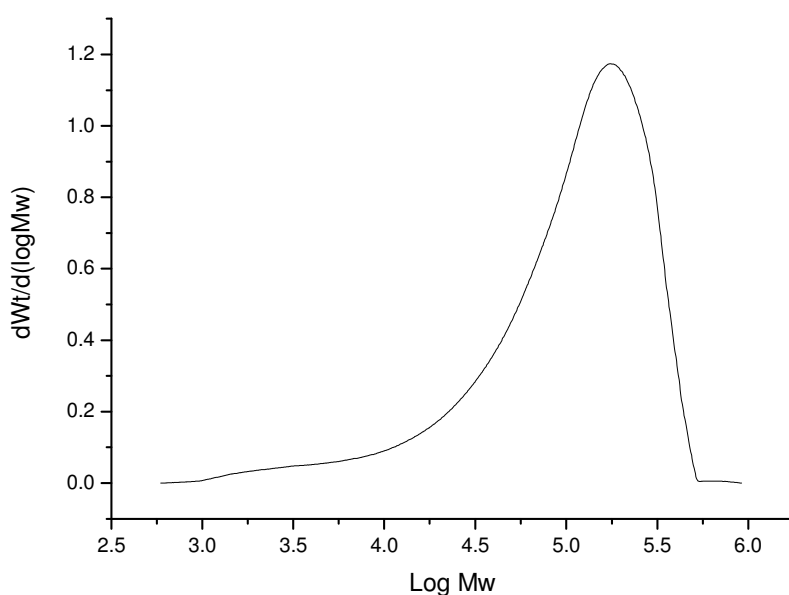


Figure 15. Molecular weight of hyaluronic acid (HA).

From the analysis through chromatography, the obtained values were,  $M_n$  37756,  $M_w$  175232 with a polydispersity of 4.64.

The maximum concentration used of HA in the preparation of PEPMHA hydrogels was of 5%. Above this concentration the viscosity of the solution was too high to allow the formation of homogeneous materials.

The molecular weight between cross-links of the PEPMHA hydrogels was also determined using different techniques and will be mentioned in the next chapter.



### 3.4. Thermal Analysis Characterization

The thermal analysis of the prepared PEPMHA polymers was determined by thermogravimetry, an analytical technique used for the investigation of the behaviour of a substance in function of the temperature, showing the thermal stability of the polymer. The decomposition profiles and associated first derivative curves of PEPMHA are shown in a typical dynamic TGA spectrum as in figure 16. This figure gives clear evidence that the polymer has a great thermal stability up to 240°C when decomposition begins. The weight loss due to degradation of this material begins around 240°C. Beyond this temperature the rate of weight loss decreases continuously as indicated in the spectrum by the different decomposition regions. The first region has a maximum decomposition rate of 241°C with a weight loss of 5.97 wt%. The second region has a maximum decomposition rate of 288°C and weight loss of 9.64 wt%. The following three regions have maximum decomposition rates at 364°C, 385°C and 414°C with respective weight loss of 38.58 wt%, 55.22 wt% and finally 78.54 wt%.

The thermal degradation of PEPMHA shows five separate degradation regions and a typical curve for the degradation of methacrylates.

The first region of weight loss detected, with maximum degradation rate at 240°C, is probably due to the cleavage of HA bonds, physically entrapped in the semi-interpenetrated system, in accordance to values reported elsewhere [9].

In previous studies of the homopolymer PEPm alone, the temperature obtained for the beginning of the polymeric system decomposition was of 226°C [10].

So, the second region should be mainly characterized by the degradation of PEPMHA bonds, and more then considering the simple summation of the two components decomposition, it denotes some form of interaction between them.

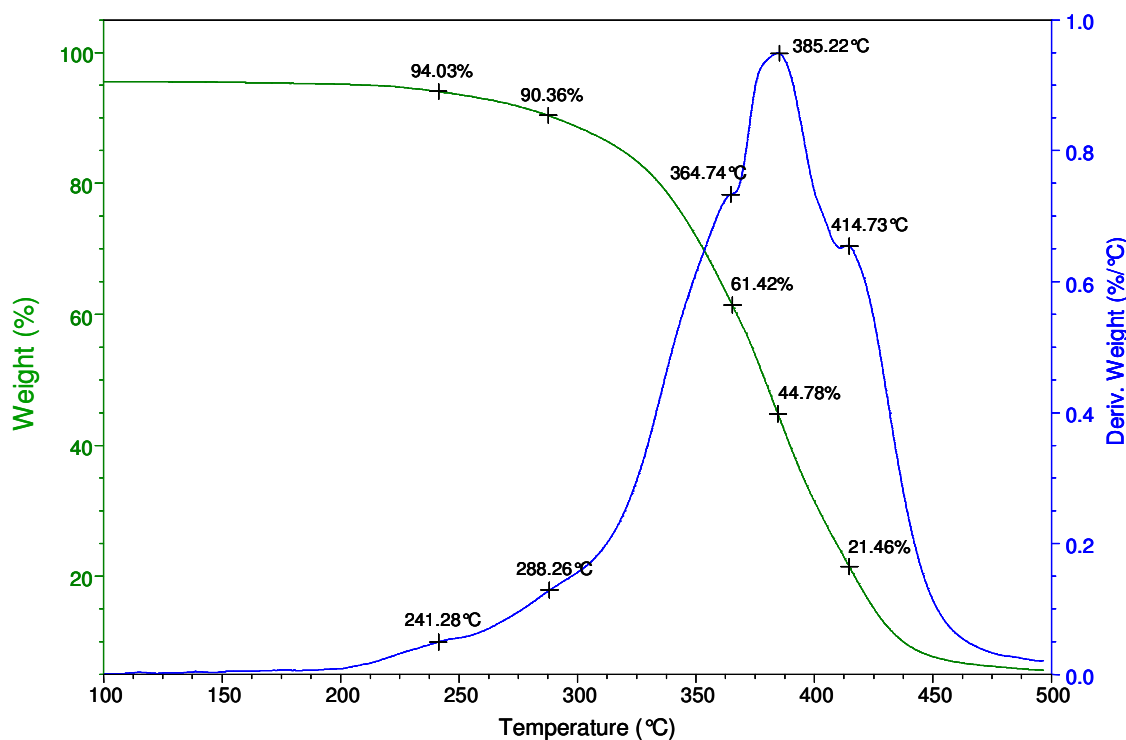


Figure 16. Thermogravimetric analysis of PEPMHA.

The subsequent regions (3-5) of main degradation of the polymer can be characterized by possible modification reactions, through lateral chains that can originate new groups or crosslinking bonds, followed by a process of radical depolymerization, where the monomer is obtained as product of degradation [11].

### 3.5. Macroscopic Characterization

Porosity was observed by scanning electron microscopy (SEM). Porosity, pore size, and surface area both at macroscopic and microscopic level, are widely recognized as important morphological parameters for a scaffold in tissue engineering. Other characteristics such as pore shape, pore wall morphology, and interconnectivity between pores of the scaffold materials also suggested to be important for cell seeding, migration, growth, mass transport, gene expression, and the formation of the new tissue [12].

In order to promote tissue growth, the scaffold must have a large surface area so that cells can penetrate the pores, and the pores must be interconnected to facilitate nutrient and waste exchange by cells deep within the construct [13].

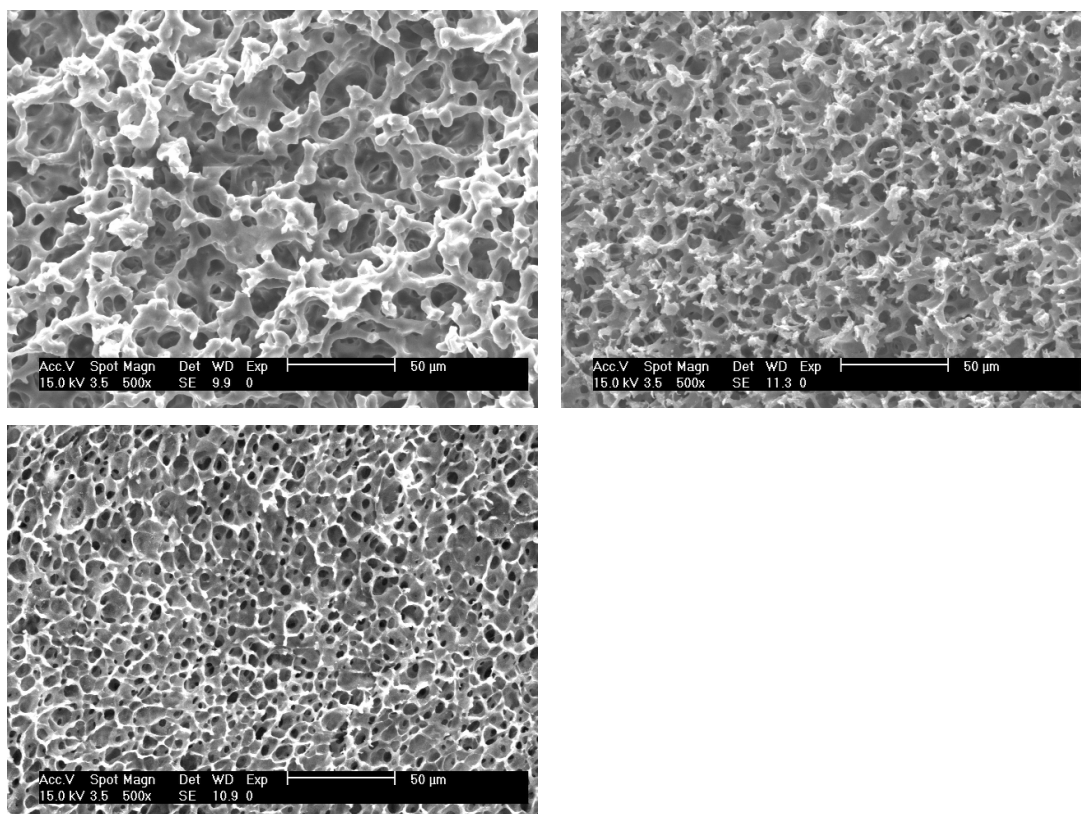


Figure 17-19. Scanning electron micrograph (500x) from 0.725M EPM polymerized in the presence of HA (1, 2.5 and 5%), using  $K_2S_2O_8$  as initiator and triethylene glycol dimethacrylate (1.7%) as a crosslinker.

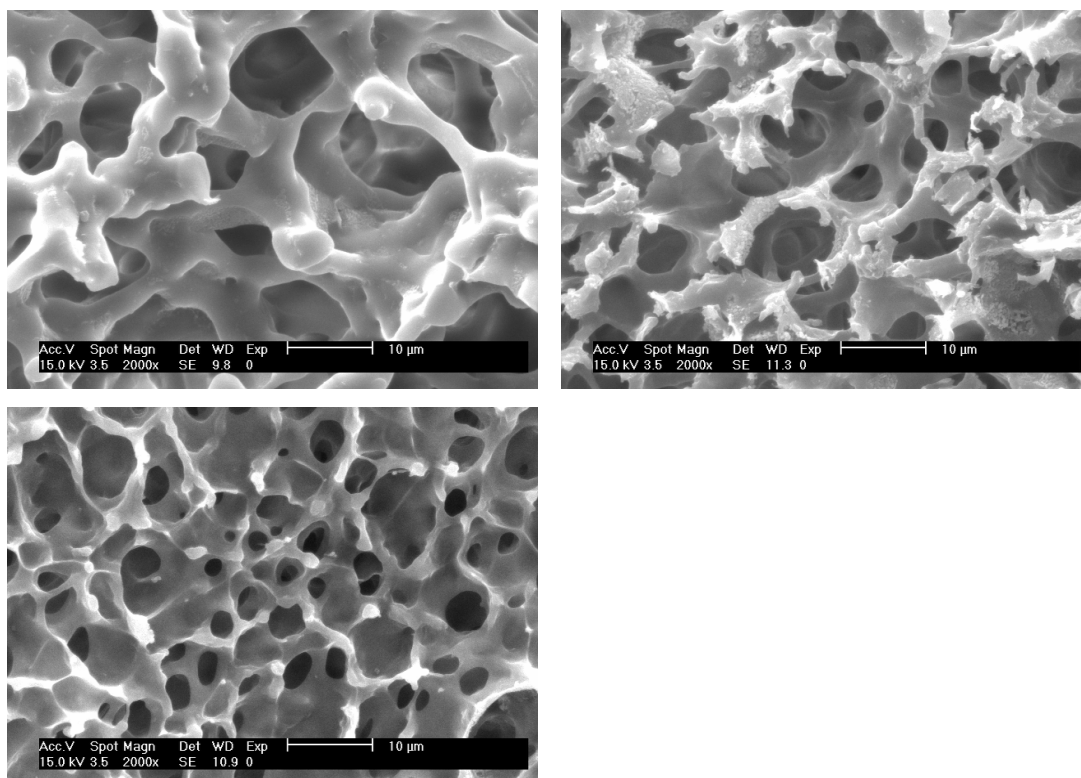


Figure 20-22. Scanning electron micrograph (4000x) from 0.725M EPM in the presence of HA (1, 2.5 and 5%), using  $K_2S_2O_8$  as initiator and triethylene glycol dimethacrylate (1.7%) as a crosslinker.

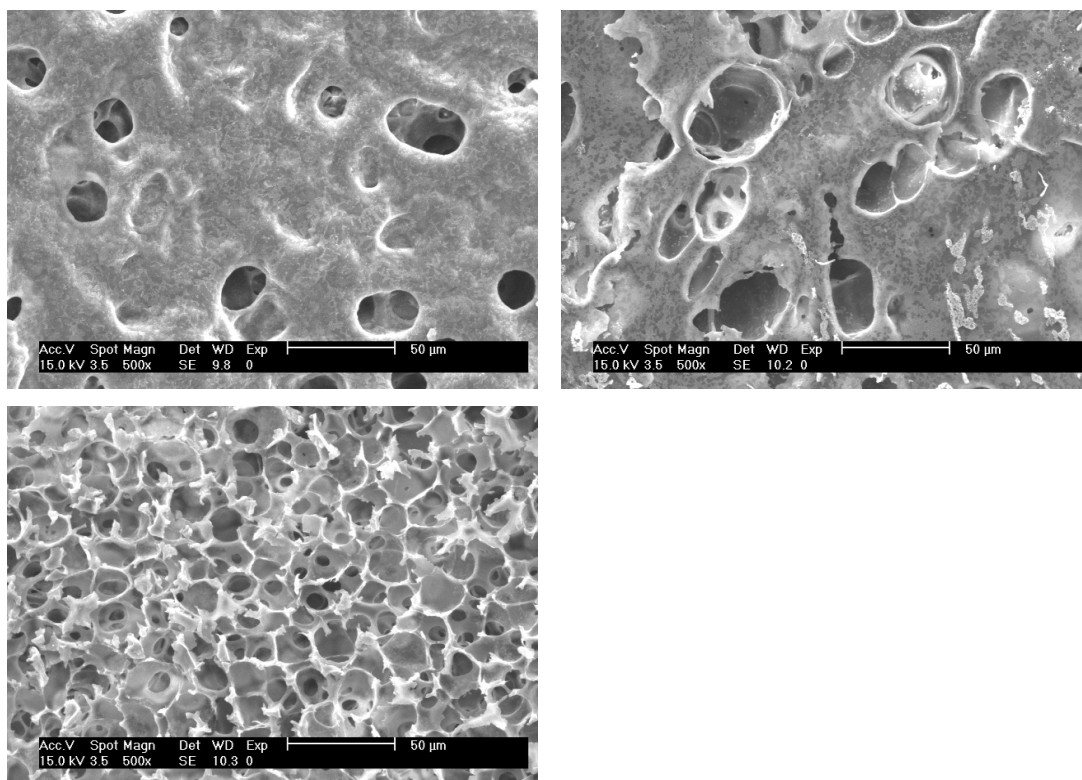


Figure 23-25. Scanning electron micrograph (500x) from 0.545M EPM polymerized in the presence of HA (1, 2.5 and 5%), using  $K_2S_2O_8$  as initiator and triethylene glycol dimethacrylate (1.7%) as a crosslinker.

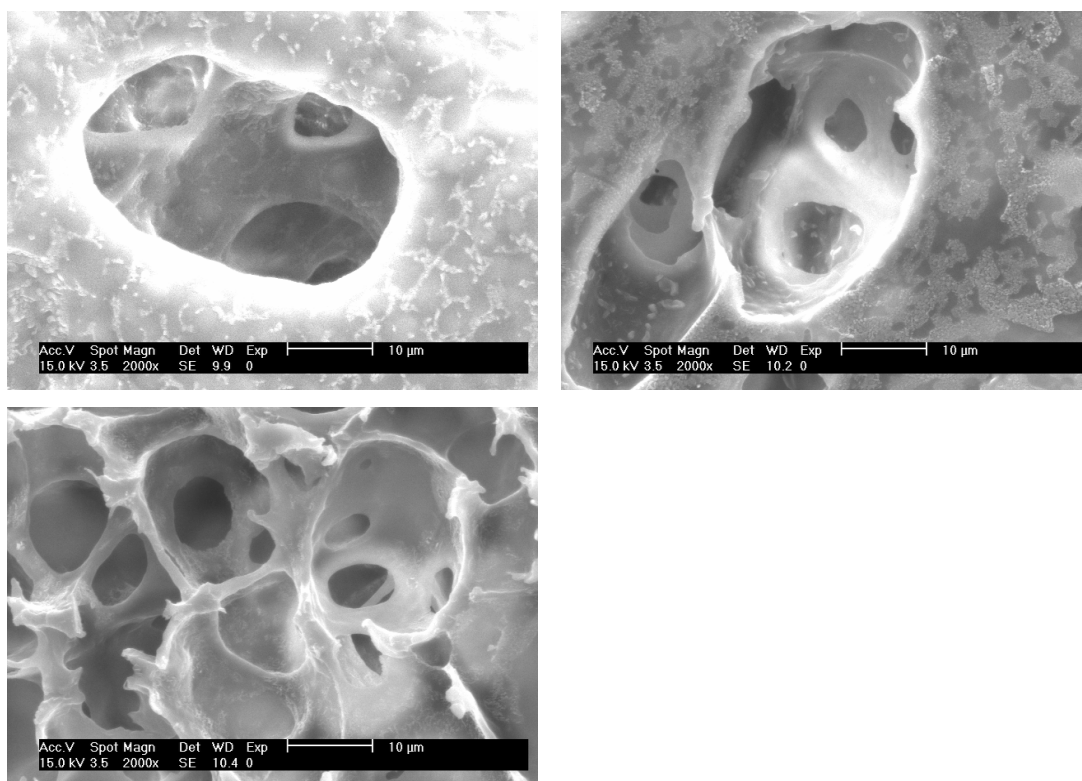


Figure 26-28. Scanning electron micrograph (4000x) from 0.545M EPM in the presence of HA (1, 2.5 and 5%), using  $K_2S_2O_8$  as initiator and triethylene glycol dimethacrylate (1.7%) as a crosslinker.

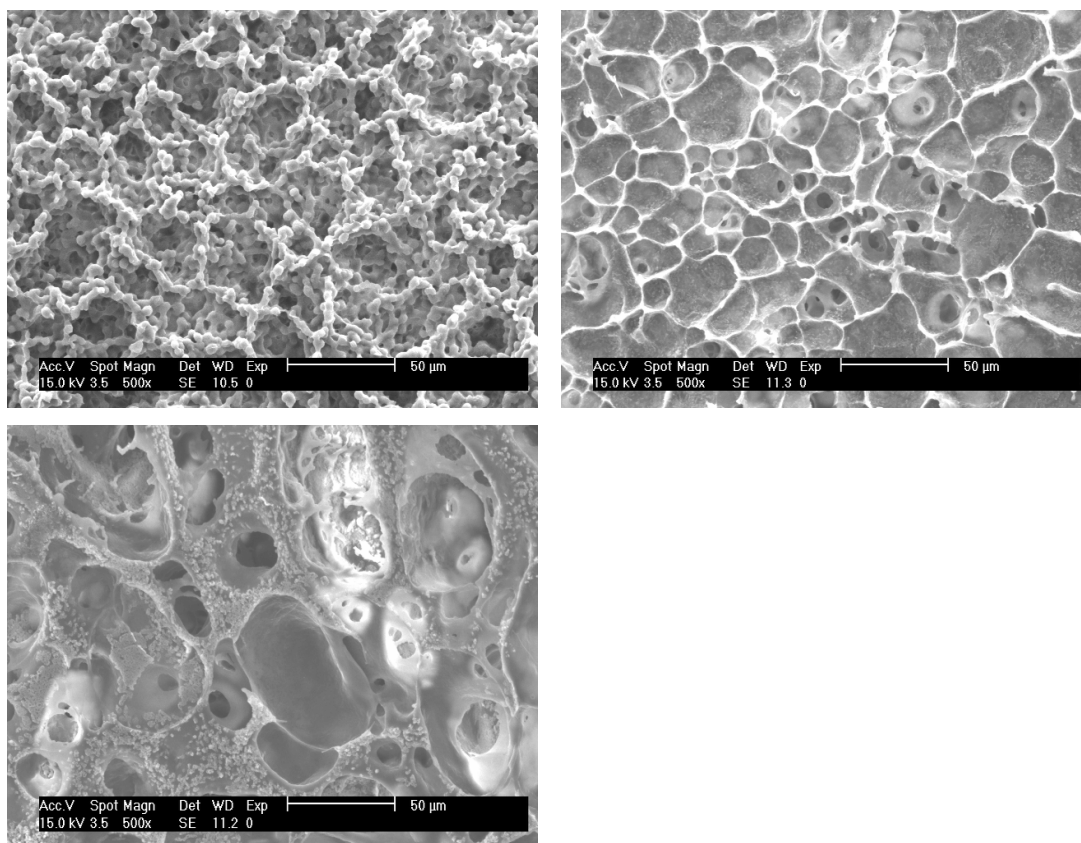


Figure 29-31. Scanning electron micrograph (500x) from 0.725M EPM in the presence of HA (1, 2.5 and 5%), using  $K_2S_2O_8$  as initiator and  $N,N'$ -methylene-bisacrylamide (2%) as a crosslinker.

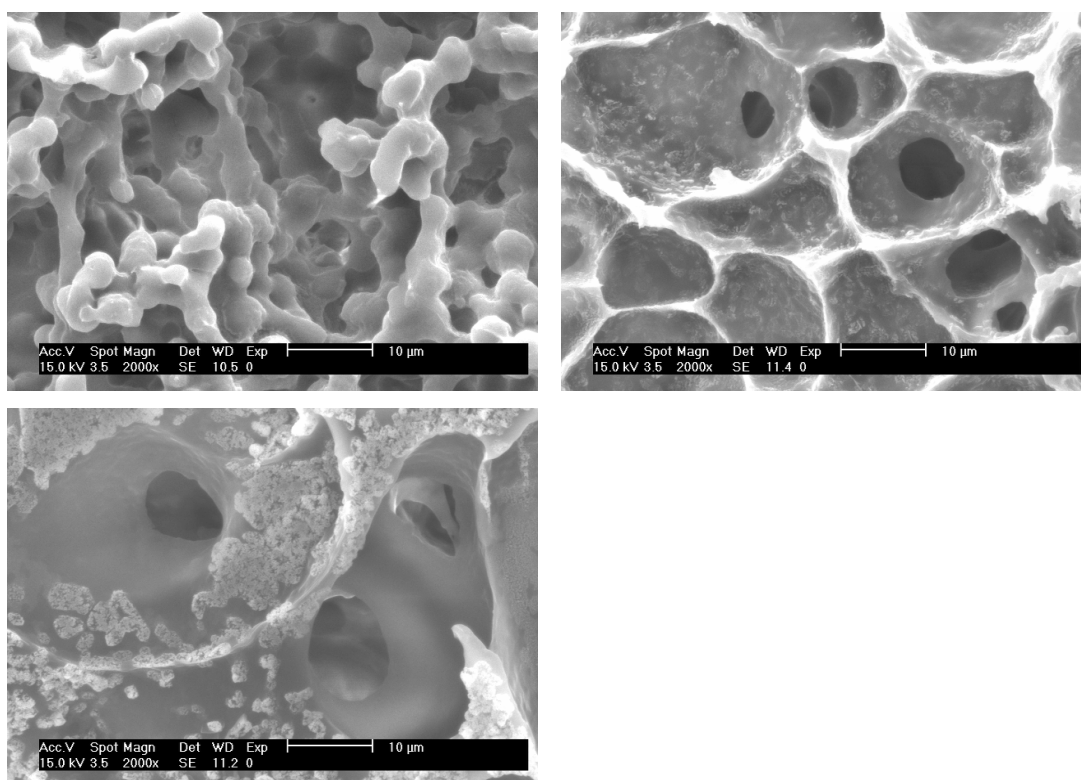


Figure 32-34. Scanning electron micrograph (4000x) from 0.725M EPM in the presence of HA (1, 2.5 and 5%), using  $K_2S_2O_8$  as initiator and  $N,N'$ -methylene-bisacrylamide (2%) as a crosslinker.

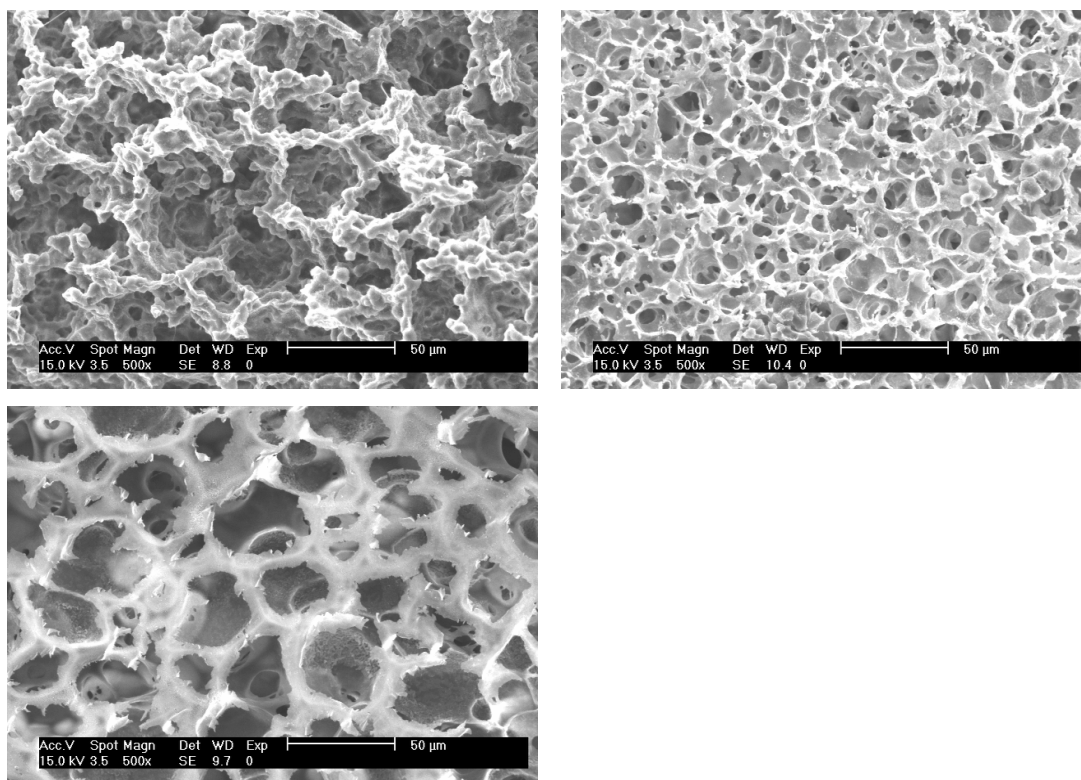


Figure 35-37. Scanning electron micrograph (500x) from 0.545M EPM in the presence of HA (1, 2.5 and 5%), using  $K_2S_2O_8$  as initiator and N,N'-methylene-bisacrylamide (2%) as a crosslinker.

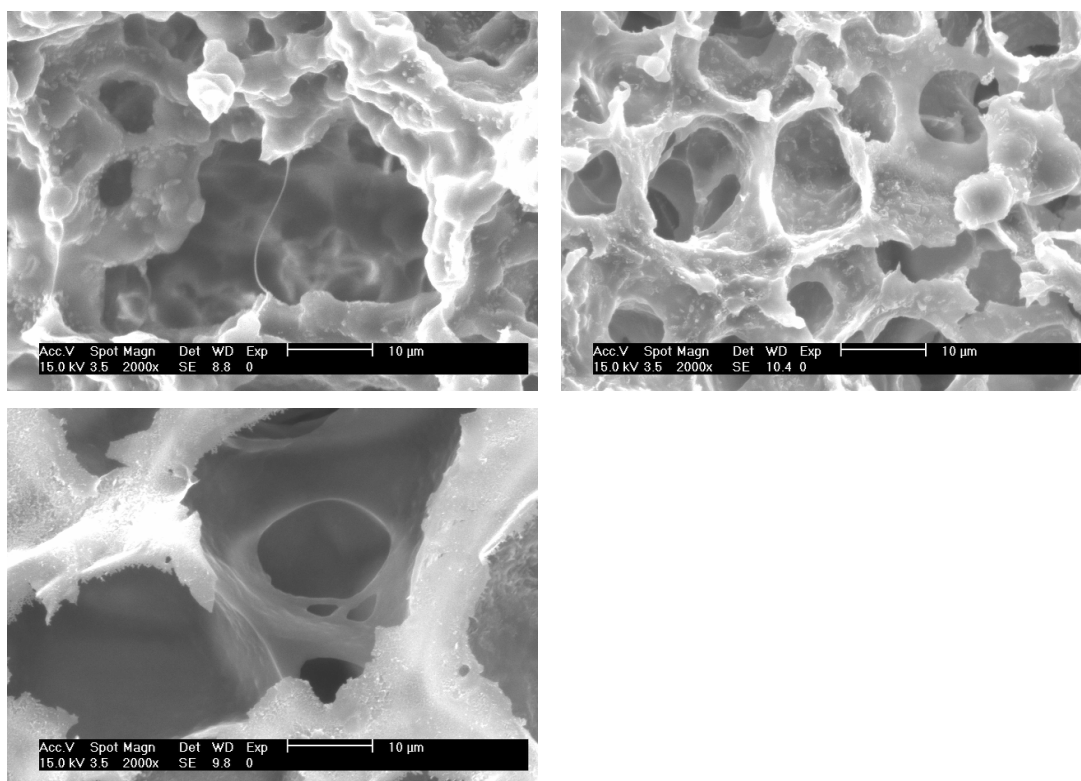


Figure 38-40. Scanning electron micrograph (4000x) from 0.545M EPM in the presence of HA (1, 2.5 and 5%), using  $K_2S_2O_8$  as initiator and N,N'-methylene-bisacrylamide (2%) as a crosslinker.

The SEM photographs were taken in order to one speculate of how the scaffolds structure would appear. The scaffolds prepared with triethylene glycol dimethacrylate present a more defined and homogenous porous structure. When observed at higher magnifications, the pores were similar in size and their shape is more spherical (fig.20-22). Scaffolds also appeared to present high porosities, but small pore sizes (10-35  $\mu\text{m}$ ). In scaffolds prepared with different concentrations of EPM, namely 0.725 and 0.545M, it was seen that the different polymeric concentration resulted in different porosities. In general, a polymer solution of higher concentration produced a denser structure, which implicates less porous structure.

### 3.6. Porosity determination by pycnometry

The freeze drying method leads to porous materials, as it can be seen from the micrographs of figures 17-40.

The porosity was estimated by measuring the real and apparent densities,  $\rho_r$  and  $\rho_{ap}$ , respectively, of the samples, as described in the methodology section of this chapter.

The porosity values obtained by this technique are quoted in table 5 together with the real and apparent densities.

Table 5: Apparent and real densities and porosity measurements for the different PEPM-HA based materials.

PEPMHA hydrogels		Apparent density ( $\text{g.cm}^{-3}$ )	Real density ( $\text{g.cm}^{-3}$ )	Density ( $\text{g.cm}^{-3}$ )	Porosity (%)
EPM 0.545M BIS 2% $\text{K}_2\text{S}_2\text{O}_8$ $2 \times 10^{-2}\text{M}$	HA 1%	1.41	1.16	1.21	-21.17
	HA 2.5%	1.42	1.14	1.25	-24.65
	HA 5%	0.56	0.82	0.69	31.28
EPM 0.725M TriEGDMA 1.7% $\text{K}_2\text{S}_2\text{O}_8$ $2 \times 10^{-2}\text{M}$	HA 1%	0.83	1.53	0.54	45.87
	HA 2.5%	0.40	1.17	0.35	65.40
	HA 5%	1.10	0.95	1.15	-15.29
EPM 0.725M BIS 2% $\text{K}_2\text{S}_2\text{O}_8$ $2 \times 10^{-2}\text{M}$	HA 1%	1.52	1.10	1.38	-37.75
	HA 2.5%	0.73	1.23	0.59	40.95
	HA 5%	0.93	1.14	0.81	18.83

Although some of the values of the apparent density approach the real values, this method didn't show to be accurate enough to determine the porosity. This can be to some extent attributed to the swelling of the hydrogels in ethanol, although the same occurred when xylene was used (data not shown). The walls of the pores would then suffer deformation altering the porous structure and impeding the determination of the porosity (negative values). Also, samples size might have influenced the results.

Comparing the real density of the produced materials to PEPM alone ( $1.14 \text{ g.cm}^{-3}$ ) there is a significant influence of the hyaluronic acid highest concentration, in this parameter, mainly in the case of the first and second polymeric systems indicated in table 5. The determined values were in accordance to the concentration of hyaluronic acid present, conferring a higher hydrophilic character, thus decreasing the density of the material as it would create more hydrogen bonds with the water molecules.

### 3.7. Determination of the mechanical properties of PEPMHA polymeric systems

Although increased porosity and pore size facilitate tissue ingrowth into a material, the result is a reduction in the mechanical properties, since this compromises the structural integrity of the scaffold.

The mechanical properties of the PEPMHA polymeric systems were determined performing consecutive frequency sweeps extending from 0 to 15 Hz, at a temperature of 37°C.

Storage modulus ( $G'$ ) and the loss tangent,  $\tan \delta$  responses for PEPMHA hydrogels were plotted as functions of strain modulation as in figures 41-43.



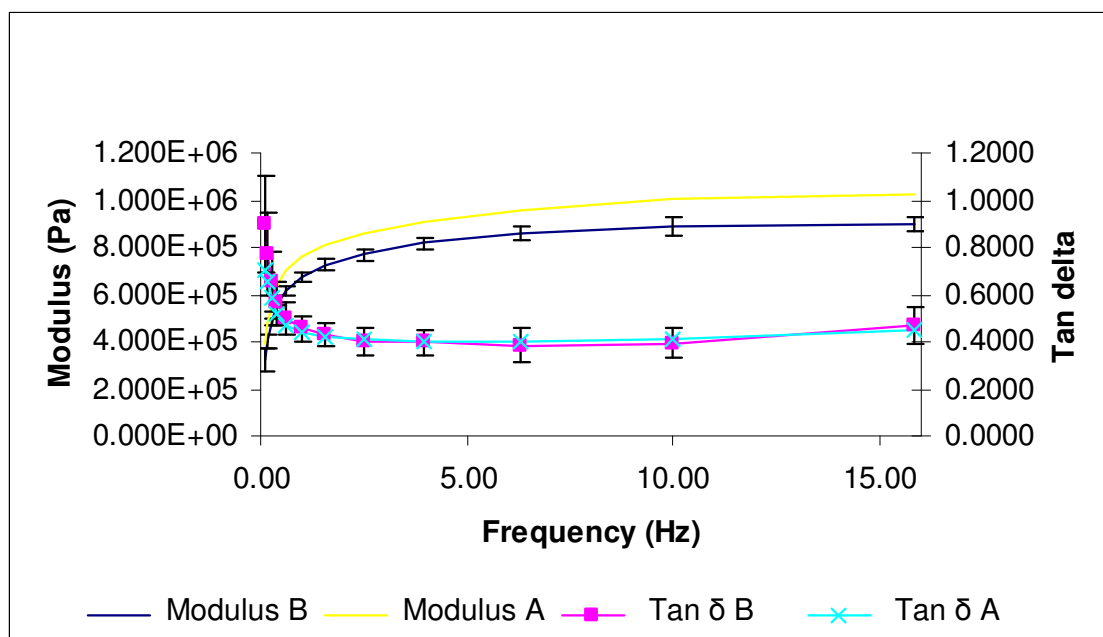


Figure 41. DMA response as a function of frequency (0-15 Hz) for PEPMHA hydrogels prepared with the following compositions: EPM 0.545M, BIS 2%,  $K_2S_2O_8$   $2 \times 10^{-2}M$ , HA 2.5% (sample A) and HA 5% (sample B).

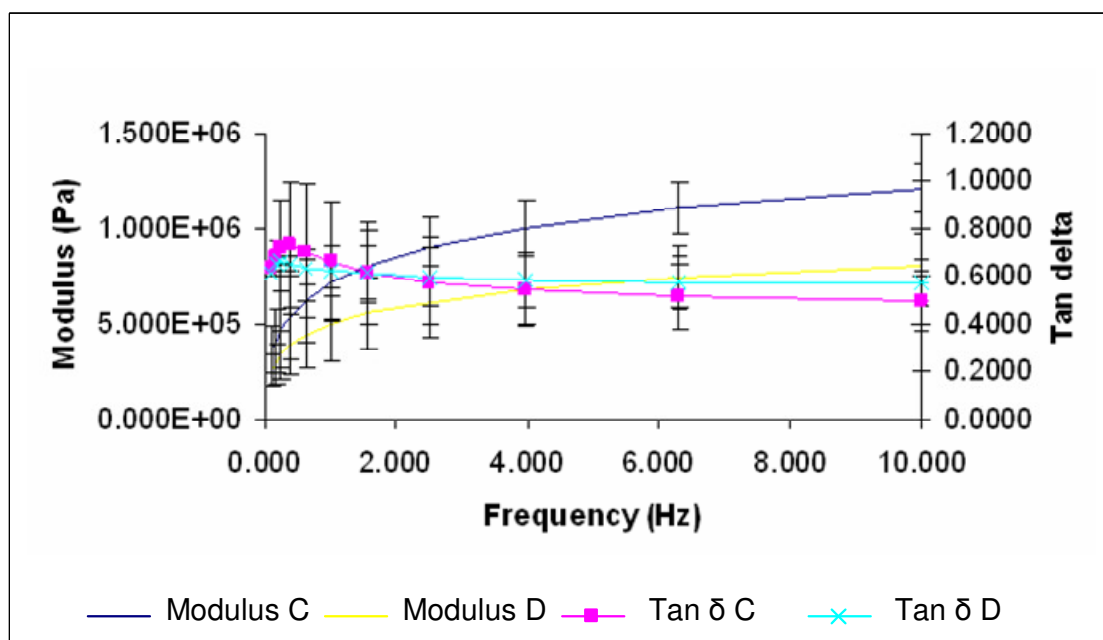


Figure 42. DMA response as a function of frequency (0-15 Hz) for PEPMHA hydrogels prepared with the following compositions: EPM 0.725M, BIS 2%,  $K_2S_2O_8$   $2 \times 10^{-2}M$ , HA 1% (sample C) and HA 2.5% (sample D).

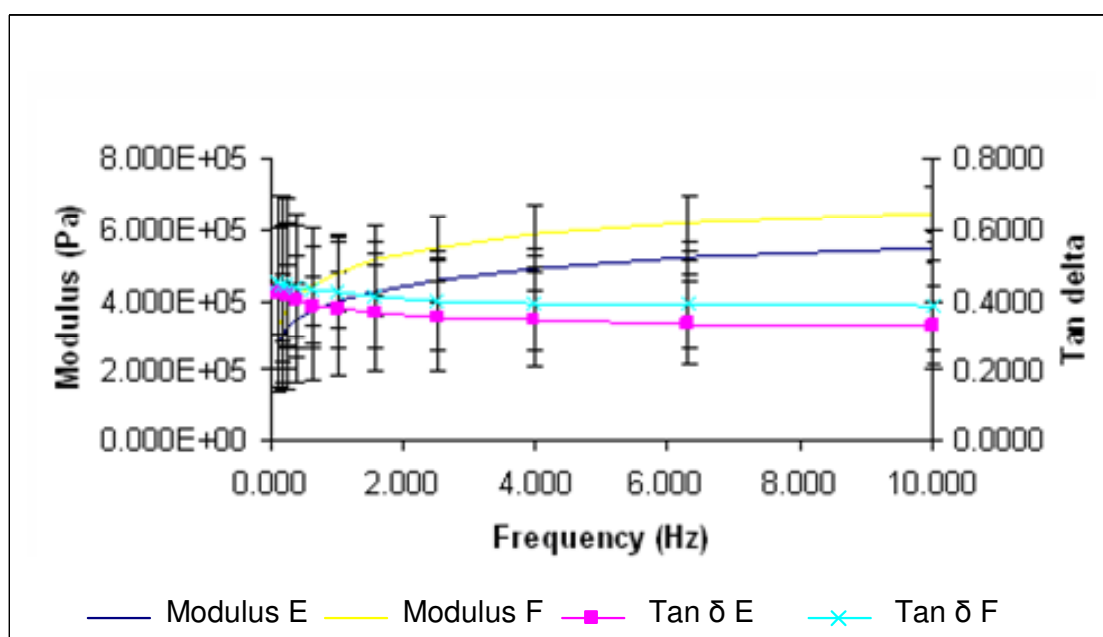


Figure 43. DMA response as a function of frequency (0-15 Hz) for PEPMHA hydrogels prepared with the following compositions: EPM 0.725M, TriEGDMA 1.7%,  $K_2S_2O_8$   $2 \times 10^{-2}M$ , HA 2.5% (sample E) and HA 5% (sample F).

The storage modulus for all samples monotonically increases with increasing frequency, which is consistent with the time-temperature superposition principle. The higher storage modulus means that the material has stronger elastic response at higher frequency.

Error bars in figures 42 and 43 are relatively high because of the heterogeneity and reduced dimension of the samples. However, the results were considered for comparison and reflect the average behavior of the hydrogels.

Further on, the obtained values for the storage modulus of PEPMHA hydrogels swollen in distilled water at 37°C, until equilibrium was reached, were summarized in figure 44. There is a clear influence of the concentration of monomer used as well as the nature and concentration of the crosslinker.

In hydrogels prepared with N,N'-methylene-bisacrylamide, an increase in the concentration of monomer used, previous to the polymerization, leads to the formation of more robust hydrogels with higher modulus of storage. As expected, when the amount of crosslinker is diminished, the hydrogels modulus,  $G'$ , decreases.

PEPMHA polymeric systems crosslinked with triethylene glycol dimethacrylate show a significant decrease in the storage modulus in relation to any of the hydrogels prepared with N,N'-methylene-bisacrylamide.

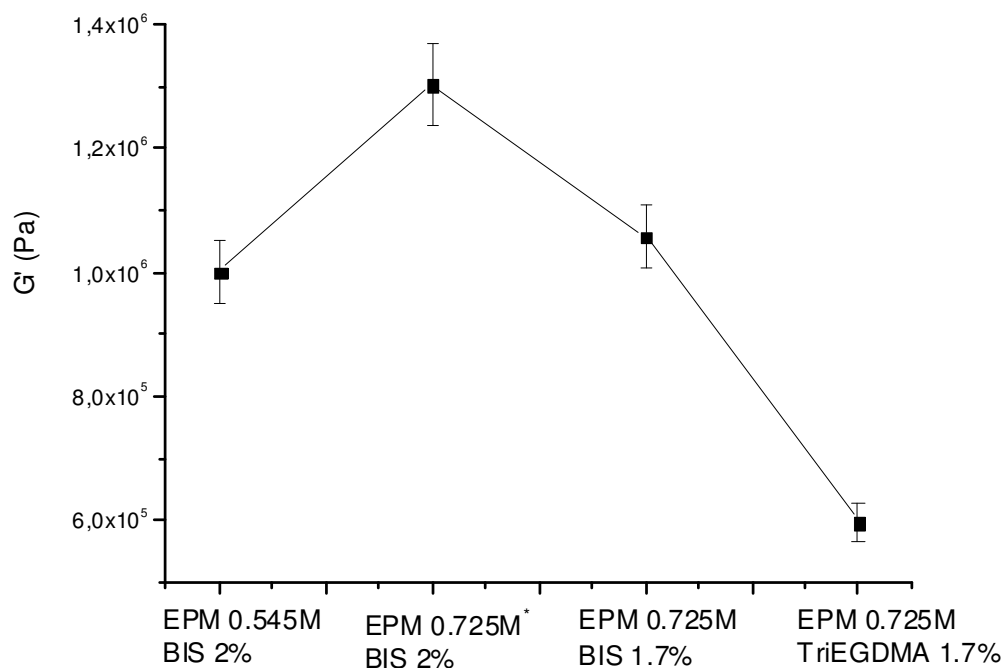


Figure 44. Storage modulus as a function of the content of EPM and nature/content of crosslinker for PEPMHA hydrogels in the equilibrium of swelling. The concentration of HA present is the same for all the hydrogels, namely 2.5%. (\* In this case,  $\text{Na}_2\text{S}_2\text{O}_8$  was used as an initiator. It was seen that both the structure and hydrogels properties didn't seem to be affected when compared to hydrogels prepared with  $\text{K}_2\text{S}_2\text{O}_8$ .) The measurements indicated were determined for a frequency of 10 Hz.

Variations on the mechanical properties may be due to some degradation, cross-linking effect or changes on the equilibrium moisture content of the samples.

The quantity of water in hydrogels determines partly their mechanical and biological properties. The challenge with hydrogels is to obtain optimal mechanical strength without decreasing cell viability and function. The next chapter is dedicated to water uptake studies and how they can be related to the material's mechanical properties.

#### 4. Bibliography

1. A. Abajo. J., C., Gallardo, A., et al, Ciencia y Tecnología de Materiales Poliméricos. Vol. I. 2004, Madrid: CSIC.
2. O. Wichterle, Lim, D., Hydrophilic gels for biological use. Nature, 1960. 185: p. 117-118.
3. B.D. Ratner, A.S. Hoffman, F.J. Schoen and J.E. Lemons, Biomaterials Science- An Introduction to Materials in Medicine. 2nd ed. 2004: Elsevier Inc.
4. R. L. Reis and J. San Román, Biodegradable Systems in Tissue Engineering and Regenerative Medicine. 2005: CRC Press.
5. J.S. Oh, Kim, J.M., Lee, K.J., and Bae, Y.C., Swelling behaviour of N-isopropylacrylamide gel particles with degradable crosslinker. European Polymer Journal, 1999. 35: p. 621-630.
6. E. Yilmaz, Adali, T., Yilmaz, O., Bengisu, M., Grafting of poly(ethylene glycol dimethacrylate) onto chitosan by ceric ion initiation. Reactive & Functional Polymers, 2007. 67: p. 10-18.
7. N. González, C. Elvira and J. San Román, Hydrophilic and hydrophobic copolymer systems based on acrylic derivatives of pyrrolidone and pyrrolidine. Journal of Polymer Science, Part A: Polymer Chemistry, 2003. 41(3): p. 395-407.
8. M.Y. Alkrad J.A., Stroehl D., Wartewig S., Neubert R., Characterization of enzymatically digested hyaluronic acid using NMR, Raman, IR, and UV-Vis spectroscopies. Journal of Pharmaceutical and Biomedical Analysis, 2003. 31(3): p. 545-550.
9. B.E. Milella E., Massaro C., Ramires P.A., Miglietta M.R., Fiori V., Aversa P., Physico-chemical properties and degradability of non-woven hyaluronan benzylic esters as tissue engineering scaffolds. Biomaterials, 2002. 23: p. 1053-1063.
10. N. Gonzalez, Nuevos Sistemas Polimericos Sensibles a pH y Temperatura. Aplicaciones Biomedicas., in Physics- Chemistry. 2006, Complutense: Madrid.
11. K.M.G. Moharram M.A., Thermal Behavior of Poly(acrylic acid)- Poly(vinyl pyrrolidone) and Poly(acrylic acid)-Metal-Poly(vinyl pyrrolidone) Complexes. J Appl Polym Sci, 2006. 102(4): p. 4049-4057.

12. P.X. Ma and J.-W. Choi, Biodegradable Polymer Scaffolds with Well-Defined Interconnected Spherical Pore Network. *Tissue Eng*, 2001. 7(1): p. 23-33.
13. A.G. Mikos and J.S. Temenoff, Formation of highly porous biodegradable scaffolds for tissue engineering. *Electronic Journal of Biotechnology*, 2000. 3(2): p. 114-119.

## Chapter II- Semi-IPN behaviour in hydrated environment

### 1. Introduction

A simple definition of a hydrogel is one which refers to it as a homopolymer or copolymer network which swells in water [1]. Hydrogels might also be defined as polymeric materials which are able to absorb water and retain a significant fraction of this water in its structure without dissolving the polymer. As water enters the network the configuration of polymeric chains changes and adopts more extended forms until a state of equilibrium is reached.

The water uptake of a hydrogel is controlled by several factors such as degree of crosslinking, type and concentration of the polymer, pH and temperature of the solution. It is also important to consider the crosslinking method because each method originates different types of networks leading to different swelling profiles.

Hydrogels are systems that present both characteristics of liquids, such as diffusive transport and characteristics of solids as cohesive properties [2]. The maintenance of the properties of the liquids is mainly due to the fact that the major component of the gel is a dissolvent. In the other hand, the ability of the gel to maintain its shape, presenting an elastic modulus at frequency zero is characteristic from the solids. This modulus is a consequence of the tri-dimensional network structure present in the hydrogels. So, the determination of swelling and rheologic properties would give an insight of the structure of the produced semi- interpenetrated networks, where the crosslinker is responsible for the bonding of different monomeric chains.

This network can therefore be characterized by the average molecular weight between cross-links,  $M_c$ , which theoretical value is determined by

$$M_c = M_r / 2X$$

where  $M_r$  is the polymer molecular weight and  $X$  the molar fraction of the crosslinker in the reaction.

To characterize the network,  $M_c$  is normally determined based in two different theories:

## 1.1. Equilibrium Swelling Theory

The most well known theory for determining the number of average molecular weight between cross-links,  $M_c$ , is probably the model of Flory and Rehner [3]. This model takes into account that the cross-linked polymer chains can be represented by a Gaussian distribution and that the cross-links are, on average, tetrafunctional. It is applied for polymeric networks formed from the crosslinking of a solid polymer.

Peppas and Merrill [4] developed a similar model considering situations where the cross-links are introduced in the swollen state, this is, the crosslinking of a solution.

## 1.2. Rubber Elasticity Theory

This theory considers that when a crosslinked network is stretched, it reaches an equilibrium strain while the stress remains constant. So, the rubber elasticity theory can be used to explain such equilibrium states thermodynamically [5]. The determination of  $M_c$  can thus be obtained through viscoelastic measurements:

$$G = \left(1 - \frac{2}{f}\right) \frac{\rho R T}{M_c} v_{2,s}^{1/3} v_{2,r}^{2/3} \quad \text{equation 1.}$$

Where  $V_{2,r}$  is the volume fraction of the gel in relaxed state,  $V_{2,s}$ , the volume fraction of the gel in the swollen state,  $f$  is the functionality of junction ( $f=4$ , for tetrafunctional networks),  $\rho$  is the density for the polymeric network ( $1.14 \text{ g/cm}^3$  for PEPM without crosslinking),  $R$  is the constant for gases ( $8.31 \text{ J/mol K}$ ) and  $T$  the temperature (K). The factor  $(1-2/f)$  is a correction factor for the defects produced in the extremities of the polymeric chains and is appropriate for diluted systems as in the case of hydrogels. In the case of perfect networks, this factor is equal to the unity. The equilibrium modulus is determined by  $G = G' + iG''$ ,  $G'$  as the storage modulus and  $G''$  the loss modulus. If  $G' \gg G''$  then the storage modulus  $G'$  can replace the equilibrium modulus in the equation 1. The volume fractions can also be determined experimentally as explained further in the methods section of this chapter.

### 1.3. Objective

The dual nature presented by the PEPMHA systems, namely the sensitivity to temperature presented by the PEPM and the sensitivity to pH by the HA is the basis of this chapter, where the water uptake response to the different stimulus is studied.

The average molecular weight between cross-links is also one of the parameters that influences the swelling profile of the hydrogels and thus calculated.

In the end, both the swelling degree and the molecular weight between cross-links should be intimately related to the mechanical performance of the materials in an aqueous environment. This way we could foresee the capability of adapting these hydrogels for tissue engineering applications.

## 2. Material and Methods

### 2.1. Water Uptake/Swelling Studies

The crosslinked hydrogels (PEPM with HA 1, 2.5 and 5%), obtained in long cylindrical shapes, were cut into small discs, that were immersed in vials with phosphate buffer solutions at pH 10, 7.4 and 2. The vials were set in a temperature- controlled bath at 20 °C and 37°C.

The study of the hydration degree was followed by measuring the weight of hydrogels in the swollen state. Basically, samples' weight was recorded by periodically removing them from the swelling media, blotting with absorbent tissue, weighting and re-placing them in the same media, until the samples reached an equilibrium penetrant uptake.

The **hydration degree** was determined gravimetrically according to the following expression:

$$\% S = \frac{W_t - W_0}{W_0} \times 100$$

Where %S is the swelling percentage, and W<sub>t</sub> and W<sub>0</sub> are the weight of the swollen (at time t) and dried sample respectively.



## 2.2. LCST determination by water uptake

PEPM polymers were shown to have a negative sensitivity with temperature in aqueous solutions [6]. According to various studies, thermosensitive polymers present a variation in their swelling degree dependent on the temperature being below or above their LCST. Therefore, the low critical solvent temperature of the crosslinked hydrogels can be determined by the study of the equilibrium swelling ratio to different temperatures. The hydrogels were cut in the same way as for the water uptake studies and immersed in vials in a phosphate buffer solution at pH 7.4. The vials were set in a temperature- controlled bath at 20 °C up to 50°C, increasing the temperature 3°C each 24h.

The same experiment was performed for other two sets of pH, 2 and 10.

## 2.3. Determination of the average molecular weight between cross-links

Volume fractions in the relaxed and swollen state,  $V_{2,r}$  and  $V_{2,s}$  were determined by thermogravimetric analysis, using a thermobalance TGA7 Perkin-Elmer.

The volume fraction of the polymer in the relaxed state,  $V_{2,r}$  can be defined as:

$$V_{2,r} = \frac{V_p}{V_p + V_{agua}} = \frac{\frac{m_r}{\rho_p}}{\frac{m_r}{\rho_p} + \frac{m_{agua}}{\rho_{agua}}} = \frac{\frac{m_r}{\rho_p}}{\frac{m_r}{\rho_p} + \frac{m - m_r}{\rho_p}} = \frac{1}{1 + \frac{\rho_p}{\rho_{agua}} \left( \frac{m - m_r}{m_r} \right)} \quad \text{equation 2.}$$

where  $m_r$  is the weight of the gel in the relaxed state,  $m$  is the weight of the gel in a determined time point of the swelling process,  $\rho_p$  is the density of the polymer (1,14 g/cm<sup>3</sup> density of PEPM was taken as the polymer density [6]) and  $\rho_{water}$  is the density of water (1,00 g/cm<sup>3</sup>) (equation 2).

In the other hand, when the absolute swelling degree of the hydrogel is considered, it is necessary to determine the weight of the dried hydrogel,  $m_0$ .

$$V_{2,r} = \frac{1}{1 + \frac{\rho_{polimero}}{\rho_{disolvente}} \left( \frac{m_r - m_0}{m_r} \right)} \quad \text{equation 3.}$$

The same formula can be applied to the polymer volume in the swollen state:

$$V_{2,s} = \frac{1}{1 + \frac{\rho_{polimero}}{\rho_{disolvente}} \left( \frac{m_s - m_0}{m_s} \right)} \quad \text{equation 4.}$$

where  $m_s$  is the polymer weight in the swollen state.

Experimentally the weights were obtained by the following method:

Hydrogel samples both in the relaxed state or swollen in water until reaching the equilibrium, were introduced in the woven of the TGA at 100°C (boiling point of water), maintaining that temperature until obtaining a constant weight. The measurement of the weight of the samples before and after the evaporation of water, provided the weights  $m_r$ ,  $m_s$  and  $m_0$  that can be replaced in equations 3 and 4 and therefore used to calculate  $V_{2,r}$  and  $V_{2,s}$ .

The obtained values will after be inserted in equation 1, for the determination of the molecular weight between cross-links.

### 3. Results and Discussion

#### 3.1. Water Uptake

A fundamental relationship exists between the swelling of a crosslinked polymer in a solvent and the nature of the polymer and the solvent. The swelling profile of a three dimensional structure in a suitable solvent is one of the most important parameters in swelling measurements [7].

So with the goal of studying the swelling behaviour of the hydrogels, the water uptake of initially dry hydrogels was followed for a time period up to 700 hours. Studying the response of hydrogels with different composition, it could be seen a controlled hydrophilic balance in response to the hydrophilic character both of the PEPM and the HA. After immersion in phosphate buffer solutions, PEPMHA hydrogels, readily swollen up to an extension of 300 to 600%. The weight swelling ratios, or the equivalent water uptakes, were plotted as functions of time.

### 3.1.1. Effect of the composition of hydrogels

Hydrogels with different composition, with variations in the monomer (EPM) concentration, solvent (HA) concentration, polymerized with two different types of crosslinkers (N, N'-methylene bisacrylamide or triethylene glycol dimethacrylate) were submitted to aqueous environments using different pH and temperatures in order to study the effect of these parameters in their water uptake degree.

#### 3.1.1.1. pH sensitivity of hydrogels

Hydrogels were immersed in phosphate buffer solutions of pH 2, 7.4 and 10, at 20°C. Swelling representative curves are shown in figures 45-56.

- Swelling isotherms of PEPM-HA hydrogels using triethylene glycol dimethacrylate as crosslinker:

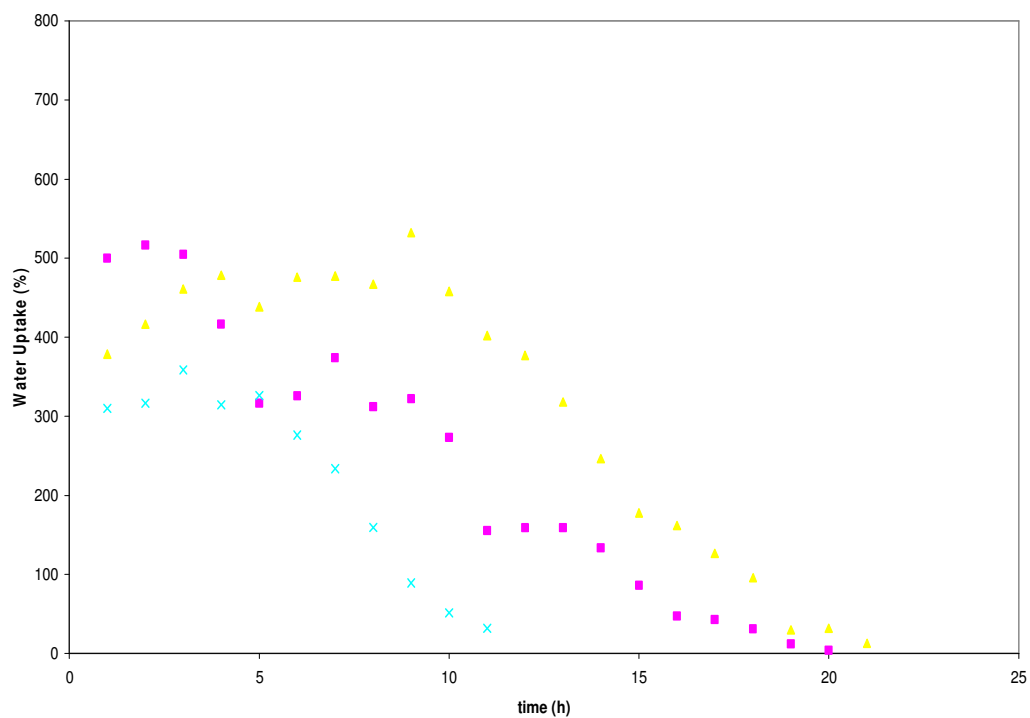


Figure 45. Swelling isotherms of 0.545M PEPMHA (1, 2.5 and 5%), with 1.7% triethylene glycol dimethacrylate as crosslinker, at pH 2.

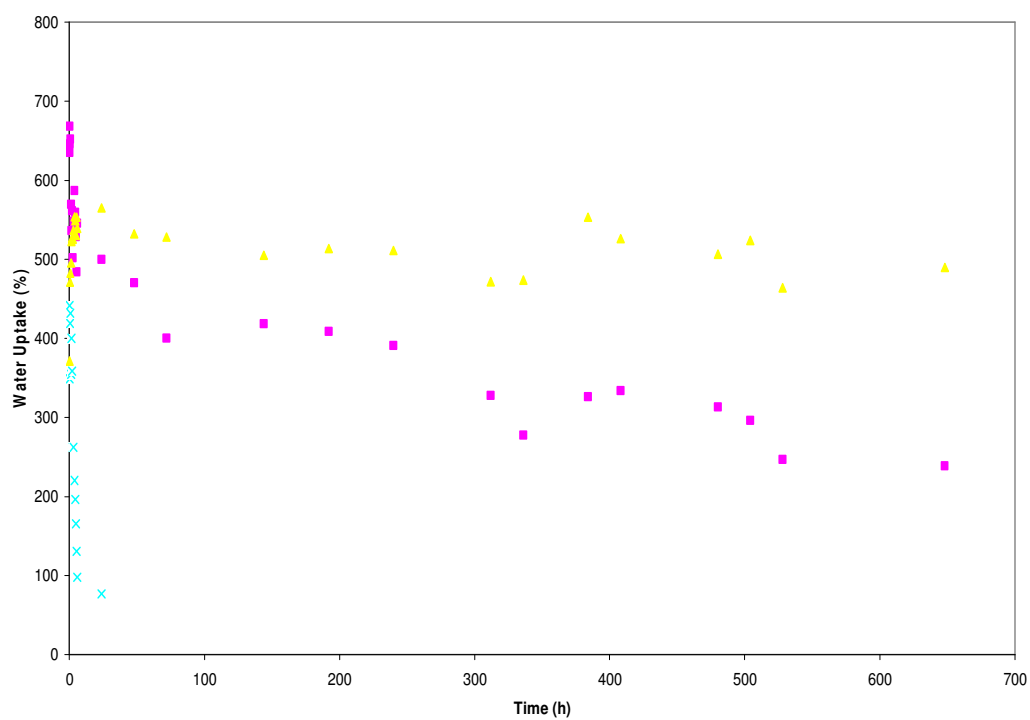


Figure 46. Swelling isotherms of 0.545M PEPMHA (1, 2.5 and 5%), with 1.7% triethylene glycol dimethacrylate as crosslinker, at pH 7.4.

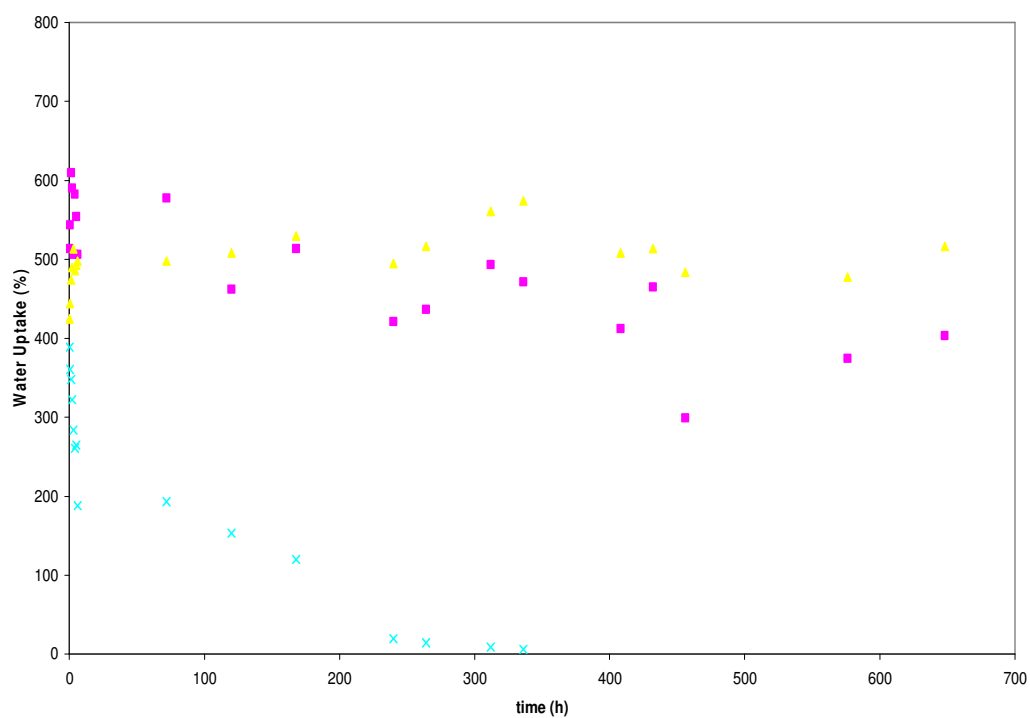


Figure 47. Swelling isotherms of 0.545M PEPMHA (1, 2.5 and 5%), with 1.7% triethylene glycol dimethacrylate as crosslinker, at pH 10.

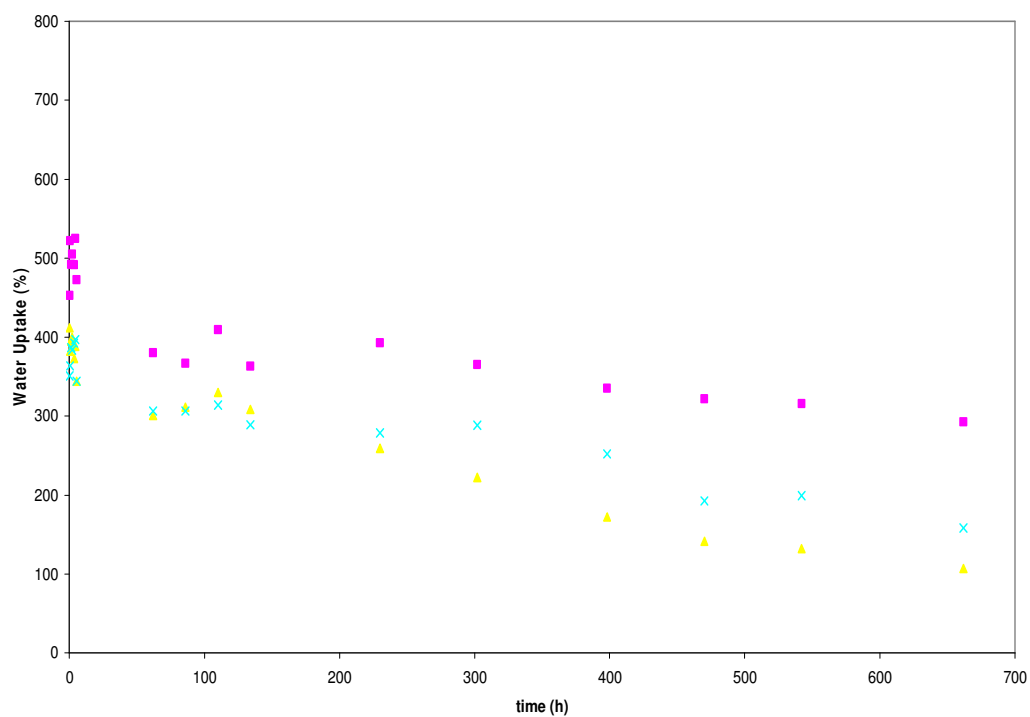


Figure 48. Swelling isotherms of 0.725M PEPMHA (1, 2.5 and 5%), with 1.7% triethylene glycol dimethacrylate as crosslinker, at pH 2.

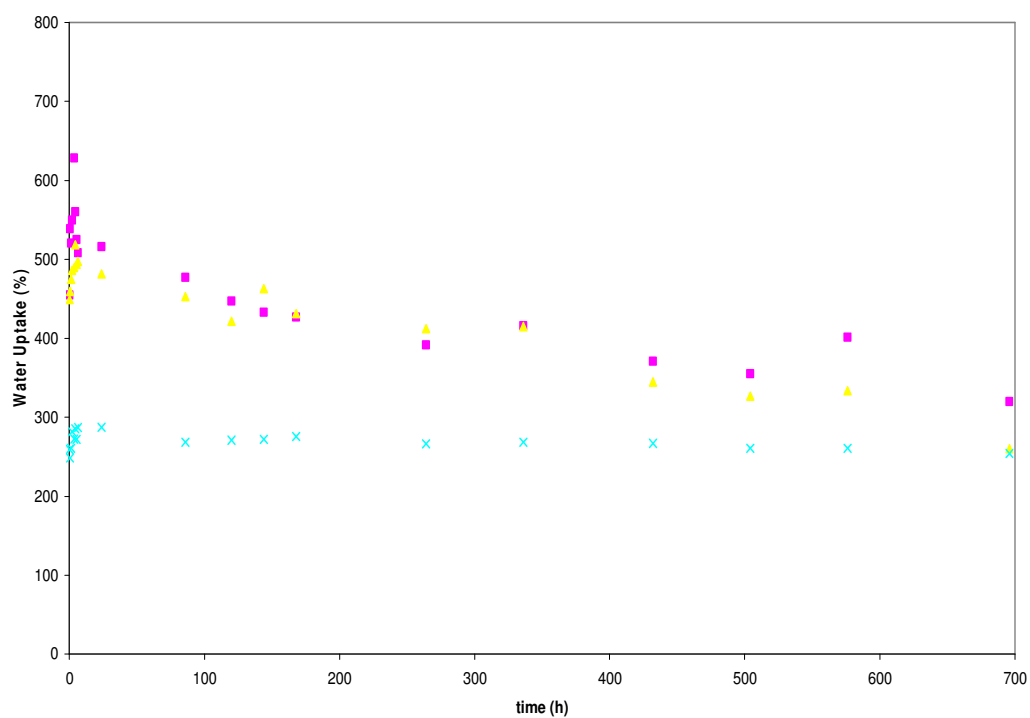


Figure 49. Swelling isotherms of 0.725M PEPMHA (1, 2.5 and 5%), with 1.7% triethylene glycol dimethacrylate as crosslinker, at pH 7.4.

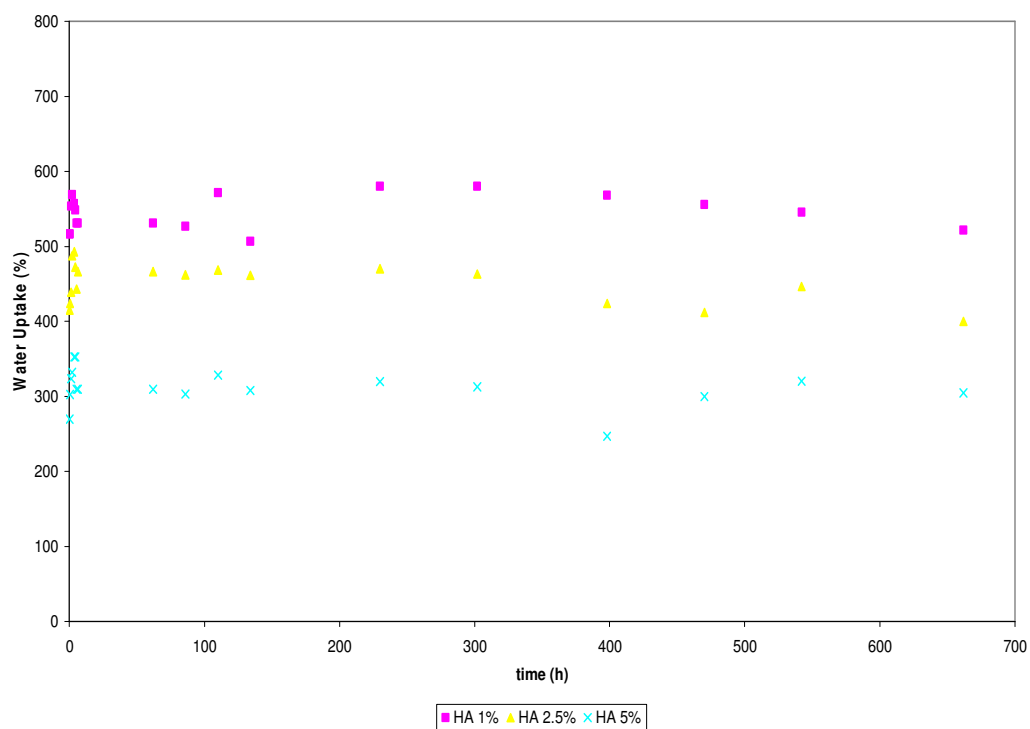


Figure 50. Swelling isotherms of 0.725M PEPMHA (1, 2.5 and 5%), with 1.7% triethylene glycol dimethacrylate as crosslinker, at pH 10.

- Swelling isotherms of PEPM-HA hydrogels using N, N'-methylene bisacrylamide as crosslinker:

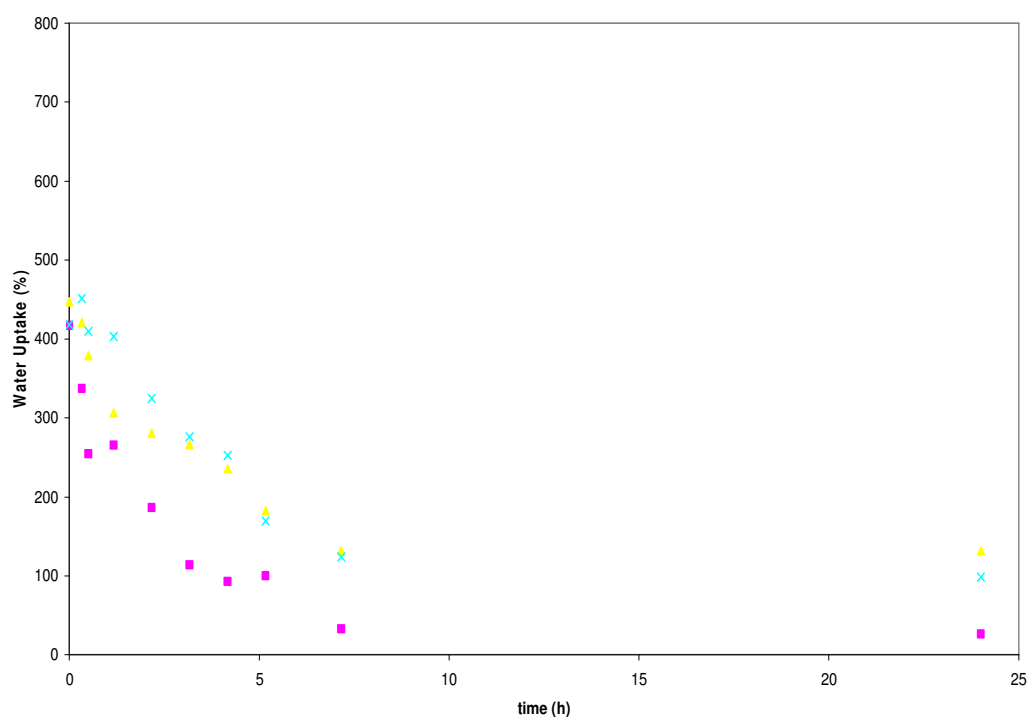


Figure 51. Swelling isotherms of 0.545M PEPMHA (1, 2.5 and 5%), with 2% N, N'-methylene bisacrylamide as crosslinker, at pH 2.

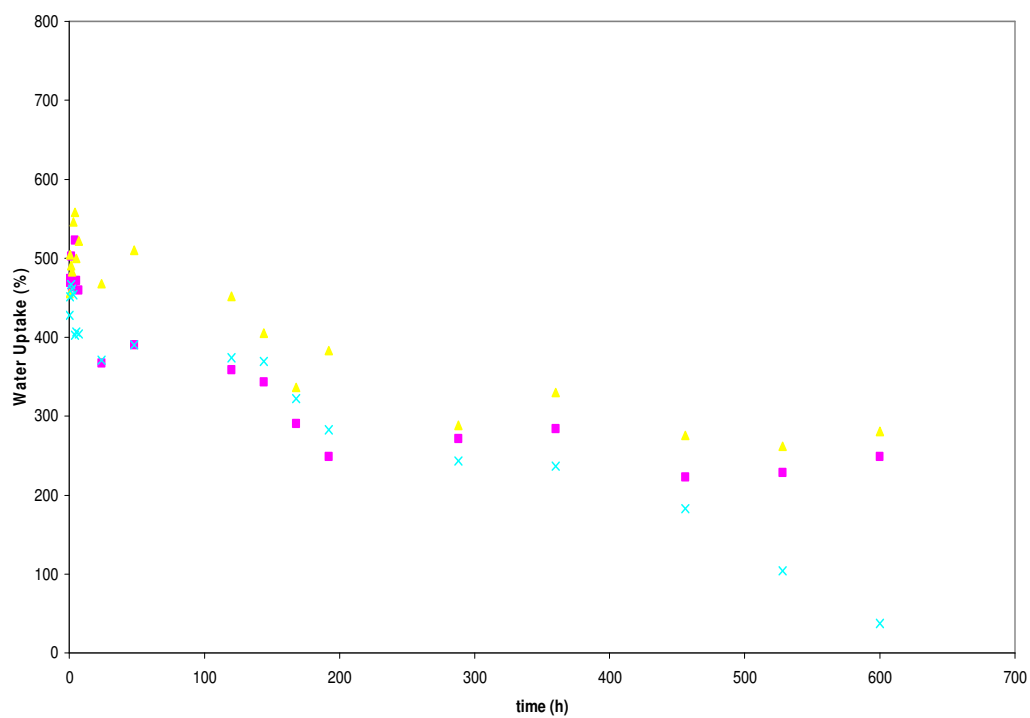


Figure 52. Swelling isotherms of 0.545M PEPMHA (1, 2.5 and 5%), with 2% N, N'-methylene bisacrylamide as crosslinker, at pH 7.4.

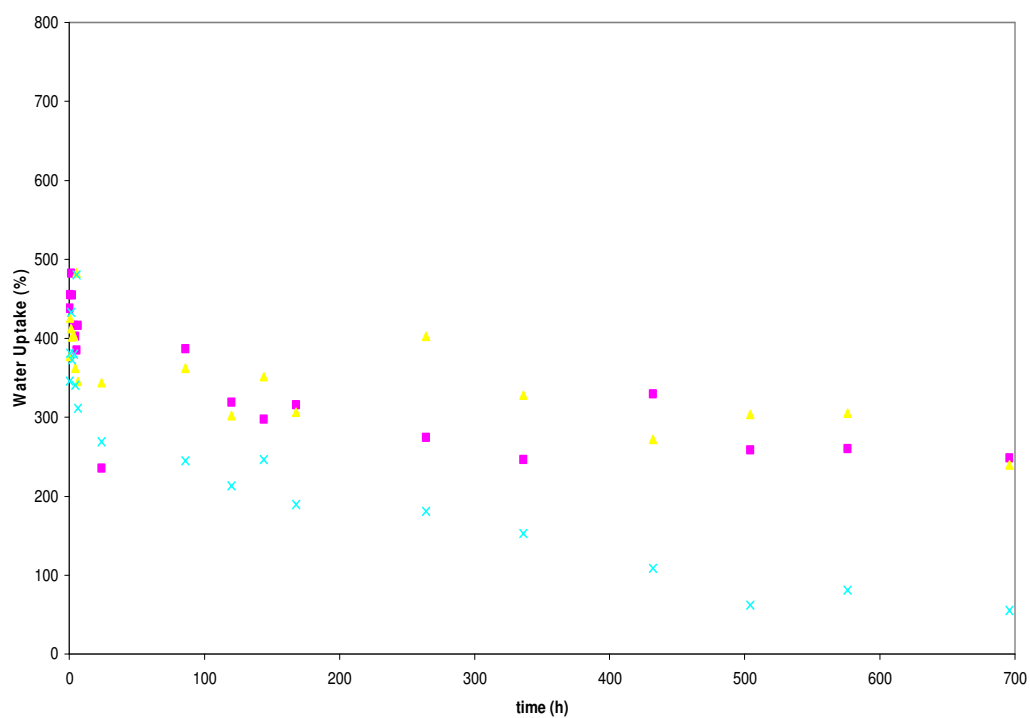


Figure 53. Swelling isotherms of 0.545M PEPMHA (1, 2.5 and 5%), with 2% N, N'-methylene bisacrylamide as crosslinker, at pH 10.

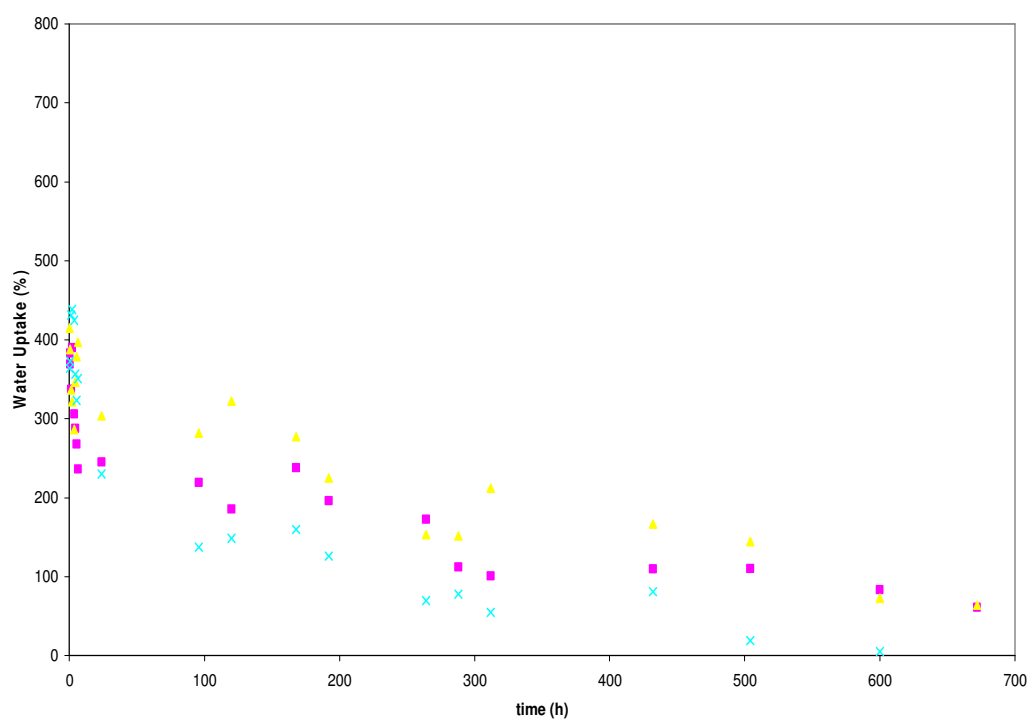


Figure 54. Swelling isotherms of 0.725M PEPMHA (1, 2.5 and 5%), with 2% N, N'-methylene bisacrylamide as crosslinker, at pH 2.



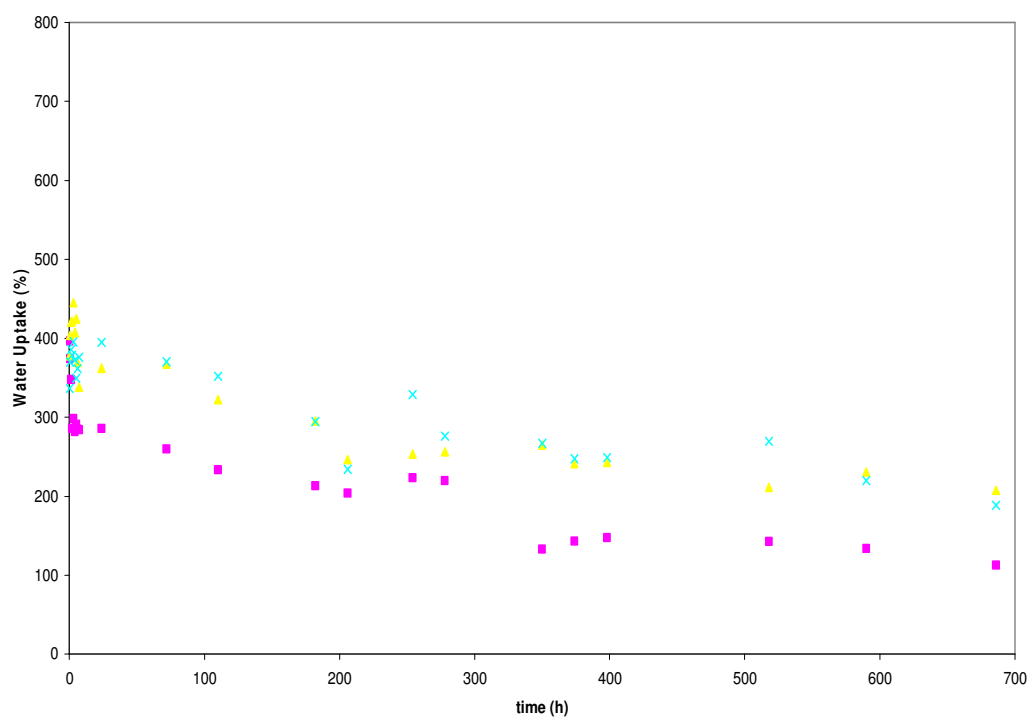


Figure 55. Swelling isotherms of 0.725M PEPMHA (1, 2.5 and 5%), with 2% N, N'-methylene bisacrylamide as crosslinker, at pH 7.4.

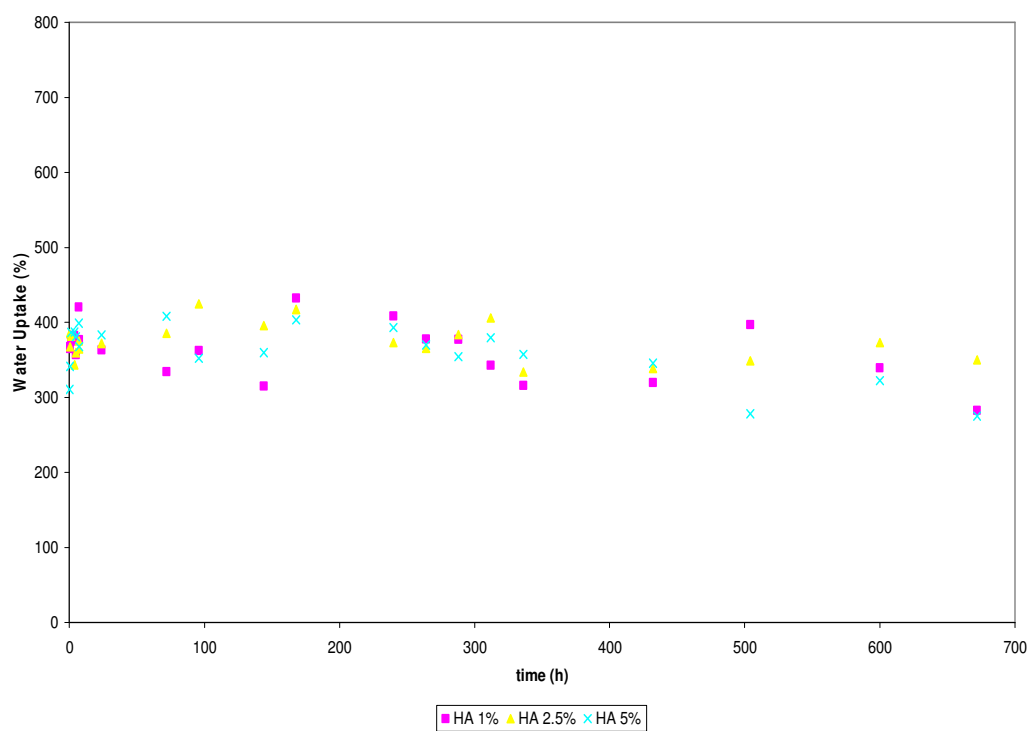


Figure 56. Swelling isotherms of 0.725M PEPMHA (1, 2.5 and 5%), with 2% N, N'-methylene bisacrylamide as crosslinker, at pH 10.

Figures 45-56 show the variation of the water uptake in equilibrium regarding the polymeric system composition.

Regarding the nature of the hyaluronic acid, presenting sensitivity to external stimulus, as variations in the pH, when the carboxylic acid groups on the glucuronic acid residues are below the pKa (3-4), they are in the COOH form [8]. As the pH of the solution increases, the COOH becomes ionized to COO<sup>-</sup>, and the repulsion between the charges causes the hydrogels to swell. At pH 7, then, these groups are predominantly ionized, and the hyaluronan molecule is a polyanion that has associated, exchangeable cation counterions to maintain charge neutrality. So, it is conceivable that the isotherms show a solubilization with immersion time, more significant at pH 2 that might be also supported by a partial hydrolysis of the PEPM. Systems prepared with poly(methacrylic) acid and alginate have shown a similar behavior [9].

In concern to the nature of the crosslinkers, although both are known to be very hydrophilic and flexible, providing highly free water swellable hydrogels, systems prepared with triethylene-glycol-dimethacrylate reached higher water uptake degrees and presented better stability than systems prepared with N,N'-methylene-bisacrylamide. Also, in the case of hydrogels prepared with TriEGDMA it was not observed an increase in the water uptake degree when the concentration of HA was higher, as it was expected. In the other hand, this behaviour was seen for hydrogels with BIS as a crosslinker.

#### 3.1.1.2. Temperature sensitivity of hydrogels

The temperature sensitivity of the hydrogels was assessed by swelling the hydrogels in a phosphate buffer solution at pH 7.4, at 20°C (as in the previous section) and at body temperature, 37°C.

The equilibrium in the systems incubated at body temperature was reached in the first 100 hours and after this period, the water uptake degree showed to be independent with time.

In the following figures are shown the differences between the water uptake degrees of the different groups.

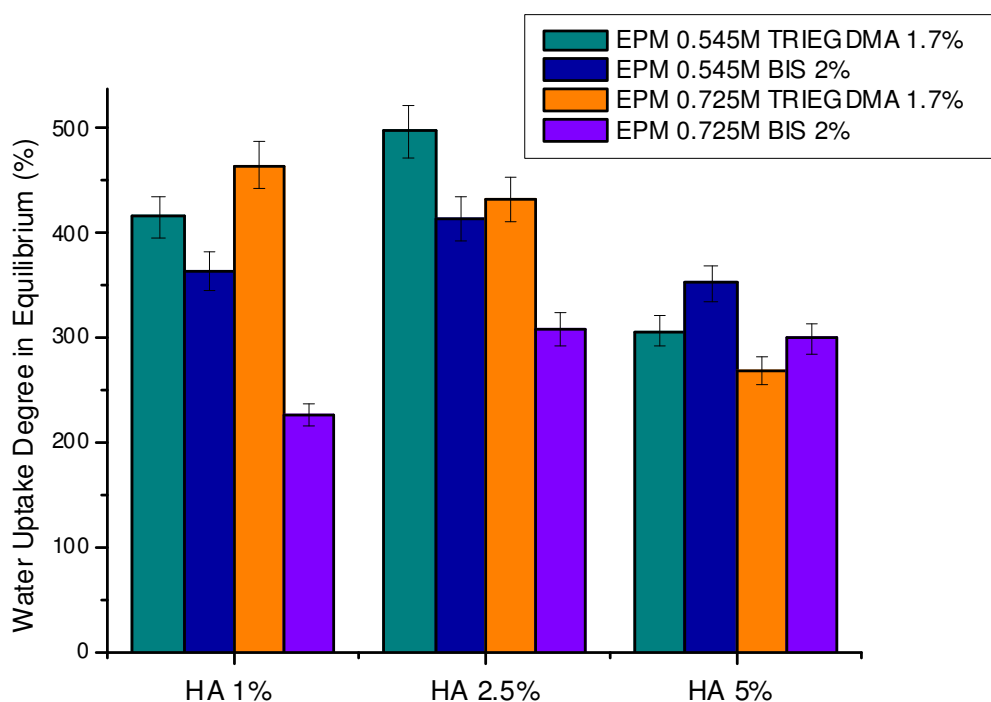


Figure 57. Water uptake degree of PEPMHA polymeric systems in equilibrium, using TriEGDMA or BIS as crosslinkers and  $K_2S_2O_8$  as initiator, at 20°C, pH 7.4.

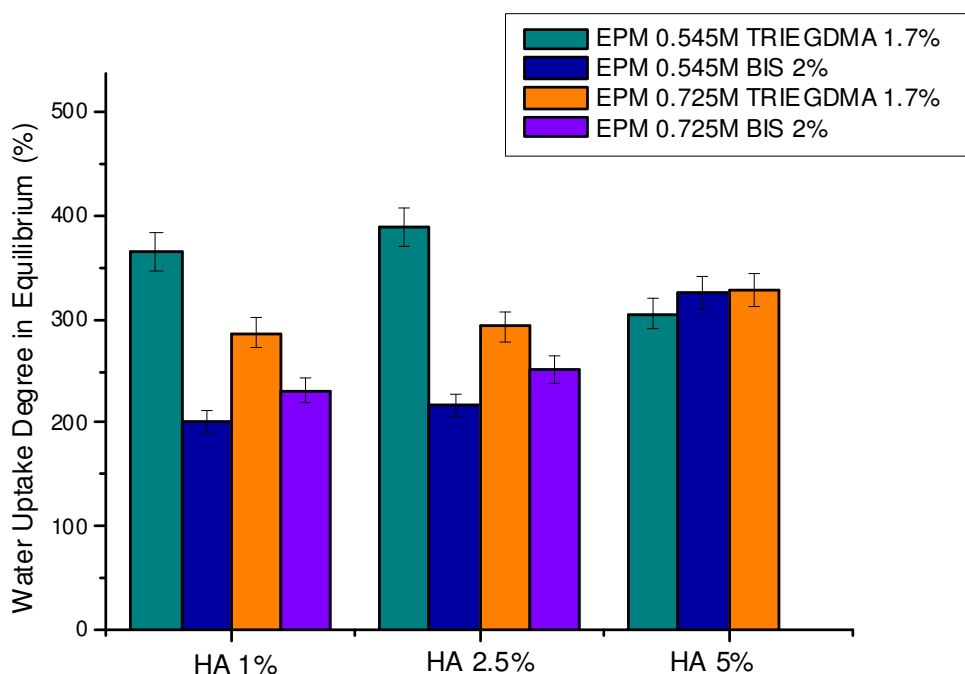


Figure 58. Water uptake degree of PEPMHA polymeric systems in equilibrium, using TriEGDMA or BIS as crosslinkers and  $K_2S_2O_8$  as initiator, at 37°C, pH 7.4.

When hydrogels were incubated at different temperatures a different behaviour was seen regarding the composition.

In the systems studied the hydration rate increased with the proportion of hydrophilic monomer used, except for higher values of HA used. However, the differences shown were not statistically different ( $p < 0.05$ , one way analysis of variance, ANOVA). So, obviously, at the selected temperatures and pH 7.4, the carboxylic group of the PEPM and both the nature of the crosslinkers and the effective crosslinking degree are actively determining the water retention character.

In the systems incubated at 20°C, when TriEGDMA is used as the crosslinker, an increase in the EPM concentration led to an increase in the water uptake capability.

In the other hand, when BIS is the crosslinker, the opposite is observed.

When the temperature of the aqueous solution where hydrogels were immersed is 37°C, the water uptake response of the materials changed. So, in this case, when TriEGDMA is the crosslinker, an increase in the EPM concentration led to a decrease in the water uptake, as for the systems prepared with BIS, an increase in the EPM augmented the water retention capability.

A more effective crosslinking using BIS would explain a lower water uptake in the systems prepared with this crosslinker.

Also, we could predict that the polymerization was rather heterogeneous, as the increase in the viscosity of the HA solution would difficult the formation of cross-links, as for hydrogels prepared with HA 5%.

Despite the differences caused within groups, there is clear evidence that the water uptake degree was higher in hydrogels incubated at 20°C. If we take into account previous studies from González et al., the PEPM presented a temperature sensitive character, where the transition temperature was of 34°C [2]. Therefore, the temperatures here mentioned are situated below (20°C) and above (37°C) this limit. So, once more the values obtained were in accordance with the reported ones. The hydrogels were more swollen at lower temperatures.

### 3.2. LCST determination by water uptake

As mentioned before, there are hydrosoluble polymers that present the property of diminishing their solubility when the temperature is augmented and precipitating at a critic temperature, LCST. This phenomenon is influenced by the variations of molecular interactions in response to temperature. These type of polymers present both hydrophilic and hydrophobic groups thus presenting an amphipilic character (Figure 59). It is the presence of these groups and the strength of the molecular interactions that will command the water and salts permeability when the temperature is altered.

So, above the LCST, as the hydrophobic interactions are dominant the polymer precipitates and there is a decrease in the water content; below the LCST, hydrogen bonding between hydrophilic segments of the polymer chain and water molecules are the dominant interactions, leading to enhanced dissolution in water and the swelling of the hydrogel.

As mentioned before, PEPM, due to its hydrophilic groups, as the cyclic amide in the pyrrolidone, can create hydrogen bonds with the water molecules and presents a LCST of 34°C. Although in comparison with other methacrylate based polymers as poly(N-acryloyl pyrrolidone) – LCST of 56°C, presents a lower transition temperature due to the presence of hydrophobic groups shown in the image (Figure 59).

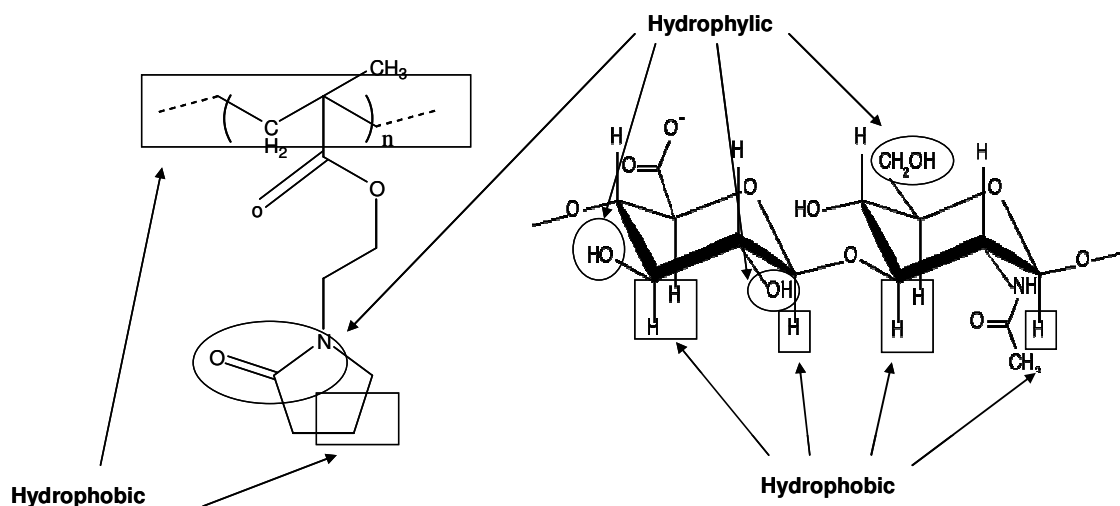


Figure 59. Structure of HA and the homopolymer PEPM and its respective hydrophilic and hydrophobic groups.

Crosslinked systems prepared from thermosensitive polymers present a critical transition temperature related to the LCST [6]. So, it would be expected that with the crosslinking of the EPM in the presence of a highly hydrophilic biopolymer, HA, the transition temperature would be increased.

To determine the critical temperature of the crosslinked systems, it was performed a study of the swelling degree in equilibrium in response to temperature variation. Hydrogels were immersed in phosphate buffer solutions, at different temperatures and different pH.

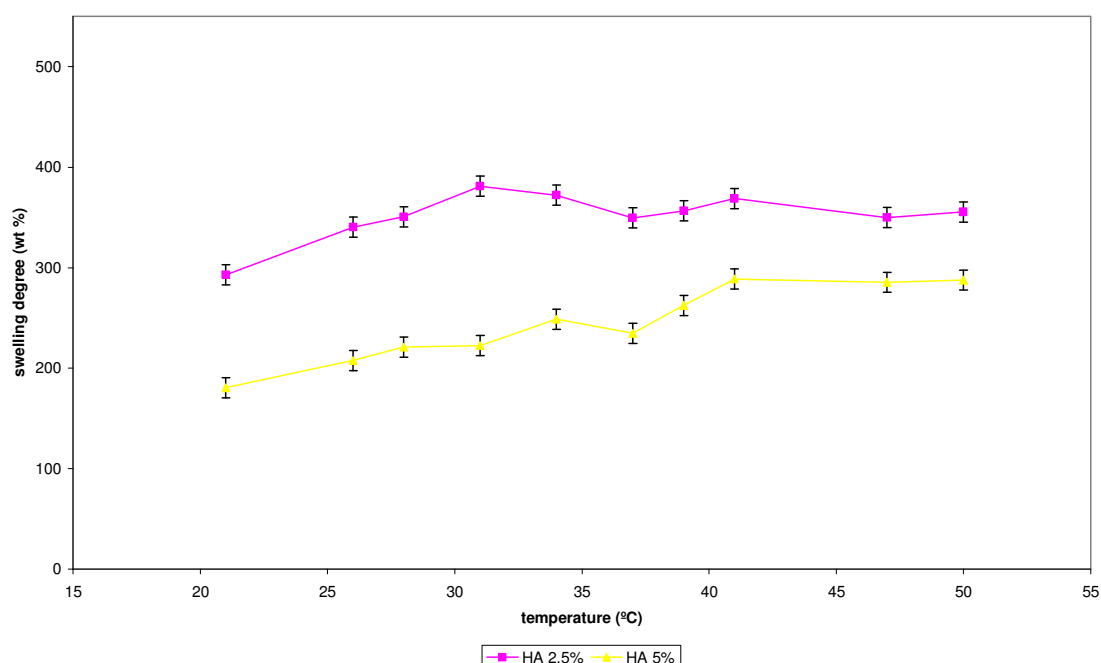


Figure 60. Influence of the temperature in the swelling degree in equilibrium of polymeric systems with EPM 0.725M, BIS 2%,  $K_2S_2O_8$   $2 \times 10^{-2}M$ , HA 2.5 and 5%, in an aqueous phosphate solution with pH 7.4.

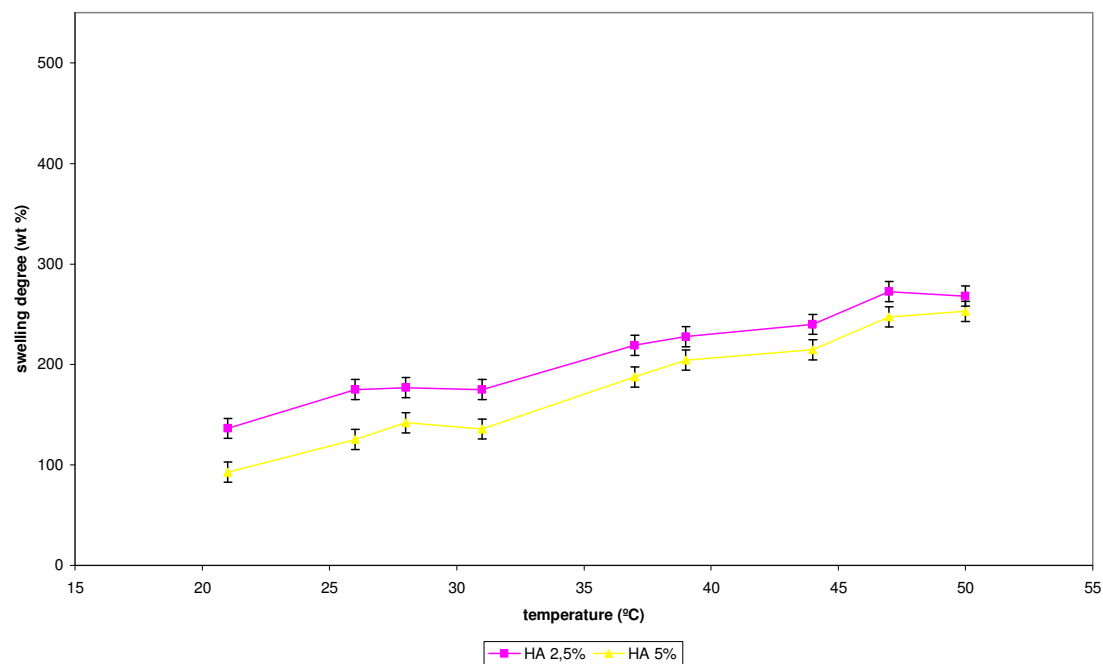


Figure 61. Influence of the temperature in the swelling degree in equilibrium of polymeric systems with EPM 0.725M, BIS 2%,  $K_2S_2O_8$   $2 \times 10^{-2}M$ , HA 2.5 and 5%, in an aqueous phosphate solution with pH 2.

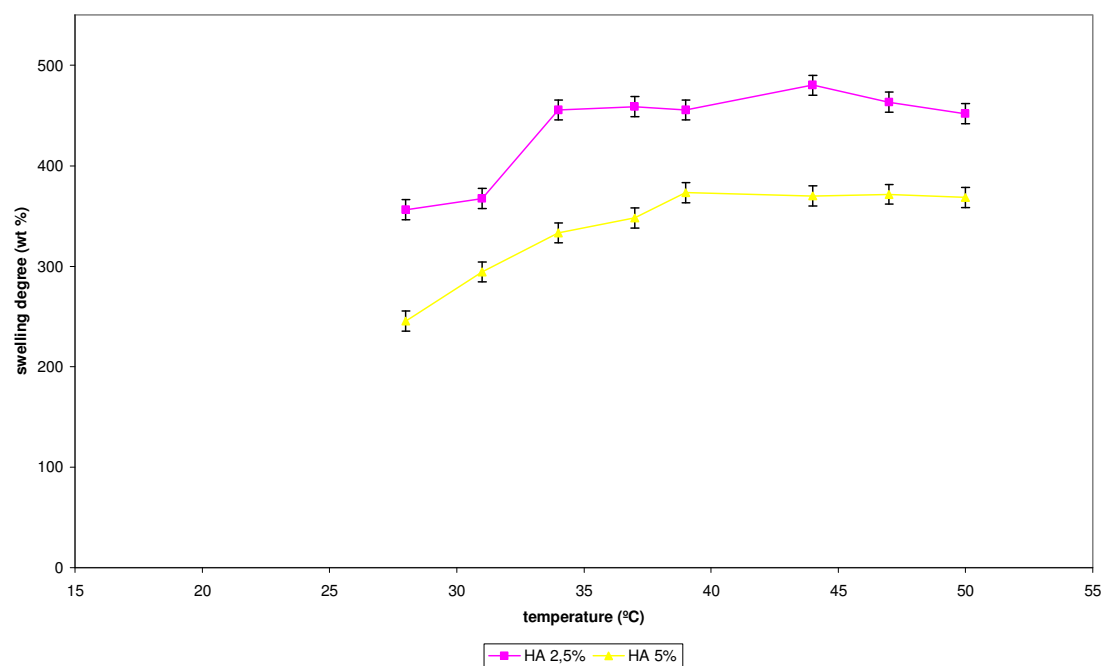


Figure 62. Influence of the temperature in the swelling degree in equilibrium of polymeric systems with EPM 0.725M, BIS 2%,  $K_2S_2O_8$   $2 \times 10^{-2}M$ , HA 2.5 and 5%, in an aqueous phosphate solution with pH 10.

In this experiment it could be determined whether the crosslinked hydrogels presented a volume variation in response to the different temperatures.

Although there was in fact a volume variation, this was not significant in order to prove the existence of two different states of the polymeric network, expanded and collapsed when the temperature was either below or above the critical temperature determined for crosslinked PEPM in previous work [6].

In the case of PEPMHA systems, the water uptake degree has increased approximately 1.5 times at higher temperatures.

What can be assumed from these facts is that probably the carboxylic groups of the hyaluronic acid bonds with water are controlling the water uptake degree and mismatching the thermo-responsive character of the PEPM.

So, with an increase of temperature, the flexibility augments inducing an increase in the water uptake capability.

In concern with the different pH used, there was a clear effect on the swelling degree when the pH was altered. At a pH below 7.4, the swelling diminished and when hydrogels were incubated at a higher pH, the swelling increased. This fact is again explained by the ionisable character of the molecule of hyaluronic acid and the conformation the molecule acquires when in presence of solutions with different acidity [9].

### 3.3. Determination of the average molecular weight between cross-links

One of the basic parameters that describe the structure of a hydrogel is the average molecular weight between cross-links ( $M_c$ ).

In other words, it describes the average molecular weight of polymer chains between two consecutive junctions. These junctions may have different nature, chemical cross-links, physical entanglements, crystalline regions, or even polymeric complexes.

In the case of swelling-controlled release systems and hydrogels used for drug delivery, it is important that the swelling increases progressively with time, but also that the mesh size of the hydrogel is able to molecularly accommodate the drug. Therefore, the mesh size of the network is also an important parameter for prediction of hydrogel permeability [10].

As mentioned before, several theories were proposed to calculate the molecular weight between cross-links. For this study, rubber elasticity theory was taken into account.



### 3.3.1. Volume fractions determination

From thermogravimetric analysis, volume fractions in the relaxed and swollen state conditions could be determined (Figure 63). For hydrogels where the total monomer concentration used in the initial polymerization mixture was the same, the volume fractions in the relaxed state were very similar within the different compositions and showed an increase, when comparing to hydrogels with lower concentration of total monomer present.

However, in the swollen state, an increase in the initial total amount of monomer, maintaining the amount of crosslinker (BIS 2%), was accompanied by a decrease in the volume fraction, which was expected as these networks become more robust and dense, swelling more, hence the fraction of dissolvent in the same volume of sample is higher. Again, when using TriEGDMA as crosslinker, an increase in the concentration of HA makes the volume fraction of these hydrogels decrease, inducing the gels to swell more.

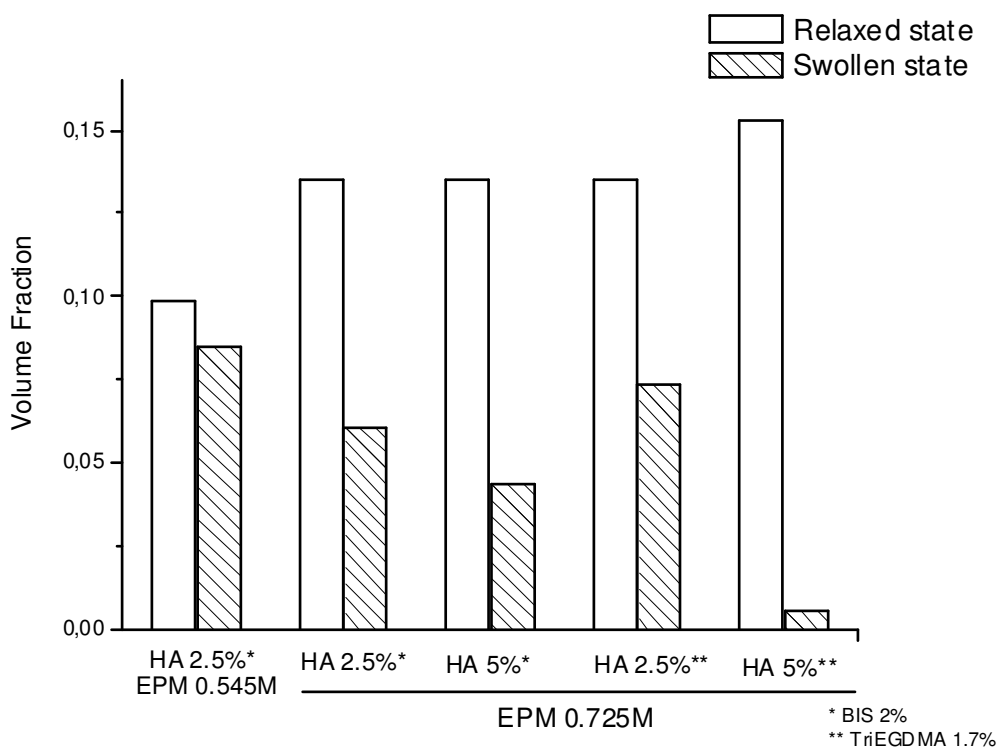


Figure 63. Volume fraction in the relaxed and swollen state of PEPMHA.

The most plausible reason for this occurrence should be related to the heterogeneous character of the hydrogels, as seen in other studies with polyacrylamide crosslinked hydrogels using N,N'-methylene-bisacrylamide or tyrosine-lysine-tyrosine dimethacrylate (DMTLT). As a result, the structure of the hydrogels would present regions with different density of crosslinking. And, as also reported in other studies, regions more crosslinked will disperse light and reduce the visible light through the hydrogel. Therefore the different opacity obtained for PEPMHA hydrogels within different composition [11].

### 3.3.2. Determination of the $M_c$

Using experimental values of  $G'$ , relaxed and swollen state volumes,  $V_{2,r}$  and  $V_{2,s}$  respectively, and equation 1, average molecular weight between cross-links,  $M_c$ , was determined.

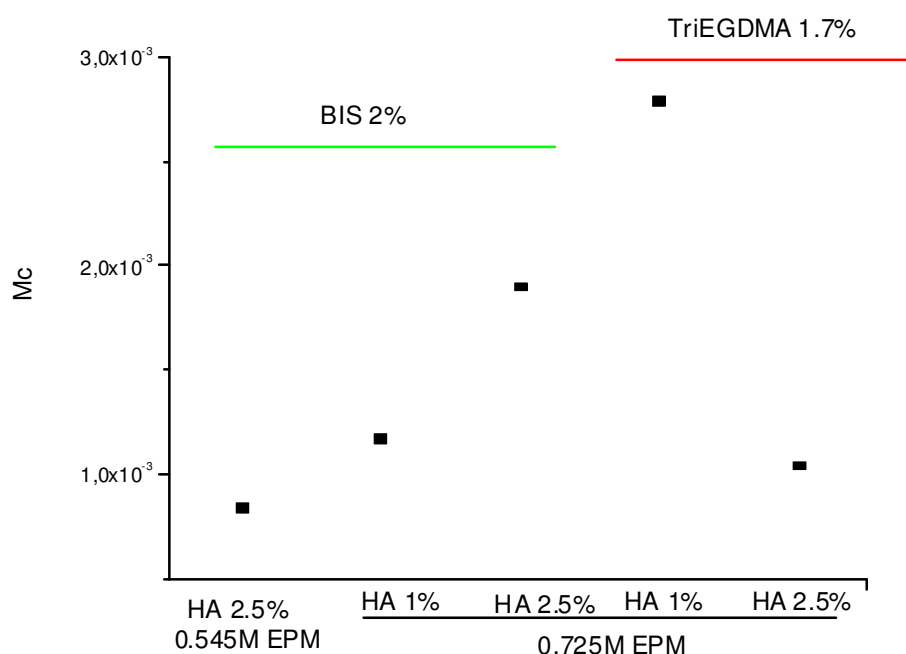


Figure 64. Average  $M_c$  values in relation to the different hydrogels.

It is very difficult to give a reasonable explanation of the values of  $M_c$  for both systems because of the different reactivity of the acrylamide and methacrylic double bonds, but it is clear from the average  $M_c$  values, determined by viscoelastic measurements, in concern to the different hydrogels, there is an effect of the monomer concentration and the viscosity increment due to the hyaluronic acid concentration (Figure 64).

It must be noted that, as stated in diverse literature, the values of  $M_c$  obtained through viscoelastic experiments aren't as accurate as the ones given by swelling experiments. In the first case, entanglements (which tend to increase the modulus) and other characteristics of the chains, such as the distribution of the acrylic nodes in the polymer chains, and the effective branching and crosslinking according to the chemical structure of the crosslinker monomers, will have a stronger influence on the mechanical properties, and ultimately in the calculated values of  $M_c$ .

### 3.4. Relation between swelling and mechanical properties of the PEPMHA hydrogels

The following table and graphic synthesise some of the determined parameters concerning swelling and mechanical properties:

Table 6: Mechanical properties and water uptake degree (at pH 7.4, 37°C, 48h after immersion) of PEPMHA hydrogels with different compositions. The modulus indicated was measured for a frequency of 10 Hz.

	<b>EPM 0.545M</b>		<b>EPM 0.725M</b>			
	<b>BIS 2%</b>				<b>TriEGDMA 1.7%</b>	
	<b>HA 2.5%</b>	<b>HA 5%</b>	<b>HA 2.5%</b>	<b>HA 5%</b>	<b>HA 2.5%</b>	<b>HA 5%</b>
<b>G' (Pa)</b>	1,001x10 <sup>6</sup>	8.849x10 <sup>5</sup>	1.303x10 <sup>6</sup>	6.930x10 <sup>5</sup>	5.77x10 <sup>5</sup>	6.997x10 <sup>5</sup>
<b>tan δ</b>	0.4068	0.3950	0.4081	0.6425	0.2471	0.29
<b>ρ<sub>real</sub> (g.cm<sup>-3</sup>)</b>	1.14	0.82	1.23	1.14	1.17	0.95
<b>Water uptake (%)</b>	195.71	330.6	240	275	324	330

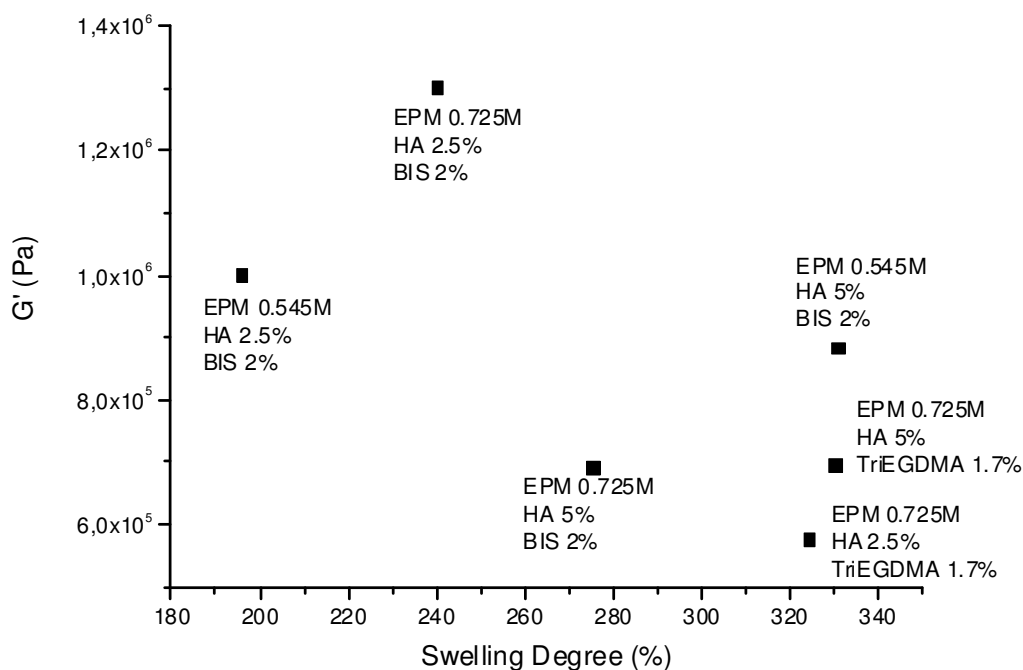


Figure 65. Storage modulus as a function of the equilibrium degree of swelling in PEPMHA hydrogels in an aqueous solution of pH 7.4.

When comparing the nature of the crosslinkers, apart from being in a higher concentration, the molecule of BIS is clearly promoting the formation of more cross-links, affecting the mechanical strength of the hydrogels (higher modulus) and their water uptake capacity (lower swelling degree), although in published work the modulus of several materials was not found to depend on the type of crosslinking agent used when less than 5% of the crosslinking agent was used [12].

In general, when the amount of HA used is increased, there is an increase in the swelling degree, thus revealing that the molecule of HA is enhancing the bonds with the surrounding water molecules, as predicted in the beginning of the study. This increase is accompanied by a decrease in modulus and thus being responsible for the reduction of the mechanical strength of the materials.

In the other hand, when the amount of HA is fixed, and EPM concentration varied, the increase in the monomer concentration leads, in the case of HA 2.5%, to an increase of mechanical strength and an increase of swelling. Now, when the amount of solvent used during the polymerization is large, the crosslinking agent will tend to form cycles rather than cross-links. This change will reduce the effective cross-link density, thus lowering the material strength. So it would be expected an increase of the  $G'$  due to the formation

of a material more robust. However, this result should be accompanied by a decrease in the swelling degree, which didn't happen. What probably is happening is that with a higher concentration of the monomer, the HA molecule is more likely to become more entrapped within the hydrogel and thus conferring a higher water uptake degree than the foreseen.

However, the same didn't happen when HA 5% was used. Within these systems, an increase in the initial concentration of monomer was followed by a diminution both in the mechanical strength and swelling degree of the hydrogels. A possible explanation might have to do with the high viscosity of the dissolvent that may impede in the formation of cross-links, decreasing the effective crosslinking degree, responsible for a decrease in the modulus of the material and preventing the physical entanglement of the HA molecules to the system.

#### **4. Conclusions**

The prediction and control of mechanical properties in hydrogels is of great importance in assessing the applicability of hydrogels. The mechanical properties can be intimately related to the polymer structure, crosslinking density and the degree of swelling, and through variations in the polymeric composition, crosslinking degree and agents, polymerization conditions it is possible to manipulate the mechanical properties of the hydrogels. As said previously, the challenge with hydrogels concerns obtaining optimal mechanical strength whilst maintaining their hydrophilic character. Hydrogels containing high water level (>95% wt.) have usually a compressive strength lower than 0.01 Pa.

So, after the description and analysis of the several parameters in the last 2 chapters we were able to conclude that:

PEPMHA polymeric systems are environmentally sensitive, and that the degree of swelling can be altered by changes in temperature and acidity:

- at physiological pH and at different temperatures (20 and 37°C) there is a higher influence possibly due to crosslinker nature and the carboxylic group of the PEPM;

- when pH is varied or both pH and temperature, the ionisable character of HA plays a more active role, mismatching the amphiphilic character of the PEPM;

The molecule of HA clearly affects the mechanical performance of the hydrogels and their water uptake capability.

In order to look for better polymerization times, effectiveness in the polymerization reaction that would influence in the mechanical performance and water uptake retention, a new approach to these materials was used. Instead of using temperature as the vehicle of conducting the polymerization, we intended to use light.

Further in this thesis there is a chapter dedicated to the use of photopolymerized PEPMHA hydrogels and the study of their properties.

## 5. Bibliography

1. N.A. Peppas and A.G. Mikos, Preparation Methods and Structure of Hydrogels. Hydrogels in Med and Pharm, 1986: p. 1-26.
2. E.F. González, Preparación y caracterización de nuevos geles interpenetrados de agarosa-poliacrilamida, in Instituto de Ciencia y Tecnología de Polimeros. 2007, Complutense: Madrid.
3. R.R.J. Flory P.J., Statistical mechanics of crosslinked polymer networks. I. Rubberlike elasticity. J Chem Phys, 1943. 11: p. 521.
4. M.E.W. Peppas N., Crosslinked hydrogels considered as swollen elastic networks. J Appl Polym Sci, 1977. 21(1763).
5. M. Peppas N., A.G., Hydrogels in Medicine and Pharmacy: Volume I: Fundamentals. 1987, Boca Raton, Florida: CRC Press.
6. N. Gonzalez, Nuevos Sistemas Poliméricos Sensibles al pH y Temperatura. Aplicaciones Biomédicas, in Physics-Chemistry. 2006, Universidad Complutense: Madrid.
7. H. Kaplan and A. Güner, Characterization and Determination of Swelling and Diffusion Characteristics of Poly(N-vinyl-2-pyrrolidone) Hydrogels in Water. Journal of Applied Polymer Science, 2000. 78(5): p. 994-1000.
8. V.C. Hascall, Laurent, T.C., Hyaluronan: structure and physical properties. 1997.
9. S.J. Kim, Yoon, S.G., Lee, Y.H., Kim, S.I., Bending behavior of hydrogels composed of poly(methacrylic) acid and alginate by electrical stimulus. Polymer International, 2004. 53(10): p. 1456-1460.
10. C.S. Brazel, Peppas, N.A., Mechanisms of solute and drug transport in relaxing, swellable, hydrophilic glassy polymers. Polymer, 1999. 40(12): p. 3383-3398.
11. P.P. Ibañez, Sistemas Poliméricos Inteligentes con Entrecruzamiento Biodegradable, in Departamento de Química Macromolecular. 2006, Universidad Complutense: Madrid.
12. K.S. Anseth, Bowman, N., Peppas, L.B., Mechanical properties of hydrogels and their experimental determination. Biomaterials, 1996. 17(17): p. 1647-1657.

## **Chapter III- Evaluation of the cellular behaviour in PEPMHA cell-constructs**

### **1. Introduction**

Until now, it was shown that varying the composition, including monomer concentration, crosslinkers, molecular weight, polymerization techniques, among others, have influenced chemical, physical and mechanical properties of the materials.

Tissue Engineering is a novel area that uses cells, biomaterial scaffolds, and signalling molecules for the repair of diseases and/or regeneration of trauma- related tissue defects [1].

Bovine articular chondrocytes were isolated from articular joints and expanded in conventional monolayer cultures to provide a sufficient number of cells. When articular chondrocytes are expanded in two dimensional culture conditions, the process of amplification causes a dedifferentiation of the chondrocytes, a process during which cells regain their ability to divide, lose their rounded morphology to a typical spindle-like or stellate cell shape, leading the cells to assume a fibroblast-like phenotype [2, 3]. This is accompanied by an alteration in the cells expression profiles [4].

The collagen types, namely II, IX, X and XI are traditionally considered specific for cartilage, being collagen type II the major protein produced by chondrocytes in articular cartilage. Thus, it is very common the use of immunolocalization of collagens test to verify their expression during the expansion and proliferation of chondrocytes.

So, in the case of dedifferentiated cells, there is a switch in their collagen production from types II, IX and XI to types I, III and V [5].

As cells start to reach confluence and multipack in tri-dimensional structures they begin to re-differentiate, regaining the normal articular cartilage-specific matrix molecules, like the collagen type II.

For this reason, it is critical to study the redifferentiation of cells and their phenotypic changes. In the case of cartilage-tissue engineering, their chondrogenic potential and the importance of a homogenous distribution of vital cells in a heterogeneously composed biomaterial that acts as a cell carrier, represent main prerequisites to generate efficient tissue substitutes.



## 1.1. Objective

We intend to study and describe the ability of the proposed polymeric systems to support chondrocytes growth in vitro.

Until the present time, any effect of cell-biomaterial interactions on cell attachment, activity, morphology or phenotype retention has been documented.

A series of novel synthetic- natural based polymers with varying proportion rates and using different crosslinkers have been prepared. As cited in chapter I, the use of a synthetic polymer would allow a better control of the biomaterial properties, allied to a greater biocompatibility of the natural based polymer.

It is of high relevance note that the molecular weight of HA has been reported to affect a variety of cell types. Cells have specific responses to HA of different sizes. It seems that high molecular weight HA does not initiate a program of gene expression, whereas a variety of genes that regulate biological properties are expressed in response to lower molecular weight HA [6-8].

So, we expect that the presence of the hyaluronic acid, of low molecular weight, in the semi-IPNs produced will enhance the cell proliferation.

The effect of the different polymeric systems to support chondrocytes attachment and expansion will be then assessed.

The experimental work concerning biocompatibility studies to be presented in this chapter will be divided in two sections:

- a first section where the viability of different cell types will be evaluated, and their adhesion to the different PEPMHA hydrogels;
- a second section, where cells, in the case of maintaining viability will be tested to engineer a cartilage-like tissue, studying the cells adhesion and proliferation and the formation of an extracellular matrix with active production of specific molecules and their quantification.

## 2. Materials and Methods

### 2.1. Scaffolds production

The materials were processed as in chapter I, and for biocompatibility assays the following groups were used:

Table 7: Scaffolds composition as for the amount of monomer 2- ethyl (2-pyrrolidone) methacrylate (EPM) polymerized in the presence of hyaluronic acid (HA), using  $K_2S_2O_8$  as the system free radical initiator and triethylene glycol dimethacrylate (TriEGDMA) or N, N'-methylene bisacrylamide (BIS) as the crosslinkers.

Group	J	K	L	M
[Monomer] EPM	0.545M	0.545M	0.725M	0.725M
[Initiator] $K_2S_2O_8$	$2 \times 10^{-2}M$	$2 \times 10^{-2}M$	$2 \times 10^{-2}M$	$2 \times 10^{-2}M$
Crosslinker %	1.7% TriEGDMA	2% BIS	1.7% TriEGDMA	2% BIS
Polymer HA %	1%- J <sub>1</sub> 2.5%- J <sub>2</sub> 5%- J <sub>3</sub>	1%- K <sub>1</sub> 2.5%- K <sub>2</sub> 5%- K <sub>3</sub>	1%- L <sub>1</sub> 2.5%- L <sub>2</sub> 5%- L <sub>3</sub>	1%- M <sub>1</sub> 2.5%- M <sub>2</sub> 5%- M <sub>3</sub>

### 2.2. Sample sterilisation

Scaffolds were sterilised under U.V. light irradiation for approximately 12 hours, both sides.

### 2.3. Sample preparation

After being sterilised, scaffolds were washed several times, first with phosphate buffered saline (PBS) and after with basic medium, where they were allowed to swell for 24 h, 37°C, prior to cell seeding. The reason for this is so that the scaffolds would reach the plateau of their swelling degree curve, with few variations in their physical structure, namely pore size, avoiding this property to influence the cells attachment and spreading.

## 2.4. Controls preparation- agarose gels

The agarose gels served as reference materials for normal cellular activity and their preparation involved simultaneous cell encapsulation (2.6.2.1. Seeding agarose gels for TE).

## 2.5. Cell isolation and expansion

### 2.5.1. Bovine cartilage dissection

Articular cartilage was harvested from bovine metacarpophalangeal joint of adult animals (18-24 months) within 4 hours of slaughter. Tissue was sprayed with industrial methylated spirit (IMS), and the hoof and upper leg were wrapped in aluminium foil and sprayed with IMS. The limb was transferred to a class II laminar flow cabinet and the joint capsule cut to open the articular joint. Tendons and ligaments were carefully severed and the cartilage surface exposed. Full depth cartilage slivers were taken and placed in PBS. Care was taken not to remove the subchondral bone. The excised cartilage slivers were cut into small (approximately 3 mm x 3 mm) sections.

### 2.5.2. Bovine chondrocyte isolation

Chondrocytes were isolated by sequential enzymatic digestion.

The cartilage slivers were washed twice with PBS and incubated with 0.25% (w/v) trypsin for 30 minutes at 37°C with agitation, followed by washing in complete medium to inhibit further enzymatic activity. The cartilage pieces were subsequently incubated in collagenase for 18 h at 37°C, with agitation. The cell suspension was passed through a 70 µm cell sieve and centrifuged (1000 rpm, 5 minutes) to pellet the chondrocytes. The isolated cells were washed twice in 10 ml PBS by re-suspension and centrifugation. The chondrocytes were finally re-suspended in 10 ml expansion medium and the cell number determined using a haemocytometer.

## 2.6. Cell expansion

Freshly isolated chondrocytes, prepared as described in the previous section were seeded into tissue culture Petri dishes at an initial density of  $2 \times 10^6$  cells per dish with 10 ml expansion medium. The cell number was expanded in a temperature-controlled 37°C incubator, with an atmosphere of 95% air/ 5% CO<sub>2</sub> and 95% humidity. Expansion medium was changed every 3 to 4 days until cells were almost confluent, when they were passaged. Cell monolayers were washed twice in warmed PBS and disassociated using 2 ml trypsin-EDTA (Appendix) per dish at 37°C for 5-10 minutes. Enzyme activity was blocked with 5% v/v FCS and the cell suspension was centrifuged at 1000 rpm for 5 minutes to pellet the cells (now known as passage 0 or P0). The chondrocytes were re-suspended in expansion medium before being divided to other tissue culture Petri dishes, at a density of  $1.5 \times 10^6$  cells per plate. Chondrocytes were allowed to expand until almost confluent as above and the disassociation procedures were repeated (to obtain P1 cells). Cells were also passaged according to this method, to obtain passage 2 (P2) and passage 3 (P3) chondrocytes.

### 2.6.1. Cell seeding and expansion

The next experimental part will be divided in the two sections explained in the objectives. So, a first part to assess cell's viability (Alamar Blue and SEM) and a second part for tissue engineering studies (cell seeding protocol, cell seeding efficiency, histological and immunohistochemical studies).

#### 2.6.1.1. Seeding scaffolds for preliminary cell activity test

Once the required cell number was achieved, confluent chondrocytes monolayers were harvested for seeding onto the developed polymeric scaffolds (group J-M), as follows. Scaffolds were allowed to equilibrate in 10 ml basic medium for 48h, at 37°C. Chondrocytes were removed from the culture dishes by trypsinization. The chondrocytes were pelleted by centrifuging at 1000 rpm, 5 min and the cell pellet resuspended in basic medium. Hydrogels were placed individually into 24 well culture plates. Each hydrogel was fully covered by expansion medium (800 µl) and cells were

seeded at a concentration of  $2 \times 10^4$  cells per well. Tissue culture well plates were transferred to an incubator (95% air/ 5% CO<sub>2</sub>, at 37°C) and placed on a magnetic stirrer. The cell suspension was gently stirred (70 rpm) until for 72h to allow cell seeding onto the hydrogels.

#### 2.6.1.2. Cell Activity- Alamar Blue Assay

For viability assessment, primary bovine chondrocytes (BC, P3), rat osteosarcoma cell line (ROS), fibroblast cell line (L929) and rat mesenchymal stem cells (MSCs, P3) were seeded as in section 2.6.1.2. All the cells types were seeded simultaneously in the same conditions but in the absence of hydrogels.

Cultured cells viability was assessed by using Alamar Blue and cellular adhesion was observed through SEM. So, for cell-constructs prepared as in section 2.6.1.1., and cells-only that served as control, the medium was carefully removed, after 72h, and replaced by fresh differentiation medium containing 10% Alamar blue<sup>TM</sup>. Cell-constructs and cells-only controls were re-placed in the incubator for different periods of time (1, 2 and 4 hours). Additionally, 3 wells with no constructs were incubated with the same concentration of differentiation medium containing Alamar blue<sup>TM</sup> that was used for incubating cell-constructs and cells-only control; this will be the dye only control to detect any reduction in the dye, in the absence of cells and/or constructs. Aliquots (200 µl) from each well were removed and placed in a 96 well plate. The OD value was assessed to determine the amount of reduced dye, using a spectrophotometer, at 570 and 600 nm.

After assessing cells viability, BC will be seeded, expanded and allowed to mature, in new PEPMHA hydrogels, as well as in agarose gels that will serve as a reference value for cells normal activity and proliferation.

#### 2.6.2. Seeding scaffolds for TE

Hydrogels were incubated for 48h in expansion medium. After the first 24h, 4 scaffold replicates were cut in a cylindrical shape, with dimensions of 5mm diameter x 3 mm thickness. In the remaining 24 hours the hydrogels would reach the swelling plateau. Bovine chondrocytes were obtained in the same manner as in section 2.6.1.1., but now

seeded at a concentration of  $5 \times 10^6$  cells per construct. In the same way, agarose constructs, used as reference were prepared and chondrocytes seeded (2.6.2.1 Seeding Agarose gels for TE). Cells were allowed to expand for 96 hours. In addition, for each group of hydrogels (group J-M) there was one specimen where no cells were seeded (construct control).

The concentration of cells used was standardised early in the experimental design to compensate concerning any possible difference in hydrogels density.

#### 2.6.2.1. Seeding agarose gels for TE

4% agarose was prepared and sterilised by autoclaving at 121°C. Passaged chondrocytes were prepared as described previously (2.6. Cell expansion).

4% agarose gel was melted and cooled to 37°C. The gel was mixed rapidly (50:50) with the cell suspension and immediately dispensed into the coated wells of the culture dish. The lid was re-placed on the culture dish and the plate incubated at 4°C for 10 min. After the gels were formed, 5 mm diameter plugs were punched and transferred to a cell culture dish and 25 ml of expansion medium was added. The culture plates were incubated at 37°C, with 95% air and 5% CO<sub>2</sub> for 96h.

#### 2.6.2.2. Seeding efficiency

After the 96 hours, the expansion medium, from cell-PEPMHA- and cell-agarose constructs, was extracted and spun down at 1000 rpm, 10 min. The pellet was resuspended and cells counted using a haemocytometer. We therefore extrapolated the average number of cells adhered to the materials (Cells<sub>A</sub>) by subtracting the cells remaining in suspension to the initial seeding concentration.

$\text{Cells}_A = \text{initial cell concentration} - \text{cell concentration in expansion medium, after 3 days}$

#### 2.6.2.3. Expansion and adhesion (7d)

After 96 h, cell-PEPMHA- and cell-agarose-constructs were moved to non-tissue culture treated Petri dishes and 25 ml fresh expansion medium were added to each

construct. Dishes were replaced in the incubator, in a gently moving orbital shaker (70 rpm). Cell-constructs remained in these conditions during 7 days.

#### 2.6.2.4. Cartilage constructs maturation (40d)

On day 7, expansion medium was removed and replaced with 25 ml of differentiation medium in order to promote the formation of a chondrogenic phenotype in the chondrocytes. Constructs were returned to the orbital shaker in the incubator and maintained at a speed of 70 rpm. Cell-constructs remained in these conditions until day 40, replacing the differentiation medium every third- forth day.

### 2.7. Characterization of the constructs

Cellular adhesion of bovine chondrocytes and ROS cells was assessed by SEM.

#### 2.7.1. Scanning electron microscopy (SEM)

##### 2.7.1.1. Fixation and alcohol dehydration

Constructs for SEM were washed using 0.1 M sodium cacodylate buffer, pH 7.4 in order to wash away any residual protein and fixed with 3% gluteraldehyde buffer for morphology and tissue composition preservation. After 30 min the solution was removed and the constructs rinsed off with PBS. It followed a secondary lipid fixation with ½ ml of 2% osmium tetra oxide for 1 hour. This was added in sufficient volume to cover samples (in a fume cupboard). The osmium tetra oxide was removed and samples washed with 0.1M sodium cacodylate buffer. Samples were then incubated in 75 % ethanol being replaced after 15 min by a solution of 95% ethanol followed by incubation in 100% ethanol for the same period of time. 100% ethanol dried over anhydrous cooper sulphate was added for 15 min, after which was removed and constructs allowed to air-dry in a fume cupboard.

#### 2.7.1.2. Mounting samples

Dry samples were mounted onto aluminium stubs using double-sided adhesive carbon tabs, and coated with approximately 25 nm of gold (3 minutes) in an Edwards S150B sputter coater. Specimens were examined in a Philips/FEI XL-20 scanning electron microscope, at an accelerating voltage of 20 Kv.

#### 2.8. Sample Processing (for cartilage-like tissue engineering cell-constructs)

On day 40, cell-constructs were removed from culture; excess medium was removed by placing them on absorbent paper, after which the constructs were weighed. The constructs were then bisected, and one half was weighed once more, frozen at -20°C, freeze dried and used for biochemical evaluation.

Cryo-embedding matrix or Optimal Cutting Temperature gel (OCT) (OCT compound BDH, Gurr®) was placed into foil cylinders on cork bases and each half of the remaining cell-construct was carefully introduced in the matrix, assuring that the cut surface was uppermost. The sample was entirely covered by extra OCT and placed in pre-cooled iso-pentane to solidify the OCT embedding matrix.

The samples were frozen with liquid nitrogen, then wrapped in laboratory film (Parafilm) to prevent desiccation, and stored at -20°C, for microscopy studies. Using a microtome, tissue sections of 8 µm were cut from the cryo-embedded samples being collected onto glass slides coated with 4% APES (Appendix) and allowed to dry overnight. Sections were then fixed for 30 minutes at 4°C, in 4% paraformaldehyde (PF) and washed twice in distilled water, followed by air-drying and storage at 4°C in a dark environment until the staining was performed.

##### 2.8.1. Histology

Most of the tissues are uncoloured which difficults their observation in the microscope. Due to this fact, there were introduced methods of colouration so that specified cell components would become visible and highlighted from others.

Most of the dyes used in histology behave as acids or bases and tend to form salinic interactions with ionisable radicals from the tissues. The following staining assays were performed:



#### 2.8.1.1. Hematoxylin and eosin stain

Hematoxylin-eosin staining was carried out in an automated machine Shandon Linear Stainer machine (Thermo Shandon, UK) according to manufacturer's instructions. Sections were stained in 0.4% hematoxylin for a total time of 4.5 min, rinsed in tap water (2 min) followed by 0.1% HCl in 70% ethanol (30 seconds) and washed again in tap water. The sections were then stained in 0.5% eosin Y for 2 min, washed with tap water, dehydrated through alcohols, cleared in xylol and mounted in DPX (Fluka/Sigma Co.).

#### 2.8.1.2. Toluidine blue stain

One drop of 1% (wt/v) toluidine blue was added onto a fixed section for a few seconds, rinsed off with distilled water. The sections were dehydrated through alcohols, dried, cleared in xylene and mounted in DPX.

### 2.9. Immunohistochemistry

The assays used for immunohistochemistry are based in specific chemical reactions or macromolecular interactions of high affinity that allow the detection of specific substances such as enzymes, DNA or RNA.

#### 2.9.1. Immunolocalization of type I and II collagen

Collagen type I and II were detected using monoclonal antibodies against collagen types I and II.

In this procedure, sections were pre-treated in 10mg/ml hyaluronidase (Sigma Co.) for 30 min at 37°C and after washed with PBS. Sections were then incubated at 37°C for 30 min with 2mg/ml pronase and again washed with PBS.

The endogenous peroxidase activity was quenched with 3% hydrogen peroxide (Sigma Co.) in 50% methanol (Aldrich) for 5 min. Sections were washed with tris-buffered saline (TBS) solution and incubated with 3% bovine serum albumin (BSA) overnight to avoid non-specific staining. These were incubated for 1 hour with a primary antibody

(collagen type I and collagen type II) in a humidified atmosphere at RT, washed twice with TBS/Tween 20 for 10 min and incubated with a secondary antibody for 1 hour at RT as before. The remaining protocol is described in the Vectastain Elite ABC kit Pk-6105 (Vector Laboratories Ltd., UK) and in the Vector DAB kit (Vector Laboratories Ltd., UK). Basically, sections were washed with TBS/Tween 20 and incubated with reagent ABC for 30 min in the same conditions, followed by 2 washes with TBS/tween 20 and treated with DAB substrate for 2-10 minutes, until a suitable colour had developed. A final wash was performed and sections were dried and mounted in DPX. Controls were performed using normal goat serum.

#### 2.9.2. Quantitative assessment of glycosaminoglycans- 1,9-dimethylmethylene blue (DMB) assay

Proteoglycans content in the matrix of the constructs was quantified by measuring the level of sulphated glycosaminoglycans (GAGs) using the 1,9-dimethylmethylene blue (DMB) dye.

Constructs were enzymatically digested to release the GAGs. 400  $\mu$ l of a digestion solution with papain (Sigma Co.) and N-acetyl cysteine (Sigma Co.) were added following incubation at 40°C until the pellet was digested.

Agarose constructs, used as controls, were digested with 1:10 agarase in the papain and N-acetyl cysteine solution, at 40°C, until the pellet was digested. After 12h the digested samples were centrifuged at 13,000 rpm for 10 min. The supernatant, containing the digested matrix proteins, was collected and stored at 4°C until the GAG assay was performed. The remaining pellet was freeze dried and then weighted to determine the remaining amount of scaffold.

A chondroitin sulphate standard solution (Sigma Co.) was prepared in water and kept refrigerated. This solution was used to prepare a standard curve of varying concentrations ranging from 0 to 50  $\mu$ g.ml<sup>-1</sup> and supernatant samples were diluted appropriately (Figure 66). 20  $\mu$ l of chondroitin sulphate standards and diluted samples were placed in duplicate into a 96-well round-bottomed plate.

DMB solution (250  $\mu$ l) was added to each well, using a multi-channel pipette.

The optical density was measured immediately using a microplate reader, at 530nm. The concentration of the GAGs in the samples was determined by comparison with the standard curve.

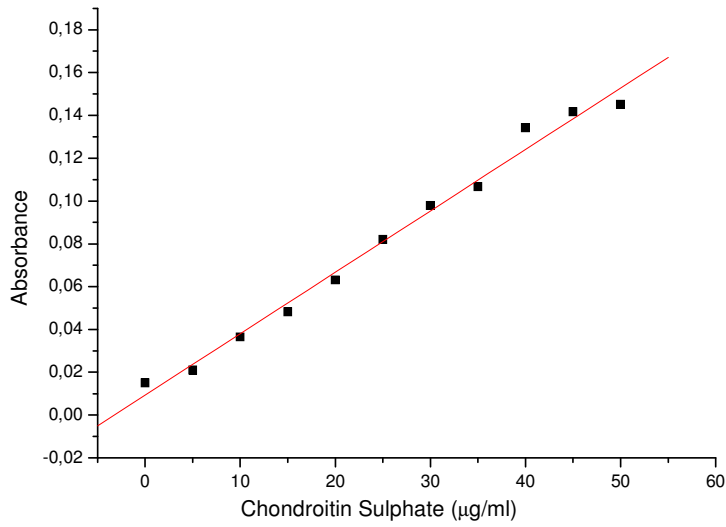


Figure 66. Example of a standard curve used for the calculations of GAG content in the engineered constructs.

The total matrix in each construct was determined using the following equation:

$$\frac{\text{Mass of GAGs} \times 100}{(Wt_1 - Wt_2)} = \text{weight \% of GAGs in construct matrix}$$

where:

- Mass of GAGs was calculated from the chondroitin sulphate standard curve
- $Wt_1$  is the mass of the dried construct before digestion with papain or agarase
- $Wt_2$  is the mass of the dried construct after digestion with papain or agarase

### 2.9.3. Statistical analysis

All data were represented as mean  $\pm$  standard error. Statistical comparisons were performed using a one-way analysis of variance (ANOVA). Differences were considered significant for  $p < 0.05$ .

Note: The protocols described in this chapter were followed or adapted for published methodology [9]. Due to better comprehension and to avoid an extensive reading on methodology presented in this chapter, a more detailed description on products or other relevant information for the assays can be found in the Appendix that can be found in the end of this memorandum.

## 3. Results and discussion

The first part of the studies on the PEPMHA hydrogels' biocompatible character had the main goal of evaluating the viability and cellular adhesion to the materials.

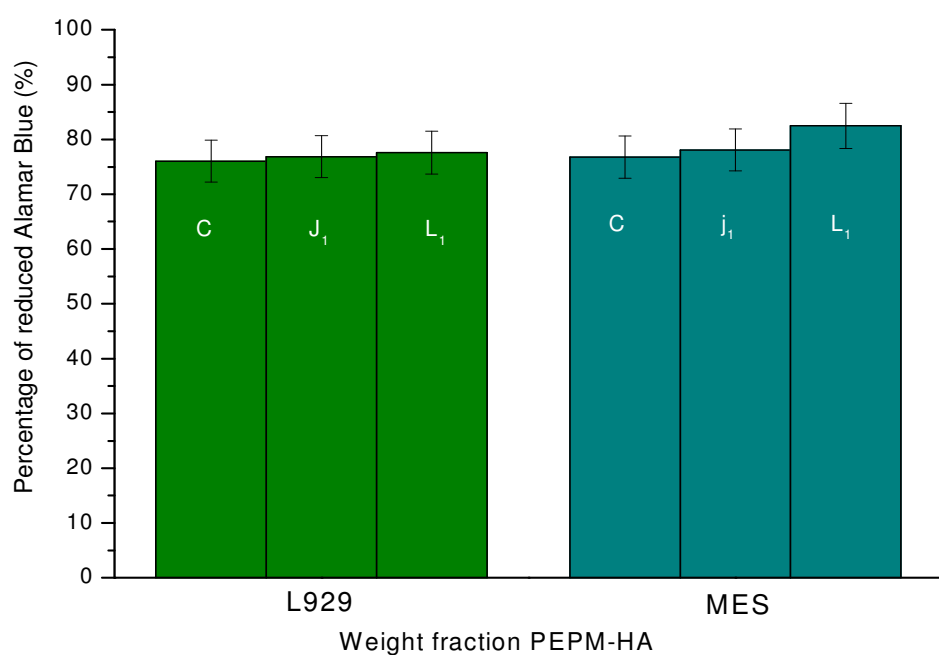
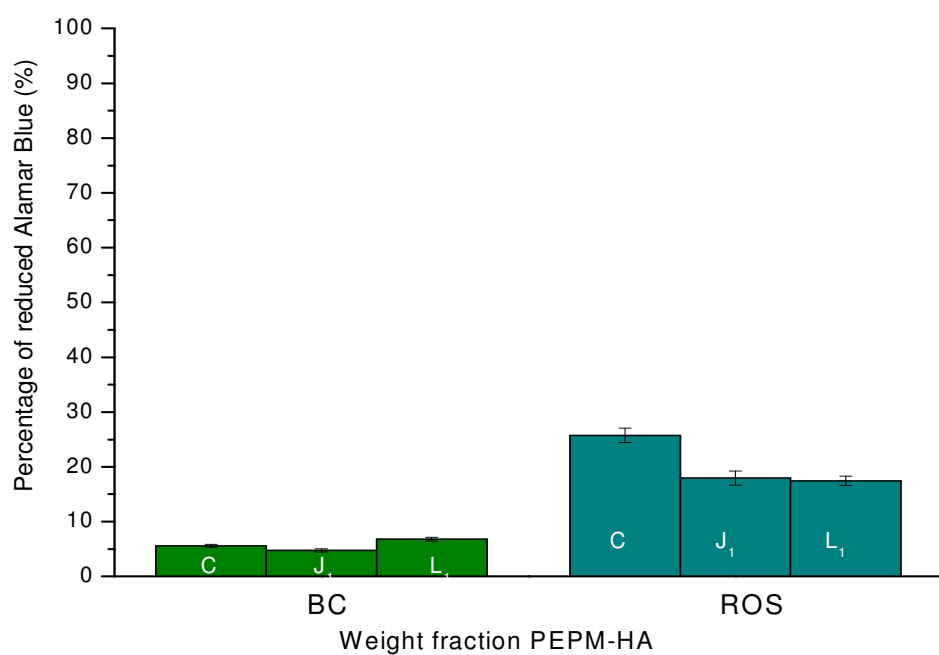
Therefore we have performed a very common assay to test cellular activity and visualized any possible cellular adhesion using scanning electron microscopy.

### 3.1. Cell activity- Alamar Blue

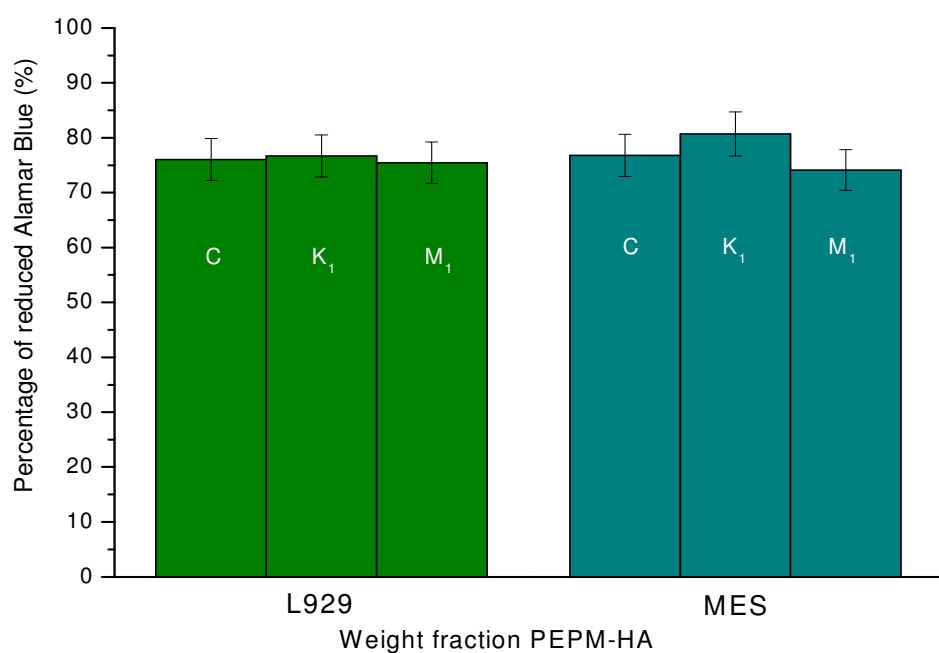
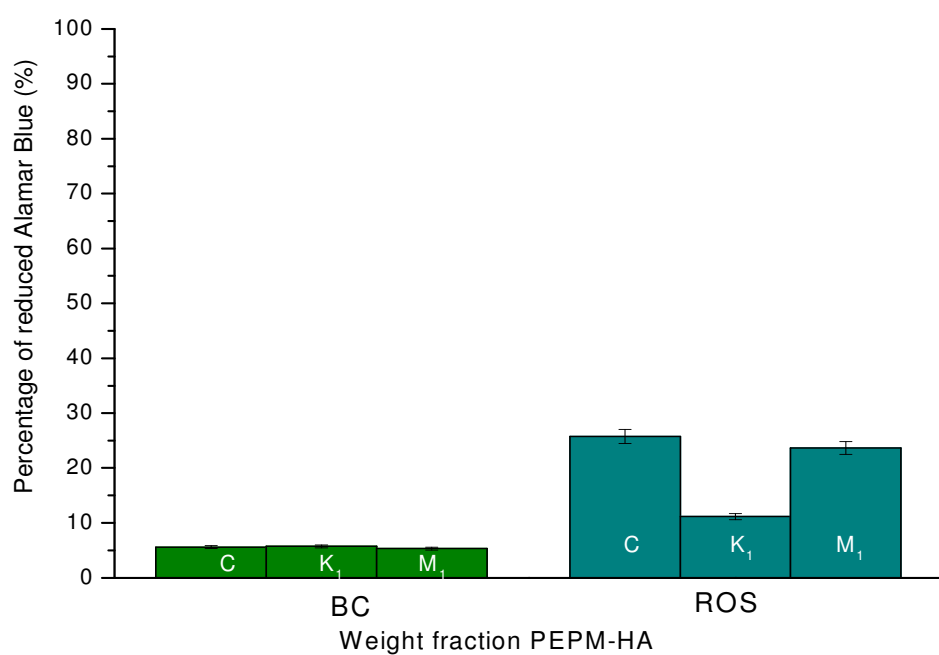
The Alamar Blue™ is a non toxic aqueous dye used in the assessment of cell viability and proliferation. As cells grow, innate metabolic activity results in a chemical reduction of dye. Continued growth will maintain a reduced environment whilst inhibition of growth will lead to an oxidized environment.

The viability test was performed using selected cell types concerning the type of future application of the elaborated scaffolds, respectively a bovine chondrocyte (BC) primary cell line, a rat osteosarcoma bone cell line (ROS), and as controls, a fibroblast cell line (L929), and rat mesenchymal stem cells (MSCs). The different cells types were seeded into PEPMHA hydrogels or in their absence (cell control) and incubated in the same conditions for 72 h. Their activity was assessed by replacing the medium for a diluted solution of Alamar Blue™ in the wells, followed by an incubation period of 2 hours and using a dye only control that consists on the dye diluted in the same concentration, but in the absence of cells or cell-constructs.

The following graphics represent the activity of the cells only controls (C), and how the presence of PEPMHA hydrogels with different composition altered their respiration (group J, L or K, M). We were also interested to see if the different cell types would respond differently to the composition of the hydrogels.



Figures 67 and 68. Viability of Bovine chondrocytes (BC), ROS, L929 and MES cells after 72h in hydrogels with different concentration of PEPM- 1%HA (Group J<sub>1</sub> - 0,545M; Group L<sub>1</sub> - 0,725M), using K<sub>2</sub>S<sub>2</sub>O<sub>8</sub> as initiator and 1,7% triethylene glycol dimethacrylate as crosslinker. Percentage of reduced dye after 2h incubation is shown in the figures.



Figures 69 and 70. Viability of Bovine chondrocytes (BC), ROS, L929 and MES cells after 72h in hydrogels with different concentration of PEPM- 1%HA (Group K<sub>1</sub> - 0,545M; Group M<sub>1</sub> - 0,725M), using K<sub>2</sub>S<sub>2</sub>O<sub>8</sub> as initiator and 2% N,N'-methylene bisacrylamide as crosslinker. Percentage of reduced dye after 2h incubation is shown in the figures.

The results are represented as a percentage of the measured absorbance of the reduced dye by the different cell types seeded on the different PEPMHA systems (Figure 67-70). From the analysis of the graphics we can see that the percentage of the reduced dye wasn't significantly altered by the presence of the different materials in comparison with the cells-only. There couldn't specify any general trend we couldn't detect any significant effect of the polymer chemistry on cell attachment except for ROS cells seeded on PEPMHA hydrogels from group K<sub>1</sub>. Even though hydrogels were purified after the polymerization, sometimes they can still contain some unreacted products of the polymerization reaction that might be toxic to cells. This might have been the case. In regard to the difference obtained for the percentage of reduced dye obtained for BC and ROS and the percentage obtained for L929 and MSCs cells, it could be explained due to a higher metabolic activity from the latter ones. As BC are the type of cells in this study with lower metabolic activity it would be expected that they had a decreased activity cellular rate due to a slower proliferation. Another possibility might be related to the standard curve. Absorbance obtained for L929 and MSCs may be already in a region of the standard curve where the peak becomes saturated, although still within the linear region, therefore giving such high percentage of reduced dye. Nevertheless the different PEPMHA hydrogels were non toxic and the different cell types seeded did remain viable. Two of the cells types, namely BC and ROS cells were after visualized through SEM in order to check the cellular adhesion.

### 3.2. SEM

For chondrocytes to maintain their phenotype it is important that they are capable to retain their rounded morphology on the biomaterial surface [10].

Cell-constructs were observed by SEM so that any effect of the polymer chemistry on cells morphology could be detected. Cellular adhesion in the PEPMHA hydrogels with different composition was observed for BC and ROS cells.

Although we could detect the presence of BC and ROS cells (Figures 71-B and 73-B) and comprove their adhesion to the materials surface, we had some difficulty in verifying this in all the different cell-constructs.

When cells adhere to a material they will be responsible for a variation in their surface. Now, the method for cells fixation is possibly interfering with the hydrophilic nature of



the porous structure of the hydrogels and affecting their integrity. The appearance of the material seeded with BC and ROS cells was completely different (Figures 71-B and 72-B). If we consider the tri-dimensional structure of the materials, what could be happening is that we have a part of the surface recovered by cells and other where cells are absent. This difference in the material surface might be affected during the fixation process, creating ruptures and collapse of the material.

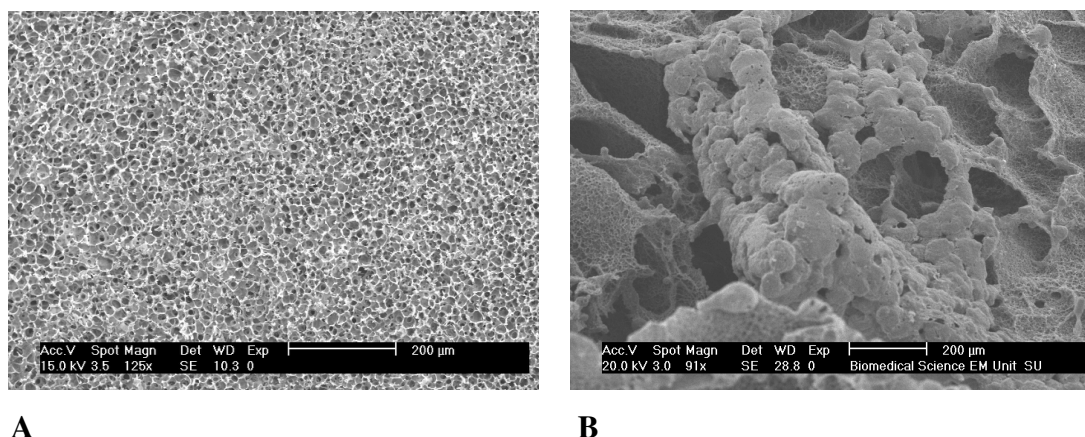


Figure 71. Scanning electron micrographs of PEPMHA scaffolds ( $J_3$ ). A: in the absence of cells; B: cell-constructs (PEPMHA seeded with BC for 3 days).

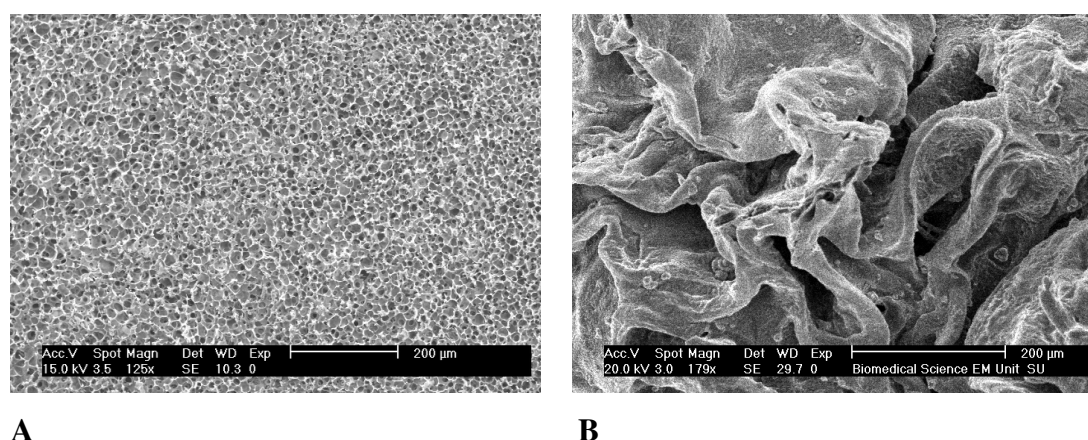


Figure 72 (A and B). Scanning electron micrographs of PEPMHA scaffolds ( $J_3$ ). A: in the absence of cells; B: cell-constructs (PEPMHA seeded with ROS cells for 3 days).

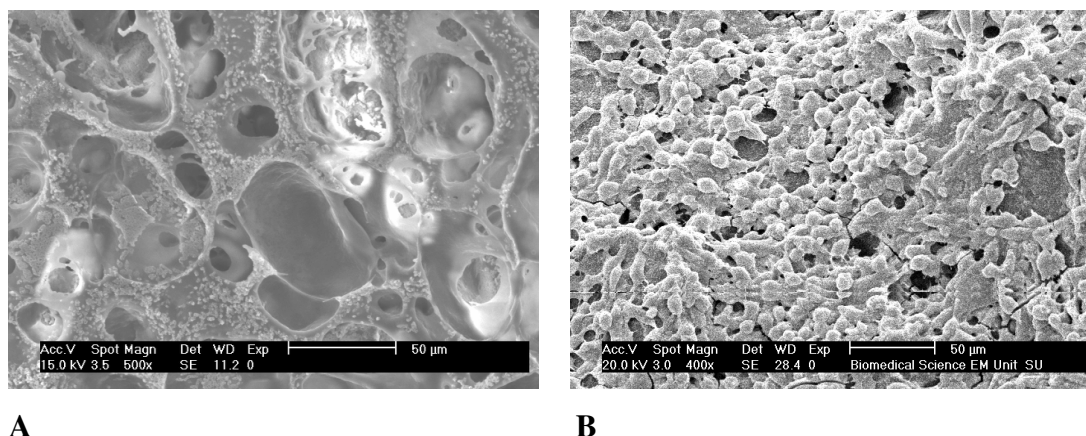


Figure 73 (A and B). Scanning electron micrographs of PEPMHA scaffolds ( $L_3$ ). A: in the absence of cells; B: cell-constructs (PEPMHA seeded with ROS cells for 3 days).

So, after a 3 days incubation period with expansion medium, and although a small agglomerate of cells could be seen, and that this method has been used successfully for different kinds of materials, we do consider that it should be optimized for the specific case of PEPMHA hydrogels.

### 3.3. Seeding Efficiency

After verifying the cells viability we performed an assay for cartilage-like tissue engineering.

Bovine chondrocytes were seeded at high cell density in PEPMHA hydrogels and expanded for 96h. After this period the effective number of seeded cells that adhered to the different hydrogels was determined. For that, we removed the cell-constructs from the wells where they were incubated and counted the cells that remained. Subtracting this value to the initial number of cells seeded would give us an approximation of the number of cells that adhered to the hydrogels. The number of cells that adhered is in fact an approximation of the real value (i.e. inferior), because some of the cells may already be in a proliferation state.

So, after seeded, bovine chondrocytes readily adhered to the surface of all PEPMHA and agarose gels, used as cells normal activity and proliferation reference. We hoped to see an influence of the chemical composition of the different scaffolds in the adhesion of the cells.

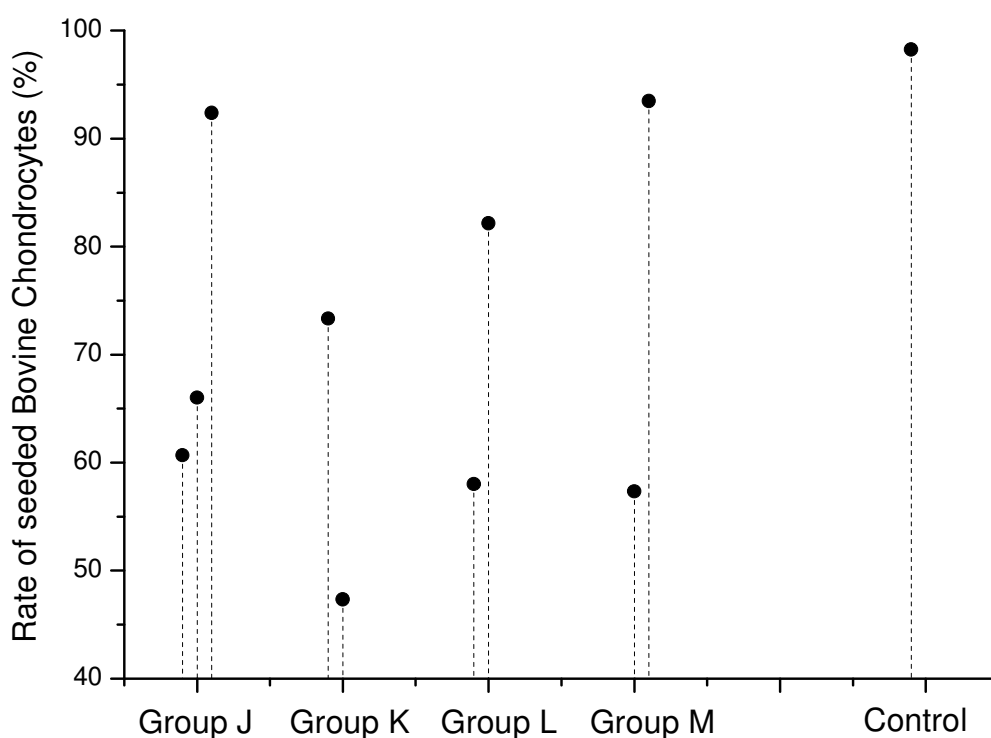


Figure 74. Rate of seeded bovine chondrocytes in 4 groups of scaffolds synthesized with different compositions; Group J:  $K_2S_2O_8$  as initiator and 1,7% triethylene glycol dimethacrylate as crosslinker, 0,545M EPM and different concentrations of hyaluronic acid,  $J_1 - 1\%$ ;  $J_2 - 2,5\%$ ;  $J_3 - 5\%$ ; Group K:  $K_2S_2O_8$  as initiator and 2% N,N'-methylene bisacrylamide as crosslinker, 0,545M EPM and different concentrations of hyaluronic acid,  $K_2 - 2,5\%$ ;  $K_3 - 5\%$ ; Group L:  $K_2S_2O_8$  as initiator and 1,7% triethylene glycol dimethacrylate as crosslinker, 0,725M EPM and different concentrations of hyaluronic acid,  $L_1 - 1\%$ ;  $L_3 - 5\%$ ; and finally Group M:  $K_2S_2O_8$  as initiator and 2% N,N'-methylene bisacrylamide as crosslinker, 0,725M EPM, and different concentrations of hyaluronic acid,  $M_2 - 2,5\%$ ,  $M_3 - 5\%$ . Agarose gels seeded with the same cell type were used as controls. The different groups were compared using an ANOVA I statistical test;  $p < 0.05$ .

In concern to the different crosslinkers used, there was a significant statistical difference between groups. However it seems that the hyaluronic acid is clearly playing a major role in influencing the cells seeding efficiency. In fact, a general trend can be observed within each group of the different polymeric systems, the rate of seeded cells increases when there is an augment on the hyaluronic acid ratio. This significant positive interference of HA was present in all groups except for group K.

The scaffolds with the highest concentration of hyaluronic acid were also the ones having the most similar rate of seeded cells when compared to agarose control gels ( $J_3$  and  $M_3$ ). Early before, Zinnerman et al., showed that hyaluronic acid is an adhesion

modulator molecule, which can mediate the early stage of cell-substrate interaction [11]. Therefore, the results shown are in accordance to the reported influence that hyaluronic acid has on cell adhesion.

### 3.4. Scaffolds for Tissue Engineering

After 96 h of incubation to promote cellular adhesion, BC were seeded and expanded during 7 days, and finally cell-constructs were incubated for an additional period of 33 days, in differentiation medium.

Cell-constructs were sectioned and immunohistological tests were performed to evaluate the presence and distribution of cells as well as the production of normal cartilage molecules synthesis that could indicate the nature of the tissue engineered constructs.

#### 3.4.1. Histology of cartilage engineered on PEPMHA scaffolds

Histological sections showed a cellular tissue in which the cells appeared to concentrate at the material's surface.

The histology processing often triggers cells expansion results, as it usually leads the contraction of structures. The detachment of cell mass observed in some of the scaffolds might have resulted from that. The nature and morphology of the material could also influence the results; the chemical composition effects in cell attachment and proliferation, due to different synthetic: natural polymer ratios, the nature of the crosslinker used, the different porosity and pore size from the scaffolds, are all characteristics well known to influence cell penetration and the diffusion of nutrients and oxygen throughout the constructs, limiting cells distribution [12].

PEPMHA systems being hydrogels have high water content, and, when frozen, their structure is altered. The high porosity presented by some of the materials, may also lead to the collapse of pores wall inducing cell detachment during the processing, as shown in figure 75. If the cells possess low matrix production they will enhance the cellular detachment process.

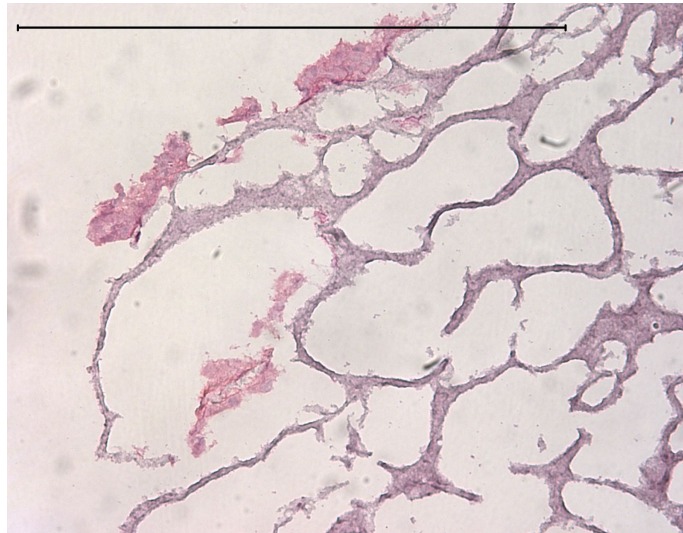


Figure 75. Light microscopy image of histology section from PEPMHA scaffold seeded with bovine articular chondrocytes, collected at day 40 of culture and stained with hematoxylin-eosin (Scale bar: 500  $\mu$ m).

#### 3.4.2. Hematoxylin- Eosin stain

Hematoxylin is a basic dye that interacts with the basophile structures of the tissues, like the nuclei as well as the regions of the cytoplasm rich in RNA, colouring them blue, whilst eosin, an acidic dye, stains the cell cytoplasm reddish.

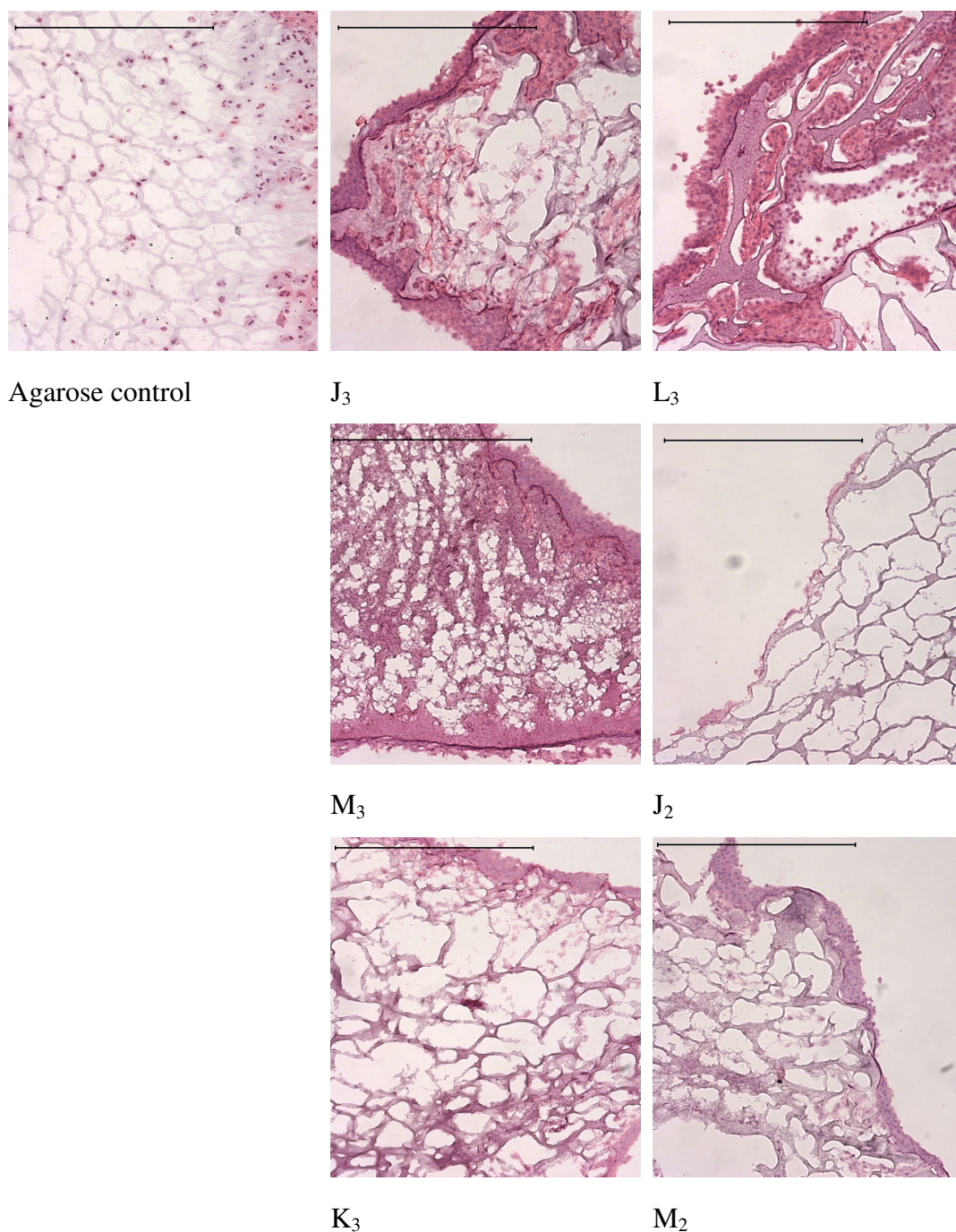


Figure 76. Light micrographs of histology sections from PEPMHA scaffolds seeded with bovine articular chondrocytes, collected at day 40 of culture and stained with hematoxylin-eosin (10x magnification; Scale bars: 500  $\mu$ m). The images correspond to the peripheral region of control agarose gel and PEPMHA constructs from the different groups (J-M).



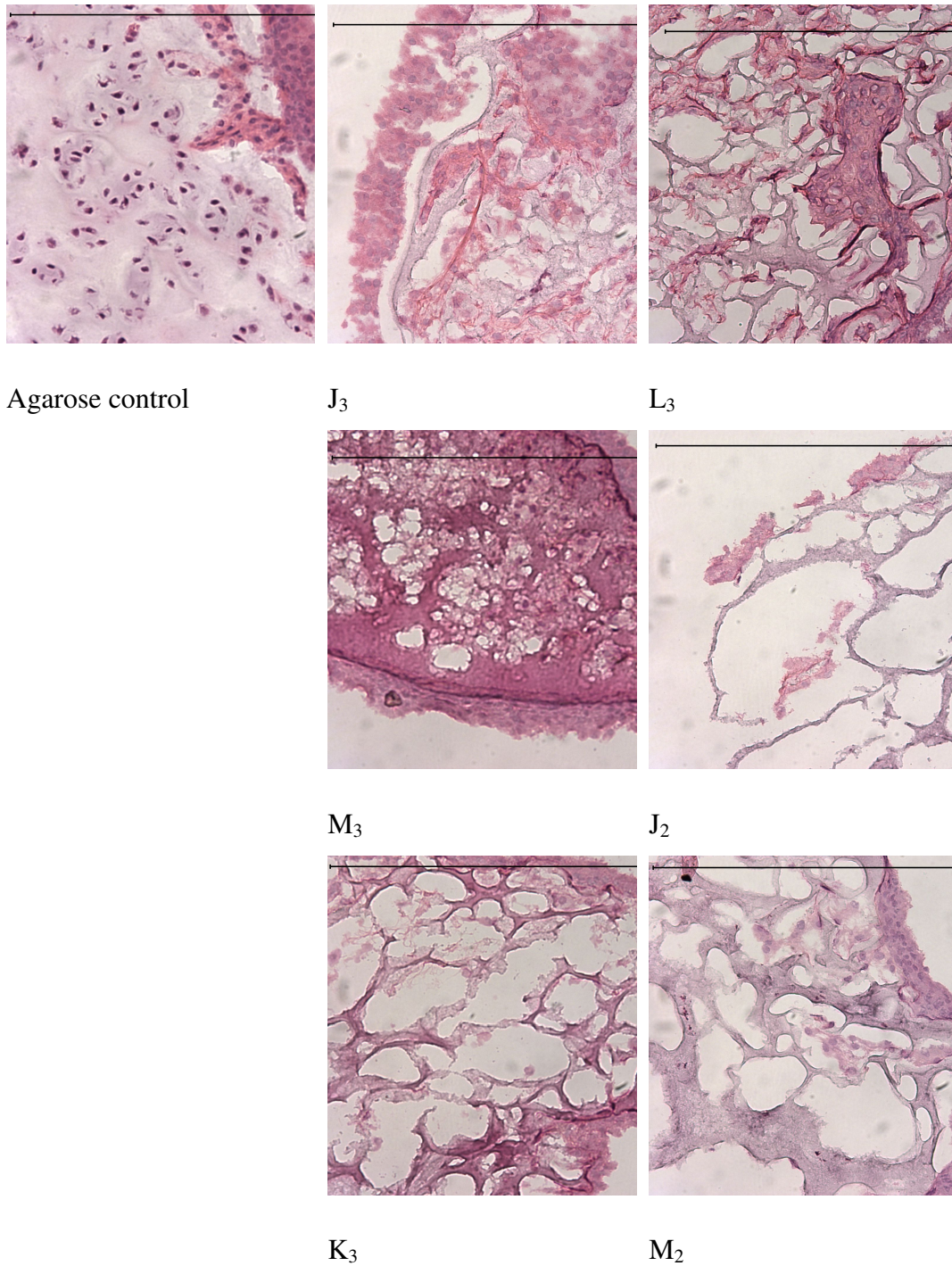


Figure 77. Light micrographs of histology sections from PEPMHA scaffolds seeded with bovine articular chondrocytes, collected at day 40 of culture and stained with hematoxylin-eosin (20x magnification; Scale bars: 500  $\mu$ m). The images correspond to the peripheral region of control agarose gel and PEPMHA constructs from the different groups (J-M).

It is evident from the images shown that cells attached and spread into some extent through the cell-construct's surface, although in most cells were lacking in the bulk.

When the polymeric material constituting the cell-construct was denser, cells weren't able to penetrate and simply attached to the surface (Figure 76, M<sub>3</sub>), whilst in the case of some highly porous cell-constructs, during the histology processing, they might have simply collapsed and released the cells present (Figure 77, J<sub>2</sub>). The absence of cells in the scaffolds bulk is normally related to inefficient cells penetration or necrosis due to high cell densities, although the first one in the PEPMHA cell-constructs seems to be more logical. This problem could be overcome through alternative methods of cell seeding, or manipulating the materials composition in order to find the optimal pore size and distribution for cells proliferation.

#### 3.4.3. Toluidine blue stain

Toluidine blue is a dye used for the detection of proteoglycans present in the extracellular matrix of hyaline cartilage. Hereby we intended to identify any GAGs present in the PEPMHA cell-constructs.



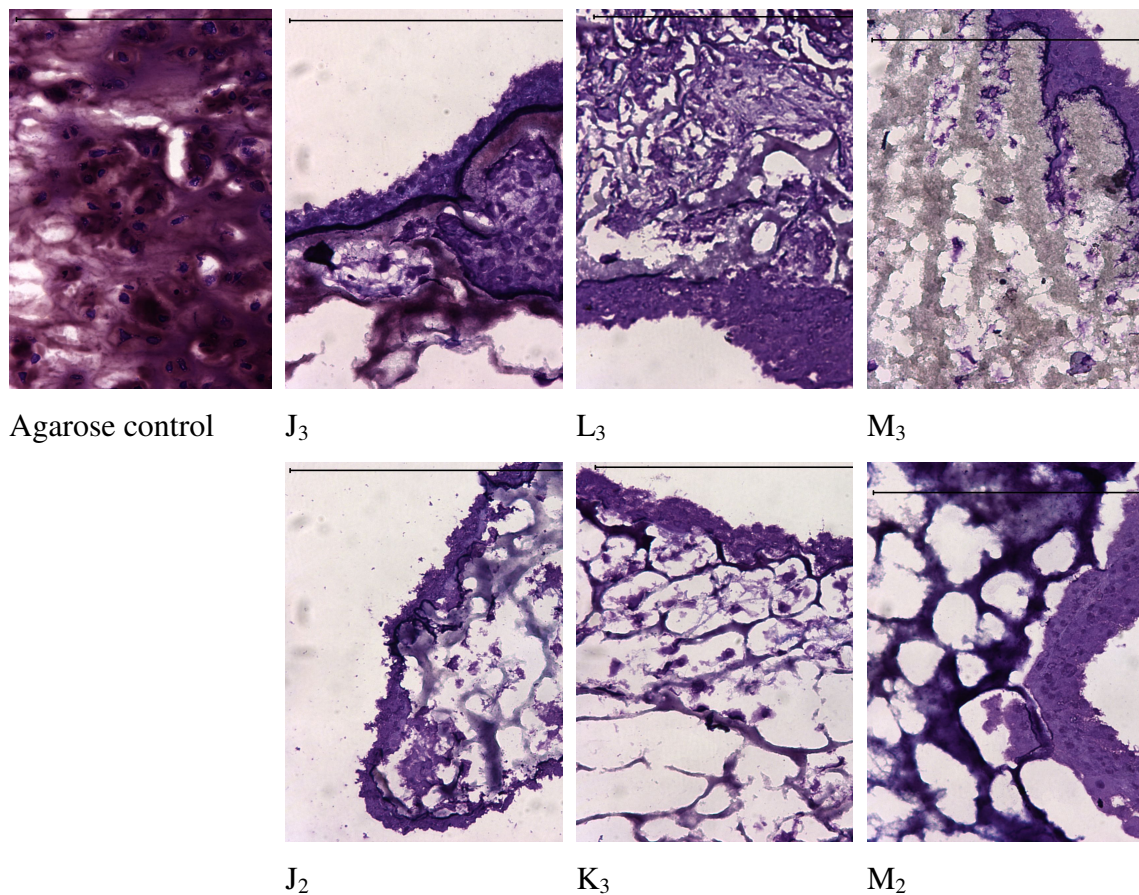


Figure 78. Light micrographs of histology sections showing the localization of glycosaminoglycans in tissue engineered cartilage on PEPMHA scaffolds after 40 days in culture. The images correspond to the peripheral region of engineered construct with bovine articular chondrocytes in agarose gel and different PEPMHA (Group J-M) hydrogels, stained with Toluidine blue (20x magnification; Scale bars: 500  $\mu\text{m}$ ).

Staining with toluidine blue was present throughout the entire sections, except for the group M<sub>3</sub>, which indicates that the chondrocytes have produced an extracellular matrix containing proteoglycans.

The images captured show the production of GAGs and also illustrate the distribution of cells (Figure 78). If observed carefully, unfortunately not that evident due to a background staining, in agarose controls, bovine chondrocytes are present throughout the entire section and more homogeneously distributed than for the PEPMHA cell-constructs where cells are even absent in some regions (M<sub>3</sub>).

We have attributed the seeding method used for the differences found. Cells were encapsulated within the agarose gels as for the PEPMHA scaffolds the seeding was done a posteriori gel formation. So, cells would be entrapped in the interior of the agarose gels leading to a more homogenous distribution, as for the PEPMHA hydrogels

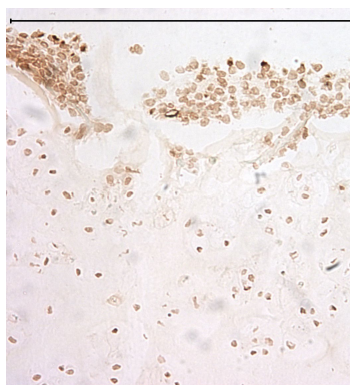
cells would have to migrate to the interior of the cell-construct, and that is the main reason why we could see a higher concentration of cells in the peripheral region. A limiting factor for cell penetration would be the hydrogel pore size. Cell penetration didn't occur in all constructs, as the pore size varied for each group. Also, we do not know whether there is a contribution of the hyaluronic acid that constitutes the hydrogel and we might as well be in the presence of some background staining due to this constituent.

### 3.4.5. Immunohistochemistry stain

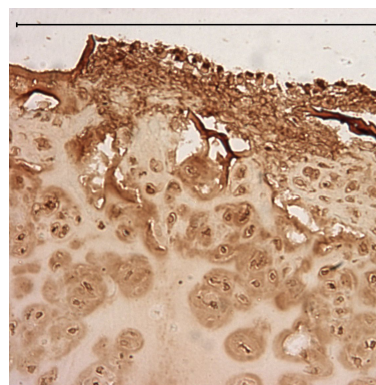
Immunohistochemical staining showed a strong presence of collagen type II mainly in the peripheral region (Figure 79, J<sub>2</sub>) and to some extent within the construct (Figure 79, L<sub>3</sub>). This was supported by the presence and distribution of glycosaminoglycans (GAGs) in the newly elaborated extracellular matrix, shown with the Toluidine Blue staining. As for collagen type I, we could see a poor staining in the periphery and almost inexistent staining throughout the constructs (Figure 79, M<sub>3</sub>).

It was also observed some cross reactivity of the antibodies with the hydrogels material (Figure 79, J<sub>3</sub>).

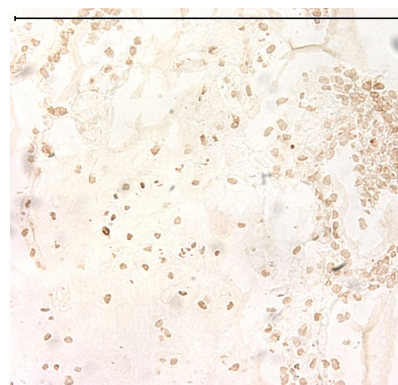
**Collagen type I**



**Collagen type II**

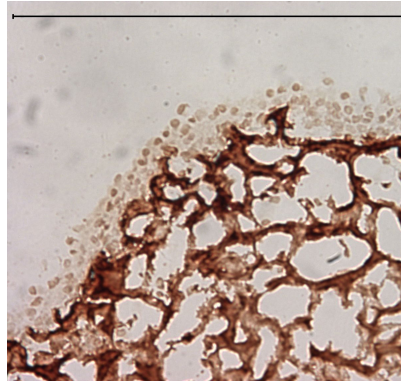
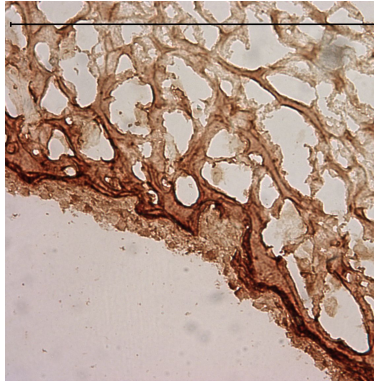
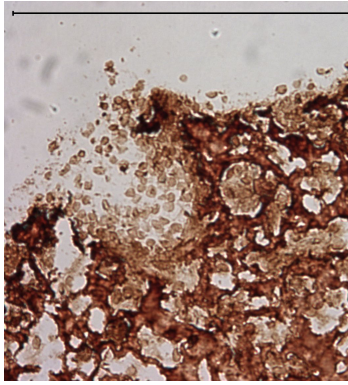


**Control**

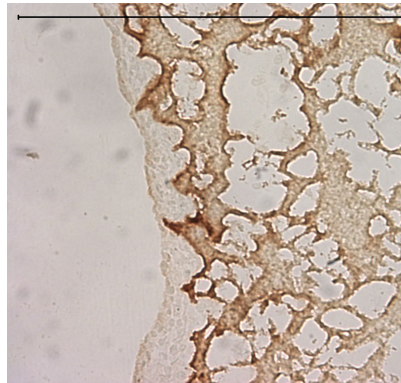
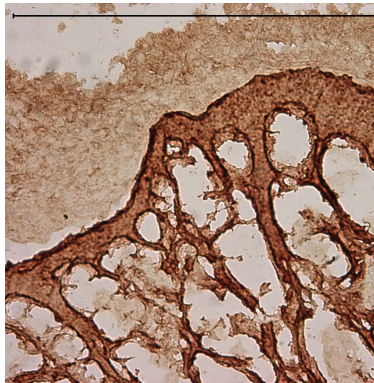
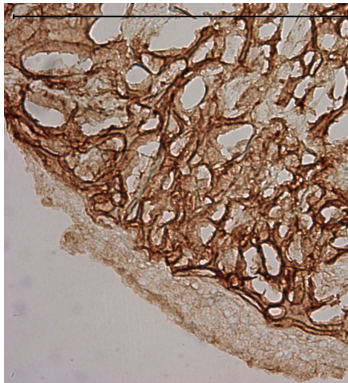


C

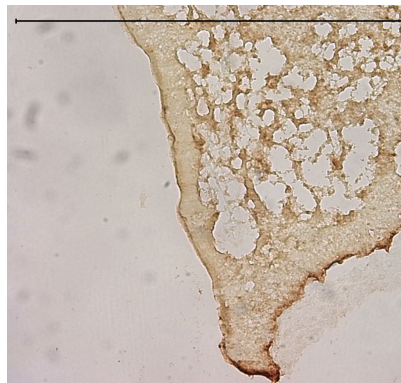
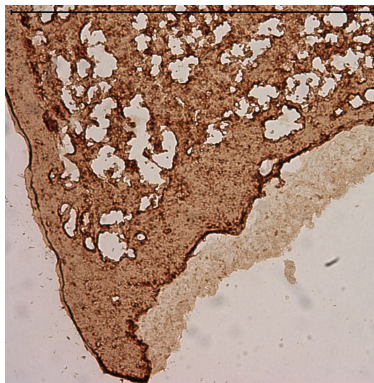
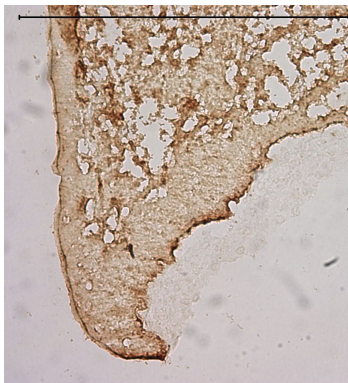




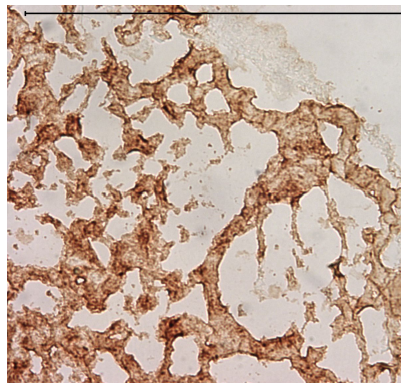
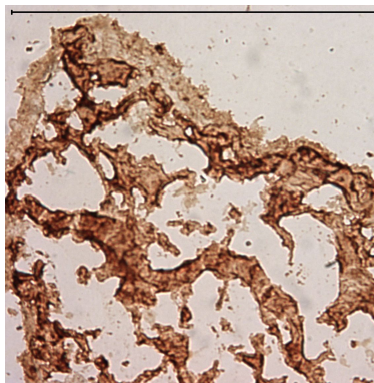
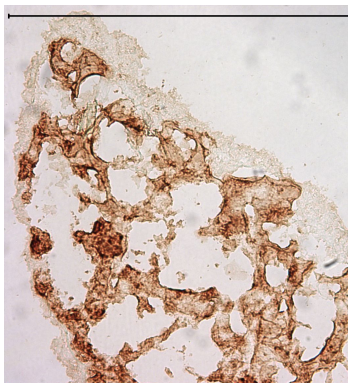
J<sub>3</sub>



L<sub>3</sub>

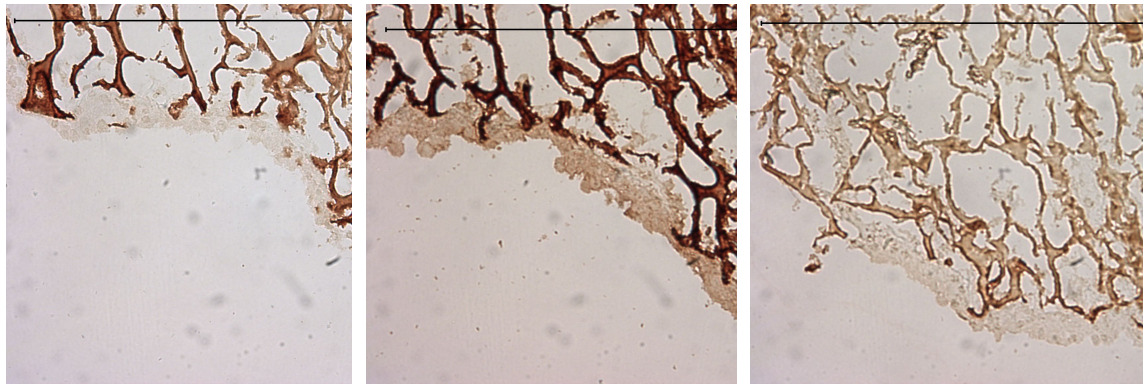


M<sub>3</sub>

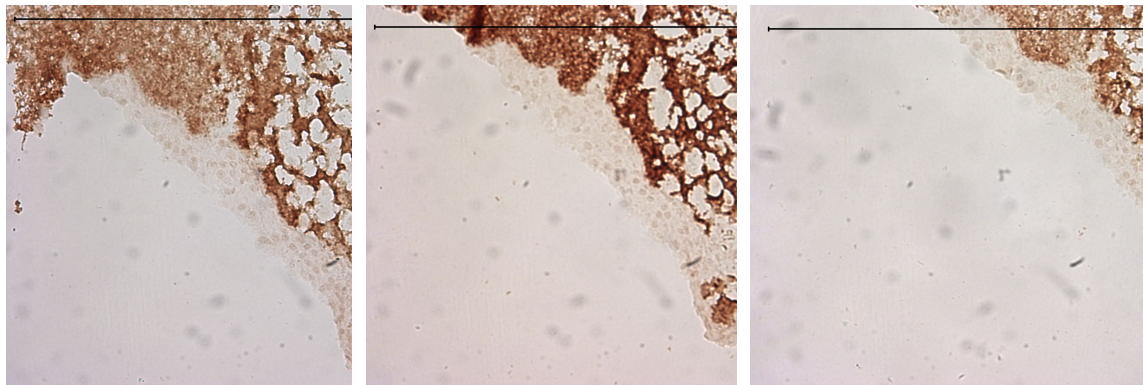


J<sub>2</sub>





K<sub>3</sub>



M<sub>2</sub>

Figure 79. Light micrographs of histology sections from PEPMHA scaffolds seeded with bovine articular chondrocytes, collected at day 40 of culture, showing the immunolocalization of collagen types I and II with a normal goat serum-control (20x magnification; Scale bars: 500  $\mu$ m). The images correspond to the peripheral region of control agarose gel (C) and different PEPMHA (Group J-M) hydrogels.

So, a predominance of collagen type II staining over collagen type I in the majority of the scaffolds inferred that bovine articular chondrocytes have maintained their chondrogenic phenotype.

#### 3.4.6. Quantification of glycosaminoglycans

After detecting the presence of glycosaminoglycans by the toluidine blue staining, we quantified the GAGs content using the DMB assay.

For this assay, PEPMHA cell-constructs were digested by papain and agarose cell-constructs were digested by agarase + papain.

Even though the digestion procedure was followed as commonly used, the PEPMHA cell-constructs didn't digest totally. This outcome could eventually influence in the determination of the total amount of matrix produced.

Even though we know that the DMB assay is specific for sulphated GAG, PEPMHA scaffolds were incubated in the absence of cells and were used as controls, in order to verify any possible interference due to material's composition, specifically because of the presence of the hyaluronic acid (non-sulphated GAG).

Figure 80 represents the amount of GAGs produced in relation to the scaffold's composition. It is noteworthy that all constructs had matrix production. However, agarose gels presented a much higher production of matrix than showed in any PEPMHA construct. As explained in the beginning of the chapter, agarose cell-constructs, serve as a reference for cell normal activity within a material in the form of a gel. We also reinforce the fact that the seeding technique was different and apparently more efficient when cells were encapsulated.

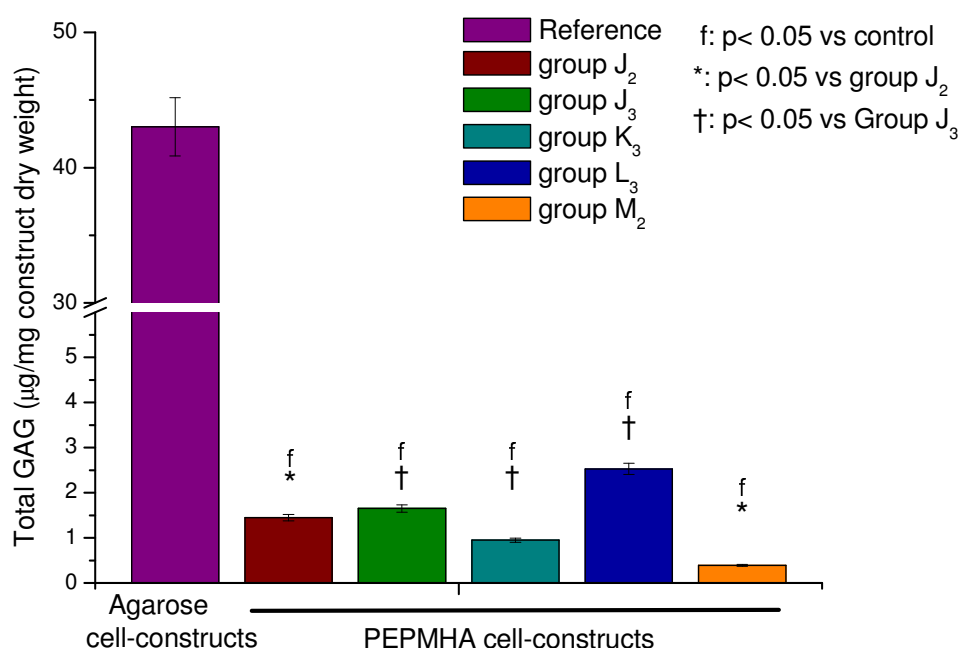


Figure 80. Comparison of the amount of matrix produced, after 40 days, in constructs of bovine chondrocytes and scaffolds with different compositions: Group J-M. Agarose constructs served as the control group. Each column represents the mean of 4 samples. The values are reported as the mean  $\pm$  SD.

The composition of the scaffolds clearly affected cells proliferation. Total GAGs' amount was significantly more influenced concerning differences in the crosslinker used or the monomer concentration than the concentration of hyaluronic acid present. We should mention that whilst performing the study some of the groups were lost. So, any observation can't be really done about the concentration of hyaluronic acid as there isn't sufficient data for that. Nevertheless, constructs fabricated with the highest concentration of monomer (0.725M EPM) and higher concentration of hyaluronic acid (5%) appeared to support the highest production of GAGs, and of course we can't neglect all the published studies, where this natural origin polymer has been added to polymeric systems as a fundamental substance.

As it is known, the ideal cell-carrier should mimic the natural environment in the cartilage ECM. The hyaluronic acid as part of the ECM components is already playing a role in regulating the expression of chondrocytes, so its application as part of a cartilage scaffold biomaterial is a very reasonable approach for enhancing chondrogenesis [13].

Regarding the specificity of the DMB assay and as mentioned before, the influence of the materials composition on this method was tested.

It was possible to determine a significantly positive interference of the non-sulphated glycosaminoglycan, hyaluronic acid, in the total amount of matrix produced by bovine chondrocytes (Figure 81).

The following graphic shows the non specificity of the DMB assay for sulphated glycosaminoglycans. So in fact we will have two variables influencing in the determined number of GAGs produced. First, this number is affected negatively by the incomplete digestion of cell-constructs, when the agarose cell-constructs digested totally. This could also explain the big discrepancy on the values obtained in the cellular adhesion for group J<sub>3</sub> that were very similar to the ones obtained in the agarose cell-constructs, in relation to the values obtained in the GAGs production by both groups and that could be correlated to the number of cells active. The second variable would be related to the non-specificity of the method in relation to the GAGs that would give us a higher content of GAGs than the real content produced.

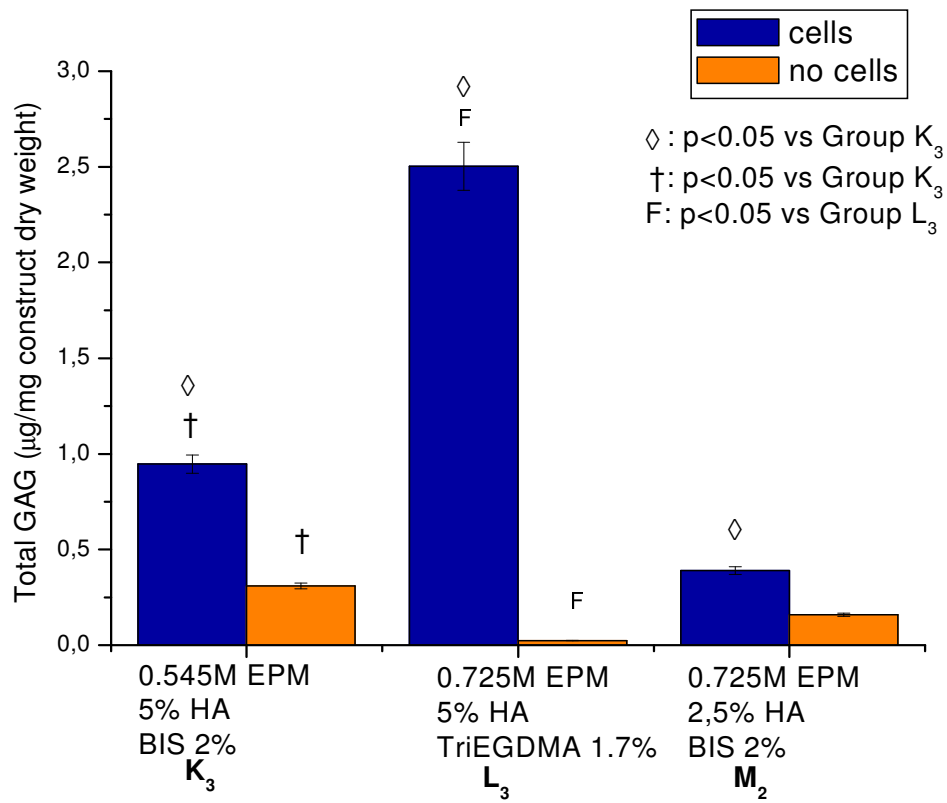


Figure 81. Comparison of the total amount of GAGs, after 40 days, in constructs of bovine chondrocytes + scaffolds with different compositions: Groups  $K_3$ ,  $L_3$  and  $M_2$ . Scaffolds presenting the same composition were also incubated in the same conditions but without the presence of cells. The values are reported as the mean  $\pm$  SD.

#### 4. Conclusions

The ability of the proposed polymeric system to support chondrocytes growth and differentiation was studied *in vitro*. It was concluded that:

The *in vitro* biocompatibility of these new polymer scaffold biomaterials was demonstrated using four different cell types (primary chondrocytes, ROS, L929 and MSCs). There was no statistical difference between the four polymeric systems investigated here. The evidence for cell adhesion, normal cell morphology, and proliferation together suggested that the biomaterials were suitable for further tissue engineering experiments.

In tissue engineering experiments, primary bovine chondrocytes (P3) were able to colonise the porous hydrogel scaffolds. However, evidence for cell penetration was limited, and detailed investigation was hampered by the collapse of the pores during sectioning. Even with this difficulty, histology showed that much of the extracellular matrix was localised outside of the scaffold, and was hyaline-like in composition (GAG and type II collagen). In summary, it appeared that the novel scaffold biomaterials supported the growth and differentiation of expanded chondrocytes, but much of the hyaline-like ECM was generated outside of the scaffold. It might be that the scaffold pores did not allow sufficient cell penetration during seeding to generate matrix throughout the bulk.

To summarise, the novel polymeric systems developed in this study showed good *in vitro* biocompatibility and supported the generation of a hyaline-like matrix by primary chondrocytes, although cell penetration and ECM production within the scaffold itself were relatively poor in these experiments. Further work might therefore best be focussed on overcoming these final challenges in the development of an advanced scaffold system for cartilage based on PEPMHA.

In chapter V we describe a brief study on photopolymerization of PEPMHA systems envisioning future cell encapsulation that might be an alternative method.



## 5. Bibliography

1. W.-J. Li, Tuan, R.S., Polymeric Scaffolds for Cartilage Tissue Engineering. *Macromol. Symp.*, 2005. 227: p. 65-75.
2. T. Aigner, Dertinger, S., Vornehm, S.I., Dudhia, J., Von Der Mark, K., Kirchner, T., Phenotypic Diversity of Neoplastic Chondrocytes and Extracellular Matrix Gene Expression in Cartilaginous Neoplasms. *American Journal of Pathology*, 1997. 150(6): p. 2133-2141.
3. A.C. MacIntosh, The Evaluation of Spider Silk as a Scaffold for Cartilage Tissue Engineering, in *School of Clinical Dentistry, Faculty of Medicine*. 2006, University of Sheffield.
4. J.T. Oliveira, Crawford, A., Mundy, J.M., Moreira, A.R., Gomes, M.E., Hatton, P.V., Reis, R.L., A cartilage tissue engineering approach combining starch-polycaprolactone fibre mesh scaffolds with bovine articular chondrocytes. *Journal of Materials Science: Materials in Medicine*, 2007. 18(2): p. 295-302.
5. R. De La Fuente, Abad, J.L., García-Castro, J., Fernández-Miguel, G., Petriz, J., Rubio, D., et al., Dedifferentiated adult articular chondrocytes: A population of human multipotent primitive cells. *Experimental Cell Research*, 2004. 297(2): p. 313-328.
6. P.W. Noble, Hyaluronan and its catabolic products in tissue injury and repair. *Matrix Biology*, 2002. 21(1): p. 25-29.
7. R. Stern, Hyaluronan catabolism: a new metabolic pathway. *Eur J Cell Biol*, 2004. 83(7): p. 317-25.
8. J.K. Kutty, Cho, E., Soo Lee, J., Vyavahare, N.R., Webb, k., The effect of hyaluronic acid incorporation on fibroblast spreading and proliferation within PEG-diacrylate based semi-interpenetrating networks. *Biomaterials*, 2007. 28(33): p. 4928-4938.
9. A.P. Hollander, Hatton, P.V., *Biopolymer Methods in Tissue Engineering. Methods in Molecular Biology*. Vol. 238. 2006: Humana Press. 147-157.
10. G.A. Hutcheon, Downes, S., Davies, M.C., Interactions of chondrocytes with methacrylate copolymers. *Journal of Materials Science: Materials in Medicine*, 1998. 9(12): p. 815-818.
11. E. Zimmerman, Geiger, B., Addadi, L., Initial stages of cell-matrix adhesion can be mediated and modulated by cell-surface hyaluronan. *Biophysical Journal*, 2002. 82(4): p. 1848-1857.

12. G.J. Vinatier C., Daculsi G., Layrolle P., Weiss P., Cartilage and bone tissue engineerin using hydrogels. *Biomed Mater Eng*, 2006. 16(4 Suppl): p. S107-13.
13. S. Yamane, Iwasaki, N., Majima, T., Funakoshi, T., et al., Feasibility of chitosan-based hyaluronic acid hybrid biomaterial for a novel scaffold in cartilage tissue engineering. *Biomaterials*, 2005. 26(6): p. 611-619.



## Chapter IV – Prediction of bone ingrowth in PEPMHA scaffolds

### 1. Introduction

A key component in tissue engineering for bone regeneration is the scaffold that serves as a template for cell interactions and the formation of bone-extracellular matrix to provide structural support to the newly formed tissue [1].

The bioactivity can thus be defined as the ability of a material to be integrated in bone structures and support bone ingrowth without breaking down or dissolving.

It was early proposed that the essential requirement for a material to bond to living bone is the formation of hydroxyapatite ( $\text{Ca}_{10}(\text{PO}_4)_6(\text{OH})_2$ ), a form of calcium phosphate, on its surface *in vivo* and this situation has also been reported to occur on the surface of materials that can bond to living bone directly in bone defects [2].

It is known that in the living body, hydroxyapatite is formed as result of a process of mineralization, designated biomineralization. During this process, the organic matrix of the bone, such as collagens, controls both the location and organization of nucleation sites as the structure and orientation of hydroxyapatite.

This formation of hydroxyapatite can be reproduced in a simulated body fluid (SBF), which is a metastable calcium phosphate solution with inorganic ion concentrations almost equal to those of human blood plasma [3].

When a material is immersed in the SBF, apatite might form and its deposition is initiated by the heterogeneous nucleation of apatite. The presence of some types of surface functional groups on a material, such as silanol  $-\text{SiOH}$ , carboxyl  $-\text{COOH}$ , phosphate  $-\text{OPO}_3\text{H}_2$  groups increase the ability to form apatite as they provide a nucleation site for apatite on the substrate [2, 4, 5]. Once the apatite nuclei are formed on the substrate, they can grow spontaneously by consuming calcium and phosphate ions from the surrounding fluid.

Takeuchi used a 1.5x SBF solution, which has an ion concentration of 1.5 times more than the 1x SBF proposed by Kokubo [3]. It is noteworthy to mention that this fact will support the idea of an apatite deposition on an organic polymer that can be triggered by the existence of specific effective functional groups, which promote heterogeneous nucleation sites, but also by an increased concentration of calcium ions in the surrounding fluid to enhance the apatite deposition.

So, the formation of a bonelike apatite on a material's surface when immersed in SBF would be useful in the prediction of the *in vivo* bone bioactivity of a material [6]. This method can and should be used for screening bone bioactive materials before animal testing, and the number of animals used as the duration of animal experiments can therefore be remarkably reduced.

## 1.1. Objective

The main goal of this study is observing the surface of the produced polymeric systems whilst incubated in SBF solution, for different time periods, detect the presence of a Ca-P layer and whether this layer is extended into the bulk of the material.

## 2. Materials and methods

PEPMHA hydrogels were prepared as before (Chapter I).

The hydrogels were washed in water and ethanol baths, for approximately 1 hour each, and then put into polystyrene films introduced individually in wells of a cell culture plate, soaked with 1.5 ml of 1.5xSBF (Table 8). The protocol for the SBF solution can be found elsewhere [3].

Below it is just elucidated the SBF composition.

Table 8: 1.5xSBF composition for preparing 1000ml solution, pH 7.4.

Order	Reagent	Amount	Purity (%)	Formula Weight
1	NaCl	12.0525 g	99.5	58.4430
2	NaHCO <sub>3</sub>	0.5325 g	99.5	84.0068
3	KCl	0.3375 g	99.5	74.5515
4	K <sub>2</sub> HPO <sub>4</sub> ·3H <sub>2</sub> O	0.3465 g	99.0	228.2230
5	MgCl <sub>2</sub> ·6H <sub>2</sub> O	0.4665 g	98.0	203.3034
6	1.0M HCl	58.5 ml	-	-
7	CaCl <sub>2</sub>	0.438 g	95.0	110.9848
8	Na <sub>2</sub> SO <sub>4</sub>	0.108 g	99.0	142.0428
9	Tris	9.177 g	99.0	121.1356
10	1.0M HCl	0-5 ml	-	-

Specimens were incubated for 1, 3, 7 and 14 days at body temperature (37°C) with medium buffer being replaced every second day.

After soaking in 1.5x SBF for the different periods of time, specimens were coated with a metal film (Au:Pd/80:20) and observed under a scanning electron microscope equipped with an X-ray energy-dispersive spectroscopy microanalyzer (EDS).

### **3. Results and discussion**

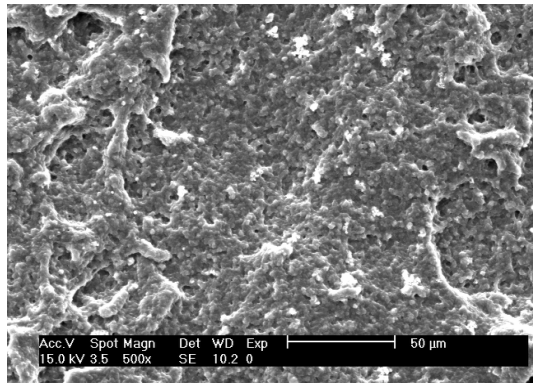
#### **3.1. SEM**

Figures 82-87 show scanning electron micrographs of the different PEPMHA hydrogels surfaces after soaking in 1.5x SBF at pH 7.4, for 1, 3, 7 and 14 days. These data enabled to follow the evolution of hydroxyapatite formation and its deposition on the surface of the different materials. So, on day 1, we observed an apparently normal surface of the material. On day 3, it is possible to detect the presence of some Ca-P nucleus, which start to expand at day 7. On day 14, the surface of the materials is already totally recovered by a layer of crystals that were observed at higher magnifications for a better comprehension of its morphology (micrographs sequence on figure 87). This behaviour was analogous for all the materials, except for the hydrogels in figure 84.

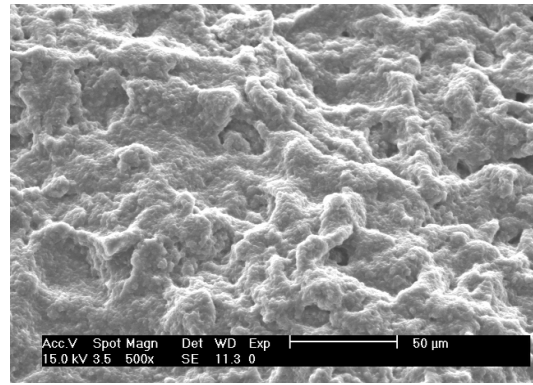
In most of the hydrogels it was in fact detected the formation of a continuous and adherent calcium-phosphate (Ca-P) layer, and evidenced the presence of a finer structure, where needle-like crystals are agglomerated to produce the so-called cauliflower morphology (Figure 82, day 7 and figure 83, day 14) [7].

Comparing all the images from the different groups of materials, the porosity seems to be affecting the apatite formation. Materials presenting a higher porosity (Figures 83, 86 and 87) appear to have induced a faster proliferation and more pronounced onto their surface than in the cases of materials less porous (Figures 82 and 84).

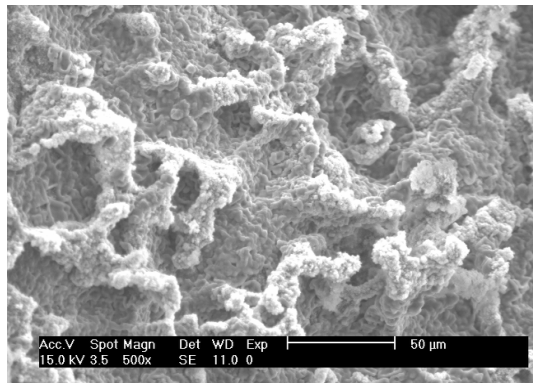
It is also noteworthy to mention that not only the apatite formed at the surface but to some extent into the materials bulk (day 14 and magnification of day 7, figure 83)



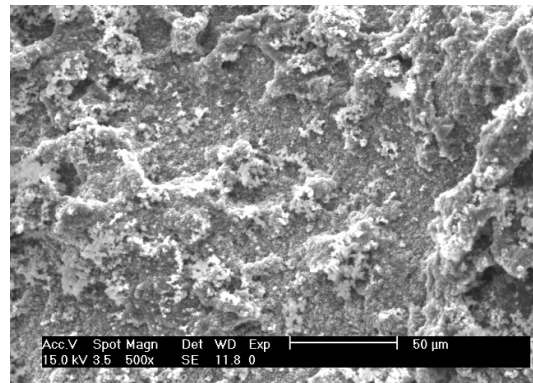
Day 1



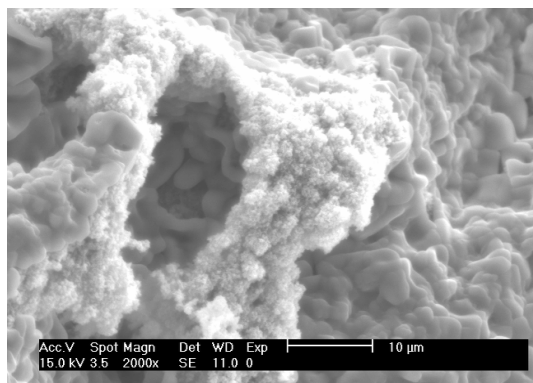
Day 3



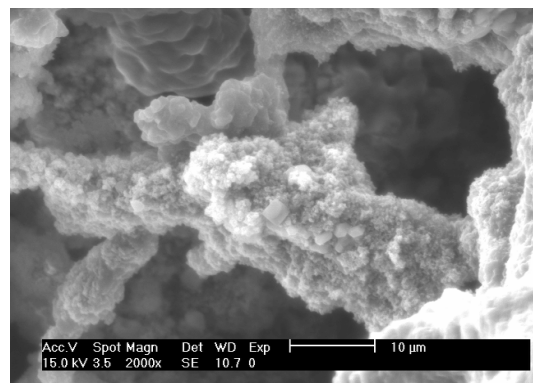
Day 7



Day 14

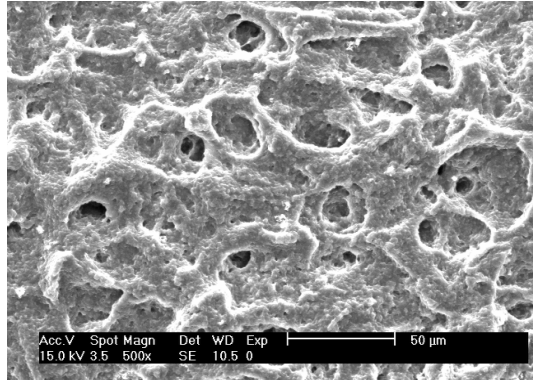


Day 7

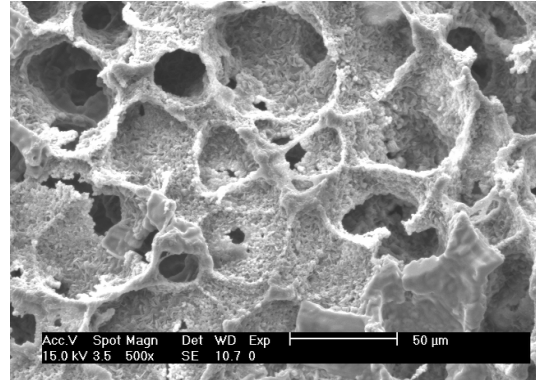


Day 7

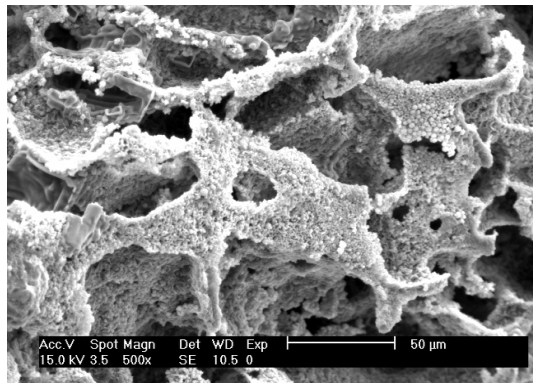
Figure 82. Scanning electron micrograph of calcium phosphates apatite like formations SEM on PEPMHA [0.545M EPM, 1% HA, 3% BIS,  $2 \times 10^{-2}$ M  $K_2S_2O_8$ ] hydrogels, after immersion in 1.5xSBF, at pH 7.4 for 1, 3, 7 and 14 days. Bottom pictures are the magnified images of the photograph taken at day 7.



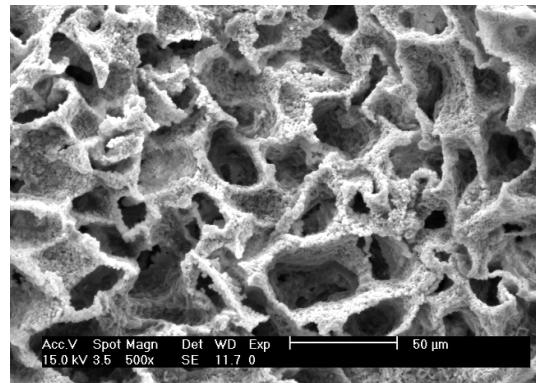
Day 1



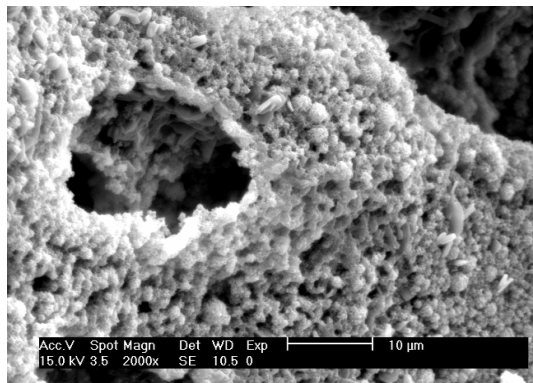
Day 3



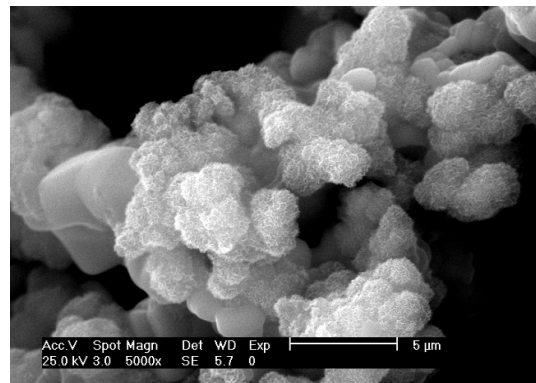
Day 7



Day 14



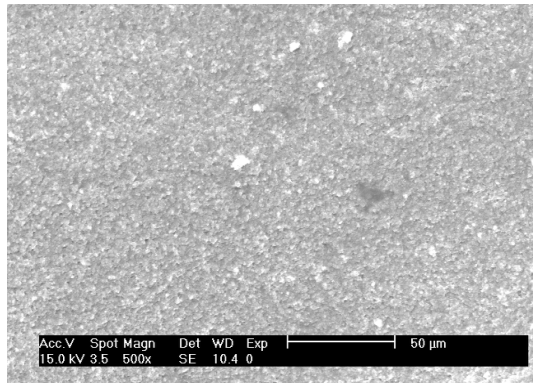
Day 7



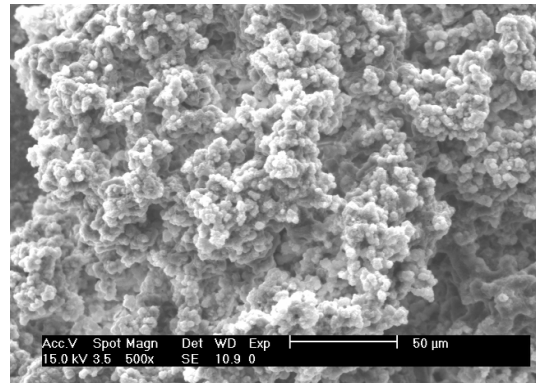
Day 14

Figure 83. Scanning electron micrograph of calcium phosphates apatite like formations on PEPMHA [0.545M EPM, 2.5% HA, 3% BIS,  $2 \times 10^{-2}$  M  $K_2S_2O_8$ ] hydrogels, after immersion in 1.5xSBF, at pH 7.4 for 1, 3, 7 and 14 days. Bottom pictures are the magnified images of the photograph taken at day 7 and 14, respectively.

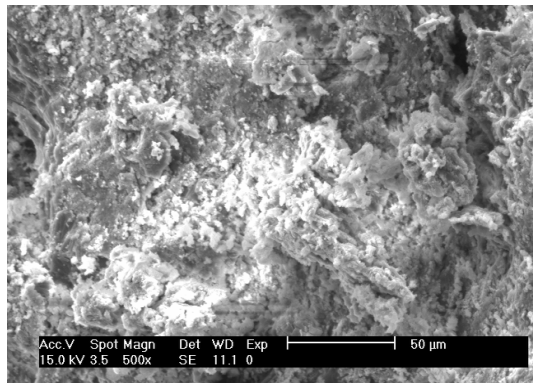




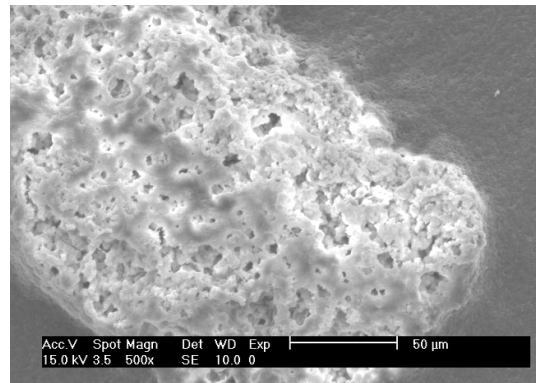
Day 1



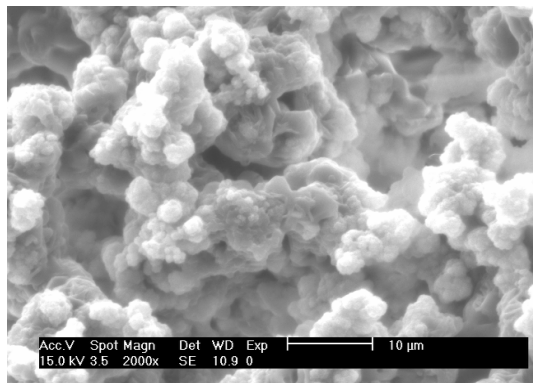
Day 3



Day 7

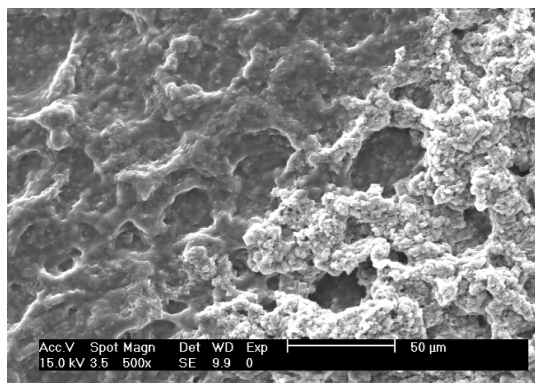


Day 14

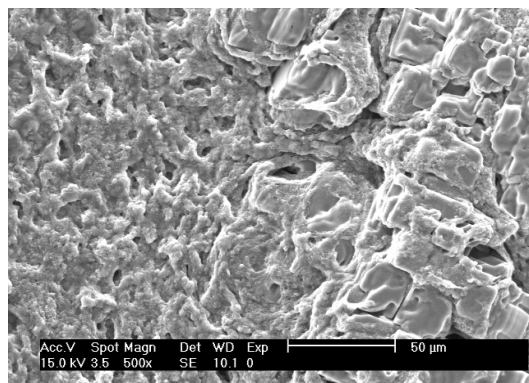


Day 3

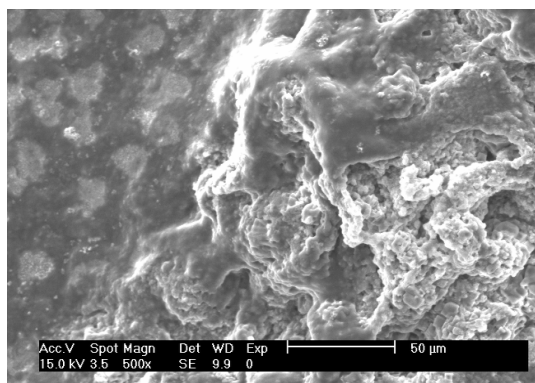
Figure 84. Scanning electron micrograph of calcium phosphates apatite like formations on PEPMHA [0.545M EPM, 5% HA, 3% BIS,  $2 \times 10^{-2}$ M  $K_2S_2O_8$ ] hydrogels, after immersion in 1.5xSBF, at pH 7.4 for 1, 3, 7 and 14 days. Bottom picture is the magnified image of the photograph taken at day 3.



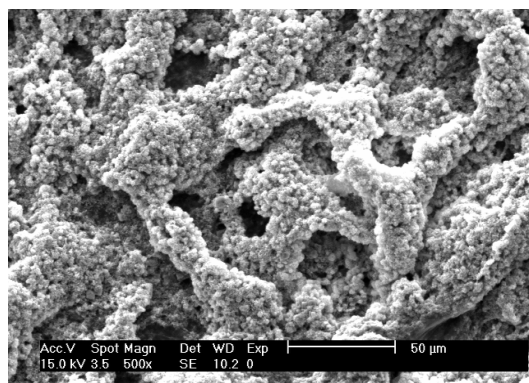
Day 1



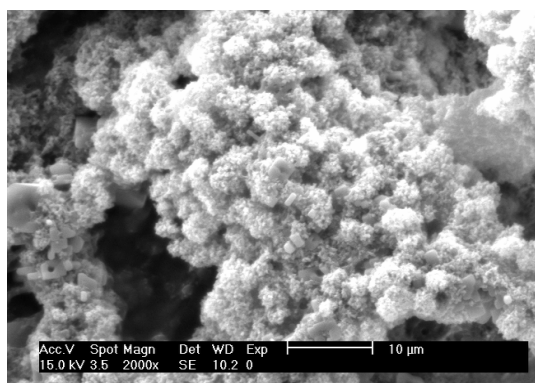
Day 3



Day 7

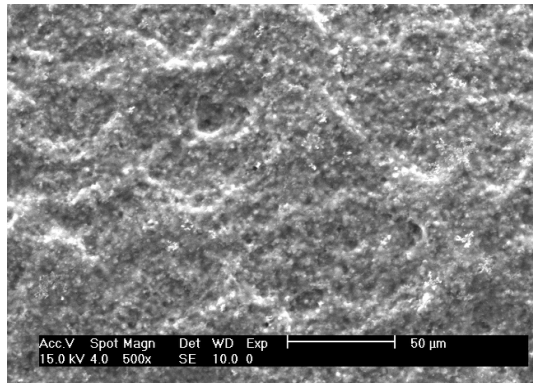


Day 14

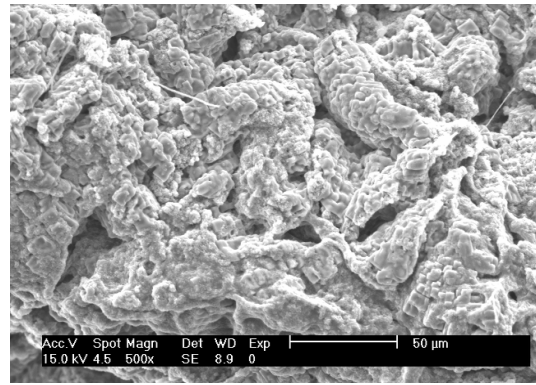


Day 14

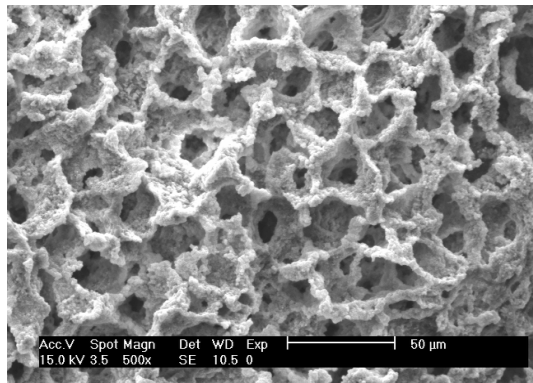
Figure 85. Scanning electron micrograph of calcium phosphates apatite like formations on PEPMHA [0.545M EPM, 1% HA, 1.7% TriEGDMA,  $2 \times 10^{-2}$ M  $K_2S_2O_8$ ] hydrogels, after immersion in 1.5xSBF, at pH 7.4 for 1, 3, 7 and 14 days. Bottom picture is the magnified image of the photograph taken at day 14.



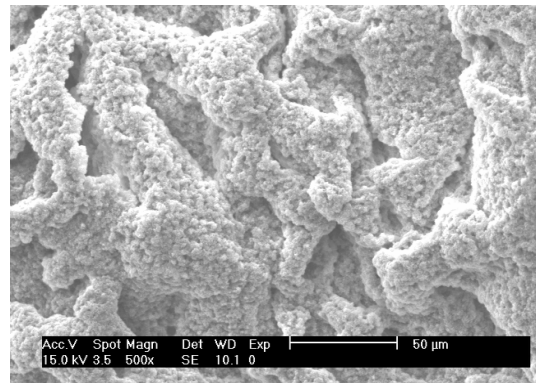
Day 1



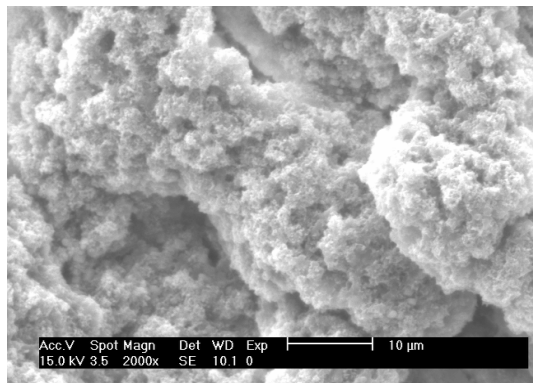
Day 3



Day 7

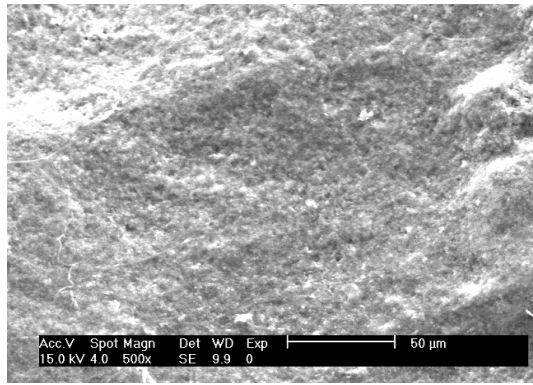


Day 14

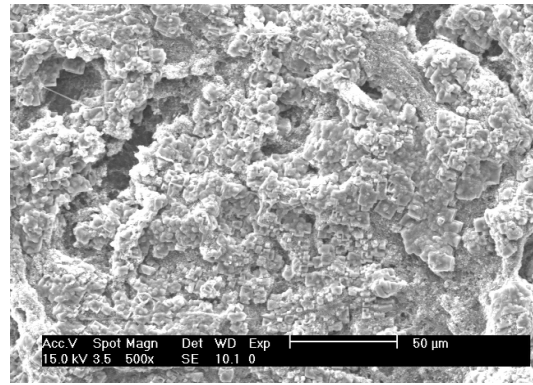


Day 14

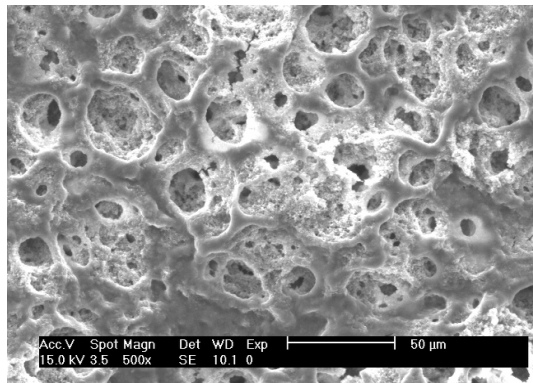
Figure 86. Scanning electron micrograph of calcium phosphates apatite like formations on PEPMHA [0.545M EPM, 2.5% HA, 1.7% TriEGDMA,  $2 \times 10^{-2}$ M  $K_2S_2O_8$ ] hydrogels, after immersion in 1.5xSBF, at pH 7.4 for 1, 3, 7 and 14 days. Bottom picture is the magnified image of the photograph taken at day 14.



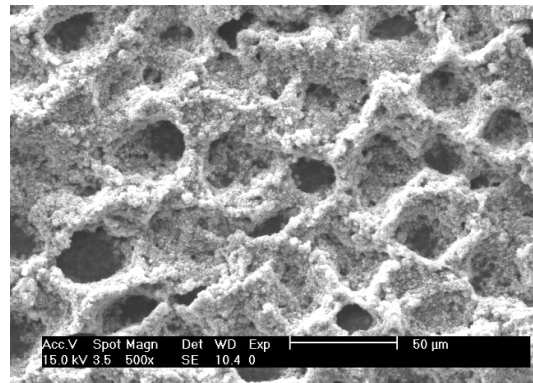
Day 1



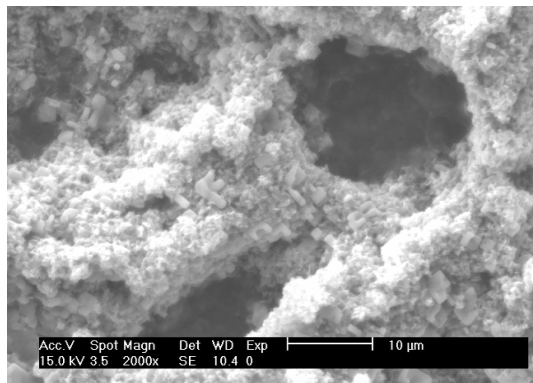
Day 3



Day 7



Day 14



Day 14

Figure 87. Scanning electron micrograph of calcium phosphates apatite like formations on PEPMHA [0.545M EPM, 5% HA, 1.7% TriEGDMA,  $2 \times 10^{-2}$ M  $K_2S_2O_8$ ] hydrogels, after immersion in 1.5xSBF, at pH 7.4 for 1, 3, 7 and 14 days. Bottom picture is the magnified image of the photograph taken at day 14.

### 3.2. EDS

The EDS spectrum for all the samples was very similar and hereby represented the results from a hydrogel chosen as an example. As it can be verified, calcium, phosphorous and oxygen were the dominant constituents of material's surface, after being soaked in 1.5xSBF, indicating the presence of a Ca-P layer (Figure 88).

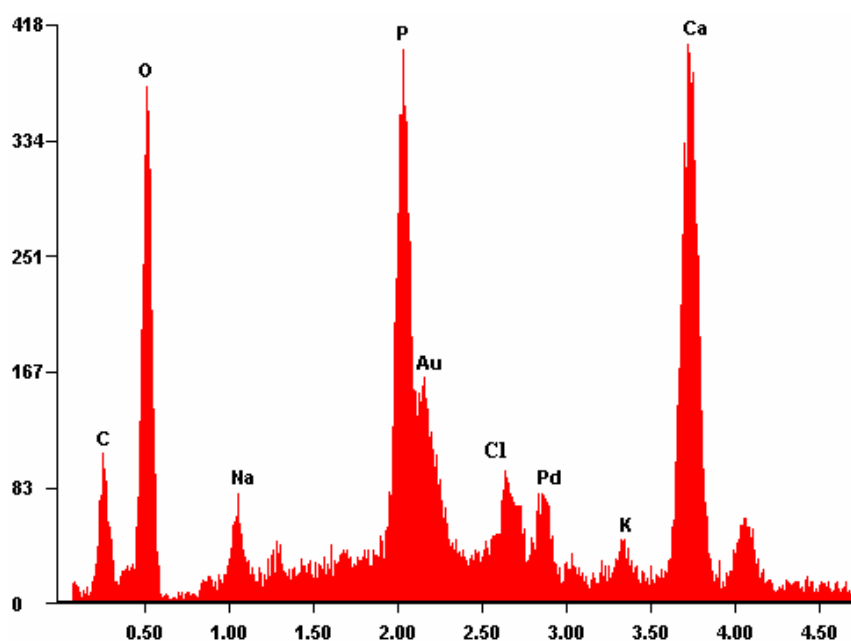


Figure 88. EDS spectrum of the surface of a PEPMHA hydrogel (0.545M EPM, HA 5%,  $2 \times 10^{-2}$ M  $K_2S_2O_8$ , 1.7% TriEGDMA) after 24 hours in 1.5xSBF immersion.

One drawback of the materials used is that some of the specimens appeared to desintegrate before the 14 days, which could lead to a differential distribution of the hydroxyapatite-like formed and for example in the case of 0.545M EPM, HA 5%, 3% BIS formulation, its gradual disappearance (Figure 84).

The deposition of hydroxyapatite on a substrate, in a metastable calcium phosphate solution, is initiated by the presence of substances that can induce heterogeneous nucleation of hydroxyapatite. Carboxyl groups are effective groups in the nucleation of hydroxyapatite from a solution that mimics the body fluid [6, 8, 9]. So, a high number of carboxyl groups, such as the ones present in the hyaluronic acid molecule, may enhance the apatite nucleation process.

Therefore it would be expected that the presence of this natural biopolymer, in the semi-interpenetrated networks of PEPMHA, would elicit a biomineralization of the substrate, with the velocity of the process directly correlated to an increase on the concentration of HA. When observing and comparing the speed of a Ca-P layer formation in the different hydrogels, it did seem that increasing the concentration of HA induced a faster induction of hydroxyapatite nucleation, except for hydrogels with the highest concentration of this polymer (HA 5%).

One can also speculate the formation of  $\text{-COOCa}^+$  complexes on the material's surface. Takeuchi has reported that the arrangement and orientation of the carboxyl functional groups, among others, influences in the hydroxyapatite nucleation, creating sites more suitable for this process [4]. The orientation of the carboxyl groups on the hyaluronic acid molecule wasn't considered in these studies, but more information about the arrangement of this functional group in the surface of the different PEPMHA hydrogels would be useful in understanding the different affinity of the materials to apatite formation, helping in the design of polymeric structures that would be more well suited for the induction of hydroxyapatite nucleation.

The water uptake capability of the PEPMHA hydrogels should also be considered hence it might generate a higher adhesive strength of the Ca-P. Again and as reported in other studies, a strong bond can be formed between the polar groups of the polymer and the calcium ions of apatite layer.

### 3.3. FTIR-ATR analysis

The following FTIR-ATR spectra allow us to compare the composition of the surface of a PEPMHA hydrogel before and after being incubation in 1.5xSBF for 7 and 14 days.

The most important bands that can be assigned for the PEPMHA were as determined in Chapter I. So, between 2800- 3200, N-H and O-H; between 1600-1800, C=O; between 1400-1500,  $\text{CH}_2\text{-N}$  and around 1200,  $\text{O-CH}_2$ . After PEPMHA hydrogels have been incubated in SBF we could assign the appearance of new bands: between 1550-1400 and around 875, characteristic from  $\text{CO}_3^{2-}$  groups, and between 1000-1100 and around 960, characteristic from  $\text{PO}_4^{3-}$  [10, 11]. These bands indicate the presence and nature of carbonate-hydroxyapatite.

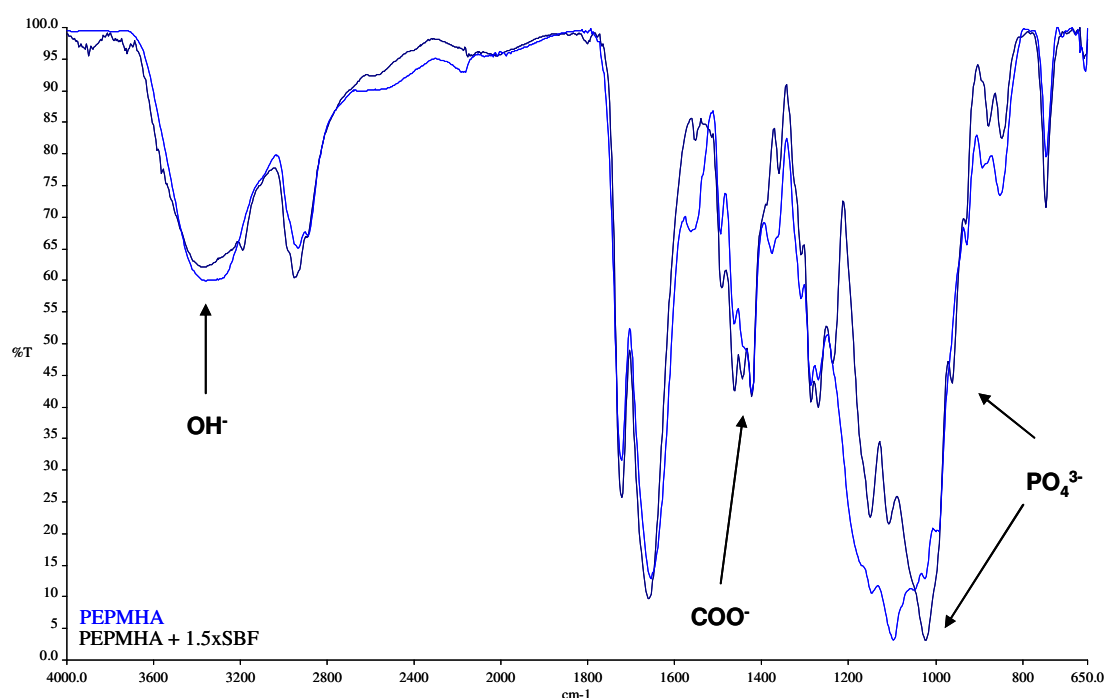


Figure 89. FTIR-ATR spectrum of PEPMHA hydrogel (0.545M EPM, HA 5%,  $2 \times 10^{-2}$  M  $K_2S_2O_8$ , 1.7% TriEGDMA) before and after 7 days of incubation in 1.5xSBF immersion.

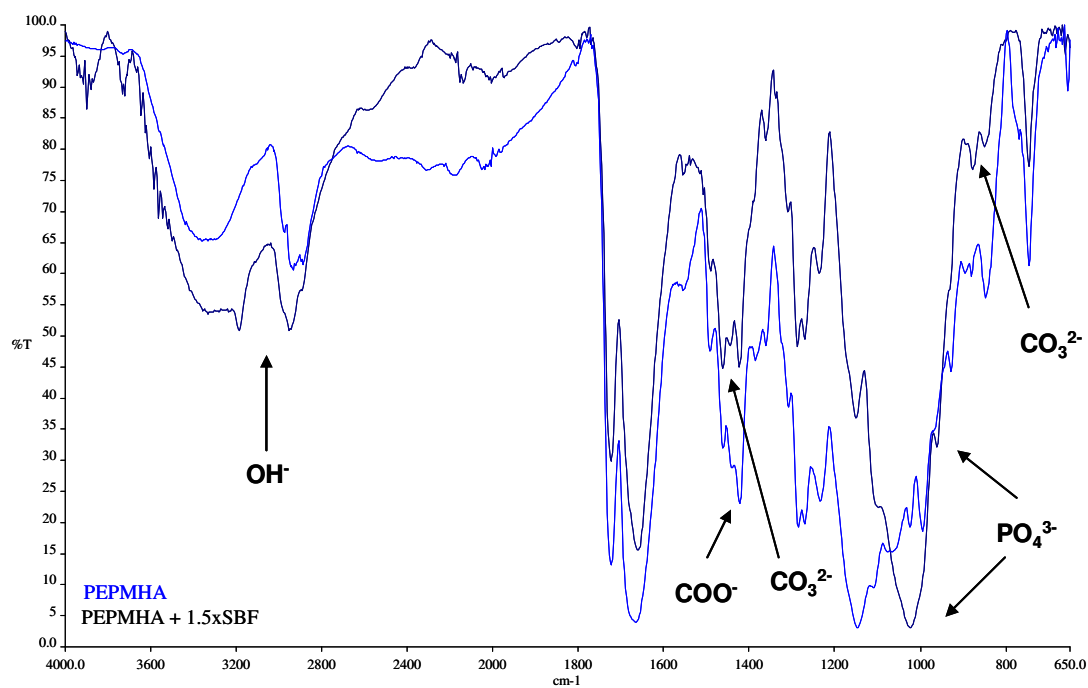


Figure 90. FTIR-ATR spectrum of a PEPMHA hydrogel (0.545M EPM, HA 5%,  $2 \times 10^{-2}$  M  $K_2S_2O_8$ , 1.7% TriEGDMA) before and after 14 days of incubation in 1.5xSBF immersion.

The evolution of the spectra with immersion times shows an increase of the strength of the bands from the characteristic groups of hydroxyapatite and decrease on the assigned bands for the PEPMHA from day 7 to day 14 is proportional to the quantity of hydroxyapatite deposited. This is, on day 7 the layer of the hydroxyapatite is only partially covering the polymer, so the characteristic bands of the polymeric system overlap have a broader signal and overlap the characteristics bands of the hydroxyapatite (Figure 89). Now, on day 14 as the hydroxyapatite is nearly totally covering the materials surface and thus interfering in the detection of the polymer groups (Figure 90). So, the comparison with a spectrum of PEPM not soaked on SBF makes it possible to assign the observed bands to the phosphate groups present in HA or other calcium phosphate minerals [12].

#### 4. Conclusions

In summary, the degree of the ability for apatite to form on the surface of a material, in SBF, can be used to predict the degree of *in vivo* bone bioactivity of a material. Thus, a material able to form apatite on its surface, in SBF, will rapidly bond to living bone as a result of apatite formation on its surface in a short period within the living body.

From the results obtained we could conclude that:

- the produced PEPMHA hydrogels were bioactive (hydroxyapatite formation);
  - o after 3 days it was already possible to observe hydroxyapatite deposition and day 7 for almost or even total covering of the material's surface;
- PEPMHA hydrogels produced with 0.545M EPM, 2.5% HA,  $2 \times 10^{-2}$ M  $K_2S_2O_8$ , either using BIS or TriEGDMA as the crosslinking agent, were the materials inducing a faster Ca-P layer formation.

The results obtained indicate that these materials should exhibit bone-bonding potential *in vivo*. Therefore we can predict the usability of these materials for bone tissue engineering.



## 5. Bibliography

1. A. Tampieri, G. Celotti and E. Landi, From biomimetic apatites to biologically inspired composites. *Anal Bioanal Chem*, 2005. 381(3): p. 568-76.
2. A. Takeuchi, C. Ohtsuki and e. al., Heterogenous nucleation of hydroxyapatite on protein: structural effect of silk sericin. 2005. 2(4): p. 373-378.
3. T. Kokubo and H. Takadama, How useful is SBF in predicting in vivo bone bioactivity? *Biomaterials*, 2006. 27(15): p. 2907-15.
4. A. Takeuchi, Ohtsuki C., Miyazaki T., Tanaka H., Yamazaki M., Tanihara M., Deposition of bone-like apatite on silk fiber in a solution that mimics extracellular fluid. *Journal of Biomedical Materials Research*, 2003. 65A(2): p. 283-289.
5. A.L. Oliveira, C.M. Alves and R.L. Reis, Cell adhesion and proliferation on biomimetic calcium-phosphate coatings produced by a sodium silicate gel methodology. *J Mater Sci Mater Med*, 2002. 13(12): p. 1181-8.
6. T. Kawai, C. Ohtsuki, M. Kamitakahara, T. Miyazaki, M. Tanihara, Y. Sakaguchi and S. Konagaya, Coating of an apatite layer on polyamide films containing sulfonic groups by a biomimetic process. *Biomaterials*, 2004. 25(19): p. 4529-34.
7. C.V. Ragel, M. Vallet-Regi and L.M. Rodriguez-Lorenzo, Preparation and in vitro bioactivity of hydroxyapatite/solgel glass biphasic material. *Biomaterials*, 2002. 23(8): p. 1865-72.
8. M.T. Tanahashi M., Surface functional group dependence on apatite formation on self-assembled monolayers in a simulated body fluid. *J Biomed Mater Res*, 1997. 34: p. 305-315.
9. C. Ohtsuki, Kamitakahara, M., Miyazaki, T., Coating bone-like apatite onto organic substrates using solutions mimicking body fluid. *Journal of Tissue Engineering and Regenerative Medicine*, 2007. 1(1): p. 33-38.
10. Y. Wang, Yang, C., Chen, X., Zhao, N., Biomimetic Formation of Hydroxyapatite/collagen Matrix Composite. *Adv Engineering Materials*, 2006. 8(1-2): p. 97-100.
11. T. Tolga Demirtas, A.G. Karakeçili and M. Gumusderelioglu, Hydroxyapatite containing superporous hydrogel composites: synthesis and in-vitro characterization. *J Mater Sci Mater Med*, 2008. 19(2): p. 729-35.

12. L.F. Boesel, S.C. Cachinho, M.H. Fernandes and R.L. Reis, The in vitro bioactivity of two novel hydrophilic, partially degradable bone cements. *Acta Biomater*, 2007. 3(2): p. 175-82.



## **Chapter V- Photopolymerization of PEPMHA systems**

After studying the properties of PEPMHA materials and verifying that cells maintain their viability and are able to proliferate in the presence of those materials, we intended to use a different approach for a faster preparation of the hydrogels in order to perform future cell encapsulation.

The following chapter gives an insight of preliminary studies to the elaboration of new photopolymerizable hydrogels based in EPM and hyaluronic acid.

### **1. Introduction**

The development of biodegradable and biocompatible photopolymerized polymers has arise as a possible strategy to reduce the invasiveness and cost of biomaterial implants designed to be used in wound healing and tissue repair.

We are mainly focused on hydrogels that can be photopolymerized in vivo and in vitro using ultraviolet (UV) light.

Photopolymerization is used to transform a monomer or macromer solution into a hydrogel in a fast and controllable manner under ambient or physiological conditions [1]. Allying this technique to the use of injectable materials would facilitate the formation of hydrogels in situ, using transdermal photopolymerization, which uses the transmission of light through tissue to photopolymerize an injected solution.

Photopolymerization presents several advantages over conventional polymerization techniques. Spatial and temporal control of the gelation process, fast curing rates at room or physiological temperatures and minimal heat production, are some of the features that contribute for its choice [2-4].

In addition, through some other characteristics like: being operational at low temperature, under aqueous condition, and by requiring a low initiator concentration, photopolymerization can minimize the damage to the entrapped bioactive agents or cells during hydrogels formation [5].

This technique is applied in the development of electronic, polymeric and optical materials, membranes, coatings, food industry and surface modifications [6]. Other common application of photopolymerization is the fabrication of complex three dimensional scaffolds with tailored properties and precisely placed cells and growth

factors [7] or even scaffolds with specific patterns promoting the control of cell behaviour, cell-cell communication and cell migration [8].

### 1.1 Photopolymerization Reactions

Photopolymerization reactions, to form linear or crosslinked polymeric structures, are driven by light-sensitive chemicals, designated photoinitiators (PI) that generally produce free radicals when exposed to specific wavelengths of light.

These reactions have both natural and synthetic origin precursors with one similarity; their backbone needs to have a photopolymerizable group, normally located at one or both ends of the structure. There are some natural occurring polymers, and many synthetic monomers and macromers fulfilling this requirement. Others might undergo determined chemical reactions to modify their structure enabling them to be photoreactive and to undergo photopolymerization. For example, methacrylic anhydride, methacryloyl chloride, and glycidyl methacrylate are examples of chemicals that may be used to add methacrylate groups to a polymer chain [9-12].

A variety of photoinitiators, each with a specific absorption spectrum, are available and continuously being developed. As mentioned before, they are involved in free radical photopolymerization reactions, which mechanism consists in 4 steps: photoinitiation, propagation, termination, and eventually inhibition. Basically, a photon from a light source excites or dissociates the PI into a high-energy radical state that is responsible for the induction of the material polymerization.

There are three possible mechanism of photoinitiation, depending on the mechanism of photolysis, namely: radical photopolymerization through photocleavage, hydrogen abstraction and cationic photopolymerization, having the latest different applications in tissue engineering. Description of the mechanisms can be found elsewhere [1].

Photopolymerization in these applications can be carried out as bulk (also known as homogeneous) or by interfacial photopolymerization and, both *ex* or *in vivo* (*in situ* photopolymerization). Bulk photopolymerization is more commonly used. It consists in the dissolution of the PI in a monomer(s)/ macromer solution that will be irradiated with an adequate light source to form polymerized or crosslinked materials. In interfacial photopolymerization the PI is firstly adsorbed onto the surface of interest that will be exposed to the photopolymerizable mixture and after irradiated. So, the photo-reaction

occurs where the precursor solution is in contact with the adsorbed PI, namely at the tissue interface.

This is a unique technique because it allows the isolation of a group of cells or tissues through the creation of a thin lining of polymer, normally inferior to 100  $\mu\text{m}$ . This technique has been continuously referred for cell encapsulation, where the polymer membrane allows sufficient immunoprotection and eases the diffusion of nutrients and metabolism products [13]. It has been applied in the treatment of type I diabetes, the prevention of blood vessels constriction following catheter-based interventions, stem cell-based therapies for cartilage repair or augmentation therapies.

The above mentioned applications involve single membranes that are generally formed in a single procedural step. However, it is difficult to obtain single membranes that possess all the properties required for a specific application. Hence, the use of multilayers would provide more precise properties in the case of a single material not being able to achieve the requirements for a determined application. This can be obtained by varying the composition or concentration of the precursor solution in each individual layer [14].

## **1.2. Cell Encapsulation**

Cell encapsulation aims to isolate determined viable cell populations within semi-permeable membranes from a specific surrounding environment. This technology has evolved in the sense of transplanting allogeneic or xenogeneic cells and tissues through an immunological barrier without the need for immunosuppression, providing potential therapy for a wide range of diseases, for instance renal failure or diabetes [15]. Avoiding the administration of immunosuppressant drugs, scientists overcome cross unwanted side effects that their systemic use might lead to, especially concerning the non-specific suppression of the immune system, facilitating opportunistic infections and other adverse complications.

By encapsulating the cells with a semi-permeable membrane, it allows a bidirectional diffusion of molecules. The membrane is permeable to nutrients that are required to the metabolic maintenance of cell function, as well as it permits the diffusion of cell products out of the membrane, providing an immunological protection by restraining the migration of antibodies and cell fragments across the barrier.

Depending on the choice of the membrane's material and the time point when the membrane is produced around the viable cells, cells will be subjected to different entrapment conditions.

The distinct procedures result in capsules with different permeabilities, specific physicochemical characteristics, and present different biocompatibility that contribute to variations in the host response and subsequent success rate of the encapsulated cells.

### **1.2.1 Cell Incorporation Routes**

Encapsulation techniques can be classified as macro or microencapsulation.

Membranes produced through macroencapsulation are in general composed of thermoplastic materials that enable the development of intra and extravascular therapeutic devices to treat endocrine, metabolic and nervous system disorders. This approach is well defined elsewhere [16].

In the other hand, microencapsulation techniques are based in hydrogels, where the reduced scale of the capsules produced is considered advantageous in concern to mass transport, and natural polymers are generally preferred because of their low/non toxicity, low immunogenicity and thereafter good biocompatibility. Examples of this are: modified polysaccharides such as hyaluronic acid derivatives [17], dextran, collagen [6] or inter-penetrating networks formed by chitosan/HEMA [18]. But also synthetic origin ones were already reported: multivinyl macromers that can reach high degrees of conversion through photopolymerization [19] like: poly(ethylene glycol) (PEG) acrylate derivatives, PEG methacrylate derivatives, poly(vinyl alcohol) (PVA) derivatives, poly(ethylene glycol) dimethacrylate (PEG-DM) and poly(lactid acid)-*b*-poly(ethylene glycol)-*b*-poly(lactid acid) dimethacrylate (PLA-*b*-PEG-*b*-PLA DM) [20].

The concept of microencapsulation was first demonstrated in the 1960s with protein encapsulation into stable microspheres with semipermeable polymer membranes. Since then, microencapsulation technologies for immobilization of a variety of biologically active species have been applied for developing bioreactors, biosensors and hybrid bioartificial organs [21].

There are two possibilities for the incorporation of cells into the scaffolds: seeding the cells onto the surface of scaffolds after the scaffold fabrication (docking the cells within low shear stress regions generated by the material structure) or the incorporation of cells

during the fabrication process. The later would allow the direct encapsulation of cells in gels increasing the efficiency and uniformity of cell seeding in concern with solid scaffolds [22].

The encapsulation of cells within gels was proposed as a method that enables the scalable expansion of anchorage dependent cells within bioreactors. Yet, the immobilization of cells in larger volumes compromises the viability of the cells in the core of the capsule due to the difficulty of access of sufficient levels of oxygen and nutrients [23].

After the first reports on successful cell microencapsulation, using polyelectrolyte complexation of polyanionic alginate with polycationic poly (L-lysine), many other techniques, have been developed [24]. Capsules can be formed from water soluble alginate polymers using an aqueous complex coacervation process. However, this type of microcapsules usually has lower mechanical strength due to possible highly hydration and the interaction between the polymeric layers be done trough ionic bonding instead of stronger covalent bonding. An attempt is being made to improve the mechanical strength by a two-step encapsulation process to form microcapsules with four separate layers [21].

Thermo-responsive hydrogels present a number of potential advantages for cell encapsulation, including fast thermal-induced gelation in aqueous surroundings and a high water content imparting a softness that reduces local tissue irritation and ensures good biocompatibility. However, this high water content may result in potential instability of the system, with poor mechanical integrity that would lead to their dissolution. This problem might be overcome with the addition of an extra membrane [15]. It is important to keep in mind that the polymer networks should present reversible gel-transition near physiological temperatures, in order to enable the cell's survival during the process.

Other cell encapsulation routes based in hydrogels, by extrusion, simply-oil-in-water dispersion, interfacial precipitation, conformal coating and in situ and photo polymerization are also being developed and improved.

These techniques have been employed using different kind of cells, namely, vascular interstitial cells, fibroblasts, HepG<sub>2</sub> cells, hepatocytes, vascular smooth muscle cells, stem cells, chondrocytes and human bone marrow derived mesenchymal stem cells [9, 21, 25-28], with applications in bone, cartilage, kidney, heart and DNA delivery systems [25, 29-32].



Although the concept of cell encapsulation might present new opportunities in the field of tissue engineering and guided tissue repair, it should be kept in mind that this encapsulation is limited to a micrometer scale.

For this reason, the increased control in spatial resolution with photopolymerization has brought an income to the design of scaffolds on a scale that ranges the micrometer to even nanometer level [4], as well as processing techniques given by rapid prototyping, such as: photopatterning, and both capillary force-, photo-, soft- and stereo-lithography [23, 33-36].

This processing methods offer the technology that enables the manipulation of polymeric systems with encapsulated bioactive components such as growth factors, cells and drugs [22].

### **1.3. Objectives**

When developing a successful scaffold for tissue engineering, several questions arise such as: how to tailor the architecture of the scaffold to provide adequate transport, mechanics, degradation and how to obtain a uniform cell density as the scaffold thickness is increased, over the range of potential defects, from partial to full thickness defects. This question is especially important in the case of cartilage repair.

Bryant et al., demonstrated that photopolymerization reactions offer flexibility for generating cell carriers from a range of macromer chemistries, providing a route to allow the same scaffold to serve multiple functions, like mechanical support as well as cellularly recognizable environment [32].

One should also keep in mind that hydrogel polymerization parameters such as photoinitiator, type and concentration, UV intensity, and duration of UV exposure will influence both in the material's properties as well as in the encapsulated cell viability [27, 37]. It is also important to assess the response of the encapsulated cells to the material used for encapsulating, as well as the response of the surrounding host cells.

We intend to direct preliminary studies in order to characterize some properties of the photopolymerized PEPMHA systems for future applications in cell encapsulation routes.

## 2. Material and methods

Considering this revising chapter, we focused on a bulk photopolymerization formed with PEPMHA polymeric systems.

### 2.1. Bulk Photopolymerization Process

The photoinitiator Irgacure 2959 (2-hydroxy-1-[4-(2-hydroxyethoxy)phenyl]-2-methyl-1-propanone, Ciba Chemicals, Figure 89) was dissolved in 70% ethanol. The resulting photoinitiator solutions were protected from light and stored at room temperature until use.

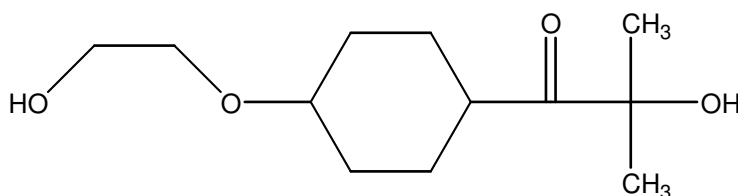


Figure 89. Chemical structure of the photoinitiator Irgacure 2959.

Photoinitiator (0,006 up to 1% w/w) was added to the hydrogel precursor solution, composed by 0.0018M EPM dissolved in HA (1 and 2%, Bioiberica), upon exposure to an UV light source (UV Spot Light Source, Lightningcure<sup>TM</sup> L8868, Hamamatsu), irradiated with long wavelength (364 nm, 1.53 mW/m<sup>2</sup>; and 313 nm, 0.54 mW/m<sup>2</sup>), at room temperature. The distance between the UV-irradiating source and the surface of the solution (6 and 8 cm) presents other variable studied. After being polymerized, hydrogels formed were washed to remove any unreacted products and freeze-dried.

### 2.2. Characterization of the materials

#### 2.2.1. Spectrometric Techniques

Absorbance was determined using a UV/Vis spectrometer Lambda 35, PerkinElmer.

### 2.2.2. Spectroscopic Techniques

ATR-FTIR method as described in chapter I.

### 2.2.3. Thermal Analysis Techniques

Thermogravimetric analysis was described in chapter I.

### 2.2.4. Microscopic Techniques

The pore size was estimated using SEM images (Philips XL30-ESEM) at 15 kv. Freeze-dried specimens of PEPMHA prepared through photopolymerization were thinly metal-coated (Au:Pd/80:20) and observed by SEM. The SEM photographs were taken at low (500x) magnifications.

### 2.2.5. Dynamic Mechanical Analysis

As in chapter I.

### 2.2.6. Swelling properties

This method was described in chapter II- water uptake/swelling studies.

## **3. Results and discussion**

From the moment that a material is irradiated with light, this should polymerize in an adequate time, designated clinic time, and that is dependent, for each case, on the final application of the product. This polymerization process is dependent of the formulation of the materials used and the concentration and chemical structure of its components. This process also depends on the intensity of the incident light and wavelength of the irradiation.

### 3.1. Preparation of PEPMHA hydrogels through bulk photopolymerization

Before starting with the polymerization reaction, the absorbance of the components of the photopolymerization system was determined, in order to verify that the species present wouldn't compete for the light absorption.

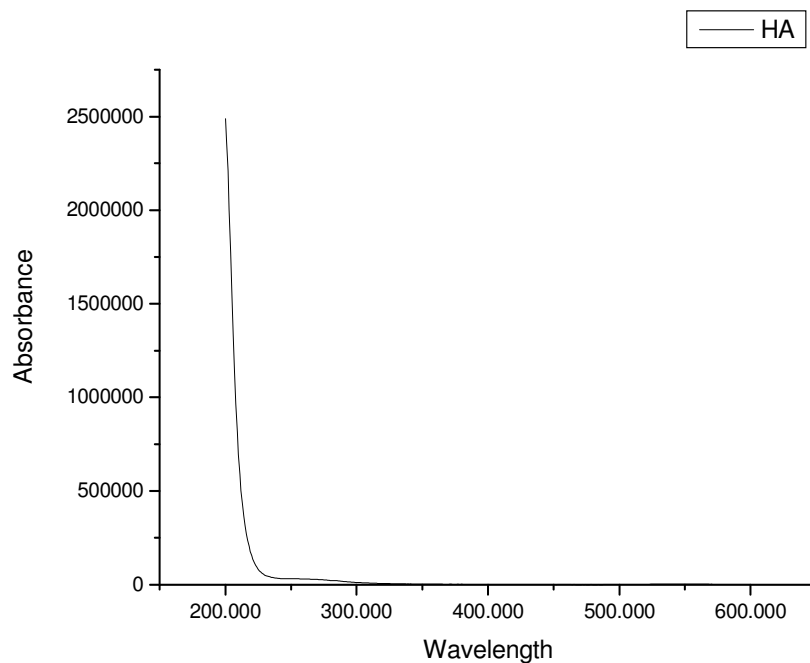


Figure 91. Hyaluronic acid absorbance in function of the wavelength.

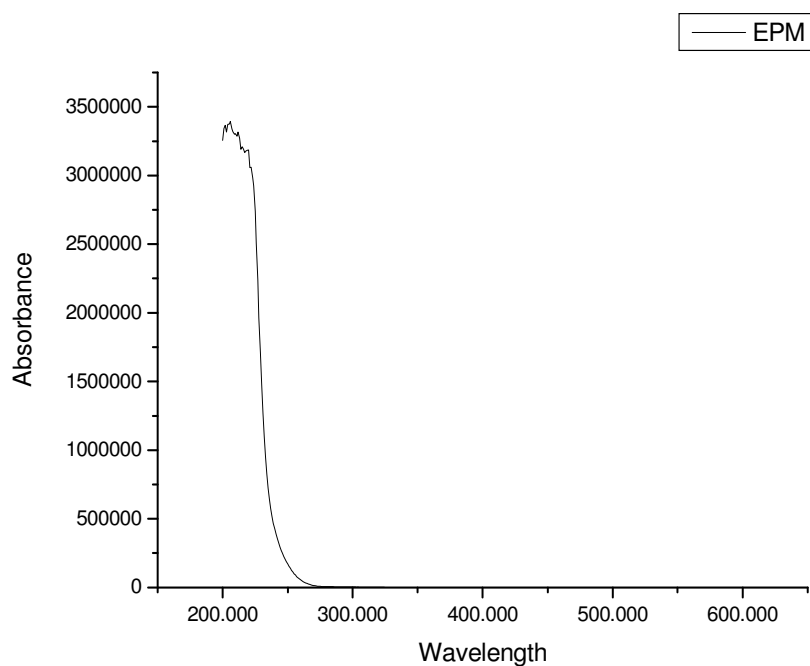


Figure 92. EPM absorbance in function of the wavelength.

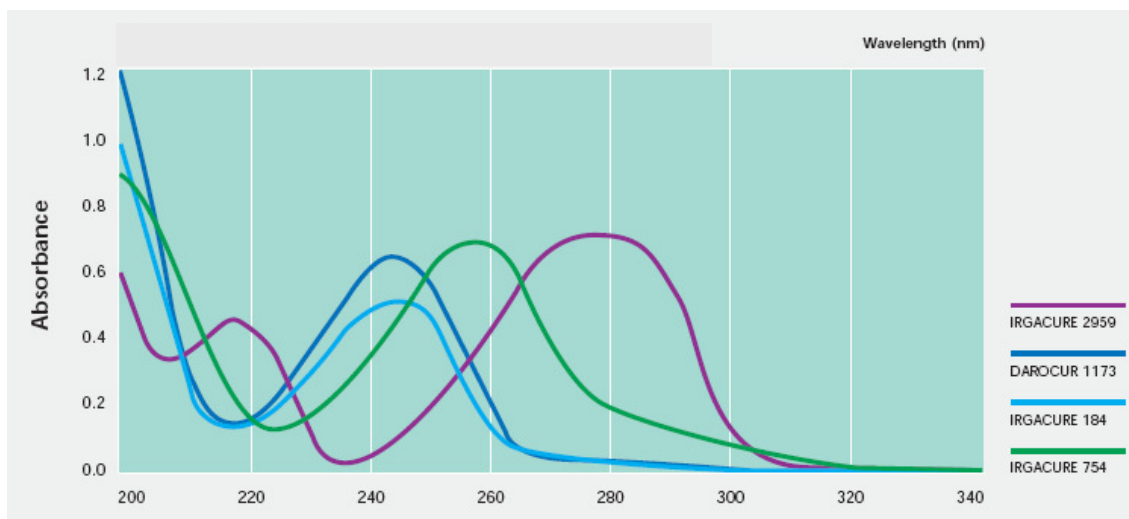


Figure 93. I2959 absorbance in function of the wavelength [38].

Absorption peaks from the monomer EPM and biopolymer HA are below the 300nm (Figures 91, 92). As for the photoinitiator, the higher absorption peak was determined to be 276nm (Figure 93). Although the absorbance of these PI at the wavelength range of the UV lamp used, namely 364 and 313 nm, is reported as being less than 10%, it has been proven in published studies, to be sufficient to induce photopolymerization, and most importantly it is also cytocompatible [37].

Bulk photopolymerization conditions were optimized after the study of the effects of some selected factors, namely, distance to the source of light, irradiation time, monomer concentration, dissolvent concentration and finally the photoinitiator concentration, within a range that has already been reported as biocompatible.

In the following table are summarized some of the conditions that these study was focused on.

Table 9: Photopolymerization conditions and reactants concentrations.

EPM (M)	HA (%)	Distance to source of light (cm)	Photoinitiator (%)
0.0018	1	6	0.5
			1
		8	0.5
			1
	2	6	0.006
			0.02
		8	0.5
			1

Photo-PEPMHA systems were obtained with high yields (70%), although it would be important to assess in the future the conversion rate of the monomer. In general, it is very difficult to obtain total conversion of the double bonds present. This is mainly due to the formation of a very viscous tri-dimensional network that entraps the monomer molecules that haven't reacted, avoiding their incorporation to the polymeric chains.

Unreacted monomer can have significant effects on the mechanics and biocompatibility, with severe implications for biological applications. For example, low conversions can decrease the mechanical properties of a biomaterial, and when implanted, unreacted and potentially toxic monomer can leach out from the construct and have prejudicial effects on the surrounding tissue. So, it is of high importance obtaining conversions approaching the 100%.

The minimum time of irradiation which resulted in an insoluble hydrogel was of 2 minutes. Then, the yield of the gel phase increases by increasing the irradiation time until approximately 45 min. But, for longer periods, it decreased probably because of partial photodegradation that occurs as a consequence of a prolonged exposure to UV light. Similar results were obtained in other reported studies [39].

The precursor solutions photopolymerized resulted in soft consistent hydrogels with white colour. This fact might be a barrier for the hydrogels formation hence the colour would affect a homogenous light incidence through all sites of the sample, leading to a heterogeneous polymerization, specifically with polymerized surfaces and non-polymerized bulk.

## 3.2. Characterization of the materials

### 3.2.1. Spectroscopic Techniques

The produced hydrogels were characterized by FTIR spectra.

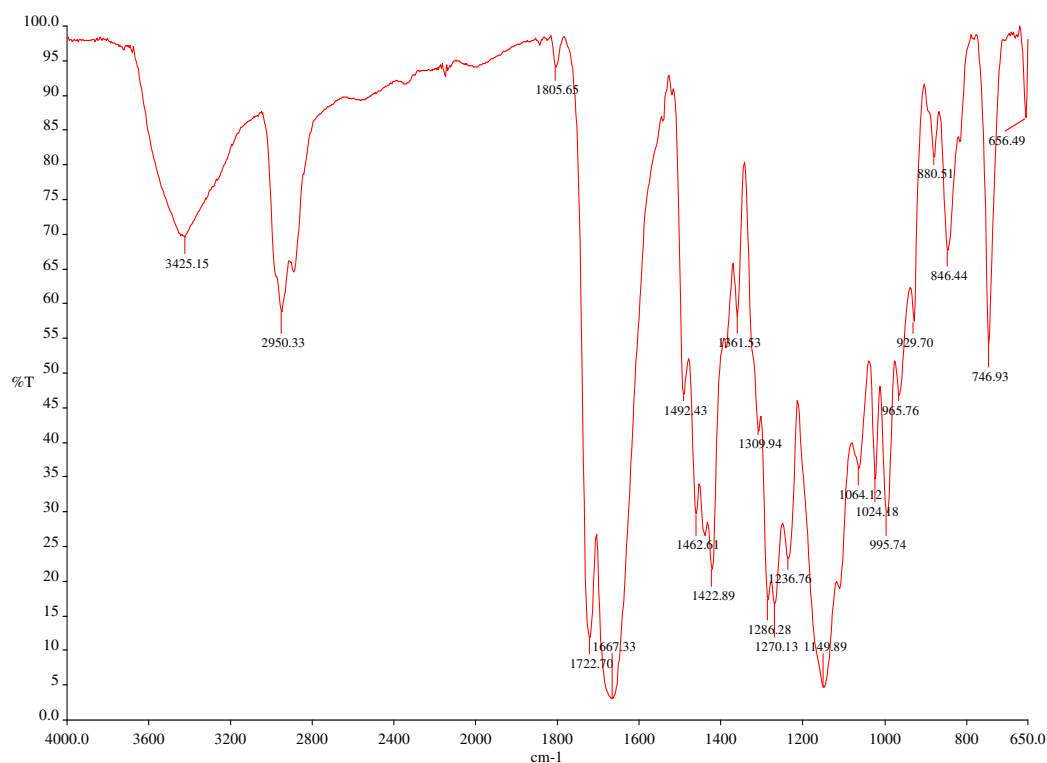


Figure 94. FTIR-ATR of PEPMHA prepared through photopolymerization.

The FTIR-ATR for the prepared photopolymerized systems (PEPMHA) was as follows: ( $\nu$ , cm<sup>-1</sup>), 3425 (N-H, O-H), 2950 (C-H), 1722 (C=O), 1667 (C=O cycle), 1422 (CH<sub>2</sub>-N), 1270 (O-CH<sub>2</sub>) (Figure 94). If we compare this results to the ones obtained for the polymers prepared to thermal polymerization, as in Chapter I, Figure 10, there is a small shift of the absorption values towards the left, meaning that the bonds between the mentioned groups are stronger. This makes sense in the way that the presence of crosslinkers in the thermal polymerization is expected to decrease the energy needed to change the vibration bonds of the polymer as they are weaker.

### 3.2.2. Thermal Analysis Characterization

The decomposition profile and associated first derivative curves of photo-PEPMHA hydrogels are shown in the spectrum from figure 95.

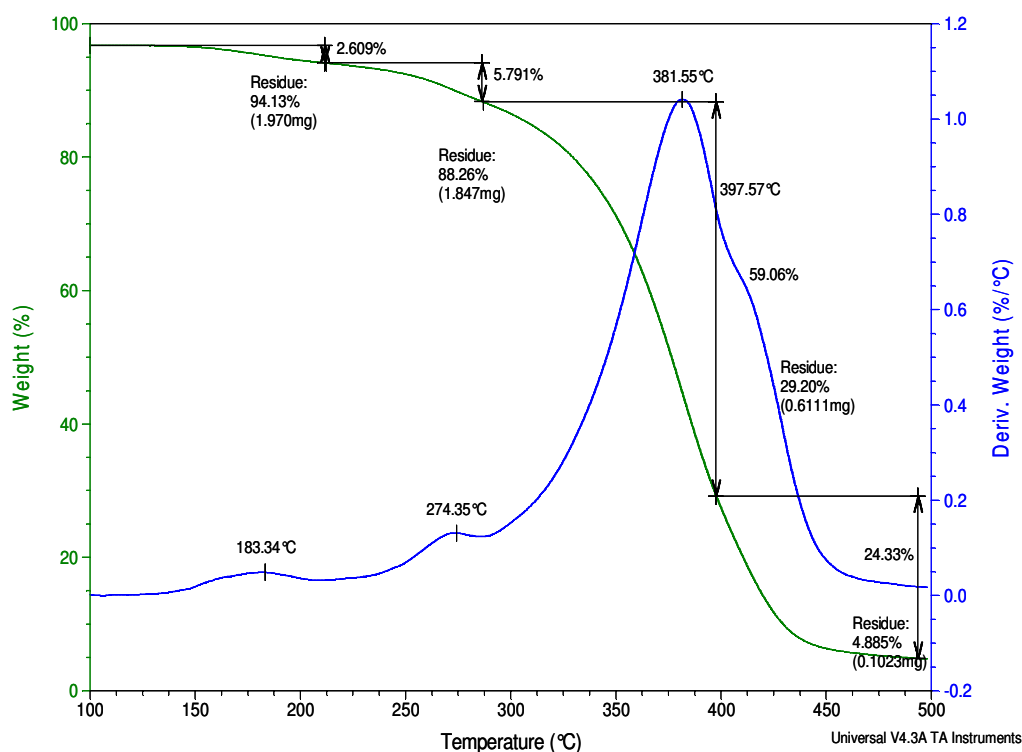


Figure 95. Thermogravimetric analysis spectrum of photo-PEPMHA.

The photopolymerized PEPMHA systems presented thermal stability up to 183°C, when decomposition began. The thermal decomposition of these polymeric systems can be defined by four regions, with maximum decompositions rates at: 183.34 °C (2.609 %wt loss), 274.35°C (5.791% wt loss), 381.55 °C (29.20% wt loss) and 397.57°C (4.885% wt loss). The obtained results were similar to the ones obtained for the PEPMHA systems prepared in chapter I, although the identified regions of thermal decomposition of the polymeric systems obtained through photopolymerization have maximum decompositions rates at temperatures inferior to the ones obtained in chapter I. This might be due to the fact that there weren't used any crosslinkers in the photopolymerization reaction.



### 3.2.3. Macroscopic Characterization

Porosity was observed by scanning electron microscopy (SEM).

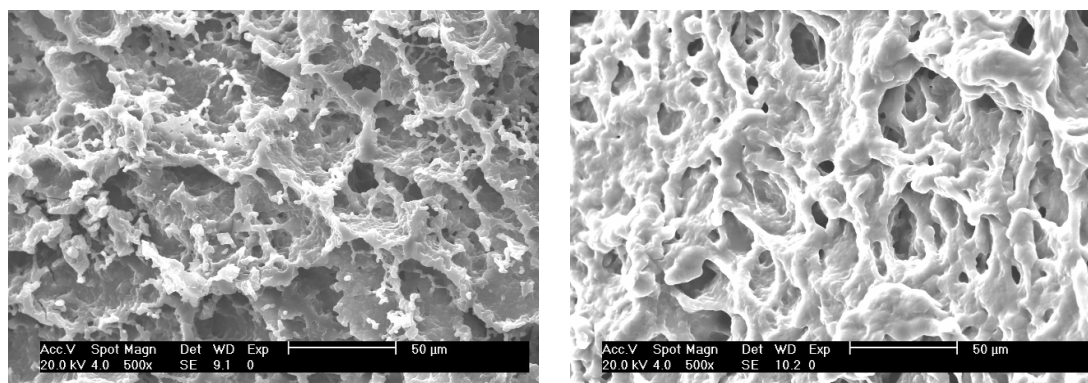


Figure 96. Scanning electron micrographs (500x) from 0.0018M EPM polymerized in the presence of HA 1%, using I2959 (0.5% w/w) as photoinitiator, at 8 and 6 cm from source of light, respectively.

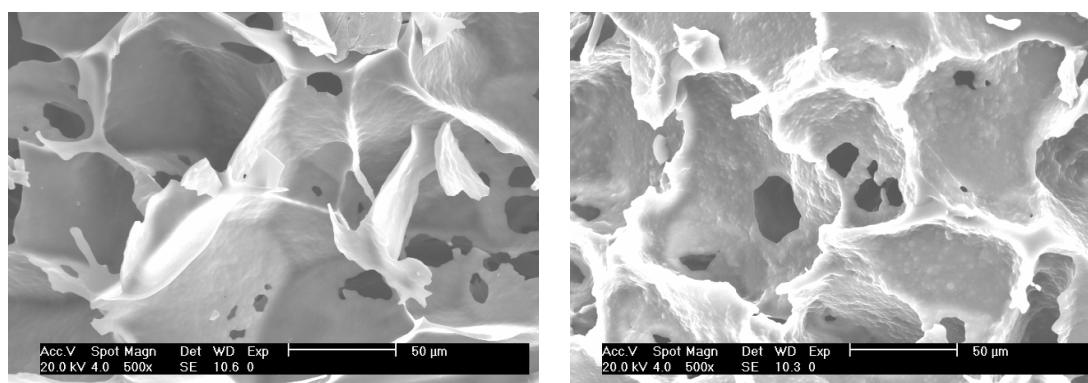


Figure 97. Scanning electron micrographs (500x) from 0.0018M EPM polymerized in the presence of HA 2%, using I2959 - 0.5 and 1% w/w, respectively, as photoinitiator, at 8 cm from source of light.

When the distance to the source of light was varied in the polymerization reaction, there were produced materials with small changes in their morphology- sharpen edges (left image, 8 cm) and rounded edges (right image, 6cm) (Figure 96).

A greater influence was observed when the concentration of hyaluronic acid was increased. In this case the hydrogels present a honeycomb type of porous structure, with a smooth surface for hydrogels polymerized in the presence of a lower concentration of PI (left image, 0.5%) and a rough surface for hydrogels polymerized in the presence of a higher concentration of PI (right image, 1%), (Figure 97).

So, obviously the different parameters varied in the polymerization reaction are influencing in the morphology of the obtained hydrogels. This will be important to

consider when cellular studies are developed because it is well known that cellular adhesion is sensitive to the surface morphology.

### 3.2.4. Swelling behaviour of the photopolymerized PEPMHA hydrogels

Hydrogels were swollen in aqueous solutions of pH 7.4, at 37°C.

The water uptake degree of the photopolymerized PEPMHA hydrogels was followed until equilibrium was reached.

In the SEM images captured it was obvious that the concentration of the photoinitiator present in the reaction, hyaluronic acid concentration and distance to source light influenced in the structure of the gels formed. The following graphics intend to elucidate the effects of such parameters in the swelling behaviour of the different materials.

As earlier mentioned, the hyaluronic acid was a component added to the polymeric system in order to increase, not only the biocompatibility with cells but the water retention character of the systems.

So, in this first section, two different concentrations of hyaluronic were tested.

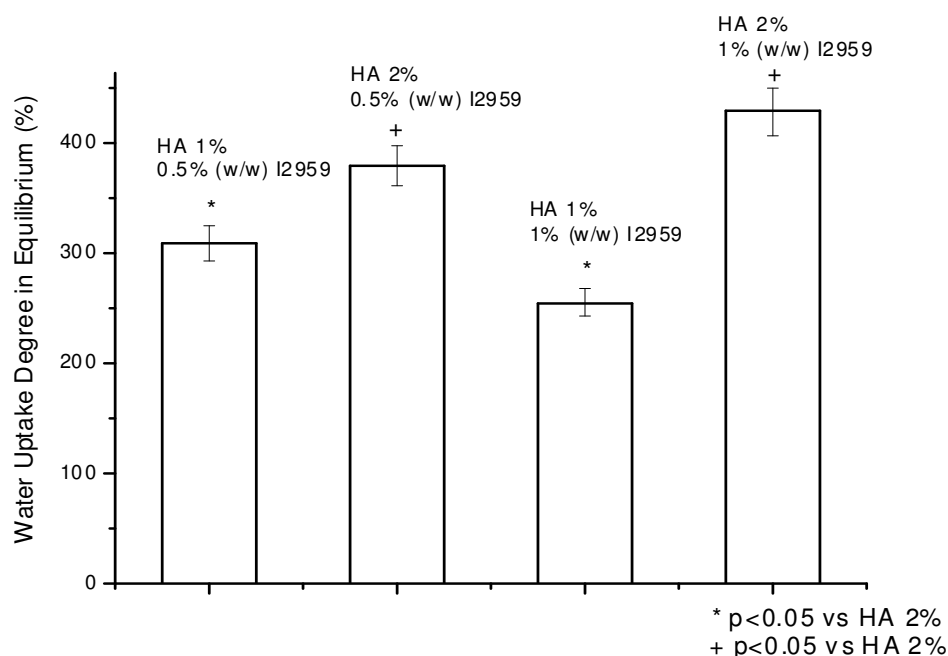


Figure 98. Water uptake degree in aqueous solution (pH 7.4, 37°C), of photopolymerized PEPMHA hydrogels in equilibrium, using 0.0018M EPM, HA 1 and 2% and different concentrations of the photoinitiator I2959, namely 0.5% and 1%, at 8cm of the source of light.

Figure 98 shows that with an increase in the concentration of the hydrophilic component of the polymerization system, hyaluronic acid, there was a significant increase in the water uptake degree reached in equilibrium. In hydrogels with a higher content in HA, there was also a positive effect on the water uptake retention with the increase on concentration of the photoinitiator used.

In order to affect as minimum as possible future cell's viability in future studies, lower concentrations of photoinitiator were tested and the swelling behaviour of the produced hydrogels was followed along time. As stated before, all the concentrations used were able to form hydrogels, and as seen in figure 99, show a good stability along immersion time in aqueous solutions.

Again, a higher initial concentration of photoinitiator led to hydrogels with a higher capacity of water retention.

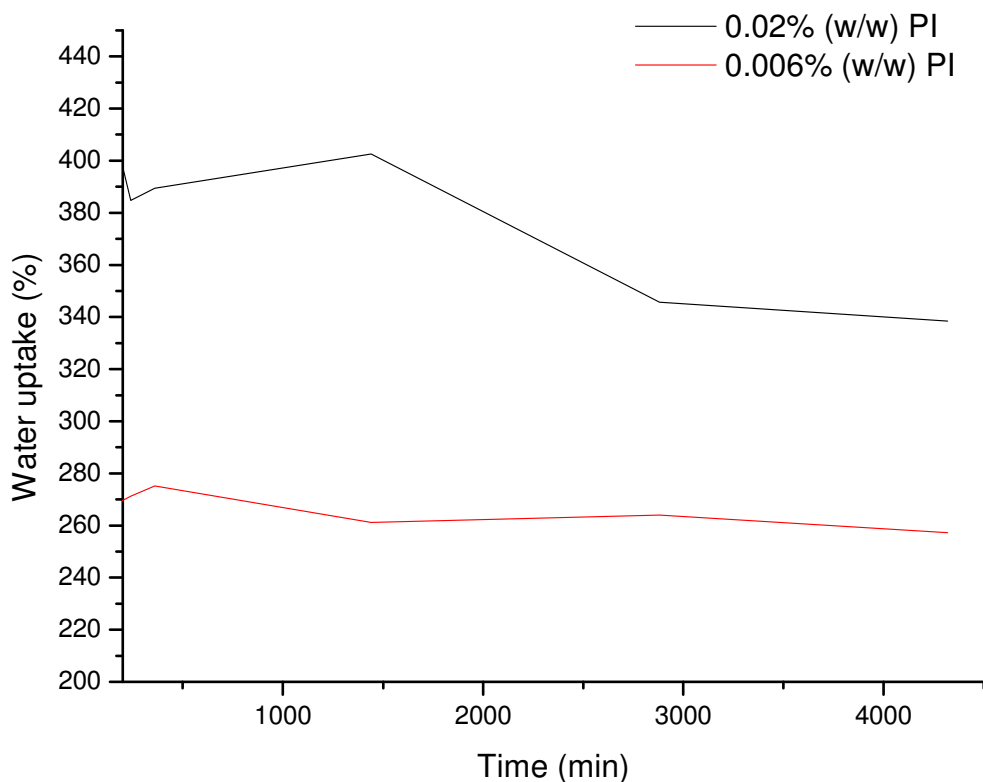


Figure 99. Water uptake degree in aqueous solution (pH 7.4, 37°C), of photopolymerized PEPMHA hydrogels, using 0.0018M EPM, HA 2% and different concentrations of the photoinitiator I2959, namely 0.02% and 0.006%, at 6cm of the source of light.

It was also tested the swelling degree of hydrogels polymerized at different distances to the source of light (6 and 8 cm).

When varying the distance to the source of irradiation we are actually changing the intensity of the light. In the case the pre- polymerization solution is closer to the source of light, the incident light is less disperse and therefore possess a higher intensity.

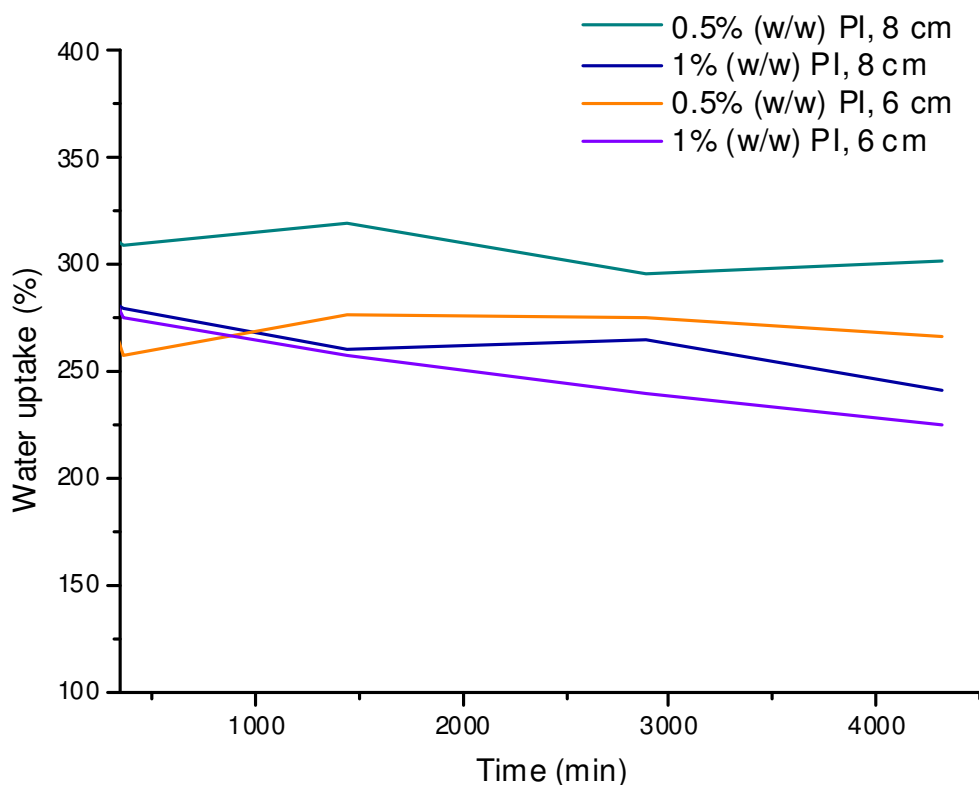


Figure 100. Water uptake degree in aqueous solution (pH 7.4, 37°C), of photopolymerized PEPMHA hydrogels, using 0.0018M EPM, HA 1%, and different concentrations of the photoinitiator I2959, namely 0.5% and 1%, at 6 and 8cm of the source of light.

It is evident from the analysis of figure 100 that this factor is influencing in the structure of the materials produced, influence that can be translated into a difference in the swelling degree. Hydrogels that were formed at a higher distance from the source of light were capable of absorbing more water than hydrogels formed closer from the light, for the same concentration of all the species involved in the photopolymerization reaction. Now, the fact that at lower distances, the intensity of the incident light is higher and would probably increment the velocity of the reaction, creating materials with decreased mechanical properties and thus correlated to a higher swelling degree.

This is only a supposition because the velocity of the reaction wasn't controlled. It was only our goal to have a brief characterization of these materials in order to direct future studies.

### 3.2.5. Mechanical Performance of the photopolymerized PEPMHA hydrogels

The mechanical performance of the photopolymerized hydrogels was assessed in an aqueous environment, pH 7.4, at body temperature. Figures 101 and 102, show the modulus ( $G'$ ) and  $\tan \delta$  of some of the materials.

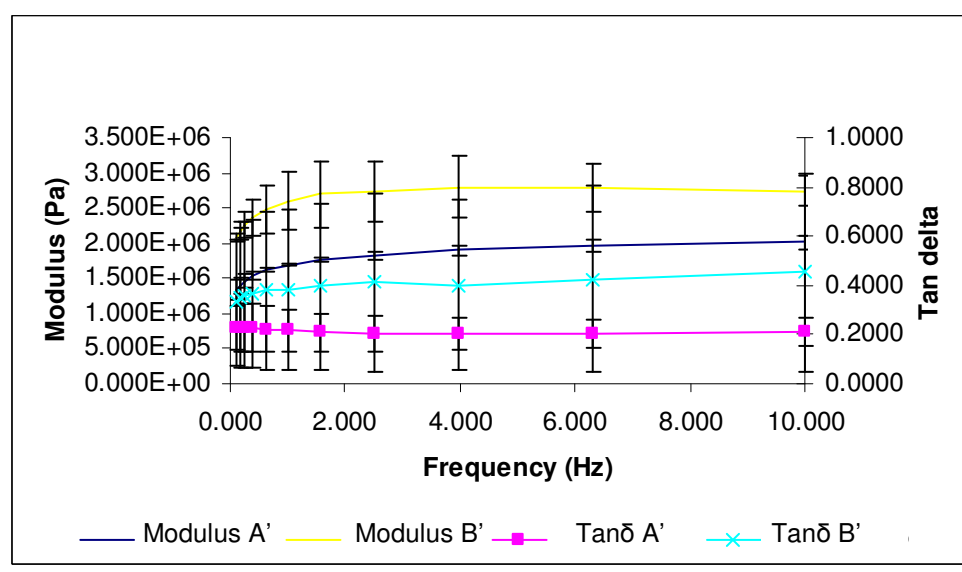


Figure 101. DMA response as a function of frequency (0-10 Hz) for photopolymerized PEPMHA hydrogels prepared with the following compositions: EPM 0.0018M, HA (1%), using I2959 (0.5% w/w) as photoinitiator, at 8 and 6 cm from source of light, respectively, sample A' and sample B'.

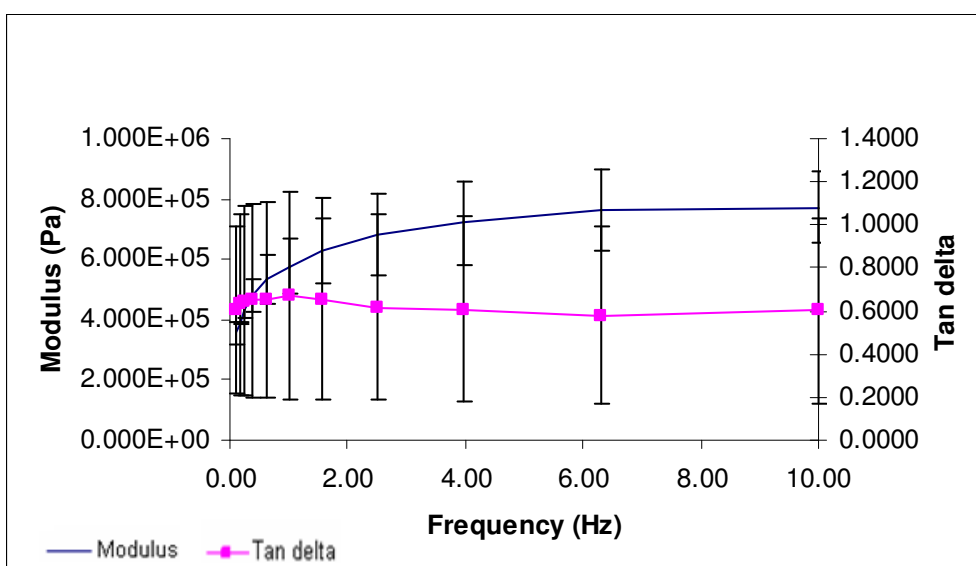


Figure 102. DMA response as a function of frequency (0-10 Hz) for photopolymerized PEPMHA hydrogels prepared with the following compositions: EPM 0.0018M, HA (2%), using I2959 0.5% (w/w) as photoinitiator, at 8 cm from the source of light.

In the first graphic, the variable studied was the distance to the source of light.

In this case, with an increase of the distance, the modulus decreased. This result will be in accordance with the increase in the water uptake degree, in equilibrium, with the distance to the source of light, observed previously.

When a higher distance is fixed and we vary the concentration of hyaluronic acid present, the modulus decreased. This result is concordant with the values of swelling for the studied materials (table 10).

Table 10: Modulus and water uptake degree (%) at equilibrium of photopolymerized PEPMHA hydrogels prepared with EPM 0.0018M, HA (1 and 2%), I2959 0.5% (w/w), at 6 and 8 cm from the source of light.

<b>G' (Pa)</b>	<b>Water uptake in equilibrium (%)</b>	<b>HA (%)</b>	<b>Distance to source of light (cm)</b>
$2.74 \times 10^6$	272.40	1	6
$2.00 \times 10^6$	305.63		8
$8.56 \times 10^5$	371.61	2	8

Finally, when comparing the modulus between the hydrogels prepared in chapter I and using the photopolymerization process, the latter ones present higher values. The same is observed in relation to the degree of water retention, for similar concentrations of hyaluronic acid. If we also consider the porous structure of the hydrogels produced by

both methods, the photopolymerized hydrogels possess an enormous decrease in their porosity, which could be correlated to higher modulus values.

So, in fact, the photopolymerization method was a faster method to prepare PEPMHA hydrogels, not as porous as the ones prepared by thermal activation, therefore with increased mechanical strength and an increased water retention capacity.

#### **4. Conclusions**

The synthesis reaction of EP with methacryloyl chloride in the presence of triethylamine besides forming a monomer with increased reactivity comparing to vinylpyrrolidone, the EPM, is also a simple method for the addition of photoreactive groups.

The formation of hydrogels networks in an aqueous environment can occur with high conversions of monomer due to the high mobility of reacting species during the gel formation, decreasing future problems concerning stability on the mechanical properties or release of unreacted monomer in toxic concentrations to cells.

The formation of thick hydrogels in photopolymerization can sometimes be a problem in the attenuation of the incident light that is absorbed by the initiator molecules. In the future we may also consider the use of photobleaching initiators, in which the initiator radicals absorb light at different wavelengths than the initiator specie, or even dual initiators that provoke the increase in the temperature of the photopolymerization system allowing its initiation through a thermal process, and permitting high conversions in sites where light does not reach.

Both mechanical performance and swelling properties were enhanced using this method of polymerization.

Considering the characteristics mentioned and all the advantages from the photopolymerization method, further studies will be performed to optimize the systems and assess cells viability and proliferation within these materials, in order to use them for cell encapsulation.

## 5. Bibliography

1. R. Barbucci, P. Torricelli, M. Fini, D. Pasqui, P. Favia, E. Sardella, R. d'Agostino and R. Giardino, Proliferative and re-differentiative effects of photo-immobilized micro-patterned hyaluronan surfaces on chondrocyte cells. *Biomaterials*, 2005. 26(36): p. 7596-605.
2. J. Elisseeff, K. Anseth, D. Sims, W. McIntosh, M. Randolph and R. Langer, Transdermal photopolymerization for minimally invasive implantation. *Proc Natl Acad Sci U S A*, 1999. 96(6): p. 3104-7.
3. J. Elisseeff, K. Anseth, D. Sims, W. McIntosh, M. Randolph, M. Yaremchuk and R. Langer, Transdermal photopolymerization of poly(ethylene oxide)-based injectable hydrogels for tissue-engineered cartilage. *Plast Reconstr Surg*, 1999. 104(4): p. 1014-22.
4. J. Elisseeff, W. McIntosh, K. Anseth, S. Riley, P. Ragan and R. Langer, Photoencapsulation of chondrocytes in poly(ethylene oxide)-based semi-interpenetrating networks. *J Biomed Mater Res*, 2000. 51(2): p. 164-71.
5. Q. Li, J. Wang, S. Shahani, D.D. Sun, B. Sharma, J.H. Elisseeff and K.W. Leong, Biodegradable and photocrosslinkable polyphosphoester hydrogel. *Biomaterials*, 2006. 27(7): p. 1027-34.
6. B. Baroli, Review photopolymerization of biomaterials: issues and potentialities in drug delivery, tissue engineering, and cell encapsulation applications. *Journal of Chemical Technology and Biotechnology*, 2006. 81(4): p. 491-499.
7. B. Baroli, V.P. Shastri and R. Langer, A method to protect sensitive molecules from a light-induced polymerizing environment. *J Pharm Sci*, 2003. 92(6): p. 1186-95.
8. S. Zhang, L. Yan, M. Altman, M. Lasse, H. Nugent, F. Frankel, D.A. Lauffenburger, G.M. Whitesides and A. Rich, Biological surface engineering: a simple system for cell pattern formation. *Biomaterials*, 1999. 20(13): p. 1213-20.
9. D.L. Nettles, T.P. Vail, M.T. Morgan and M.W. Grinstaff, Photocrosslinkable Hyaluronan as a Scaffold for Articular Cartilage Repair. *Annals of Biomedical Engineering*, 2004. 32(3): p. 391-397.
10. J.A. Burdick, C. Chung and X. Jia, Controlled Degradation and Mechanical Behaviour of Photopolymerized Hyaluronic Acid Networks. *Biomacromolecules*, 2005. 6(1): p. 386-391.



11. Q. Li, C.G. Williams, D.D. Sun, J. Wang, K. Leong and J.H. Elisseeff, Photocrosslinkable polysaccharides based on chondroitin sulfate. *J Biomed Mater Res A*, 2004. 68(1): p. 28-33.
12. J. Trudel and S.P. Massia, Assessment of the cytotoxicity of photocrosslinked dextran and hyaluronan-based hydrogels to vascular smooth muscle cells. *Biomaterials*, 2002. 23(16): p. 3299-307.
13. K.T. Nguyen and J.L. West, Photopolymerizable hydrogels for tissue engineering applications. *Biomaterials*, 2002. 23(22): p. 4307-14.
14. S. Kızıle, E. Sawardecker and F. Teymor, Sequential formation of covalently bonded hydrogel multilayers through surface initiated photopolymerization. *Biomaterials*, 2006. 27(8): p. 1209-1215.
15. H.F. Lu, E.D. Targonsky, M.B. Wheeler and Y.L. Cheng, Thermally induced gelable polymer networks for living cell encapsulation. *Biotechnol Bioeng*, 2007. 96(1): p. 146-55.
16. H. Uludag, P. De Vos and P.A. Tresco, Technology of mammalian cell encapsulation. *Adv Drug Deliv Rev*, 2000. 42(1-2): p. 29-64.
17. K.H. Bae, J.J. Yoon and T.G. Park, Fabrication of hyaluronic acid hydrogel beads for cell encapsulation. *Biotechnol Prog*, 2006. 22(1): p. 297-302.
18. L.-T. Ng and S. Swami, IPNs based on chitosan with NVP and NVP/HEMA synthesised through photoinitiator-free photopolymerisation technique for biomedical applications. *Carbohydrate Polymers*, 2005. 60(4): p. 523.
19. S.J. Bryant, R.J. Bender, K.L. Durand and K.S. Anseth, Encapsulating chondrocytes in degrading PEG hydrogels with high modulus: engineering gel structural changes to facilitate cartilaginous tissue production. *Biotechnol Bioeng*, 2004. 86(7): p. 747-55.
20. M.A. Rice and K.S. Anseth, Encapsulating chondrocytes in copolymer gels: bimodal degradation kinetics influence cell phenotype and extracellular matrix development. *J Biomed Mater Res A*, 2004. 70(4): p. 560-8.
21. C.H. Quek, J. Li and T. Sun, Photo-crosslinkable microcapsules formed by polyelectrolyte copolymer and modified collagen for rat hepatocyte. *Biomaterials*, 2004. 25: p. 3531-3540.
22. R. Landers, U. Hubner, R. Schmelzeisen and R. Mulhaupt, Rapid prototyping of scaffolds derived from thermoreversible hydrogels and tailored for applications in tissue engineering. *Biomaterials*, 2002. 23(23): p. 4437-47.

23. J. Yeh, Y. Ling, J.M. Karp, J. Gantz, A. Chandawarkar, G. Eng, J. Blumling, 3rd, R. Langer and A. Khademhosseini, Micromolding of shape-controlled, harvestable cell-laden hydrogels. *Biomaterials*, 2006. 27(31): p. 5391-8.
24. A.M. Sun and M. Klaus, Microencapsulation of pancreatic islet cells: A bioartificial endocrine pancreas, in *Methods in Enzymology*. 1988, Academic Press. p. 575.
25. A. Alhadlaq and J.J. Mao, Tissue-engineered osteochondral constructs in the shape of an articular condyle. *J Bone Joint Surg Am*, 2005. 87(5): p. 936-44.
26. K.S. Masters, D.N. Shah and L.A. Leinwand, Crosslinked hyaluronan scaffolds as a biologically active carrier for valvular interstitial cells. *Biomaterials*, 2005. 26(15): p. 2517-2525.
27. G.H. Underhill, A.A. Chen and D.R. Albrecht, Assessment of hepatocellular function within PEG hydrogels. *Biomaterials*, 2007. 28(2): p. 256-270.
28. T. Taguchi, L. Xu and H. Kobayashi, Encapsulation of chondrocytes in injectable alkali-treated collagen gels prepared using poly(ethylene glycol)-based 4-armed star polymer. *Biomaterials*, 2005. 26(11): p. 1247-1252.
29. M.R. Kim and T.G. Park, Temperature-responsive and degradable hyaluronic acid/Pluronic composite hydrogels for controlled release of human growth hormone. *J Control Release*, 2002. 80(1-3): p. 69-77.
30. S.J. Bryant and K.S. Anseth, The effects of scaffold thickness on tissue engineered cartilage in photocrosslinked poly(ethylene oxide) hydrogels. *Biomaterials*, 2001. 22(6): p. 619-26.
31. D.A. Wang, C.G. Williams, Q. Li, B. Sharma and J.H. Elisseeff, Synthesis and characterization of a novel degradable phosphate-containing hydrogel. *Biomaterials*, 2003. 24(22): p. 3969-80.
32. S.J. Bryant, K.A. Davis-Arehart and N. Luo, Synthesis and Characterization of Photopolymerized Multifunctional Hydrogels: Water-Soluble Poly(Vinyl Alcohol) and Chondroitin Sulfate Macromers for Chondrocyte Encapsulation. *Macromolecules*, 2004. 37(18): p. 6726-6733.
33. V.A. Liu and S.N. Bhatia, Three-dimensional photopatterning of hydrogels containing living cells. *Biomedical Microdevices*, 2002. 4(4): p. 257-266.
34. A. Khademhosseini, G. Eng, J. Yeh, J. Fukuda, J. Blumling, 3rd, R. Langer and J.A. Burdick, Micromolding of photocrosslinkable hyaluronic acid for cell encapsulation and entrapment. *J Biomed Mater Res A*, 2006. 79(3): p. 522-32.

35. K. Arcaute, B.K. Mann and R.B. Wicker, Stereolithography of three-dimensional bioactive poly(ethylene glycol) constructs with encapsulated cells. *Ann Biomed Eng*, 2006. 34(9): p. 1429-41.
36. R. Petzold, H.F. Zeilhofer and W.A. Kalender, Rapid prototyping technology in medicine--basics and applications. *Comput Med Imaging Graph*, 1999. 23(5): p. 277-84.
37. C.G. Williams, A.N. Malik, T.K. Kim, P.N. Manson and J.H. Elisseeff, Variable cytocompatibility of six cell lines with photoinitiators used for polymerizing hydrogels and cell encapsulation. *Biomaterials*, 2005. 26(11): p. 1211-8.
38. C.S.C. Inc, Photoinitiators for UV Curing- Key Products Selection Guide.
39. G. Pitarresi, P. Pierro, F.S. Palumbo, G. Tripodo and G. Giammona, Photo-cross-linked hydrogels with polysaccharide-poly(amino acid) structure: new biomaterials for pharmaceutical applications. *Biomacromolecules*, 2006. 7(4): p. 1302-10.

## **General Summary and Conclusions**

### **PHYSICOCHEMICAL AND MECHANICAL CHARACTERISTICS**

Hydrogels can be produced from natural origin polymers or from synthetic polymers. Ultimately a combination between both seems an excellent alternative to combine their characteristics in order to produce materials that can better suit their application.

Hydrogels are highly valuable scaffold materials for three-dimensional culture of cells due to their biomimetic nature. In fact, hydrogels like cartilage and bone tissue contain a high amount of physiological fluids held by a macromolecular matrix. They are able to replace the native extracellular matrix in many of its functions, organizing cells into three dimensions, providing mechanical support to the newly formed tissue and allowing the diffusion of nutrients to and from the cells.

The formation of hydrogel networks in aqueous environments can occur with high conversions of monomer due to the high mobility of reacting species during the gel formation, decreasing future problems concerning stability on the mechanical properties or release of unreacted monomer in toxic concentrations to cells.

The prediction and control of mechanical properties in hydrogels is of great importance in assessing their applicability. Mechanical properties can be intimately related to the polymer structure, crosslinking density and swelling degree. Through variations in the polymeric composition, crosslinking degree and agents as well as polymerization conditions it is possible to manipulate the mechanical properties of the hydrogels.

Concerning all these aspects, we have used a polymer of synthetic origin (PEPM) together with a natural origin one (HA). The polymerization of EPM occurred through free radicals in solution (HA) and in the presence of crosslinkers with different nature (TriEGMA or BIS).

So, after the description and analysis of the several parameters we concluded that:

- PEPMHA polymeric systems were environmentally sensitive, and that the degree of swelling could be altered by changes in temperature and acidity;
- The molecule of HA clearly affected the mechanical performance of the hydrogels and their water uptake capability;

In order to look for better polymerization times, effectiveness in the polymerization reaction that would influence in the mechanical performance and water uptake retention, a new approach to these materials was used. Instead of using temperature as the vehicle

of conducting the polymerization reaction, we intended to use light. Both mechanical performance and swelling properties were enhanced using this method of polymerization.

Considering the characteristics mentioned and all the advantages from the photopolymerization method, further studies will be performed to optimize the polymeric systems and assess cells viability and proliferation within these materials, in order to use them for cell encapsulation.

## **BIOLOGICAL BEHAVIOUR AND BIOCOMPATIBILITY**

The development of hydrogels offers new opportunities for the tissue engineering field as well as for setting up culture systems *in vitro* that mimic the three-dimensional organization and differentiated function of tissues.

The ability of the new biomaterial scaffolds, PEPMHA, to support chondrocytes growth and differentiation was studied *in vitro*. It was concluded that, the novel polymeric systems developed in this study showed good *in vitro* biocompatibility and supported the generation of a hyaline-like matrix by primary chondrocytes, although cell penetration and ECM production within the scaffold itself were relatively poor. Further work might therefore best be focussed on overcoming final challenges, concerning methodology and biomaterial's nature, in the development of an advanced scaffold system for cartilage based on PEPMHA.

The degree of *in vivo* bone bioactivity of a material can be predicted by the degree of ability for apatite to form on the surface of a material in SBF. Thus, a material able to form apatite on its surface in SBF, will rapidly bond to living bone as a result of apatite formation on its surface in a short period within the living body.

So, examination of apatite formation on the surface of a material in SBF is an useful tool for predicting the *in vivo* bone bioactivity of a material.

From the incubation of PEPMHA hydrogels on SBF it was observed the formation of a Ca-P layer that is indicative of the bioactive character of these materials.

Finally, and to summarize, the novel materials synthesized in this work presenting different properties may be used to mimic the extracellular matrix of bone or cartilage and considered as a future vehicle to be used in regenerative medicine and both cartilage and bone tissue engineering.

## **Conclusiones Generales**

### **CARACTERISTICAS FISICO-QUIMICAS Y MECANICAS**

La predicción y control de las propiedades mecánicas de los hidrogeles es de elevada importancia para sus aplicaciones. Las propiedades mecánicas pueden estar íntimamente relacionadas con la estructura del polímero, la densidad de entrecruzamiento y el grado hinchamiento y, a través de variaciones en la composición polimérica, agentes entrecruzantes, grado de entrecruzamiento y las condiciones de la reacción de polimerización.

La formación de hidrogeles en medios acuosos puede realizarse con elevados grados de conversión de monómero, debido a la elevada movilidad de las especies presentes en la reacción. Este hecho va a evitar problemas relacionados con la estabilidad del hidrogel como soporte polimérico, así como la posible liberación de monómero que no haya reaccionado en concentraciones tóxicas para las células. Obviamente hay que considerar la viscosidad de las especies presentes en la reacción de polimerización y su influencia en la movilidad de las cadenas macromoleculares durante el proceso de polimerización. A partir de la descripción y análisis de diversos parámetros verificamos que:

- los sistemas poliméricos de PEPMAH son sensibles a cambios “ambientales” y que su grado de hinchamiento es dependiente de variaciones a temperatura y acidez del medio;
- el ácido hialurónico influye en las propiedades mecánicas y grado de hinchamiento de los hidrogeles;

Los procesos de polimerización se han realizado utilizando iniciación térmica y fotoquímica con la finalidad de evaluar las posibilidades de aplicación de los sistemas preparados mediante ambas técnicas.

La activación fotoquímica utilizando como foto-iniciador el Irgacure 2959, dio muy buenos resultados, dando lugar a sistemas homogéneos en presencia del ácido hialurónico.

Los resultados obtenidos ponen de manifiesto que:

- La cantidad inicial de fotoiniciador, concentración del monómero y de ácido hialurónico, distancia a la fuente de luz, influyen en la porosidad, propiedades mecánicas y grado de hinchamiento de los materiales sintetizados;
- Se observó una mejoría en las propiedades mecánicas y grados de hinchamiento, siendo más elevados para los hidrogeles obtenidos por las reacciones inducidas por la luz que a través de la activación térmica;

Aunque el estudio de estos factores en la velocidad de polimerización no fue analizado, se debe considerar como una línea de investigación futura para optimizar el método así como el estudio de la viabilidad celular y proliferación en estos materiales para su utilización en encapsulamiento celular.

## **COMPORTAMIENTO BIOLÓGICO Y BIOCOMPATIBILIDAD**

Las propiedades de los biomateriales definen su biocompatibilidad, el comportamiento mecánico y sus prestaciones como soporte polimérico a corto y largo plazo. Los fenómenos de interacción que se desencadenan desde el momento en que un biomaterial se encuentra en presencia de un medio biológico están determinados por la estructura y composición de este mismo.

Para determinar la biocompatibilidad de los materiales sintetizados a través de una reacción de polimerización inducida por la temperatura, se sembraron distintos tipos de células en los mismos - condrocitos primarios, ROS, MSC y L929.

Se observó que:

- Los 4 tipos distintos de células mantuvieron su viabilidad cuando fueron sembrados en presencia los distintos materiales;
- Evidencias de adhesión celular, morfología normal de las células, y su proliferación en los hidrogeles sugirieron su aplicación en estudios para ingeniería del tejido cartilaginoso;
- En los estudios para ingeniería tisular, los condrocitos sembrados fueron capaces de colonizar los hidrogeles. La estructura porosa del material está posiblemente influyendo en la penetración celular;

- Los condrocitos fueron capaces de producir una matriz extracelular, localizada predominantemente en la superficie de los materiales, lo que se puso de manifiesto a través de su composición hialina (GAG y colágeno de tipo II);

Futuros estudios deberán considerar: la elevada retención de medio acuoso por parte de los hidrogeles y el cambio de sus propiedades en relación al medio, que por supuesto influirá en la adhesión y proliferación celular; el carácter hidrofílico que poseen estos materiales también será un factor limitante en el caso de algunos métodos de análisis; el método de sembrar las células deberá ser perfeccionado. En este contexto, el estudio preliminar de la aplicación de la fotopolimerización a estos materiales puede aportar beneficios considerables.

Finalmente, se evaluó también la bioactividad de los materiales y se observó la formación de una capa de Ca-P con los característicos cristales en forma de aguja, presentando la típica morfología “coliflor”. Esta morfología es indicativa del carácter bioactivo de estos materiales y su posible aplicación en la ingeniería de los tejidos óseos.





## Appendix

### A- Mechanical Properties (in relation to Chapter I)

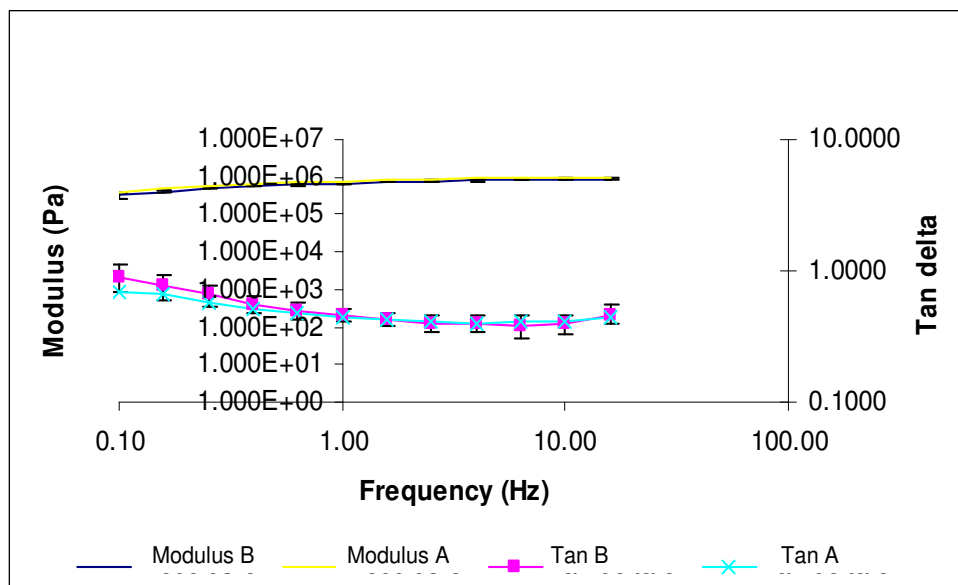


Figure 1. DMA response as function of frequency (0.10-100 Hz) for PEPMHA hydrogels prepared with the following compositions: EPM 0.545M, BIS 2%,  $K_2S_2O_8$   $2 \times 10^{-2}$ M, HA 2.5% (sample A) and HA 5% (sample B).

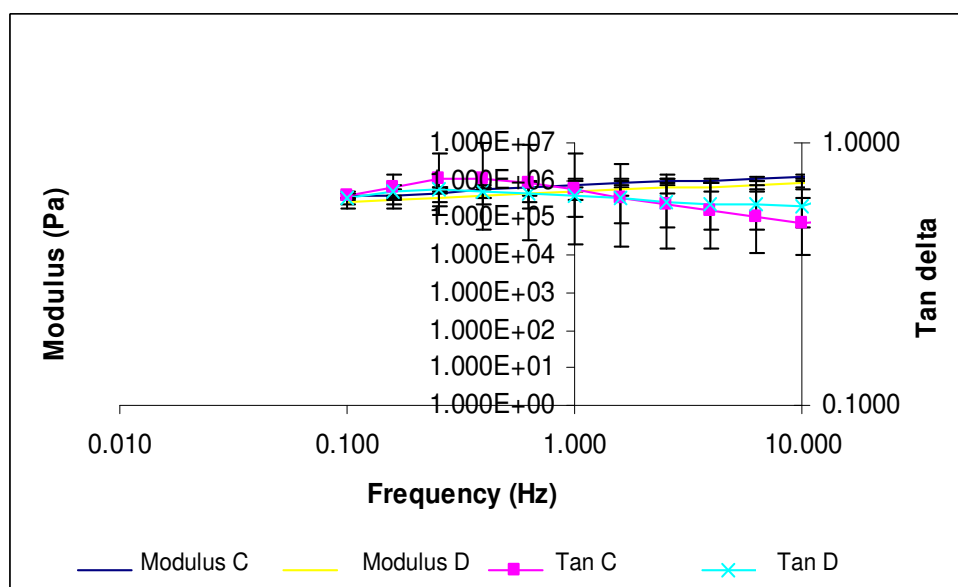


Figure 2. DMA response as function of frequency (0.010-10 Hz) for PEPMHA hydrogels prepared with the following compositions: EPM 0.725M, BIS 2%,  $K_2S_2O_8$   $2 \times 10^{-2}$ M, HA 1% (sample C) and HA 2.5% (sample D).

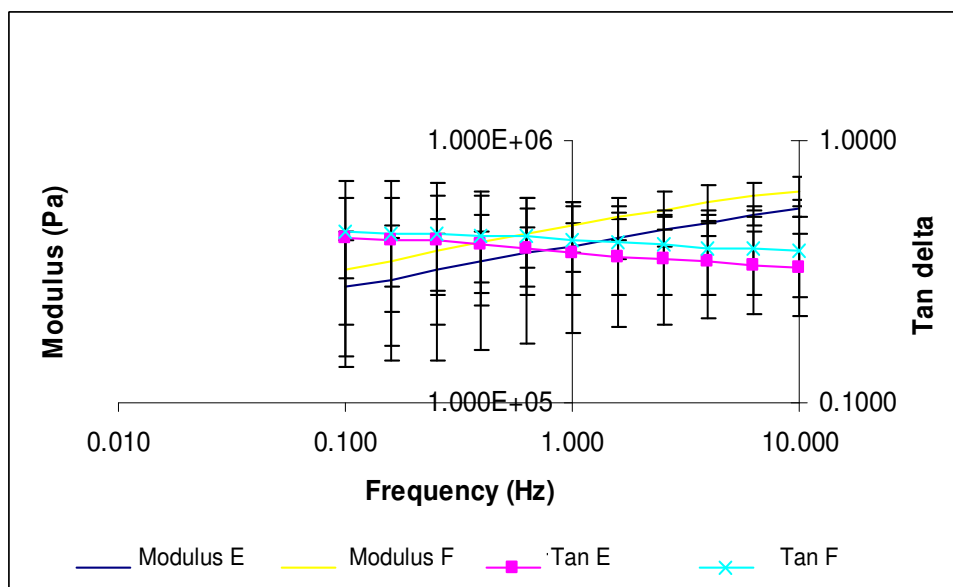


Figure 3. DMA response as function of frequency (0.010-10 Hz) for PEPMHA hydrogels prepared with the following compositions: EPM 0.725M, TriEGDMA 1.7%,  $K_2S_2O_8$   $2 \times 10^{-2}$ M, HA 2.5% (sample E) and HA 5% (sample F).

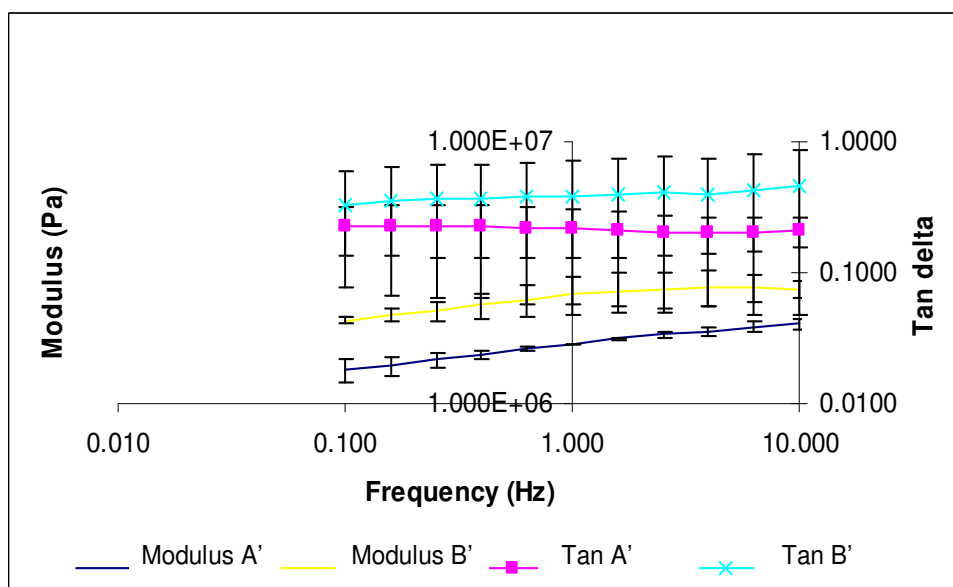


Figure 4. DMA response as function of frequency (0.010-10 Hz) for photopolymerized PEPMHA hydrogels prepared with the following compositions: EPM 0.0018M, HA 1%, using I2959 (0.5% w/w) as photoinitiator, at 8 and 6 cm from source of light, respectively, sample A' and sample B'.

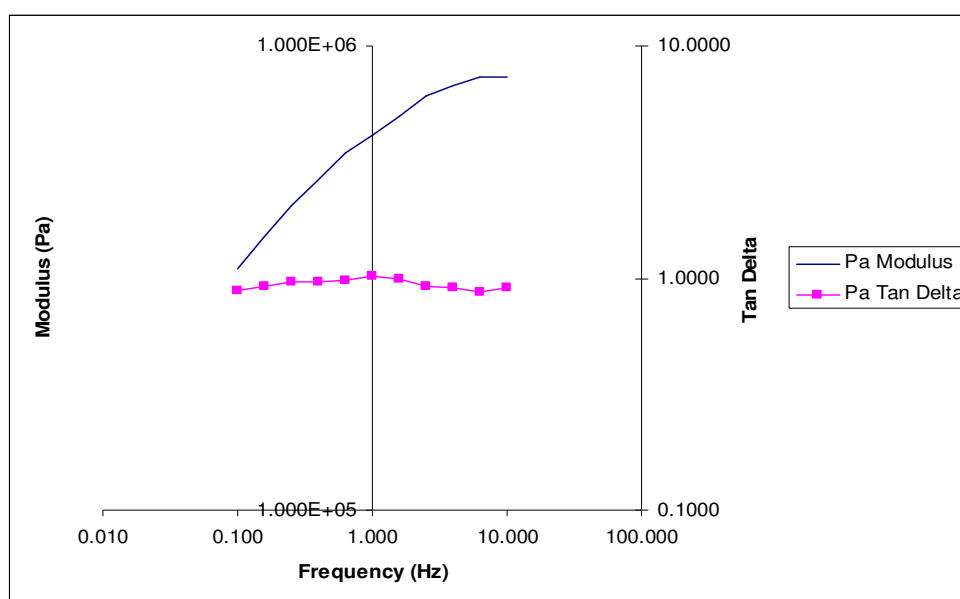


Figure 5. DMA response as function of frequency (0.010-100 Hz) for photopolymerized PEPMHA hydrogels prepared with the following compositions: EPM 0.0018M, HA 2%, using I2959 (0.5% w/w) as photoinitiator, at 8 from source of light.

## B- Cells Biology (in relation to Chapter III)

### 1. Sample sterilization

- Class II laminar flow cabinet
- Phosphate buffered saline (PBS): 10x  $\text{Ca}^{2+}$  /  $\text{Mg}^{2+}$  free phosphate buffered saline, sterile, diluted to 1x PBS stock solution with sterile distilled water
- Basic medium: Dulbecco's Modified Eagle's Medium (DMEM; high glucose formula containing GLUTAMAX-1, Gibco BRL®, Cat. 15630), containing 10 mM HEPES buffer pH 7.4 (Gibco BRL®, Cat. 15630), 10000 units/ml penicillin/10000  $\mu\text{g/ml}$  streptomycin (Gibco BRL®, Cat. 15140) and supplemented with MEM non-essential amino acids

### 2. Cell isolation and expansion

- Bovine metacarpophalangeal joints from skeletally mature animals (>18 months) were obtained from a local abattoir within 4 hours of slaughter
- Rat osteosarcoma cell line (ROS 17/28, Merk. Inc., USA)
- L929, fibroblast cell line (European Collection of Cell Cultures, ECACC, Salisbury, UK)
- Rat mesenchymal stem cells, were isolated from the femurs of young (5-6 week-old) male Wistar rats (Charles Rivers Animal Suppliers, UK)

#### 2.1. Bovine chondrocytes isolation

- Class II laminar flow cabinet
- Dissection tray and aluminium foil
- PM40 post-mortem handle and blades
- Tri-gene virucidal disinfectant (MediChem International, Sevenoaks, UK)
- 70 % v/v industrial methylated spirit (IMS)
- Sterile scalpels, blades and forceps
- Sterile syringe filters: cellulose acetate membrane, 0.22  $\mu\text{m}$  (Orange Scientific, Braine-l'Alleud, Belgium)

- 1 x Phosphate buffered saline (PBS)
- Foetal calf serum (FCS) (Biowest Ltd, Nuaille, France)
- Basic medium: (see in section 1 of this appendix)
- Complete medium: Basic Medium (see section 1 of this appendix) containing 10 % (v/v) foetal calf serum (heat-inactivated, Gibco BRL®, Cat. 10108).
- Trypsin (see section 2.2.)
- Collagenase: 2 mg.ml<sup>-1</sup> bacterial collagenase (EC 3.4.24.3 Closridiopeptidase A [Sigma-Aldrich, Poole, UK]), in complete medium, sterilised by passing through a 0.22 µm millipore filter. Approximately 20 ml was used per dissected joint
- Haemocytometer
- Cell sieve: 70 µm pore size (BD Biosciences Europe, Erembodegem, Belgium)

## 2.2. Cell expansion

- Class II laminar flow cabinet (Walker Safety Cabinets Ltd, Glossop, UK)
- bFGF: basic fibroblast growth factor (FGF<sup>2</sup> Cat. 100-18B, PreproTech, London, UK) [Stock solution: 10 µg.ml<sup>-1</sup> bFGF in PBS, containing 1 mg.ml<sup>-1</sup> bovine serum albumin. This stock solution was stored in 100 µl aliquots at -20°C]
- 1x Phosphate buffered saline (PBS)
- Foetal calf serum (FCS) (Biowest Ltd, Nuaille, France)
- Expansion medium: complete medium (see section 2.1. of this appendix) containing 1µl/ml of stock bFGF solution, added immediately prior to use [N.B. final concentration of bFGF was 10 ng.ml<sup>-1</sup>]
- Trypsin-EDTA: 0.05% wt/v porcine trypsin and 0.02% wt/v EDTA• 4Na in Hank's Balanced Salt Solution containing phenol red
- Tissue-culture grade petri dishes, 100 mm diameter (Greiner bio-one Ltd, Stonehouse UK). Sterile
- Multi-place magnetic stirrer: mounted within a temperature controlled 37°C incubator with an atmosphere of 95% air / 5% CO<sub>2</sub>, 95% humidity

### **3. Cell seeding and adhesion for TE**

#### **3.1. Seeding scaffolds**

- Class II laminar flow cabinet (Walker Safety Cabinets Ltd, Glossop, UK)
- PEPMHA scaffolds
- Agarose scaffolds
- Haemocytometer
- Non-adherent culture dishes, 100 mm diameter (Greiner bio-one Ltd, Stonehouse UK). Sterile
- Multi-place magnetic stirrer: mounted within a temperature controlled 37°C incubator with an atmosphere of 95% air / 5% CO<sub>2</sub>, 95% humidity
- 19 or 21 G sterile syringe needles
- Expansion medium (see section 2.2.)

#### **3.2. Expansion and adhesion (7 days)**

- Class II laminar flow cabinet (Walker Safety Cabinets Ltd, Glossop, UK)
- PEPMHA scaffolds
- Agarose scaffolds
- Expansion medium
- Non-adherent culture dishes, 100 mm diameter (Greiner bio-one Ltd, Stonehouse UK)
- Expansion medium: basic medium

#### **3.3. Cartilage construct maturation (40days)**

- Class II laminar flow cabinet (Walker Safety Cabinets Ltd, Glossop, UK)
- PEPMHA scaffolds
- Agarose scaffolds
- Non-adherent culture dishes, 100 mm diameter (Greiner bio-one Ltd, Stonehouse, UK)

- L-ascorbic acid: a stock solution of 50 mg.ml<sup>-1</sup> L-ascorbic acid (in basic medium (see section 1.) was freshly prepared when required (Sigma- Aldrich, Poole, UK)
- Insulin: from bovine pancreas (Cat. no I5500, Sigma-Aldrich, Poole, UK). A stock solution of 1 mg.ml<sup>-1</sup> insulin in 10 mM acetic acid was prepared and sterilised by passing through a 0.22 µm millipore filter. The stock solution was stored in 250 µl aliquots at -20°C
- Non-adherent culture dishes, 100 mm diameter (Greiner bio-one Ltd, Stonehouse, UK). Sterile
- Differentiation medium: basic medium (see section 1) and 10 % v/v foetal calf serum (heat-inactivated, Gibco BRL®, Cat. 10108), supplemented with stock 1 mg/ml insulin (see above) and 1µl/ml of stock 50 mg/ml L-ascorbic acid solution (see above)

#### **4. Characterisation of scaffolds and constructs**

##### **4.1. SEM**

- Cacodylate buffer 0.1 M sodium cacodylate in H<sub>2</sub>O at pH 7.4
- 3% wt/v glutaraldehyde (Agar Scientific, Stansted, UK) in 0.1 M PBS (see section 1)
- 2% aqueous osmium tetroxide (OXKEM, Berkshire)
- Ethanol (75% v/v, 95% v/v, 100% v/v, and 100% v/v dried over anhydrous copper sulphate)
- Fume cupboard
- Double-sided adhesive carbon tabs (Agar Scientific)
- Edwards S150B sputter coater with gold target
- Philips/FEI XL-20 scanning electron microscope

##### **4.2. Cell Viability**

- Alamar Blue™ (BioSource Europe, S.A.B-1400 Nivelles, Belgium)
- 96- well flat bottom plates (Corning Life Sciences, Acton MA, US)
- Differentiation medium: as in section 3.3.



- Non-adherent culture dishes, 100 mm diameter (Greiner bio-one Ltd, Stonehouse UK)
- Multichannel pipette
- Polarstar Galaxy spectrophotometer, operated with Fluostar Galaxy software (BMG Labtech GmbH, Offenburg, Germany)

### **4.3. Construct processing for histology and Immunohistochemistry**

- Cork discs
- Aluminium foil
- Isopentane
- Liquid nitrogen
- OCT cryo-embedding compound (VWR International, UK)
- Microtome (Leica CM 3050 S. Leica, UK)
- Glass slides coated in 4% APES (3-aminopropyltriethoxysiloxane in acetic acid)
- Paraformaldehyde: 4% paraformaldehyde (w/v in PBS), pH 7.4
- Parafilm

#### **4.3.1. Histology**

- Distilled water
- Ethanol
- Xylene
- Glass coverslips
- DPX mountant
- Toluidine Blue: 1% wt/v Toluidine blue (Sigma-Aldrich, UK) in 0.5% wt/v sodium borate in distilled water, filtered
- Hematoxylin (acidified commercial preparation, 0.4%, Thermo Electron Corp., UK)
- Eosin Y (0.5% commercial preparation, 0.4%, Thermo Electron Corp., UK)

#### 4.3.2. Immunohistochemistry

- 1 x Phosphate buffered saline (PBS)
- Hyaluronidase: 10 mg.ml<sup>-1</sup> bovine testicular hyaluronidase (EC 3.2.1.35, Sigma-Aldrich, Poole, UK) in PBS
- Hydrogen peroxide (Sigma, Co, 3% (v/v) in methanol (Aldrich)
- TBS: 0.61% w/v tris(hydroxymethyl)methylamine (BDH, Poole, UK) and 0.81% w/v NaCl in distilled water, pH 7.5-7.6
- TBS/ Tween 20: TBS (see above) containing 0.05% v/v Tween 20 High salt wash: 0.61% w/v Tris and 2.5% w/v NaCl in distilled water
- BSA blocking solution: 30 mg.ml<sup>-1</sup> bovine serum albumin (Sigma-Aldrich, Poole, UK) in TBS/Tween 20 (see above)
- Antibody diluent: 10 mg.ml<sup>-1</sup> bovine serum albumin (Sigma-Aldrich, Poole, UK) in TBS/Tween 20 (see above)
- Primary antibody for collagen type I: 0.4 mg.ml<sup>-1</sup> stock solution of anticollagen type I antibody (Cambridge Bioscience, Cambridge, UK), diluted 1:100 in antibody diluent (see above), containing 50 µl.ml<sup>-1</sup> normal rabbit serum (N.B. final concentration 4 µg.ml<sup>-1</sup> anti-collagen type I antibody)
- Primary antibody for collagen type II: 0.4 mg.ml<sup>-1</sup> stock solution of anticollagen type II (Cambridge Bioscience, Cambridge, UK), diluted 1:20 in antibody diluent (see above), containing 50 µl.ml<sup>-1</sup> normal rabbit serum (N.B. final concentration 20 µg.ml<sup>-1</sup> anti-collagen type II antibody)
- Normal goat serum control: 10 µg.ml<sup>-1</sup> stock solution of normal goat serum in antibody diluent (see above), diluted 1:150 in antibody diluent containing 50 µl.ml<sup>-1</sup> normal rabbit serum (N.B. final concentration 67 nl.ml<sup>-1</sup> normal goat serum)
- Vectastain© *Elite* ABC kit (Pk-6105), with biotinylated goat IgG (Vector Laboratories Ltd, Peterborough, UK)
- DAB substrate kit for peroxidase (Vector Laboratories Ltd, Peterborough, UK)
- Methyl green stain (Vector Laboratories Ltd, Peterborough, UK)

#### 4.4. Quantitative assessment of glycosaminoglycans

- Dimethylmethylen Blue (DMB) dye solution: 0.016 g.L<sup>-1</sup> DMB (Aldrich, Gillingham, UK), in distilled water containing 0.04 M glycine, and 0.04 M NaCl. Stirred for at least 2 hours, covered with foil. pH adjusted to 3.0 with HCl (BDH Laboratory Supplies, Poole, UK) and volume to 500 ml. Stored at room temperature, away from light
- Papain: 0.5 mg.ml<sup>-1</sup> (from papaya latex, Cat. P4762, EC 3.4.22.2, Sigma-Aldrich, Missouri, USA)
- N-Acetyl cysteine: 0.96 mg.ml<sup>-1</sup> (Sigma-Aldrich, UK)
- Agarase: 10 µl.ml<sup>-1</sup> (Cat. A6306, EC 3.2.1.81, Sigma), [Stock solution: 1000 units.ml<sup>-1</sup>, prepared in PBS, and stored in 100 µl aliquots at -20°C]
- Chondroitin 4-sulphate: Na salt from bovine trachea, [Stock solution: 50 µg.ml<sup>-1</sup>, prepared in distilled water, and stored in 100 µl aliquots at -20°C]
- 96- well flat bottom plates (Corning Life Sciences, Acton MA, US)
- Centrifuge (MSE Harrier 18/80, Sanyo, UK distributor)
- Multichannel pipette
- Polarstar Galaxy spectrophotometer, operated with Fluostar Galaxy software (BMG Labtech GmbH, Offenburg, Germany)